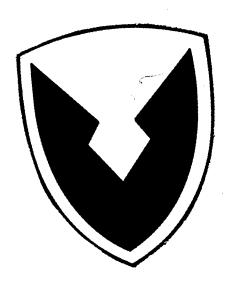
TECHNICAL REPORT NO.

9560

TECHNICAL LIBRARY REFERENCE COPY

RESEARCH REPORT NO. 6

November 1966



PERMANENT FILE COPY

20020814015

The Land Locomotion Laboratory

Distribution of this document is unlimited.

COMPONENTS RESEARCH & DEVELOPMENT LABORATORIES

WARREN, MICHIGAN U.S. ARMY TANK AUTOMOTIVE CENTER

The findings in this report are not to be construed as an official Department of the Army position, unless so designated by other authorized documents.

CITATION OF EQUIPMENT IN THIS REPORT DOES NOT CONSTITUTE AN OFFICIAL INDORSEMENT OR APPROVAL OF THE USE OF SUCH COMMERCIAL HARDWARE.

Distribution of this document is unlimited.

Destroy this report when it is no longer needed. Do not return it to the originator.

100

RESEARCH REPORT NO. 6

Ву

THE STAFF

of

THE LAND LOCOMOTION LABORATORY

November 1966

AMCMS CODE: 5022.11.82200 DA PROJECT: 1-V-0-21701-A-045

ABSTRACT

This report is a comprehensive collection of technical papers written by the Staff of the Land Locomotion Laboratory. Its purpose is to offer, in a single volume, a picture of the state-of-the-art of soil-vehicle mechanics.

The following topics are covered: Description of Soil Stress-Strain Behavior in Vertical and Horizontal Directions and Its Use in Vehicle Performance Prediction; The Analysis of Wheel Performance in Soft Soil; Vehicle Ride Characteristics Studies; Application of Dimensional Analysis in Land Locomotion Mechanics; Remote Area Soil Strength Prediction by Means of Soil Analogs; Description of a Portable Soil-Strength Measuring Apparatus; Field Tests with a Wheeled Soil Strength Measuring Device; Discussion on a Terrain Profile Recorder; and Novel High Mobility Vehicle and Component Concepts.

Reproduced From Best Available Copy

Copies Furnished to DTIC Reproduced From Bound Originals

ACKNOWLEDGEMENT

This Research Report is the result of an extensive effort by Mr. Zoltan J. Janosi, Chief of the Theoretical Land Locomotion Mechanics Section of the Laboratory. Mr. Janosi was given the task of organizing a comprehensive review of the State-of-the-art of land locomotion mechanics. He was expected to assign papers to various staff members and assure that deadlines were met. Because of many conflicting tasks, it was not possible to maintain the schedule proposed for the report making its publication date much later than we desired. The results of Mr. Janosi's efforts are satisfying in that a review is presented that could only be exceeded by the preparation of a major text.

TABLE OF CONTENTS

Paper No.		Page No.
	Abstract	iii
	Acknowledgement	iv
	Introduction	1
1.	Hegedus, E., and Liston, R. W., "Recent Investigati of Vertical Load-Deformation Characteristics of Soils"	ons 2
2.	Wills, B. M. D., "Horizontal Shear in Soil-Vehicle Mechanics"	21
3.	Hanamoto, B., "Vehicle Ride Characteristics"	46
4.	Janosi, Z. J., "State-of-the-Art of the Analysis of Soft Soil Performance of Wheels"	121
5.	Czako, T. F. and Janosi, Z. J., "State-of-the-Art o Vehicle Performance Prediction"	f 152
6.	Liston, R. A., "Dimensional Analysis in Land Locomo tion Problems"	- 167
7.	Harrison, W. L., Jr. and Bong-Sing Chang, "Soil Strength Prediction by Use of Soil Analogs"	209
8.	Spanski, P., "Portable Soil Test Devices"	242
9.	Sloss, D., 'Wheeled Bevæmeter Field Tests"	254
10.	Martin, L. A., "Terrain Geometry Measuring Equip- ment"	272
11.	Liston, R. A., "Unusual Vehicle and Component Concepts"	278
	Distribution List	320
	DD Form 1473	

INTRODUCTION

One of the functions assumed by the Land Locomotion Laboratory at its inception was the dissemination of the results of mobility research. Although a significant amount of mobility research was in progress during the early postwar period, there were few outlets available for the publication of technical papers. The Land Locomotion Laboratory began publication of a bulletin which included a variety of papers and solicited comments, discussions, and articles. But since the bulletin did not produce the desired response, our Research Report series was initiated. The Research Reports consisted of a series of papers describing work done by or for the Laboratory. With the exception of Research Report No. 5, the reports did not follow a theme but attempted a journal-like format.

Research Report No. 5 had a specific theme: the land locomotion soil value system and its applications. This report was very successful and indicated the value of establishing a theme for the reports which could be examined in depth. However, with the formation of the International Society for Terrain-Vehicle Systems in 1962 and the appearance of the "Journal of Terramechanics" in 1964, the need for the Research Report with its journal format disappeared. The present report is the last of the journal-like reports which will be prepared by the Laboratory. Subsequent research reports will summarize the state-of-the-art within a single topic which will be treated in detail. It is proposed, for example, that Research Report No. 7 appear in approximately six months and consider the topic of Walking Machines.

Research Report No. 6 is an ambitious undertaking which attempts to present a review of the state-of-the-art of land locomotion mechanics as viewed by the Land Locomotion Laboratory. The preparation of the report has been much more time consuming than had been anticipated and is published approximately one year late. The papers appearing in the report were, for the most part, completed in early 1965 but they still remain current. In some cases subsequent work was done, but unless earlier papers contained errors of fact which were identified by subsequent studies, no attempt was made to up-date the results. However, the reader is cautioned that the papers represent the state-of-the-art approximately two years ago.

RECENT INVESTIGATIONS OF VERTICAL

LOAD-DEFORMATION CHARACTERISTICS OF SOILS

By: E. Hegedus R. A. Liston

The fundamental assumption of the Bekker method for off-the-road vehicle performance evaluation is that it is possible to predict vehicle sinkage and motion resistance on the basis of plate penetration tests. Furthermore, it is assumed that the constants associated with the equations of the load-sinkage relationships represent soil properties and are independent of plate shape and size. Based on these assumptions, a general theory for soil-vehicle systems has been developed. The approach is primarily experimental. To obtain soil parameters, the penetration of two small plates of different sizes is required in order to determine $k_{\rm C}$, $k_{\rm C}$, and n, which govern the plate sinkage problem. This approach is very attractive, since it is a straightforward procedure which attempts to describe a complex phenomenon on the basis of a simple test. At the present time, a purely theoretical approach to soil vehicle mechanics is lacking because a general failure theory for soils does not exist.

However, if the plate test is to be a useful tool in the mobility field, the following requirements have to be satisfied:

- a. A good fit of experimental load-sinkage curves with an equation involving soil properties and plate geometry.
- b. A minimum rate of penetration, above which pressuresinkage curves are the least affected by the speed of penetration must be maintained.
- c. Knowledge of size and shape effects is imperative in order to produce the same soil parameters in a soil with arbitrarily selected plates. If this requirement is not met, then one needs to know how far it is possible to extrapolate plate test results to loading areas having different size and form.

The description of research endeavors into the above requirements is the purpose of this article.

Bekker (1) suggested that pressure-sinkage relationships for all soils can be described by the equation

$$p = (\frac{k_c}{b} + k_p) z^n \dots 1.$$

$$a_1 = k_c/k_1 + k_{\emptyset}$$

$$\mathbf{a}_2 = \mathbf{k}_c/\mathbf{b}_2 + \mathbf{k}_{\phi}$$

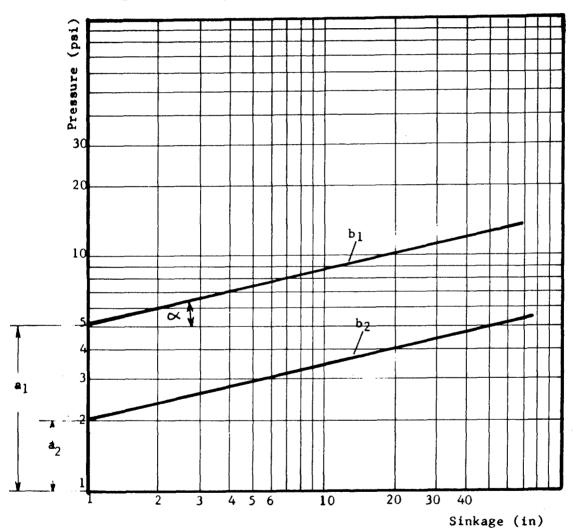


Figure 1

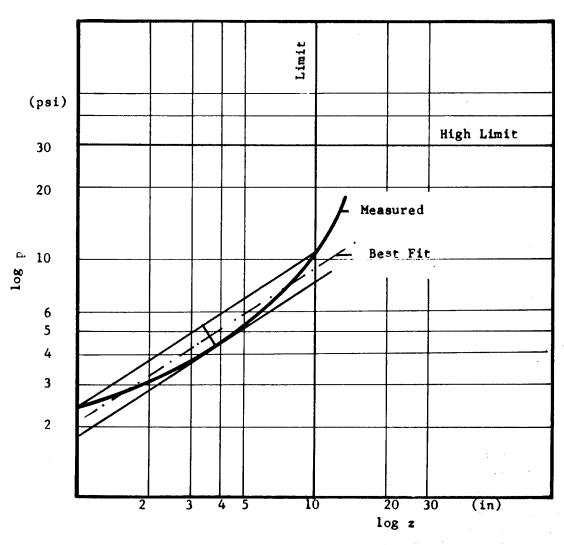


Figure 2

The evaluation of load-sinkage parameters k_c , k_f , and n, is done by plotting two experimental pressure-sinkage curves obtained from two plates of different size on log-log paper, and the best fitting straight line is drawn (Figure 1). k_c , k_f , and n, can be obtained from the intercepts and slopes of p_1 and p_2 curves respectively. It is important that the straight lines drawn most closely approximate the actual pressure-sinkage curves; therefore, Reece (2) proposed the so-called "minimum error method".

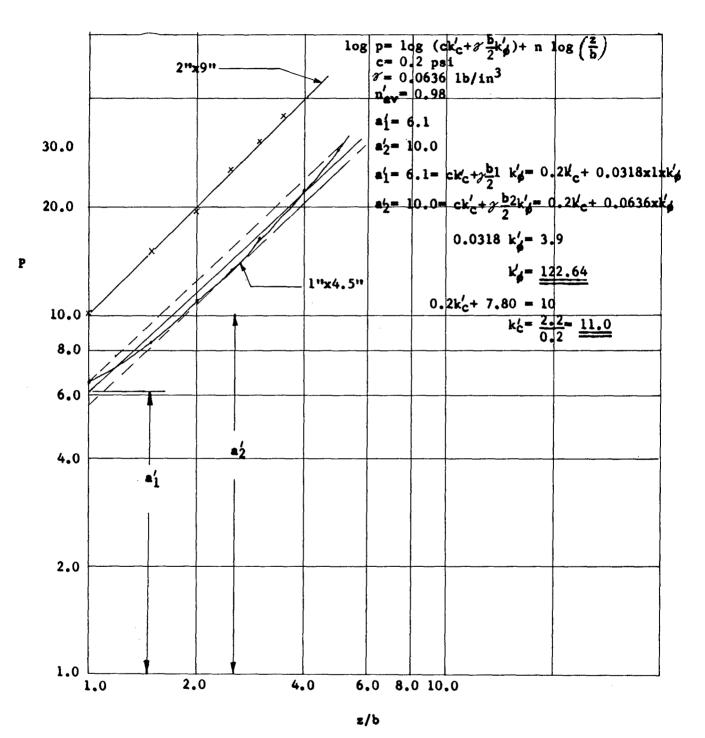
According to Reece, the curve fitting procedure requires the setting of practical limits of a stress-strain curve along which the best fit is desired. The parts of the stress-strain curves below one inch sinkage (z) are neglected since $z \le 1$ in. is not likely to cause a mobility problem. Sinkages over ten inches are also neglected, since most vehicles would be immobilized if they sank that far. However, if 30 psi occurs at less than 10 in. sinkage, then 30 psi is taken as the upper limit for any land vehicle.

Taking the portion of stress-strain curve which is defined by the above limits, the end points are connected (Figure 2).

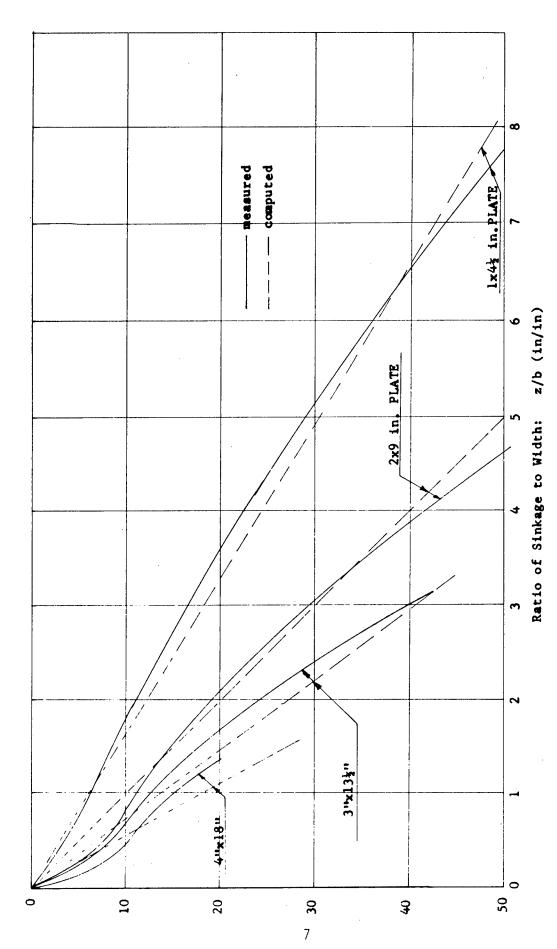
The line parallel to AB, but having the same maximum error, (e), at the ends, as well as in the middle, will represent the best fitting straight line to the experimental points. This line is situated midway between the chord and the tangent. The justification of this procedure is described in Reference 2.

Equation 1 has often been criticized on the ground that it is in contradiction with well established bearing capacity theories and the dimensions of k_c , and k_f , and a function of n. In order to overcome some of the disadvantages of Bekker's equation, Reece (3) proposed to describe pressure-sinkage relationships for soils as follows:

The form of Equation 2 is very similar to Meyerhof's bearing capacity equation. The desirable features of the equation are that k_c^{\dagger} and k_c^{\dagger} are dimensionless quantities and the equation incorporates soil shear strength parameters. It is in accord with bearing capacity theories since the supporting power of the soil is directly proportional to the width of the footing. In Equation 2, k_c^{\dagger} and k_c^{\dagger} are true cohesive and frictional moduli of deformation since, for k_c^{\dagger} a cohesionless soil (c = 0), k_c^{\dagger} has no influence. Therefore,



EVALUATION OF k_c' , k_b' , and n from REECE'S EQUATION Figure 3



p vs. z/b CURVES FOR CONSTANT 1/b RATIOS OF FOOTINGS IN SATURATED OTTAWA SAND

Figure 4

$$p = \frac{\gamma_b}{2} \qquad k_b \left(\frac{z}{b}\right)^{n'} \qquad \dots \qquad 3$$

To evaluate k_c^{\prime} , k_c^{\prime} , and n^{\prime} of Equation 2, pressure-sinkage curves with two plates of different widths must be available. The technique of evaluating k_c^{\prime} , k_c^{\prime} , and n is identical to the procedure described for obtaining k_c^{\prime} , k_c^{\prime} , and n. Figure 3 shows the procedure in detail, where the Reece method is employed to rectangular plate sinkage curves obtained in a saturated Ottawa sand. All pertinent information is in the data.

Taking plate sizes 1" x $4\frac{1}{2}$ " and 2" x 9" as a basis for obtaining k_c , k_c , and n, the question remains, how good are these values when applied to predicting the load sinkage characteristics of larger plates? In this case, the 3" x $13\frac{1}{2}$ " and 4" x 18" plates are preferred. Only after the predictions prove to be satisfactory is it possible to conclude that k_c , k_c , and n' may be soil parameters, and they are practically independent from plate size.

A comparison of Reece's equation with plate sinkage test data is shown in Figure 4. The correlation performed in the figure is good, however, not better than one would expect to get from the Bekker approach. This equation, like Bekker's, is purely empirical. k' and k' are artificially made to be dimensionless parameters by introducing the cohesion (c) and the bulk density (1) of the soil. It will be shown later that z/b is not a significant soil parameter except for cohesive soils.

Applying Equation 2 to circular plate test data in the same soil, an entirely different set of k', and k', and n' were obtained. This makes it clear that the constants associated with the equation do not represent soil properties. They are functions of plate form and possibly size. For this reason, Reece (3) proposed the use of long infinite strip footings for penetration tests. He argued that most off-the-road vehicles penetrate the soil with long narrow contact area; also, a future theoretical treatment appears to be more hopeful if infinite strips are involved. The long narrow contact area, however, is seldom met in the case of wheels.

Noteworthy suggestions derived from the Reece approach are that soil shear strength parameters must, somehow, be tied into the loadsinkage equation and a relationship should exist between $k_{\rm C}^{\rm I}$ and $k_{\rm C}^{\rm I}$, and the angle of internal friction of the soil. Present investigations at the Land Locomotion Laboratory by Dr. B. M. D. Wills are expected to yield answers to some of these propositions.

Equations 1 and 2, described in the preceding, do not fit stress deformation curves obtained in soft clays (Figure 5), unless the separate straight-line portions of the log p-log z curve are described separately. This idea is highly impractical since an equation consisting of the sum of at least two terms having different sets of constants (soil properties), and slopes would have to be used to predict, for example, the vehicle sinkage. Wills found that the complete pressure deformation curves of this type can be accurately expressed by a single equation

This equation is also an empirical formula which is suitable for the description of a particular type of stress-strain curve. Vehicle-evaluation equations based on this type of pressure distribution function are not available as yet. The use of Equation 4 would be a departure from the original Bekker scheme, because he assumed that the load-sinkage relationships for all soils can be adequately described by Equation 1.

Dr. Ehrlich of the Stevens Institute of Technology has been working on a basic load-sinkage equation based on a power series. The purpose of the study is, not only to obtain a better fit to load-sinkage data, but also to investigate the shape and form effects of plates on load-sinkage relationships. At the time of this writing, no conclusive results of Ehrlich's study were available.

During the past few years, plate penetration studies performed at the Land Locomotion Laboratory involve the investigation of the effect of penetration (5) rate and plate size and form effects on stressstrain characteristics of soils (6).

Before 1963, the technique employed for obtaining soil values from plate penetration tests has been used with little regard as to what effect, if any, speed would have on load-sinkage curves. As a result, penetration tests have been conducted using a set sinkage speed chosen arbitrarily. However, according to recent papers in the literature (7), strain rate and loading rate tests conducted on saturated sand show a definite influence of speed on the stress-strain characteristics of soils. Since field conditions warrant the necessity of testing in saturated material, the effect of sinkage rate on load-sinkage relationships was investigated at the Land Locomotion Laboratory.

Seven small scale footings, having circular, rectangular, and square contact areas, were subjected to a constant rate of penetration

ranging from 0.2 in./min. to 1,750 in./min. in a saturated Ottawa sand. With increased rates of penetration, the resistance of soil penetration increased. The most significant effect occurred prior to failure; the effect being a considerable increase in bearing strength of the soil. A typical pressure sinkage curve with load as parameter, is shown in Figure 6. Sixty inches per minute was observed as the critical deformation rate at which the mode of failure changed. For sinkage rates slower than 60 inches per minute, local failure occurred; for higher sinkage rates, general shear failure was predominant. The above conclusions were true for all footings tested except for the 3/4 x 4 in. strip footing which failed due to general shear failure occurring at all sinkage rates tested.

Pressure differences between the lowest (0.6 in./min.) and highest (1,750 in./min.) rates of penetration at post failure deformations were as high as 30%. The pressures deviating for strain rates over 60 in./min. were 10% or less for all footings tested and were considered negligible.

It was concluded that in order to produce the same mode of failure in the soil in each penetration test, and to have the least speed effect on load-sinkage relationships, the penetration tests should be performed at the speed of 60 in./min. or higher. Increased strength with increased rates of penetration was attributed to inertia effects and, also, to the change in the mode of failure of the sand.

The following discussion will be concerned with size and form effects of plates on load-sinkage relationships. The problem is two-fold:

- a. To define soil parameters so that they will be independent of plate.
- b. To determine the range of validity for extrapolating small plate data to predict the load-sinkage behavior of large loading areas.

When examining the accuracy of a proposed pressure-sinkage equation based on plate sinkage, first, one has to determine whether the plate sinkage data can be used to predict plate sinkage. That is, can the behavior of a small plate allow one to predict the behavior of a larger plate? When considering model-prototype relationships, an obvious approach is to treat the problem by means of dimensional analysis.

The objective was to derive an equation relating pressure and sinkage on the basis of dimensional analysis. The equation would be evaluated on the basis of its ability to predict the sinkage of a large plate from data established by means of a test using a small, or model,

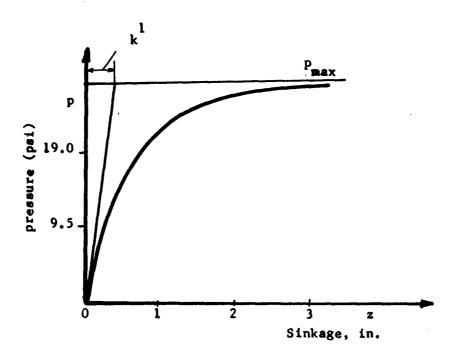
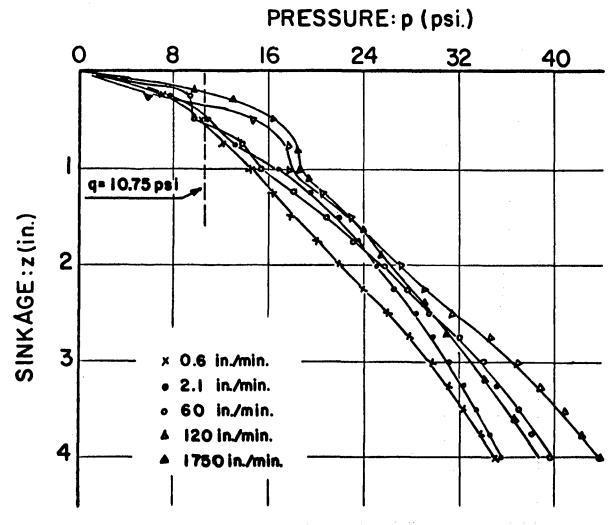


Figure 5



PRESSURE SINKAGE CURVES FOR A 3 IN. DIA. FOOTING IN SAND
Figure 6

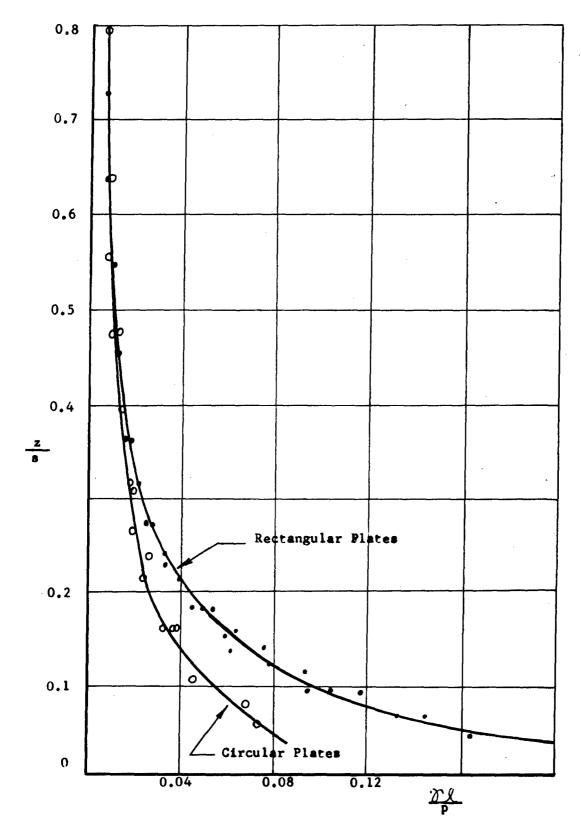


Figure 7

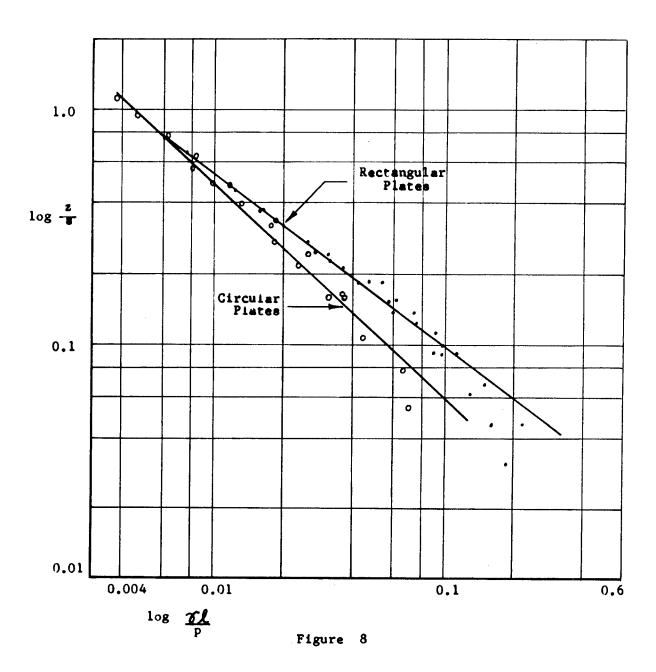


plate. The accuracy of predicting sinkage and the accuracy of predicting work involved in sinking to a given depth were to be investigated.

Assuming that the pressure sinkage (p-z) relationship in soils is governed by the following variables: the circumference of the plate (s), characteristic length of the plate (ℓ) , bulk density of the soil (7), cohesion (c), and angle of internal friction (p), the following functional relationship was obtained for a frictional soil,

$$\frac{z}{s} = f_1 \left(\frac{\gamma \ell}{p}\right) . (\not b) \right] 5.$$

and for a soil having both cohesion and friction,

The above equations were written for a constant rate of penetration and for a semi-infinite soil mass.

Let us first examine Equation 5. According to Equation 5, if one uses plates of several different lengths and circumferences in a cohesionless soil (c = 0, \mathcal{J} = constant, ϕ = constant), then for a given ℓ/p ratio, the z/s ratios must be constant. In other words, z/s versus $\mathcal{I}\ell/p$ curves must collapse. If actual test results support this conclusion, then a new pressure-sinkage relationship can be found involving the above variables which will take plate size effects into account and, no doubt, the equation will be dimensionally constant.

The z/s vs. \mathcal{H}/p relationship was successfully applied to load sinkage data obtained with footing sizes ranging from three to 72 in. in dry sands, a wet sand, and in snow (6). A typical z/s vs. $\mathcal{T}\ell/p$ relationship for wet Ottawa sand having c=0.2, p=30, and $\mathcal{T}=110$ lb./ft. is shown in Figure 7. By applying Equation 5 to soils having a "fair" amount of cohesion, it can be seen that a reasonable collapse of load sinkage data can be achieved. The applicability of Equation 5 covers that range, as it is pointed out in Reference 6, in which the contribution of the cohesive component of the soil is less than 50% of the total bearing capacity.

Figure 7 shows a plot of the load-sinkage data obtained from plates of different sizes in terms of dimensionless parameters. It can be seen that nearly all points are situated along an experimental

curve for plates of a given geometrical shape. Therefore, if the equations of the experimental curves are known, it can be assumed that the load-sinkage relationship under large contact areas can be predicted on the basis of small model tests.

By plotting z/s vs. $\mathcal{T}l/p$ relationships on log-log paper, a well defined straight line function resulted for sands and snows tested. Figure 8 shows the log-log plot of the variables shown in Figure 7. The equation of these straight lines may be described as follows:

$$\log \left(\frac{z}{s}\right) - \log A = m \left(\log \frac{f\ell}{p} - \log B\right) \dots 7.$$

where "A" and "B" are the ordinate and abscissa, respectively, of any point along the straight line and "n" is the slope of the straight line. They are dimensionless constants associated with soil properties and plate geometry.

Eliminating the logs on both sides of Equation 7 and solving for p, one gets

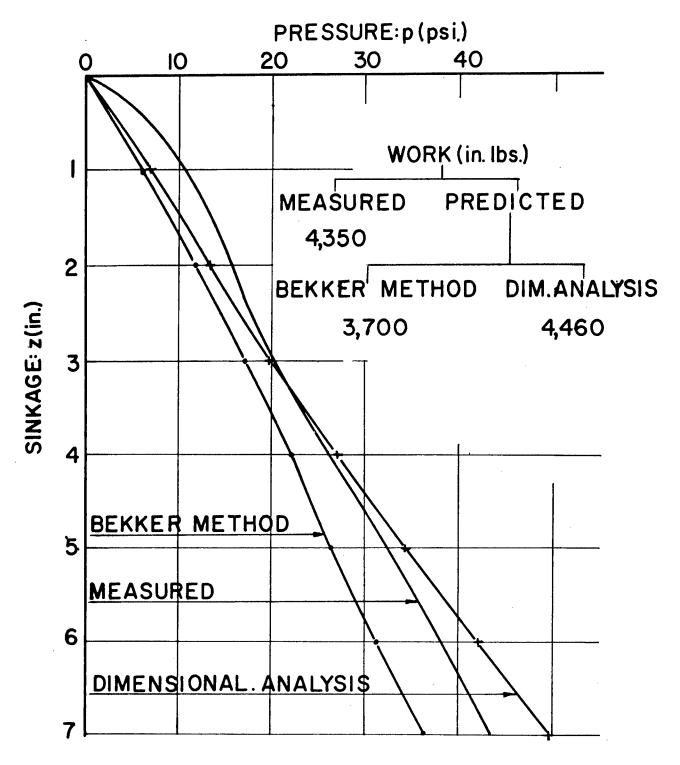
$$p = \frac{\mathcal{S}l}{A^n B} \left(\frac{z}{s}\right)^n \dots 8.$$

where $n = -\frac{1}{m}$

Theoretically, only one load-sinkage curve is necessary for the evaluation of the constants associated with Equation 8, and for the prediction of the load-sinkage behavior of a large loading area from a small plate test. However, the accuracy of such predictions can obviously be improved if data from several plate sinkage tests are averaged when determining the plate sinkage equation.

In order to evaluate the usefulness of the proposed equation, two criteria were investigated: the accuracy of predicting the pressure-sinkage relationship of a prototype plate, using a small plate as a model and the accuracy of predicting the work involved in sinking a prototype plate to a given depth.

One set of data analyzed was obtained by means of circular plates in wet Ottawa sand. A two-inch diameter plate was used as the "model" and the load-sinkage characteristics of the six-inch diameter plate were predicted. The comparison of measured and computed values for the above two criteria is shown in Figure 9. The "dimensional" data produced a more accurate prediction of both sinkage and work of the



COMPARISON OF RELATIONSHIPS FOR THE 6 in. Dia. FOOTING INSATURATED OTTAWA SAND.

Figure 9

circular plate than Equation 1. The analysis of data involving rectangular plates revealed (6), however, that the Bekker approach resulted in a more accurate prediction of p-z relationship, while the dimensional approach produced a better prediction of work.

It is pointed out that Equation 8 does not give a general stress-strain relationship for all plate forms, but only for a constant plate form and variable plate size. That is, a different set of constants, A, B, and n, is associated with each geometrical configuration.

The upper limit for extrapolating model footing data to prototype footings is not known at the present time. Available experimental data (6) show that a 1×4.5 in footing is adequate to predict the load-sinkage behavior of a 4×18 in. footing. The 4×18 in footing has sixteen times greater contact area than the 1×4.5 in footing. Load-sinkage tests with large loading areas at the Land Locomotion Laboratory are expected to answer this problem and, also, what the minimum plate size should be to predict the load-sinkage behavior of a vehicle.

It is clear, from Equation 6, that it is impossible to apply the preceding analysis to cohesive soils without referring to model soils. It is possible to devise a scaled soil but the effort does not appear to justify the result because each natural soil of interest would demand a model soil which would be dependent both on the prototype soil and the scale factor.

Considerable attention has been devoted to the possibilities of scaling plate sinkage in cohesive soils at Ohio State University (8) and at Syracuse University (9). Several dimensionless parameters have been tried for load-sinkage curves obtained with footings of various sizes and shapes. It is not clear yet which are the most significant sinkage and pressure parameters controlling scaling in cohesive soils.

It is suspected, however, that the scaling of plate tests in cohesive soils will not be successful until qualitative similarity of the pressure distribution beneath a plate is obtained. This qualitative similarity has been assumed to exist in most studies to date and is unjustified.

To sum up the status of the load-sinkage problem, the following conclusion is appropriate.

The new load-sinkage relationships resulting from recent investigations either are not general enough to cover most soils, or are not significantly more accurate to warrant the rejection of Bekker's equations. It is, therefore, recommended that until a more significant improvement in load-sinkage description is found, Equation 1 be used for frictional and frictional-cohesive soils. It is recommended that Equation 4 be evaluated for adaptation to purely cohesive soils.

REFERENCES

- 1. Bekker, M. G., "Theory of Land Locomotion", University of Michigan Press, Ann Arbor, Michigan, 1956.
- 2. Reece, A. R., "Curve Fitting Technique in Soil Vehicle Mechanics", Journal of Terramechanics, Vol. 1, No. 2, 1964.
- 3. Reece, A. R., "Problems of Soil Vehicle Mechanics", Land Locomotion Laboratory, Report No. 8470 (LL 97), U.S. Army Tank-Automotive Center, Warren, Michigan, 1964.
- 4. Wills, B. M. D., "Rolling Resistance in Theory and Practice", Journal of Terramechanics, Vol. 1, No. 4, 1965.
- Haley, P. W. and E. Hegedus, "Pressure Sinkage Relationships in in Soils - Part I", Land Locomotion Laboratory, Report No. 82. U. S. Army Tank-Automotive Center, Warren, Michigan, 1963.
- 6. Liston, R. A. and E. Hegedus, "Dimensional Analysis of Load Sinkage Relationships in Soils and Snow", Land Locomotion Laboratory, Report No. 100, U. S. Army Tank-Automotive Center, Warren, Michigan, 1964.
- 7. "First Interim Report on Dynamic Soil Tests", Massachusetts Institute of Technology, Cambridge, Massachusetts, 1959.
- 8. Perloff, W. H., "Study of the Pressure-Penetration Relationship for Model Footings on Cohesive Soil", Progress Report No. 3, submitted to the Land Locomotion Laboratory, U. S. Army Tank-Automotive Center, Warren, Michigan, 1964.
- 9. Li, W. H. and L. J. Goodman, "Plastic Behavior of Soils in the Study of Land Locomotion Problems", Progress Report No. 9, submitted to the Land Locomotion Laboratory, U. S. Army Tank-Automotive Center, Warren, Michigan, 1964.

HORIZONTAL SHEAR IN SOIL VEHICLE MECHANICS

By: Dr. B. M. D. Wills

Coulomb's equation has long been fundamental to all problems of civil engineering soil mechanics which deal with the ultimate strength and failure of soils (1). It was not until 1944, however, that Micklethwaite used a modified form of this equation to predict the maximum tractive effort of a vehicle in soil, and thereby made a highly significant contribution to what is now known as the science of soil-vehicle mechanics (2). According to Micklethwaite, the unit shear strength beneath a vehicle of weight W, and ground contact area A, is given by:

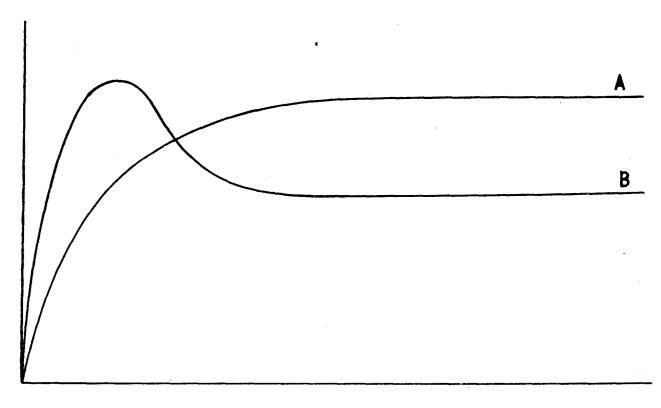
The cohesive component of soil strength is given by the apparent cohesion of the soil, c, which is independent of the normal pressure on the shearing area. The frictional component is a function of the normal pressure and ϕ the angle of internal friction resistance of the soil.

Total shear force or gross tractive effort is given by:

This equation is immediately useful not only in predicting gross tractive effort but also in assessing the relative importance of the cohesive and frictional components of soil shear strength.

Typical soil shear stress deformation curves are shown in Figure 1. Characteristic of all soils is the rapid increase of shear stress to a maximum value at a particular deformation. The overall shape of a curve is determined by the soil type and its physical condition. In general, loose sands and clays will retain their maximum value as shown by curve A, Figure 1. Compacted sands, loams and agricultural top soils sometimes show a peak and then a fall-off to a residual shear stress, curve b, Figure 1. The value of the maximum





Deformation, in.

Figure 1. Experimental Shear Stress/Deformation Curves.

shear stress is also determined by the soil type and its physical condition as well as the normal pressure acting on the area being sheared. Figure 2 shows the effect on shear strength of different normal pressures for one of the soil types shown in Figure 1. The characteristic shapes of the shear stress deformation curves can be obtained with all types of shear tests although the effective size of the sample under test will determine the deformation scale of the curve.

The methods available to the civil engineer for the measurement of soil shear strength may be classified into three types of tests, namely: translational, torsional, and triaxial. The translational or direct shear box test is essentially a linear two-dimensional test on a small and highly confined soil sample. It is a laboratory test best suited for use with sands rather than clay soils because of the difficulty in placing a specimen in the shear box.

Several workers have attempted to measure soil strength by means of torsion shear tests on solid or annular cylindrical specimens (3). The resulting apparatus in each case was extremely complicated and only suitable for laboratory use. The principal advantages of this type of apparatus are that the cross sectional area of the specimen does not change during the test, unlike the translational test, and that it is suitable for measuring displacement. The annular shearing apparatus is superior to the solid cylindrical type in that the angular displacement is much more uniform across the specimen. It is more difficult to prepare the specimen, however, especially for undisturbed soils.

The triaxial shear test is a sophisticated laboratory experiment carried out on a small cylindrical specimen under controlled (axial and radial) external pressures and drainage conditions (4). It offers the most accurate method for the determination of the maximum shearing resistance and the stress strain relationship of the specimen up to failure. Due to the deformation of the specimen, however, it is not suitable for measuring the stress-strain relationship after failure. The triaxial test is more suitable for use with clays than with free running soils due to the difficulty of preparing a specimen. In either case it requires much time and effort to obtain a strength envelope. The excellence of the triaxial test for the civil engineer lies in the ability to subject the specimen to the state of stress and drainage existing at depth in a soil.

It would seem then that the standard methods for measuring the shear strength of soil in civil engineering practice are essentially laboratory experiments carried out on small soil samples, and require undisturbed samples if field conditions are to be reproduced. This is always a difficult and laborious task, and in most cases, it is virtually impossible (5). In soil-vehicle mechanics it is the shear strength of the soil at the surface which is of prime importance, and it is essential in the majority of cases that a shear test be carried out in situ if soil strength parameters are to be related to field conditions. A field test is also almost obligatory in soil-vehicle mechanics because of its convenience and possible speed.

Several attempts have been made to measure soil shear strength in the field by means of the torsion shear test. The shear vane, for example, is principally an instrument for measuring maximum soil shear strength at depth in clay soils, although it may be used on the surface (6). Its use is limited to clays as it can only be used on the soil under field load conditions and is unable to separate the cohesive and frictional components of soil shear strength. The National Institute of Agricultural Engineering (N.I.A.E.) torsion shear box is principally an apparatus for measuring the shear strength of agricultural top soils (5). It can also be used to measure horizontal deformation with either a solid or annular shear box, a large circular scale and a pointer but this makes what is essentially a simple and effective method for measuring the maximum shear strength of soils into a slow, unwieldly and laborious operation. The soil sheargraph is basically the same instrument except that a very small shear head is used. The normal load is applied by hand and the shear strength is recorded directly (7).

The foregoing tests are primarily concerned with the measurement of maximum shear strength and can be used together with Micklethwaite's equation to predict maximum gross tractive effort. Maximum shear stress is only developed, however, after a certain deformation, which depends on the soil condition and sample size, Figure 2. Micklethwaite's equation, therefore, which is based on the assumption that maximum shear stress is developed immediately with deformation will always over-estimate gross tractive effort. The equation also has a rather limited use as it can only predict one particular set of performance conditions, albeit important ones, rather than an overall performance curve.

Bekker was the first to realize the importance of the soil shear stress-deformation relationship in the prediction of the overall performance curve of a vehicle (8). He suggested that the shear test could be used as a model of the soil shear strength-deformation characteristics beneath a slipping wheel or track, and adapted the torsion shear test for field use in this respect. He used an annular shear head with grousers attached which rested on the soil; thus,

requiring no excavation and through which a torque could be applied to the soil under different normal loads. An annulus was used in preference to a length of rigid track because it avoided any bulldozing effect and lent itself to simpler apparatus and speedier operation. By using the apparatus in the field in this way soil strength and deformation parameters pertinent to vehicle performance can be measured.

The mode of horizontal soil deformation in a shear test is quite different to that beneath a slipping wheel or track. In the former the deformation is the same throughout the shearing area and is always equal to the displacement of the shear plate. In the latter, the deformation increases from zero at the front end of the contact area to a maximum value at the back, and is dependent on the slip rate of the vehicle. Slip, i, can be defined as the ratio of horizontal deformation, j, to the distance, x, a vehicle would travel without slip during the same time interval. Soil deformation can then be expressed by:

This equation expresses the fact that deformation increases linearly along the length of the ground contact area and is directly proportional to slip. It can be seen that the shear stress-deformation curve obtained with the shear annulus is equivalent, as regards the deformation scale, to that obtained beneath a vehicle at 100% slip, as the deformation is then equal to the movement of the shearing area in both cases.

Equation 2 expresses gross tractive effort as a function of ground contact area and shear stress, which is assumed to be constant in this particular case. When the shear stress is variable, the gross tractive effort is obtained by summing the forces on the elementary shearing areas over the length, ℓ , and width, b, of the contact area where:

$$H = b \int_{0}^{\ell} s dx \qquad \dots \qquad \dots$$

It is evident from Equations 4 and 5 that gross tractive effort can be evaluated over the full range of slip values by using experimental shear stress deformation values. This can be done either by graphical integration of the experimental curve or by the quicker and more convenient method of expressing the experimental curve mathematically in terms of shear stress and horizontal deformation.

Bekker proposed a general equation to describe all the possible forms of the experimental shear stress deformation curve. He did this empirically by adapting an equation relating the displacement and natural frequency of an aperiodic vibration which gave the required form of curve. The equation relates soil shear strength to soil deformation in terms of the two soil strength parameters, the normal pressure, p, and soil deformation constants $\rm K_1$ and $\rm K_2$. Therefore,

$$s = (c + p tan p) \left[\frac{e^{(-K_2 + \sqrt{K_2^2 - 1})K_{1j}}}{Y_{max}} \right]$$

$$- \frac{e^{(-K_2 - \sqrt{K_2^2 - 1})K_{1j}}}{Y_{max}} \right]$$

where Y_{max} is the maximum value of the exponential function shown within the brackets obtained by substituting, j_{opt} , the deformation value at the point of maximum shear stress.

To express an experimental curve in the above form, it is first necessary to evaluate the strength parameters c, ϕ and deformation parameters K_1 and K_2 . The strength parameters can be obtained in the usual way, without any recourse to Equation 6, by obtaining maximum shear values at several normal pressures and plotting one set of values against the other. The shape of the theoretical curve is determined by the values of the deformation parameters K_1 and K_2 . By comparing an experimental curve with a family of theoretical curves covering a wide range of K values it is possible to pick out particular values of K_1 and K_2 which describe the experimental curve.

In the present state of soil vehicle mechanics, net tractive effort or drawbar-pull can only be obtained by subtracting motion resistance from gross tractive effort:

$$DP = H - R$$
 7

Any comparison between experimental and predicted performance must necessarily evaluate both gross tractive effort and motion resistance together. The two can not be separated other than by using the measured towed rolling resistance and assuming it to be equal to the rolling resistance in the driven case and to be independent of slip. It should be noted, however, that only the prediction of gross tractive

effort is dealt with here. Bekker's soil value system is comprehensive in that it also includes the prediction of rolling resistance and consequently by means of Equation 7, vehicle field performance. With the above limitations it can only be said that Bekker's overall theory was shown to give reasonable accuracy on soil and snow for tracks but a much lower accuracy for wheels $(9,\ 10)$. It was found that Equation 6 did not describe the experimental curves too well and that it was difficult to obtain accurate K values from the experimental shear stress-deformation curves. This was especially so when the experimental curves showed no noticeable peak and the K_2 values were of a high order (11). A more precise but also a much more complicated method of measuring K values was suggested later by Sela (12).

Most of the work carried out in this field since Bekker first proposed his soil value system has been based on his original concepts of the shear test model and the kinematics of deformation. Indeed, the same type of apparatus introduced by Bekker is still used widely today (13, 14). The more recent work has attempted to obtain greater accuracy and added convenience, both theoretical and practical, by proposing new equations, although none so general as Bekker's, to describe the shear stress deformation curve.

Since Bekker's equation was proposed, it has been found that a great many soils do not peak in their shear stress deformation curve, curve A, Figure 1, In the instances where a peak does occur it can usually be neglected with negligible loss in accuracy. A much simpler experimental equation was thus proposed by Janosi and Hanamoto which only involved the two strength parameters and one deformation constant K, where soil shear stress is given by:

This equation is much easier to manipulate in the integration required to obtain gross tractive effort, and is used widely today in place of Equation 6 (11).

Two problems must be faced if the experimental shear stress-deformation curve is to be described by a theoretical equation. The accuracy of the theoretical equation must first be established, and some method of measuring the required deformation constants from the experimental curves must be decided upon.

One of the important characteristics common to Equations 6 and 8 is that maximum shear stress is reached at a constant optimum deformation, independent of the value of the normal pressure. In the case of Equation 8 where the shear stress only tends towards its

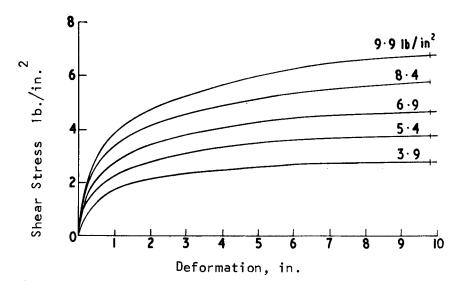


Figure 2. Shear Stress/Deformation Curves for Several Normal Pressures.

maximum value, it is more correct to say that the percentage of the maximum shear stress at any particular deformation is independent of the normal pressure. In the same instance, the use of a characteristic deformation, j_c , at which the shear stress is, say, 95% of its maximum value would be more realistic than the optimum deformation used in Equation 6. This deformation characteristic can be seen graphically in Figure 3, or can be appreciated theoretically by expressing Equation 8 in the form shown below:

It was noticed by several workers that experimental shear stressdeformation curves did not behave in this manner but showed an increasing characteristic deformation with increasing normal pressure (11, 15), Figure 2. Reece proposed a modification of Equation 8 to account for this, expressing the exponent as a function of normal pressure where:

This equation was suggested by the results obtained from a limited number of experiments with a model tracklayer on loose sand (15). The form of a family of curves described by this equation is shown in Figure 4.

Later sand experiments showed that neither Equation 8 or 10 would accurately describe the experimental shear stress-deformation curves (16). A family of such curves is shown in Figure 2. It can be seen that the curves do not have a constant $j_{\rm C}$ value as suggested by Figure 3, nor are they of the form shown in Figure 4. When plotted in the form shown in Figure 5, they do not collapse onto a single curve as would values described by Equation 8, nor do they show such a variation with normal pressure as would values described by Equation 10. The experimental curves show a gradual movement down and to the right, with increasing normal pressure. If they are to be described by an exponential equation of the form of Equation 8 then K cannot be taken as a soil constant but must be expressed as a function of some other soil parameter.

The form of the experimental curves may be explained by the fact that the volume of the specimen, or the volume of soil affected in a shear test, is important in determining deformation characteristics. The deformation that takes place at the soil surface beneath a shearing

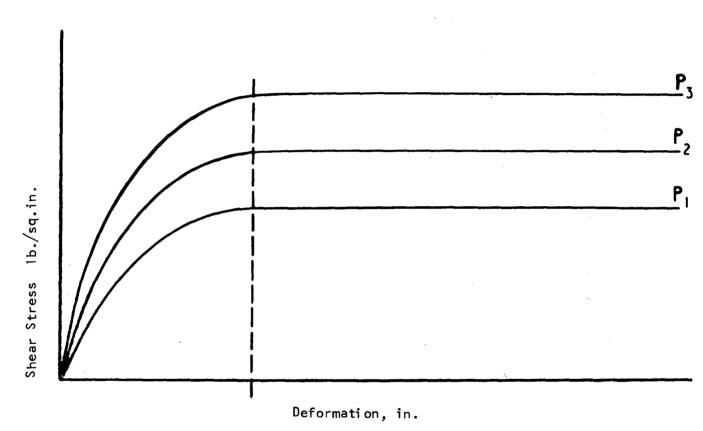


Figure 3. Shear Stress/Deformation Curves According to the Simplified Bekker Equation.

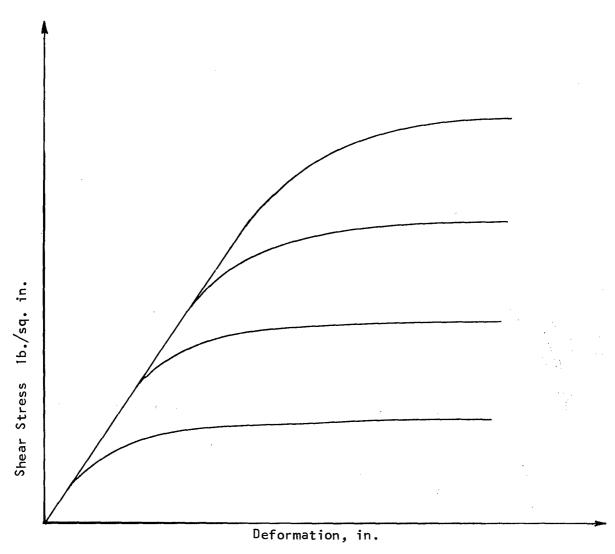
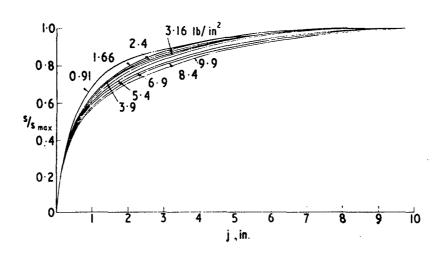


Figure 4. Shear Stress/Deformation Curves According to the Reece Equation.



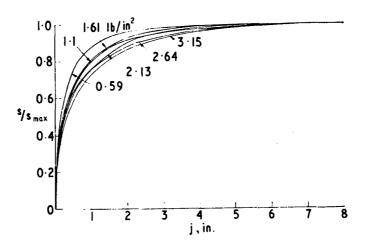


Figure 5. Theoretical Shear Stress/Deformation Curves for 8-3/4 in. Annulus (top) and 7 x 28 in. Rigid Track (bottom).

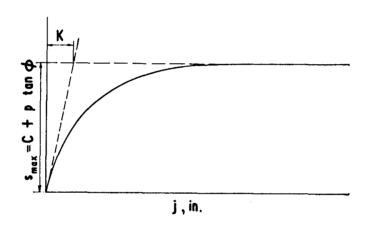


Figure 6. Determination of the Deformation Modulus after Janosi and Hanamoto.

area, before the soil strength is fully mobilized, is the sum of the deformation to failure over the effective depth of the sample and will be proportional to that depth. As the normal pressure increases, so will the effective depth of the sample with a resulting increase in the value of j_c . The translational shear box provides an excellent example in that it uses a very small sample depth and the values of j_c obtained over a wide pressure range are never more than small fractional parts of an inch.

Despite this discrepancy between theory and practice, results obtained by Janosi and Hanamoto with model crawler tractors on a farm soil and on a sand further demonstrated the utility of the semiempirical approach (11).

Gross tractive effort was obtained by substituting Equation 8 into Equation 5 when: ρ

$$H = b \int_{0}^{c} (c + p \tan \phi)(1 - e) dx$$

From Equation 4:
$$j = i_0 x$$

$$\therefore H = b(c + p \tan \phi) \left[\ell + \frac{K}{i} (e^{-i_0 \ell/K} - 1) \right] \qquad \quad 10a$$

Net tractive effort was then obtained by calculating rolling resistance values according to the Bekker theory and evaluating Equation 7. Although reasonable accuracy was obtained between experimental results and the predicted band, it is thought that the method used in determining the deformation modulus was somewhat inadequate.

Janosi and Hanamoto showed that the slope of the tangent at the origin of the shear stress deformation curve is given by differentiating Equation 8 with respect to deformation, j, and equating j to zero.

The value of K is then obtained by drawing a tangent at the origin of the experimental curve and measuring off the horizontal intercept as shown in Figure 6. It was argued by Reece that this method of obtaining K only made use of a small part of the experimental curve and then at the origin where accurate measurement is extremely difficult (11). He proposed an alternative method to make use of the full experimental

curve. Re-writing Equation 8 and expressing it logarithmically,

$$\log(1-\frac{s}{s_{\text{max}}}) = -\frac{j}{K}$$

When plotted on log-linear coordinates, this is the equation of a straight line of slope - 1/K. The experimental value of K can thus be obtained by plotting values from the experimental curve in the above form and measuring the slope of the curve, Figure 7.

Recent work carried out on loose sand has shown that the experimental shear stress-deformation curve can be far from that of the exponential form described by Equation 8 (16). It was pointed out that the determination of -K value by the tangent method can only be accurate if the experimental curve is exponential in form or close to being so over its full range. Even then, the drawing of a tangent at the origin of an experimental curve is extremely difficult and can lead to great inaccuracy. It was also shown that the logarithmic method was equally inadequate in such a case when the experimental curves are far from being exponential. Although reasonable linearity is obtained from the experimental results around the origin and lower values, Figure 7, it can be seen that taking the whole curve, which is the supposed advantage of this method, results in a large departure from linearity and the problem of determining an average K value still remains. The conclusion drawn was that the only useful method remaining

was one of visual comparison of the experimental curve with a family of theoretical curves, Figure 8. Although this method is dependent on personal judgement, it is no more so than the other methods cited. It does, however, allow for the assessment of an average K value over the full shear stress deformation curve without any distortion.

In Figure 8 experimental curves obtained with a torsion shear annulus and a linear shear track plate are compared with a family of theoretical curves and the designated K values shown. The K values obtained by the tangent method for these curves, although not shown, were 1/4 and 1/2 for the annulus and track respectively. The semilogarithmic method in this case is no different from the visual comparison method other than it is more difficult to apply due to logarithmic distortion of the scale. The accuracy of these curve fitting methods may be judged by comparing the predicted performance curves with that obtained by graphical integration of the shear stress deformation curve. This has been done for both the annulus and the track, Figure 9.

There is excellent agreement between the datum curves and the visual comparison curves in all cases.

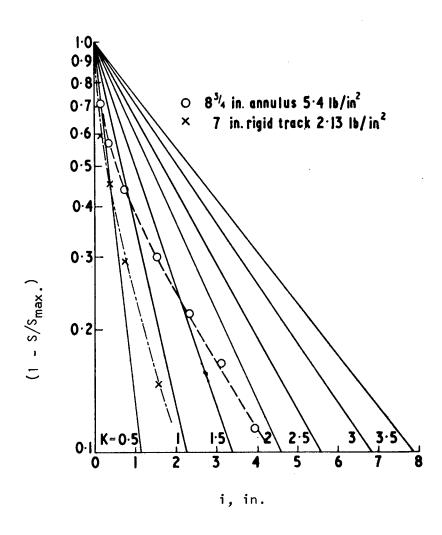
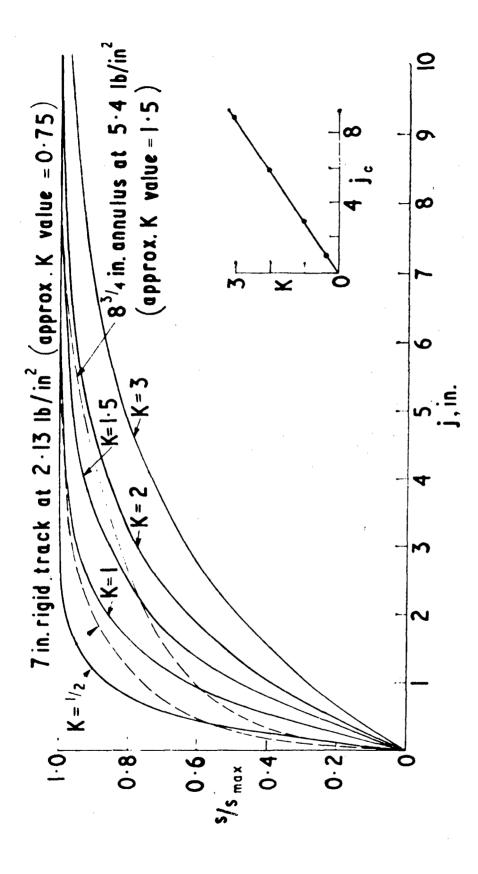
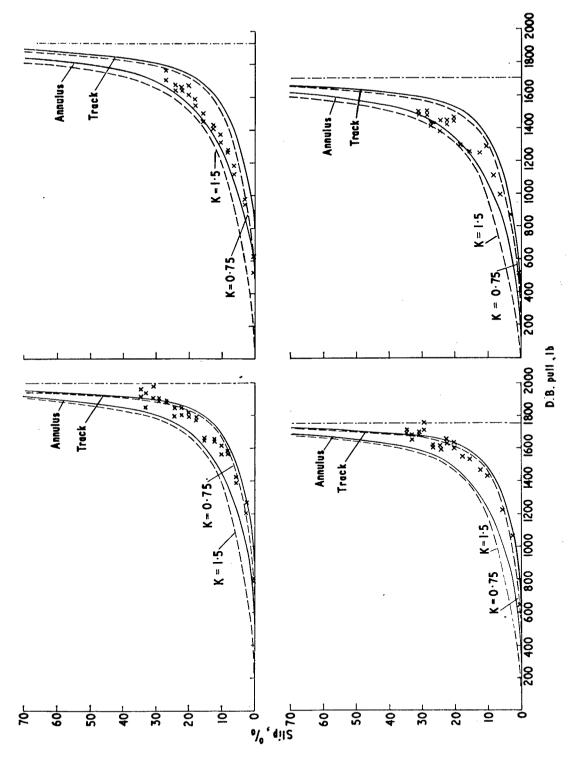


Figure 7. Determination of the Deformation Modulus $% \left(1\right) =\left(1\right) +\left(1\right)$



Comparison of Experimental Shear Stress/Deformation Curves with Exponential Curves of the Form Figure 8:



(Full lines) Annulus or Rigid Track Integration; (Broken lines) Simplified Bekker Equation; (Chain dotted lines) Micklethwaite Equation. Measured (points) and Predicted Performance of Full Length, 50" crs., (left) and 3/4 length tracks (right). (Top) 10 in. wide; (Bottom) 7 in. wide. Figure 9.

The predicted curves obtained by using the tangent method, K values would obviously be highly inaccurate for both the annulus and the track. Despite the accuracy of the visual method, even in the extreme cases cited above, it should be remembered that it is still wholly dependent upon personal judgement and is in no way different from the other methods except in degree.

The development of curve fitting techniques, similar to that suggested by Reece for pressure sinkage curves, where the personal element is completely removed, is urgently required (17).

The performance curves shown in Figure 9 would also appear to give further proof of the validity of Bekker's basic theory when applied to full size tracks. It should be remembered, however, that no attempt was made to estimate rolling resistance in this case. The predicted drawbar-pull curves were obtained from theoretical gross tractive effort values by means of the somewhat dubious assumption that the measured towed rolling resistance was independent of slip.

In the most recent work on this subject, Reece analysed the errors involved in the use of the normal torsion shear annulus and questioned the unqualified suitability of this test in the prediction of vehicle performance (17). He pointed out that the current method of using the shear annulus neglected the effect of side wall shear and drag and demonstrated by qualitative analysis that the shear annulus can often become an extremely crude apparatus in such a case. Side wall shear can be substantially reduced by decreasing the side wall area of the annulus by using shorter grousers on the nominal shearing area. The remaining error in the calculation of c and p can then be allowed for by a method suggested by Reece.

The effect of drag can be compensated for in sands by unloading the shearing area and measuring the torque required to turn the shear head. This would not be possible in clay. In such a case, the sinkage of the annulus is usually small and the drag is unimportant. On composite soils such as loams, however, where there is likely to be appreciable sinkage, the effect of drag can become highly significant, if c and p are to be measured accurately. Unfortunately there seems to be no ready way of measuring it under these conditions.

To overcome this problem and to enhance the accuracy of the shear annulus in general, Reece suggested a new type of shear head to minimize side wall and drag effects, Figure 10. The grousered shear ring A is supported from the main loading cylinder B through strain gauged cantilevers which measure the torque on the shear ring. Rubber sealing rings D bonded to the steel parts on their top and

bottom surfaces must accommodate relative movement but not transmit any appreciable force or torque.

In this way the drag is not included in the measured torque and the side wall stresses can be kept small by reducing the side wall area to a minimum.

Reece indicated that Coulomb's equation, although fundamental to soil vehicle mechanics, would seem to be inadequate in that drainage and pore water pressure effects are neglected, There is no time dependent term, and it is two dimensional in form. He pointed out, however, that the drainage problem is not as formidable as it first appears, as work on clay is normally carried out with full pore pressure and the quick undrained triaxial test is appropriate. On sand, where there is no confining head, the simple drained test is suitable. Difficulties arise, however, on composite soils such as loams and silts where test conditions somewhere between undrained and drained are required. In such a case some allowance should be made for the effective stresses being a function of vehicle speed.

The effect of rate of shearing has usually been ignored in the field of soil vehicle mechanics. Shear tests developed by the civil engineer, with shearing rates of the order of .001 inch per second, for work concerned with the long term slow deformations of the soil under foundations have been used without modification to predict the performance of ground drive equipment, with shearing rates as high as 200 inches per second. It was suggested that all shear tests be run at the same shear rate and that this should be of the same order as that developed by vehicles in the field.

Although the problems encountered in soil vehicle mechanics are almost always three dimensional in form, they are invariably resolved by means of plane strain theories. The difference between plane and three dimensional strain is evidenced in practice by the lateral flow of the soil and can best be explained in theory in terms of the magnitude of the third or intermediate principal stress. Several workers have indicated that ϕ may be dependent on the value of the intermediate principal stress and that an increase of approximately 10% in the value of p is possible between triaxial and plane strain conditions (18, 19, 20). The experimental curves shown in Figure 5 indicate that deformation characteristics are also dependent on the lateral flow conditions peculiar to the type of shear test and can result in appreciable variation in the prediction of vehicle performance, Figure 9. This is obviously a serious problem which may have a profound effect on current traction theories and, therefore, requires immediate investigation. Reece has pointed out that although a plane stress condition exists beneath a vertically loaded plate, this quickly changes to a triaxial condition when a horizontal load is applied. He has suggested that the problem could be clarified if it were possible to accurately

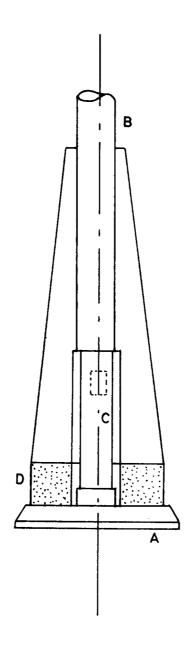


Figure 10. Improved Design of Annular Shear Device After Reece.

describe the state of stress beneath a shear plate under slip-sinkage conditions (17).

It has been shown that the Bekker shear stress deformation theory is a reasonable model of tractive vehicle performance and should provide a sound foundation upon which future improvements in this field can be made. Although much work has been carried out to test these theories, it has been sporadic in nature, confined to full size and model vehicles and restricted to certain soil types.

It is often necessary to make use of a theory as soon as it is shown to be workable rather than to await the outcome of rigorous Even so, evaluation. it is felt that the latter should not be neglected but that it should be carried out so that eventually it will give a more accurate evaluation and a better understanding of the scope and limitations of the theory in question. Although the ultimate object of work in this field is the prediction of vehicle performance, the use of a vehicle in the first place to evaluate theoretical work pertaining to a particular type of ground drive unit will tend to obscure the issue and will result in an indirect and possibly inaccurate assessment. A comprehensive series of tests should therefore be carried out under controlled conditions using a representative range of ground drive equipment with special purpose testing machines on a full range of soil types and for all important conditions of each type. A theory, thus evaluated, can then be used to predict the performance of a vehicle. Problems pertinent to and characteristic of each vehicle type will need to be considered in the light of any modifying effect on the theory. It can then be evaluated for the whole vehicle by means of vehicle tests in the field.

Future work in this field should attempt to describe the effect of lateral flow in determining shear strength and deformation moduli for different modes of shearing and for various sizes and shapes of shearing area. It has been suggested that this could be done by means of a slip-sinkage theory. This would result in the added advantage of being able to express rolling resistance as a function of slip, thus allowing for more accurate and separate evaluations of traction and rolling resistance theories. The shearing rate of all types of shear test used in soil vehicle mechanics should be standardized at a realistic value comparable to that occurring beneath a vehicle, and the effect of rate of shearing should be investigated. Ultimately, when sufficient knowledge and experience has been accumulated, it should be possible to formulate a traction theory in terms of the fundamental properties of the soil (21, 22).

FIGURES

No.

- 1. Experimental Shear Stress/Deformation Curves.
- Shear Stress/Deformation Curves for Several Normal Pressures.
- Shear Stress/Deformation Curves According to the Simplified Bekker Equation.
- 4. Shear Stress/Deformation Curves According to the Reece Equation.
- 5. Theoretical Shear Stress/Deformation Curves for 8-3/4 in Annulus (top), and 7×28 in Rigid Track (bottom).
- 6. Determination of the Deformation Modulus After Janosi and Hanamoto.
- 7. Determination of the Deformation Modulus After Reece.
- 8. Comparison of Experimental Shear Stress/Deformation Curves with Exponential Curves of the Form: -x/K v = 1 2
- 9. Measured (points) and Predicted Performance of Full Length, 50" crs., left, and 3/4 length tracks (right). Top: 10 in. Wide. Bottom: 7 in. Wide.
- 10. Improved Design of Annular Shear Device After Reece.

BIBLIOGRAPHY

- 1. Terzaghi, K., "Theoretical Soil Mechanics", John Wiley, New York, 1956.
- Micklethwaite, E. W. E., 'Woil Mechanics in Relation to Fighting Vehicles", Military College of Science, Chertsey, 1944.
- 3. Hvorslev, M. J., "Torsion Shear Tests and Their Place in the Determination of the Shearing Resistance of Soils", Symposium on Shear Testing of Soils, Proc. Am. Soc. for Testing Materials, 1939.
- 4. Bishop, A. W. and Henkel, D. J., "The Measurement of Soil Properties in the Triaxial Test", Edward Arnold. London, 1957.
- 5. Fountain, E. R., and Payne, P. D. J., "The Shear Strength of Top Soils", N.I.A.E. Tech. Memo. No. 42, 1951.
- 6. Evans, I., and Sherratt, G. G., "A Simple and Convenient Instrument for Measuring the Shearing Resistance of Clay Soils". Sci. Instrum. 25 (12), 1948.
- 7. Cohron, G. T., "The Soil Sheargraph", A.S.A.E. Paper No. 62-133.
 Washington Meeting, June, 1962.
- 8. Bekker, M. G., 'Theory of Land Locomotion', (The Mechanics of Vehicle Mobility). University of Michigan Press, Ann Arbor, Michigan, 1956.
- 9. Harrison, W. L., "Analytical Prediction of Performance for Full Size and Small Scale Model Vehicles". Proc. 1st International Conference of Mech. Soil-Vehicle Systems, Turin, 1961.
- 10. Weiss, S. J., et al, "Preliminary Study of Snow Values Related to Vehicle Performance", Land Locomotion Laboratory, Detroit Arsenal, 1962.
- 11. Janosi, Z., and Hanamoto, B., "The Analytical Determination of Drawbar-Pull as a Function of Slip for Tracked Vehicles in Deformable Soils", Proc. 1st Int. Conf. Mech. Soil-Vehicle Systems, Turin, 1961.

- 12. Sela, A. D., "On Slip and Tractive Effort", Proc. 1st. Int. Conf. Mech. Soil-Vehicle Systems, Turin, 1961.
- 13. Wills, B. M. D., "A Hydraulic Bevameter", Journal of Terramechanics, Vol. 1, No. 1, 1964.
- 14. Spansky, Paul, ''Portable Soil Testing Devices', U. S. Army Tank-Automotive Center, 1965.
- 15. Reece, A. R., and Adams, J., "An Aspect of Tracklayer Performance", A.S.A.E. Paper No. 62-623, Winter Meeting, Chicago, 1962.
- 16. Wills, B. M. D., "The Measurement of Soil Strength and Deformation Moduli and a Comparison of the Actual and Theoretical Performance of a Family of Rigid Tracks", Journal of Agricultural Engineering Research, Vol. 8, No. 2, 1963.
- 17. Reece, A. R., "Problems of Soil Vehicle Mechanics", Land Locomotion Laboratory, U. S. Army Tank Automotive Center, Warren, Michigan, Report No. 97, 1964.
- 18. Meyerhof, G. G., "Discussion of Variation in Bearing Capacity Factors with Shape and Influence of Strength in Triaxial and Plane Strain Tests", Proc. 5th Int. Conf. Soil Mech. Found. Eng., Paris, Vol. 3, 1961.
- 19. Kirkpatrick, W. M., "The Condition of Failure for Sand", Proc. 4th Int. Conf. Soil Mech. Found. Eng., London, Vol. 1, 1957.
- 20. Haythornthwaite, R. M., "Stress and Strain in Soils", Reprint from, "Plasticity", Pergamon Press.
- 21. Rowe, P. W., "Stress Dilatancy, Earth Pressures and Slopes", Journal of Soil Mech. and Found. Div., A.S.C.E. May, 1963.
- 22. Roscoe, K. H., Schofield, A. N., and Wroth, C. P., 'On the Yielding of Soils', Geotechnique, Vol. 8, No. 1, March, 1958.

VEHICLE RIDE CHARACTERISTICS

By: B. Hanamoto

The research problem in investigating travel over rough, hard, off-road terrain is one of describing the motion of vehicles and ensuing vibrational effects on vehicle components, occupants, and cargo. The study of vehicle ride characteristics resolves into: investigating the hard-ground profile as inputs to a vehicle suspension system; investigating the dynamic response of the vehicle; investigating the resulting motion within and on the vehicle for its detrimental effects on human occupants, cargo, and vehicle components. The study can be separated into three distinct but interrelated phases: description of hard-ground profile; description of vehicle response using the description of hard-ground profile as inputs; and the description of resulting ride in terms of roughness for the human occupants or in terms of its harmful effects on vehicle components and cargo.

The ultimate goal of the research endeavor is to develop a design procedure whereby off-road vehicle speeds are increased in traveling over hard terrain. It is envisioned that a vehicle designer, knowing the roughness characteristics of the terrain to be traversed and the tolerable roughness criterion which must be satisfied, can (by means of analytical methods) design the vehicle suspension system so that the dynamic response of the vehicle meets the demands of the roughness criterion. The designer then may optimize the vehicle suspension system parameters so that the vehicle response motions meet specified requirements.

A military vehicle operating off-road encounters two types of hard-ground roughness: obstacle-type roughness such as trees, stream beds, deep gulleys, large rocks, abrupt hills and stable-ground roughness, defined as the variation in elevation where influence on vehicle dynamics remains reasonably constant over distance and is free of obstacles (1). The latter type of hard-ground roughness is the one where attention has been focused.

A quantitative description of stable-ground roughness was the first requirement in this study. It became apparent that, due to the random nature of profile elevation vs. horizontal distance, deterministic characterization of roughness was impossible. Instead, statistical techniques would have to be employed.

The power spectral density (psd) description is the statistical method adopted to quantitatively characterize stable hard-ground roughness. Description of environmental roughness in terms of the

psd have been employed successfully to characterize the roughness of the sea, atmospheric turbulence and airport runways. These descriptions have proven useful to the designer of ships and aircrafts. The usefulness of the psd approach by the land vehicle designer is one of the points to be proven by the vehicle ride characteristics studies. These studies are being conducted for the Land Locomotion Laboratory by the Midwest Applied Science Corporation of West Lafayette, Indiana, primarily by Drs. Bogdanoff, Kozin and Cote.

ONE-DIMENSIONAL POWER SPECTRAL DENSITIES

OF HARD GROUND ROUGHNESS (Ref. 1).

The effect of terrain roughness on the vibration characteristics of a vehicle traveling over it is a problem of a random function used as inputs to a linear or nearly linear system and the effects on the output of the system. Its effects in such problems can be separated into the sum of effects due to frequency components. The profile heights, $h(x_i)$, on the path of a vehicle will be a function of the distance, x, along the path. The roughness of the profile will depend upon the variation of $h(x_i)$ about some medial "smoothed" terrain.

Since our concern is with the profile height variations that are responsible for producing vehicle vibration, long gradual hills must be flattened or "smoothed" so that the roughness, other than hills, is of a uniform character and the mathematical assumption of stationarity for the profile of ground heights may be satisfied.

Two methods of smoothing the profile have been used. One method consists of constructing a smooth profile by fitting paraboloids to segments of the data. This method consists of fitting second degree polynomials, H(x), to the data points $h(x_i)$. Smoothing is accomplished by taking deviations of the profile heights from heights of the polynomials fitted to the segments of the data. The actual profile may be imagined as variations about the joined parabolic curves for all the segments of the data. A parabola can remove only one hill from each segment so that when hilly ground is encountered, the number of segments will have to be increased. It was found that for hilly ground smoothed with many segments, steps occurred where the segments came together. At times, the magnitude of the steps compared to the profile height variation about the fitted curve was such that the resulting spectra were affected. Therefore, parabolic smoothing was considered appropriate when the curves fit closely but stronger smoothing was needed on hilly ground. The second method of smoothing consists of the running average type. Parabolic trends are removed. by the selection of specified coefficients. A theoretical discussion of the effects of this type of smoothing is presented in Reference 1.

The smoothed variations in profile heights for a line were first considered. Denote the deviations of the profile heights by $^{\bullet}$ d(x). These will average zero and their variations is what we mean by roughness. As a simplification of separation into frequency components, we might have

$$d(x) = \sum_{k=0}^{M} (a_k \sin^{\omega} k + b_k \cos^{\omega} k^{2}) \dots 1.1$$

Because it is unrealistic to consider that only a few frequencies are present as in Equation 1.1, we should admit all frequencies each in an infinitestimal amount. Here, however, the fact of randomness complicates matters. By random we mean that d(x) may turn out to be any one of an ensemble of functions. We have no hope of determining which one but we can determine or estimate some ensemble averages. How to deal with infinitestimal random quantities in the case of continuous frequencies presents a special problem in probability theory which will not be discussed here. It can be stated that the unrealistic, fixed frequency case converges to the realistic case. If d(x) with fixed frequencies is random, then the coefficients \mathbf{a}_k , \mathbf{b}_k must be random. This is no restriction, for we can assume that all possible frequencies are represented by the ω 's and that their absence or presence is determined by the zero coefficients.

If Equation 1.1 is written in the exponential form of the trigonometric series and if the ω_k are given for k = 0,1, 2, -, M and ω_0 = 0, then

$$d(x) = \sum_{k=-M}^{\infty} c_{k} c_{k}$$

$$c = \sum_{k=-M}^{\infty} c_{k} c_{k}$$

Note that d(x) is real because the complex terms drop out due to the change in limits. The exponential form is introduced for ease of manipulation.

where

$$\mathbf{a}_{k}^{k} = \frac{1}{2}(b_{k} - ia_{k}), \quad k > 0$$

$$\mathbf{a}_{-k}^{k} = \mathbf{a}_{k}^{k} = \frac{1}{2}(b_{k} + ia_{k}), \quad k > 0$$

$$\mathbf{A}_{o} = \mathbf{b}_{o}$$

and the asterick denotes conjugate.

We assume two main properties for the randomness of d(x). The first is that the ensemble average at any point is zero. From the linear property of the expected value (ensemble average) operation,

$$E\left[d(x)\right] = \sum_{k}^{\Sigma} E\left[d_{k}\right] e^{i\omega_{k} \times x} = 0 \dots 1.3$$

The series above, being identically zero as a function of x, must have zero coefficients, i.e.,

Our second assumption is that of stationarity. A consequence of the assumption is that any expected value of the d's must remain unchanged for different placements of the origin of x. In particular, the following does not depend on x:

$$E \left[d(x+s) \ d(x) \right] = E \left[\sum_{k=j}^{\Sigma} \alpha_{k} \alpha_{j}^{*} \right] e^{i \omega_{k} (x+s) - i \omega_{j}^{\omega} x}$$

$$= \sum_{k=j}^{\Sigma} E \left[\alpha_{k} \alpha_{j}^{*} \right] e^{i (\omega_{k} - \omega_{j}) x} e^{i \omega_{k} s}$$

$$= \sum_{k=j}^{\infty} E \left[\alpha_{k} \alpha_{j}^{*} \right] e^{i (\omega_{k} - \omega_{j}) x} e^{i \omega_{k} s}$$

$$= \sum_{k=j}^{\infty} E \left[\alpha_{k} \alpha_{j}^{*} \right] e^{i (\omega_{k} - \omega_{j}) x} e^{i \omega_{k} s}$$

In this expression we have made use of the fact that $d(x) = d^{k}(x)$ for convenience, i.e.,

$$d(x) = \sum_{k = -M}^{\infty} c^{i \omega} c^{k x}$$

$$= \sum_{k = -M}^{\infty} c^{k - i \omega} c^{k x}$$

$$= \sum_{k = -M}^{\infty} c^{k - i \omega} c^{k x}$$

$$= c^{*}(x)$$

The series on the right in Equation 1.4, which must be identically constant for all x, falls into two parts:

$$\sum_{k} E \left[\alpha_{k} \alpha_{k}^{*} \right] e^{i\omega_{k} s} + \sum_{k \neq j} E \left[\alpha_{k} \alpha_{j}^{*} e^{i(\omega_{k} - \omega_{j})x + i\omega_{k} s} \right]$$

If the $\omega_{\vec{k}}$ are all different, which we may assume from the start, the second series must be identically constant as a function of x, hence its coefficients must be zero,

$$E\begin{bmatrix} x & x \\ k & i \end{bmatrix} = 0 \quad k \neq j$$

Thus if d(x) is stationary, it is necessary that the complex coefficients be mutually uncorrelated. In this case

$$E\left[d(x+s)\ d(x)\right] = R(s) = \sum_{k}^{\infty} E\left[\alpha_{k}^{\alpha} \alpha_{k}^{*}\right] e^{i \alpha_{k}^{\alpha} s} ... 1.5$$

R(s) is called the <u>covariance function</u> of d(x).

Changing the form of Equation 1.1,

where
$$A_{k} = \sqrt{\frac{2}{a_{k}} + b_{k}}$$

$$A_{k} = \sqrt{\frac{2}{a_{k}} + b_{k}}$$

$$A_{k} = \sqrt{\frac{1}{a_{k}} + b_{k}}$$

Then
$$\left| \alpha_{k}^{2} \right|^{2} = \alpha_{k}^{2} \alpha_{k}^{2} = \frac{1}{4} \left(a_{k}^{2} + b_{k}^{2} \right) = \frac{1}{4} A_{k}^{2}$$
 (Taking $A_{k} = A_{k}$)
$$\left| \alpha_{0}^{2} \right|^{2} = \alpha_{0}^{2} = A_{0}^{2}$$

The various A_k 's arranged according to the sizes of the $^{\omega}$'s form what is called the <u>frequency spectrum</u>. Their sizes give the amounts of the frequencies present. For a continuum of frequencies this concept becomes that of a spectral density. This gives the important relationship

$$R(s) = E \left[A_0^2\right] + \sum_{\substack{k = -M \\ \neq 0}}^{M} E \left[\frac{1}{4} A_k^2\right] e^{i \omega_k s} ...1.6$$

which links the covariance function with the spectrum. Note that the components are all in phase so that

$$R(s) = E\left[A_0^2\right] + \frac{1}{2}\sum_{k=1}^{M} E\left[A_k^2\right] \cos \omega_k s \qquad ... 1.6$$

Therefore R(o) is a maximum (positive) value of R(s). The coefficients in the trigonometric series are ensemble averages and are possible to know or estimate. When the coefficients are arranged in order of the sizes of the ω_k 's, they form what is called the power spectrum of the random function d(x).

To interpret the power spectrum, imagine that the frequency values $\omega_{\bf k}$ are very close together. We have from Equation 1.6 that

$$R(o) = E \left[A_o^2\right] + \sum_{k=1}^{M} E \left[\frac{1}{2}A_k^2\right] \dots 1.7$$

From Equation 1.5

Assuming that d(x) is approximately normal and has a mean of zero, R(o) is its variance. Equation 1.8 has another interpretation through the ergodic hypothesis which says that ensemble averages may be found as limits of time averages. In particular

$$L_{\dot{T}^{m}} = \frac{1}{T} \int_{0}^{T} \left[d(x) \right]^{2} dx = E \left[\left\{ d(x) \right\}^{2} \right] = R(0) \dots 1.9$$

The left side is a measure of the average variability of d(x) over a long stretch. By Equation 1.7, this is divided into averages of uncorrelated components each of which has a separate effect on the linear system. We will be interested more in frequency bands and it is natural to consider that the total variance can be partitioned into partial variances due to frequency bands. Suppose we have several random functions, $d_1(x)$, $d_2(x)$, . . . , each of which may be represented as a trigonometric series of form Equation 1.2 with random coefficients. Since the frequencies are different we can assume the coefficients to be uncorrelated. Thus, $d_1(x)$, $d_2(x)$, . . . , are also uncorrelated so that the variance of the sum is the sum of variances

$$var [d_1(x) + d_2(x) + ...] = R_1(0) + ...$$

Calling the sum d(x), we have

$$\operatorname{var}\left[d(x)\right] = \sum_{1} \operatorname{E}\left[\frac{1}{2} \operatorname{A}_{k}^{2}\right] + \sum_{2} \operatorname{E}\left[\frac{1}{2} \operatorname{A}_{k}^{2}\right] + - - \cdot \cdot \cdot 1.10$$

where Σ means sum over those ω_k 's which are frequency components of $d_1(x)$. This shows that the variance of d(x) can be partitioned into the sums of variances of various frequency components each of which may be thought of as a separate random function, the sum of which is d(x) itself.

Two relationships will be the principal guides in estimating spectral values from profile data. The first is Equation 1.6, which links the power spectrum to the covariance function and the second is another aspect of the ergodic hypothesis;

$$R(s) = \frac{\text{Lim}}{T} \frac{1}{T} \int_{0}^{T} \left[d(x + s) d(x) \right] dx \qquad 2.1$$

We will assume a continuous power spectrum given by a spectral density function so that Equation 1.6 becomes

with $f(-\lambda) = f(\lambda)$

The quantity $f(\lambda_k)d\lambda$ or $f(^\omega_k)d\lambda$, (frequencies in radian per foot $(^\omega)$ and cycles per foot (λ) , may be associated with the value of the sum of $E\left[\frac{1}{4}A_n^2\right]$ for those ω_n within a band of width $d\lambda$ about ω_k .

Equations 1.6 and 2.1 suggest that the values of R(s) might be estimated by taking mean lagged products of the data to estimate the covariance function. Then the values of the power spectrum might be established by determining the Fourier coefficients in the expansion of R(s). Taking into account the form of the data, that is n values of an outcome of d(x) taken at evenly spaced intervals, $d(x_0 + k\Delta)$, k = 0, 1, 2, ---, n-1. We shall define a mean lagged product as

$$r_{j} = \begin{cases} \frac{1}{n-j} & \sum_{k=0}^{n-j-1} & d(x_{o} + k \Delta + j\Delta) & d(x_{o} + k \Delta) & \text{if } j \geq 0 \\ \\ \frac{1}{n-j} & \sum_{k=j}^{n-1} & d(x_{o} + k \Lambda + j \Delta) & d(x_{o} + k \Delta) & \text{if } j < 0 \end{cases}$$

Then $r_{.}=r_{.}$. It is apparent from the definition of R(s), Equation j 1.5 that

$$E[r_j] = R(j\Delta)$$

The above indicates how the covariance functions are estimated. The determination of its Fourier coefficients is accomplished by taking a linear combination of its values with cosine coefficients. The linear combinations of the r_j 's with any sort of coefficient w_j is

The expected value of this estimate is

$$E\left[\widetilde{W}\right] = \sum_{j=-M}^{m} R(j\Delta) w_{j}$$

$$= \sum_{j=-m}^{m} \int_{-\infty}^{\infty} f(\lambda) w_{j} \cos 2\pi \lambda j \Delta d\lambda$$

$$= \int_{-\infty}^{\infty} f(\lambda) \left[\sum_{j=-m}^{m} w_{j} \cos 2\pi \lambda j \Delta \right] d\lambda \cdot 2.4$$
with $W(\lambda) = \sum_{j=-m}^{m} w_{j} \cos 2\pi \lambda j \Delta$, then ... 2.5

The function $W(\chi)$, Equation 2.5, is called the "spectral window". The estimates W obtained by linear combinations of the covariance estimates are not estimates of the values of the power spectrum, but of averages of those values of $f(\chi)$ admitted by the window. By making $W(\lambda)$ have a narrow peak of unit area near λ_0 and very low values elsewhere, an estimate of the power over an interval of frequencies near λ_0 can be obtained. The properties of $W(\chi)$ arising from its form as a finite Fourier series, Equation 2.5, gives several limitations of the linear estimates. A discussion of these limitations are in Reference 1 and a modification of the windows is developed to account for the limitations imposed by the finiteness and discreteness of the data.

These limitations on the exactness of the estimates are not of a statistical nature. The statistical errors are random deviations of W from its expected value of E[W], the ultimate randomness being in the smooth profile data itself. It is assumed that this is approximately Gaussian. The main ideas of the statistical problems and their proofs may be found in Blackman and Tukey (The Measurement of the Power Spectra, Dover 1958) or in Grenander & Rosenblatt

(Statistical Analysis of Stationary Time Series, Wiley, 1957).

The estimate W, Equation 2.3, considered as a function of the n data points, is a homogeneous quadratic polynomial. In practice such polynomials in Gaussian random variables are found to have distributions that are well approximated by a Gamma distribution, i.e.

with parameters A and k in which k=1,2,--, and A > 0. It is convenient to recognize that Equation 3.1 is a generalization of a chi-squared (X^2) distribution. Equation 3.1 would be stated equivalently as, W/2A has a X^2 distribution with 2 k degrees of freedom, except that 2 k need not be an integer.

The Gamma distribution is fitted by the method of moments, that is, the values of A and k are chosen so that the first two moments of the gamma distribution match those of W.

$$4 Ak = E\left[\widetilde{W}\right]$$

$$16 A^{2}k = var\left[\widetilde{W}\right]$$

from which

$$k = \frac{\left\{ \mathbb{E} \left[\widetilde{W} \right] \right\}^{2}}{\text{var } \left[\widetilde{W} \right]}, \quad \Lambda = \frac{\mathbb{E} \left[\widetilde{W} \right]}{4 k} \quad \dots \quad 3.2$$

Using a χ^2 table, a 95% confidence interval may be found for E $\left[\widetilde{W}\right]$ by obtaining numbers L and R such that

$$P \left[L < X^2 < R \right] = .95$$

then since $\widetilde{W}/2A = 2kW/E [\widetilde{W}]$ has a Λ^2 distribution

$$P\left[\frac{2k}{R}\widetilde{W} < E\left[\widetilde{W}\right] < \frac{2k}{L}\widetilde{W}\right] = .95$$

The factors 2k/R and 2k/L give the ends of a confidence interval for the random deviations of the observed value of W from the expected W. The Table below illustrates how the width of the interval depends on the degree of freedom, 2k

2k = Degree of Freedom	<u>2k</u> R	2 <u>k</u> L
5	•39	6.02
10	.495	3.08
15	. 546	2.40
20	.622	2.09
30	.640	1.79
40	.675	1.64
50	.700	1.54
60	.720	1.48

The degrees of freedom, 2k, measure the amount of statistical error. Various requirement measures of statistical error are listed in the paper by Jenkins, "General Considerations in the Analysis of Spectra", Technometrics, Vol. 3, No. 2, May 1961, pp 133-166. They all depend ultimately on the first two moments of W. The first moment is given by Equation 2.4, i.e.,

$$E\left[\widetilde{W}\right] = \int_{-\infty}^{\infty} f(\chi) W(\chi) d\chi$$

The variance of \widetilde{W} may be approximated in a similar form by making use of the assumption of approximate normality.

$$var\left[\widetilde{W}\right] = \frac{1}{\Delta (n-m)} \int_{-\infty}^{\infty} f^{2}(\lambda) W^{2}(\lambda) d\lambda \dots 3.3$$

The proof of this formula may be found in Blackman & Tukey (Dover, 1958, cited above). It can be shown that with these two formulas, the final approximation of the degrees of freedom formula, Equation 3.2, is

$$2k \stackrel{\sim}{=} 2 \frac{n-m}{m} \qquad \dots \qquad 3.4$$

The magnitude of the statistical error may be indicated by confidence intervals. These may be found from the degrees of freedom as in the Table. The Table shows that precision increases with an increase in the degree of freedom. Equation 3.4 suggests that to increase the degrees of freedom, the number, n, of observations must be increased or the number, m, of lags must be decreased. The former increases the expense of the investigation while the latter decreases the resolution of the spectral estimates.

The foregoing has been a discussion on the one-dimensional or line spectra of hard ground roughness. A spectral program has been written for the IBM 7090 with complete details of the program available. Actual field survey data from Yuma, Arizona; Fort Knox, Kentucky; and Aberdeen, Maryland has been analyzed, and the following conclusions appear to be consistent with the results obtained:

- a. Visual observed roughness characteristics of the profile are related to characteristics of the estimated psd.
- b. The estimated psd's may be approximated with reasonable accuracy by a relatively simple class of functions.
- c. Sections of ground which appear visually to have constant roughness characteristics satisfy reasonably well the stationarity assumption on intervals of 1,000 2,000 feet.
- d. The normality assumption for the smoothed data is reasonably well satisfied although there is a consistent deviation from it.
- e. The remaining average method for removing unwanted hills, (smoothing) have proved satisfactory.

TWO-DIMENSIONAL POWER SPECTRAL DENSITY (Reference 1).

To be able to speak mathematically of the height irregularities of a piece of ground, suppose that a horizontal datum and a coordinate system on it has been established. The coordinates, x,y, in feet, locate a point on the datum and h(x,y) will denote the height, in feet, of the ground surface above the datum. The pattern of irregularities is given completely by h(x,y). In general, for another piece of ground having the same kind of irregularities, the function h(x,y) will be different. In order to extract the common character of the irregularity, the common mathematical model of a stationary random function will be expanded. As in the case of the line profile, we will be concerned with the variations of the heights from a variable datum called

the smoothed heights,

$$d(x,y) = h(x,y)$$
 smoothed height at (x,y) 4.1

d(x,y) is considered as being random and that the expected value or ensemble average, $E\left[d(x,y)\right]$, at any point is zero, thus, unchanging or stationary from point to point. More than this, it is assumed that all the characteristics of the probabilities are unchanging from point to point. This is the meaning of "stationary random functions".

In this discussion of random functions with two variables, standard notations and wording will be used and the development will be parallel to the one for functions of one variable. This may be found in the cited references of Grenander & Rosenblatt, "Statistical Analysis of Stationary Time Series", Wiley, 1957, and Blackman & Tukey, "The Measurement of Power Spectra", Dover, 1958.

The definition of the covariance is:

$$R(a,b) = E [d(x,y) d(x + a, y + b)]$$
4.2

The symbol E denotes the expected value operator or the ensemble average. Because of the stationarity or probabilistic sameness of one location to another the average does not depend on the location (x,y) but only on the "lag" (a,b). The covariance function is not random - - it is a fixed characteristic of the roughness.

a.
$$R(0.0) = E\left[\left\{d(x,y)\right\}^2\right] \ge 0$$

b. $R(a,b) \le R(0,0)$
c. $R(-a,-b) = R(a,b)$

In many applications the covariance function has been useful mostly in the form of its Fourier transform

Since $e^{i\theta}=\cos\theta+i\sin\theta$, the quantity $2\pi(xu+yv)$ must be in radians. Since x and y are in feet, 2π u and $2\pi v$ are in radians/ft., or u and v are in cycles/ft.

As with one variable transforms, this can be inverted to

$$R(x,y) = \int_{-\infty}^{\infty} \int_{-\infty}^{\infty} e \qquad F(u,v) \text{ dudv } \dots 4.5$$

The fact that R(x,y) is an even function, Equation 4.3, implies that F(u,v) is real valued and in fact

$$F(u,v) = \int_{-\infty}^{\infty} \int_{-\infty}^{\infty} e^{-2\pi i(xu + yv)} \frac{1}{2} \left[R(x,y + R(-x - y)) \right] dx dy$$

$$= \frac{1}{2} \begin{bmatrix} \infty & \infty & -2\pi i (xu + yv) \\ \int \int \int e & R(x,y) dx dy \\ -\infty & -\infty & e \end{bmatrix}$$

$$R(x,y) dx dy$$

$$R(x,y) dx dy$$

The second integral is obtained by transforming x'=-x, y'=-y then omitting the primes. The two may then be averaged to give

$$F(u,v) = \int_{-\infty}^{\infty} \int_{-\infty}^{\infty} e^{-2\pi i(xu + yv)} \left[R(x,y) + R(-x - y) \right] dx dy$$

$$= \frac{1}{2} \left[\int_{-\infty}^{\infty} \int_{-\infty}^{\infty} e^{-2\pi i(-xu - yv)} R(x,y) dx dy \right]$$

$$= \frac{1}{2} \int_{-\infty}^{\infty} \int_{-\infty}^{\infty} e^{-2\pi i(-xu - yv)} R(x,y) dx dy$$

$$+ \int_{-\infty}^{\infty} \int_{-\infty}^{\infty} e^{-2\pi i(-xu - yv)} R(x,y) dx dy$$

$$+ \int_{-\infty}^{\infty} \int_{-\infty}^{\infty} e^{-2\pi i(-xu - yv)} R(x,y) dx dy$$

$$+ \int_{-\infty}^{\infty} \int_{-\infty}^{\infty} e^{-2\pi i(-xu - yv)} R(x,y) dx dy$$

$$+ \int_{-\infty}^{\infty} \int_{-\infty}^{\infty} e^{-2\pi i(-xu - yv)} R(x,y) dx dy$$

$$+ \int_{-\infty}^{\infty} \int_{-\infty}^{\infty} e^{-2\pi i(-xu - yv)} R(x,y) dx dy$$

$$+ \int_{-\infty}^{\infty} \int_{-\infty}^{\infty} e^{-2\pi i(-xu - yv)} R(x,y) dx dy$$

which corresponds to the usual relation between even functions and cosine transforms in one variable Fourier analysis. From Equation 4.6 it follows that F(u,v) is an even function so that Equation 4.5 may be written

$$R(x,y) = \int_{-\infty}^{\infty} \int_{-\infty}^{\infty} \cos 2 \pi (xu + yv) F(u,v) du dv . . 4.7$$

Some properties of F(u,v) are

a.
$$F(-u, -v) = F(u,v)$$

b. $F(u,v) \ge 0$

b.
$$F(u,v) \ge 0$$

c.
$$\int_{-\infty}^{\infty} \int_{-\infty}^{\infty} F(u,v) du dv = R(0,0)$$
4.8

Properties, Equation 4.8, b and c, suggest that the total variance R(0,0), may be divided up into components F(u,v) at the frequency values (u,v). This is indeed the case and one can derive generalizations of the various representations of a stationary stochastic process of one variable. The spectral density function F(u,v) will be interpreted as giving the "power" of the roughness in the frequency region u(cycles/ft.). Parallel to the x-axis, and v(cycles/ft.) parallel to the y-axis. An elementary wave at this frequency will be a cosine wave cos $2\pi(xu + yv)$ which has the appearance of corregated iron on the xy plane with crests parallel to the line ux + vy = 0 and having crests evenly spaced every $\frac{1}{\sqrt{u^2 + v^2}}$ feet.

A representation theorem makes us conceive of d(x,y) as a sum of such elementary waves at different frequencies, amplitudes and phases. For purposes of power, those waves of the same frequencies are classified together. The power is analogous to the sum of the squared amplitudes.

Stationary random functions of one variable have been used in engineering for more than twenty years. Problems concerning the output of a linear system with a stationary random input are nowadays routine.

In our work, such a problem would be to determine the variable force on the driver of a motorcycle which is traveling at a uniform rate across our ground on a straight line through (x_0, y_0) at an angle to the x-axis. The input is the random function of distance, s

$$g(s) = d(x_0 + s cos < y_0 + s sin <) 4.9.$$

For a two track vehicle, the input must be regarded as two correlated random functions. In any case, the output, the variable force acting on the driver or the variable displacement of the driver, is also a random function.

A variable which runs over the rough ground is affected only by the roughness under its wheels. If its tracks are straight across a stationary field, the roughness is stationary. For a single track, Equation 4.9 gives the random function involved. The covariance function for this is

$$C(\mathcal{T}) = E \left[g(s)g(s + \mathcal{T}) \right]$$

$$= E \left[d(x_0 + s \cos \alpha, y_0 + s \sin \alpha) d(x_0 + s \cos \alpha + \mathcal{T}\cos \alpha, y_0 + s \sin \alpha) \right]$$

$$= R(\mathcal{T}\cos \alpha, \mathcal{T}\sin \alpha)$$

$$= R(\mathcal{T}\cos \alpha, \mathcal{T}\sin \alpha)$$
4.10

The spectrum function for $C(\tau)$ is the function $D(\lambda)$ that satisfies

$$C(?) = \int_{-\infty}^{\infty} e^{2\pi i \lambda T} D(\lambda) d\lambda$$

But from Equation 4.5 we have

$$R(\mathcal{T}\cos \alpha, \mathcal{T}\sin \alpha) = \int_{-\infty}^{\infty} \int_{-\infty}^{\infty} e$$

$$F(u,v) du dv$$

and if we take

$$u \cos \alpha + v \sin \alpha = \lambda$$

$$- u \sin \alpha + v \cos \alpha = \lambda \mu \qquad 4.11.$$

Then

$$\lambda \cos \alpha - \mu \sin \alpha = u$$

$$\lambda \sin \alpha + \mu \cos \alpha = v$$

and

$$|J| = \frac{\delta(\lambda, u)}{\delta(\mu, v)} = 1$$

The integral may be transformed to

$$\int\limits_{-\infty}^{\infty} e^{2\pi i \lambda t \infty} \int\limits_{-\infty}^{\infty} \left[F(\lambda \cos \alpha - \mu \sin \alpha, \lambda \sin \alpha + \mu \cos \alpha) d\mu \right] d\lambda$$

From which we have

$$D(\lambda) = \int_{-\infty}^{\infty} F(\lambda \cos \alpha - \mu \sin \alpha, \lambda \sin \alpha + \mu \cos \alpha) d\mu . . 4.12$$

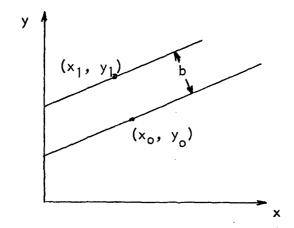
relating the linear spectra in various directions to the two dimensional spectrum.

For parallel tracked separated by a distance, b, the spectrum of each track is given by Equation 4.12. The cross variance of the two profiles is

$$H(\tau) = E \left[d(x_0 + s \cos \alpha, y_0 + s \sin \alpha) \right]$$

$$d(x_1 + s \cos \alpha + \tau \cos \alpha, y_1 + s \sin \alpha + \tau \sin \alpha)$$

$$= R(x_1 - x_0 + \tau \cos \alpha, y_1 - y_0 + \tau \sin \alpha)$$



If (x_1,y_1) is opposite (x_0,y_0) on a line perpendicular to the track, $x_1-x_0=-b\sin\alpha$ and $y_1-y_0=b\cos\alpha$. Since $H(\ell)$ is not an even function, its Fourier transform has both a real and an imaginary part. These are, respectively, its cosine and its sine transform. They give the frequency-phase difference relationship between the two tracks. As above, this complex spectrum is the function $K(\lambda)$ such that

$$H(\lambda) = \int_{-\infty}^{\infty} e^{2\pi i \lambda T} K(\lambda) d\lambda$$

and Equations 4.5 and 4.12 give

$$H(\mathcal{T}) = \int_{-\infty}^{\infty} \int_{-\infty}^{\infty} e^{2\pi i \left[(-b \sin \alpha + \mathcal{T}\cos \alpha) u + (b \cos \alpha + \mathcal{T}\sin \alpha) v \right]}$$

F(u,v)du dv

Making use again of the transformation, Equation 4.11

$$H(\tau) = \int\limits_{-\infty - \infty}^{\infty} \int\limits_{-\infty}^{\infty} e \qquad F(\lambda \cos \alpha - \mu \sin \alpha, \lambda \sin \alpha + \mu \cos \alpha)$$
 d μ d λ

From which

$$K(\lambda) = \int_{-\infty}^{\infty} e \qquad F(\lambda \cos \alpha - \mu \sin \lambda, \lambda \sin \alpha + \mu \cos \alpha) d\mu$$

$$F(\lambda \cos \alpha - \mu \sin \lambda, \lambda \sin \alpha + \mu \cos \alpha) d\mu$$

Equation 4.12 is a special case of Equation 4.13 where b = 0. for each λ , the integral is a line integral of the two dimensional spectrum along lines perpendicular to the direction, , of the track. When the track curves, the resulting roughness is not stationary unless the roughness of the field is the same in all directions. These spectra, Equation 4.13, for various , will give the conditions met by the vehicle in various directions and may be of aid in studying the effects of slowly varying non-stationarity.

The foregoing has been a discussion of the theoretical quantities associated with the stochastic process. The following will be concerned with estimating these quantities, especially the spectral function.

Estimation of a two-dimensional spectrum is an extension of one-dimensional spectral estimation. As in all statistical work data from outcomes of the random process will be used to make estimates of the desired characteristics. In our case this characteristic is the spectral density function of the covariance. Statistical estimation makes use of the fact that when repeated outcomes are averaged, the random part of the average tends to be small. This repitition may be accomplished with d(x,y) by taking the values at different places; the stationarity property is, in effect, the property that the randomness repeats itself in different places. Actually a somewhat more stringent property, the ergodic property, is necessary so that averages over (x,y) tend to ensemble averages. We will assume that this property holds.

It is convenient for computation and for measurement to take data at intersection points of a rectangular lattice. Let $\Delta_{\!\!\! \chi}$ and $\Delta_{\!\!\! y}$ be the separations of the data points in both directions and that $n_{\!\!\! \chi}$ and $n_{\!\!\! y}$ observations were taken at the points $(k\Delta_{\!\!\! \chi},\,j\Delta_{\!\!\! y}),\,k=0,1,2,\ldots$ -, $n_{\!\!\! \chi}$ - 1; $j=0,1,2\ldots$ - - $n_{\!\!\! y}$ - 1. After the smoothing of the profile, the data will consist of $n_{\!\!\! \chi}$ by $n_{\!\!\! y}$ values $d(k\Delta_{\!\!\! \chi},\,j\Delta_{\!\!\! y}).$

Only a part of the randomness is involved in this data. The covariance which underlie it are of the form

$$E\left[d(k^{\wedge}_{x}, j^{\Delta}_{y}) d(k+a)^{\Delta}_{x}, (j+b)^{\Delta}_{y}\right] = R(a^{\Delta}_{x}, b^{\Delta}_{y}) . . 5.1$$
for

$$a = 0, \pm 1, \ldots \pm n_{x}; b = 0, \pm 1, \ldots, \pm n_{y}$$

No other values of the covariance function are used to "produce" the data and we cannot, therefore, hope to make direct estimates of any but these.

The spectrum is related to the covariance function, R(x,y), by Equation 4.7

$$R(a\Delta_{x}, b\Delta_{y}) = \int_{-\infty}^{\infty} \int_{-\infty}^{\infty} \cos 2\pi (a\Delta_{x} u + b\Delta_{y}v) F(u,v) du dv$$

instead of using cosines to obtain

$$\sum_{a} \sum_{b} \cos 2\pi (a \triangle_{x} u_{o} + b \triangle_{y} v_{o}) R(a \triangle_{x}, b \triangle_{y}) \triangle_{x} \triangle_{y} \dots 5.2$$

Let us use general coefficients to obtain

$$F*(u_0,v_0) = \sum_{a} \sum_{b} w(a,b; u_0,v_0) R(a\Delta_x, b\Delta_y)$$

$$= \sum_{a \in b} w(a,b; u_o, v_o) \int_{-\infty}^{\infty} \int_{-\infty}^{\infty} \cos 2\pi (a \Delta u + b \Delta v) F(u,v) du dv$$

$$= \int_{-\infty}^{\infty} \int_{-\infty}^{\infty} \sum_{a} \sum_{b} w(a, b; u_{o}, v_{o}) \cos 2\pi \left(a \Delta_{x} u + b \Delta_{y} v\right) F(u, v) du dv$$

From this we see that $F*(u_0, v_0)$ is a weighted average of spectral values,

$$F*(u_o, v_o) = \int_{-\infty}^{\infty} \int_{-\infty}^{\infty} W(u_o, v_o; u, v) F(u, v) du dv \qquad 5.4$$

Our purpose is to obtain $F*(u_0, v_0)$, therefore

$$W(u_o, v_o; u, v) = \sum_{a \in S} \sum_{b} w(a,b; u_o, v_o) \cos 2\pi (a \Delta_x u + b \Delta_y v)$$

$$a b$$

$$...5.5$$

W(...) ideally is the Dirac or delta function of (u,v) centered at (u_0,v_0) . It is, of course, impossible to attain this ideal since W(.) is a finite Fourier series. This leads to the phenomenon of "aliasing", discussed in Reference 1, which is a limitation of accuracy resulting from sampling at intervals. A discussion is also presented on another limitation of accuracy arising from having only a finite number of data points. An obvious W(...) to try is the finite part of the Fourier series for the Dirac function.

$$\cos 2\pi (a\Delta_x u + b\Delta_y v)$$
 5.6

which corresponds to Equation 5.2. The form of W(...) is the subject of a good deal of literature and was some of the early work-that given in Blackman and Tukey, "Measurement of Power Spectra", - will be followed. This will take the direction of using as standard the W(...) given by Equation 5.6 and modifying it by filtering the final firm of W(...) is discussed in detail under "filtering" in Reference 1.

Up to now, it was assumed that the values of R(a \triangle_x , b \triangle_y) were known for a = 0, \pm 1, . . \pm n_x b = 0, \pm 1, . . \pm n_y. Actually,we will estimate these values from the weight data d(k \triangle_x , j \triangle_y). The usual estimate for an expected value, Equation 5.1, is an average

$$\frac{1}{(n_x - |a|)(n_y - |b|)} \xrightarrow{\Sigma} \xrightarrow{\Sigma} d(k\Delta_x, j\Delta_y)d(k + a)\Delta_x$$

$$(j+b)\Delta_y = r_{a,b} \dots 5.7$$

where k and j range over all the pairs on hand.

We will try to estimate values of the spectral function which are evenly spaced throughout the relevant range. Since we will have covariance values only up to m_X , m_y , the sparing of spectral values is correspondingly larger. For mathematical convenience, a spacing of 1/(2m+1) rather than 1/2m will be used, where m is m_X in the x direction and m_Y is the y direction. Thus we will try to estimate (See Equation 5.3)

$$F^*\left(\frac{\swarrow}{(2m_x+1)} \quad \frac{\swarrow}{(2m_y+1)}\right) \equiv F^*_{\swarrow} \qquad 5.8$$

with
$$\alpha = 0, \pm 1, \pm 2, \ldots, \pm m_x; \beta = 0, \pm 1, \pm 2, \ldots, \pm m_y$$

Using the coefficients $w(a,b; u_o, v_o)$ of Equation 5.2, we can calculate the estimates

$$f_{\alpha,\beta} = \sum_{a=-m_{X}}^{m_{X}} \sum_{b=-my}^{m_{y}} w \left(a,b; \frac{\alpha}{(2m_{X}+1)\Delta_{X}}, \frac{\beta}{(2m_{y}+1)\Delta_{y}}\right) r_{a,b}$$

whose expected values are F*, B

To approximate the distribution of the random variable f_{α} , β we will assume the Gamma distribution which has been found to fit well in this kind of work. The parameters A,K of the distribution will be estimated by the method of moments.

The following is the mathematical expression of our first assumption.

$$P\left[f_{\alpha,\beta} < \Delta\right] = \frac{A^{K}}{\Gamma(K)} \int_{0}^{\Delta} t^{K-1} e^{-At} dt \qquad (A.1)$$

As in the one-dimensional case, we have correspo to Equation 5.2

$$K = \frac{\left(F_{\alpha,\beta}^{*}\right)}{\operatorname{var}\left[f_{\alpha,\beta}^{*}\right]}$$

$$F_{\alpha}^{*}$$

$$A = \frac{F *_{\alpha} \beta}{4K}$$

The derivation of the formula for $Var[f_{\alpha,\beta}]$, which also gives $cov[f_{\alpha',\beta'}] = 0$ is presented in an appendix in Reference 1.

The degrees of freedom equation, also discussed in the appendix, is

$$2K \stackrel{\sim}{=} 2\left(\frac{1-g}{g}\right)^2 \qquad 5.11$$

where

$$g = \frac{m_X}{m_X} = \frac{m_Y}{n_Y}$$
, the ratio of the number of R values in

each direction to the number of profile values in each direction.

The assumptions made in the approximate calculation of var f and cov $\left[f_{\alpha',\beta},f_{\alpha',\beta'}\right]$ are as follows:

- A.2 The profile height deviations d(x,y) of Equation 4.1 are approximately Gaussian with means 0.
- A.3 The values of m_x and m_y are small in comparison to n_x and n_y so that the number of terms in the sum for different covariance estimates (Equation 5.7) are approximately the same.
- A.4 F(u,v) is essentially zero for (u,v) outside the range $1/\Delta_x$ in the u direction and $1/\Delta_y$ in the v direction so that aliasing does not occur.
- A.5 The non-zero parts of the function W(...) of Equation 5.4 are no wider than

$$\left(-\frac{1}{2n_x \Delta_x}, \frac{1}{2n_x \Delta_x}\right)$$
 by $\left(\frac{1}{2n_y \Delta_y}, \frac{1}{2n_y \Delta_y}\right)$

so that their overlap is negligible.

There is utile control over assumptions A.1 and A.2. Assumption A.5 is somewhat in conflict with the discussion on the limitation of accuracy arising from having only a finite number of data points. This has indicated that the non-zero area of w(...) should be at least a half period wide by a half period high, i.e.,

$$\frac{1}{2n_x \Delta_x}$$
 by $\frac{1}{2n_y \Delta_y}$

to come near a compromise. A relatively long Fourier expansion of Equation 5.5 must be used and the coefficient chosen with care. This means a fairly large $\rm m_x$ and $\rm m_y$ - also desirable for good resolution or closeness of spectral estimates. But A.3 requires an even larger $\rm n_y$ and $\rm n_y$. The ratio, g, of m to n should be small to obtain a large degree of freedom. Assumption A.4 relates to the size of the spacing, $\Delta_{\rm x}$ $\Delta_{\rm y}$, in the profile data.

As one can see, many factors must be considered; the desire for good resolution, statistical precision and a wide range for the values of F(u,v) require a large member of profile data. These desires must be balanced with the expense of measuring the profile and the handling of the data. Other factors such as non-stationarity and the inherent errors of measurement, which have not been taken into account here, would limit the accuracy and precision in other ways, so that the problem cannot be answered by simple and straightforward answers. The principles outlined in this discussion will help us to deal rationally with it.

The final form of the spectral estimates, discussed under "filtering", Reference 1, is:

$$f_{\alpha,\beta} = \sum_{a \ b} \sum_{b \ w(a,b)} \alpha \delta_{x} \beta \delta_{y} r_{ab}$$

$$= \sum_{a} \sum_{b} C \cos_2 \pi \left(\frac{a \alpha}{2m_x + 1} + \frac{b \beta}{2m_y + 1} \right) r_{a,b}$$

$$= \frac{1}{2m_x+1} + \frac{1}{2m_y+1} \sum_{a} \sum_{b} C C_{a,b}$$

From this we have a fundamental relation. \overline{C} is the "raw spectrum" of the covariances, $r_{a,b}$ and the coefficients C are used to smooth it by taking a running average. By this we may achieve a variety of $W(\dots)$ functions. All the filters used in practice are given in terms of the running average weights C or in terms of the coefficients C which modify the covariances before making a Fourier transformation. Corresponding to the two sides of the convolution theroem, we have two ways of computing the spectrum. We may first compute a "raw spectrum" or cosine transformation of $r_{a,b}$ and then smooth it by a running average. This is convenient when only a few of the running average coefficients $C_{j,k}$ are non-zero. Or we may modify the $r_{a,b}$ by multiplying them by factors $c_{a,b}$ then take the cosine transformation. This is done when the C's are easy to compute.

A two-dimensional spectral computer program has been written, debugged, and is now operational. The general operation of the program involves the steps:

- 1. The area data is smoothed.
- 2. The covariances of the smoothed data are computed.
- 3. A preliminary spectrum of these covariances is computed.
- 4. A trigonometric polynomial is fitted to the reciprocals of the spectral values, its coefficients are used to make a running average smoothing of the covariances.
 - 5. A new spectrum of the smoothed covariances is computed.
 - 6. The spectrum is smoothed by the Hamming method.
- 7. The spectrum is corrected using the reciprocals of the polynomial (4) as factors.

During the Summer of 1964, a survey team conducted an extensive survey of sites located in the South and Southwest and the Southeastern Sections of the United States. These profile data will be used as the input data to the spectral programs. Both the line spectra and the

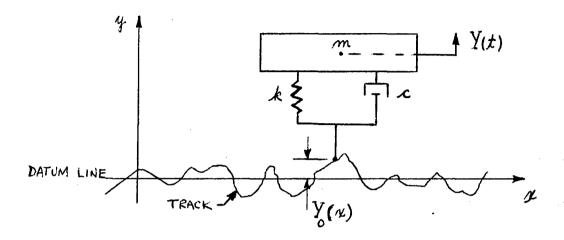
two-dimensional spectra will be determined and analyzed. The data measured at intersection points of a rectangular grid will enable us to compare the spectral characteristics of the different areas and in some way to identify and categorize hard, rough, terrain by the psd characteristics and the geographic location, geologic and geomorphologic characteristics of the terrain. It may also be possible that terrain roughness could be identified by comparison of the surveyed areas and aerial photographs of these areas. The stationarity of roughness as the direction is changed will also be investigated using the grid survey data. If terrain roughness can be categorized according to its psd characteristics and the natural terrain descriptions such as location and geologic history, the basic input to vehicles operating in these areas will be known, the first requisite in the study of vehicle ride characteristics. Another area of investigation using the survey data is the effect of terrain roughness on vehicle vibration. At one of the survey sites, vehicle vibration tests were conducted where acceleration responses of different parts of the vehicle frame as well as under the driver's seat were measured. The line profile of the vehicle ruts were also surveyed so that the input psd characteristics will be known. This brings us to the next area of investigation in the study of vehicle ride characteristics, the response of the vehicle traveling over the hard rough terrain.

BEHAVIOR OF IDEALIZED VEHICLES TRAVELING OVER HARD ROUGH TERRAIN

The following will be a discussion on the relationship of the hard rough terrain to a vehicle traveling over it. The problem is being investigated by Bogdanoff and Kozin of the Midwest Applied Science Corporation and to date only the idealized vehicle has been considered. The investigation has progressed from simple one-dimensional to two-dimensional systems and from hypothetical to actual ground profile data inputs. In determining the output responses, the major hurdle will be the problem of describing the real vehicle and its response to the various types of hard off-road terrain in which it must operate. As mentioned previously, an inroad to this problem has been made with the field measurement of the vehicle motion and the terrain over which it traveled. Comparisons will be made so that the accuracy of predicting vehicle responses by using idealized models can be assessed and where changes are needed, the direction of the modifications needed will be clearer.

The simplest case of a vehicle will be considered so as to set up most clearly the method of approach to this problem, References

2 and 3 consider the system shown below:



The spring mass is m, the linear spring constant is k, and the viscous damper constant is c. A wheel of zero radius or a point follower is in constant contact with the track. The co-ordinates of the mass center of the spring mass are given by (x,y) and we assume no rotational motion of the mass.

The track elevation $Y_{Q}(x)$, above some prescribed datum line, is assumed to be a function of a random process, Reference 4, whose functions are of the form:

where f_0,\ldots,f_n are real random variables, Reference 5, each of which is uniformly distributed over the interval $(0,2\pi)$ such that $f_{-k}=-f_k$, $k=1,2,\ldots,n$. Furthermore, the coefficients a_{-k} are given complex constants for which a_{-k} is the complex conjugate (a_k^*) of a_k , $k=1,2,\ldots,n$ and $a_0=0$. The constants f_k are given real numbers having the dimensions of length for which $f_k=-f_k$, $f_k=1,2,\ldots,n$. From these conditions $f_k=1,2,\ldots,n$ is a real random function which can be written

$$Y_{0}(x) = \sum_{k=1}^{n} 2 \operatorname{Re} \left[a_{k} e^{i\left(\frac{x}{\sqrt{k}} + \mathbf{p}_{k}\right)} \right] \qquad 6.2$$

If the a 's are real, this may be written

Hence, $Y_0(x)$ may be regarded as a superposition of cosine functions of frequencies $\lambda_j = 1/\hat{x_j}$; amplitude $2a_j$; and random phases ϕ_j . Equations 6.1 and 6.3 will be used interchangeably.

Regarding x as a parameter relative to the average operation, it can be shown that:

The mean value
$$E\left[Y_0(x)\right] = \sum_{n=0}^{\infty} a_n E\left[\frac{i(\frac{x}{k} + \sqrt{k})}{e^{k}}\right] = 0$$
 . . . 6.4

The variance
$$\sigma_{Y_0}^2 = E\left[(Y_0(x))^2 \right] = \sum_{n=0}^{n} a_k a_k^* \dots 6.5$$

Rice, Reference 6, has shown that for sufficiently large n, $Y_o(x)$ is normally distributed within a small prescribed error. That is

$$P\left[Y_{o}(x) \leq Y_{o1}\right] \stackrel{=}{=} \frac{1}{\sqrt{2\pi}} \int_{\infty}^{Y_{o1}} \frac{y^{2}}{e^{2\pi}} \int_{0}^{2\pi} e^{y^{2}} dy \dots 6.7$$

Using standard techniques, Reference 7, one can also show that for sufficiently large n, $Y_0(x)$ and $Y_0(x+\mathcal{L})$ are to within a small prescribed error, jointly normally distributed.

The power spectral density, $P_{\gamma}(\lambda)$, for non-negative λ of $Y_{o}(x)$ is, Reference 8, given by the formula:

$$P_{Y_0}(\lambda) = \frac{2}{\pi} \int_0^\infty \mu_{Y_0}(t) \cos \lambda \tau d\tau = \sum_{k=1}^n 2|a_k|^2 \delta(\lambda - \lambda_k)$$

where $\lambda_k = 1/l_k$, k = 1, . . , n and $\delta(\lambda)$ is the delta function centered at λ_k with properties

$$\int_{-\infty}^{\infty} \int (\lambda - \lambda_k) d\lambda = 1,$$

if
$$\lambda^{\perp} \neq \lambda_{k}$$

If a function of the form, Equation 6.3, is used as an input to a linear system, the output also has this form

$$Y(t) = \sum_{k=1}^{n} 2 a_{k}^{t} \cos \left(\frac{x}{k} + \beta_{k}\right) \qquad6.9$$

The coefficients a_k^{\dagger} depends only on the a_k of the k^{th} term of Equation 6.3. Then

transfer functions of the linear system. The phase of the input does not affect the amplitude of the output nor does the amplitude of the input affect the phase of the output. In many problems the ultimate effect does not depend on the phase so that only the a_n' and hence only a_n is of interest.

In the analysis of the simplest vehicle, we assume that this vehicle travels with constant horizontal velocity v_0 , so that $x = v_0$ t. The equation of motion of the mass is:

$$\ddot{Y} + 25\omega_{0}\dot{Y} + \omega_{0}^{2}Y = 25\omega_{0}\dot{Y}_{0} + \omega_{0}^{2}Y_{0} - g$$
 . . . 6.10

where
$$\omega_0 = \frac{k}{m}$$
, $2 \not \leq \omega_0 = \frac{c}{m}$, $\omega_k = \frac{v_0}{\ell_k}$ and

$$Y_{o}(t) = \sum_{-n}^{n} a_{k} e^{i(\omega_{k}t + \Phi_{k})}$$

The transient portion of the solution of Equation 6.10 will be neglected. The steady-state solution for the displacement of the mass is:

$$Y(t) = -\frac{g}{\omega_0^2} + \sum_{-n}^{n} b_k e^{i(\omega_k t + \frac{\sigma}{k})} ... 6.11$$

where

$$b_{k} = a_{k} \frac{\omega_{o}^{2} + i 2 \zeta \omega_{o} \omega_{k}}{\omega_{o}^{2} - \omega_{k}^{2} + i 2 \zeta \omega_{o} \omega_{k}}$$

The acceleration of the mass is:

and comparing the right-hand sides of 6.12 and 6.13 to Equation 6.1, for $Y_o(x)$, shows that they are identical in form. Hence, statistical parameters for $Y(t) + g/\omega_o^2$ and Y(t) may be computed from formulas similar to those used for $Y_o(x)$. Thus: $E\left[Y(t) + g/\omega_o^2\right] = 0$

$$\mu_{y}(\tau) = E\left[\left\{Y(t) + \frac{g}{\omega_{o}^{2}}\right\} \left\{Y(t+t) + \frac{g}{\omega_{o}^{2}}\right\}\right]$$

$$= \frac{n}{\Sigma} \quad b_{k} b_{k}^{*} \quad e$$

$$= \frac{g}{N} \quad b_{k} b_{k}^{*} \quad e$$

$$= \frac{n}{\Sigma} \quad b_{k} b_{k}^{*} \quad ... \quad ... \quad ... \quad 6.14$$

The power spectral density of Y(t) is

$$E\left[\ddot{Y}(t)\right] = 0$$

$$\mu_{\ddot{y}}(\tau) = \mathbb{E}\left[\ddot{Y}(t) \ddot{Y}(t+\tau)\right]$$

$$\mathcal{O}_{\ddot{y}}^{2} \mu_{\ddot{y}}(v) = \sum_{-n}^{n} \omega_{k}^{4} b_{k} b_{k}^{*} e^{i\omega_{k}}$$

$$\frac{2}{\ddot{Y}} = \mu_{\ddot{y}}(0) = \sum_{-n}^{n} \omega_{k}^{4} b_{k}b_{k}^{*}$$

. . . . 6.16

The power spectral density of Y(t) is

Returning to the variance, σ^2 , of $\left[Y(t) + g/\omega_0^2\right]$ and Y(t);

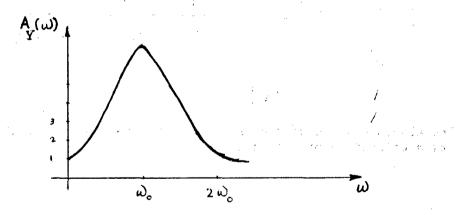
$$\mathbf{O}_{Y}^{2} = \sum_{-n}^{n} b_{k} b_{k}^{*} = \sum_{-n}^{n} b_{k}^{*}$$

$$= \sum_{-n}^{n} \int_{0}^{\omega_{0}^{2} + i \cdot 2 \cdot 5 \cdot \omega_{0} \cdot \omega_{k}} \int_{0}^{2} |a_{k}|^{2} \dots 6.18$$

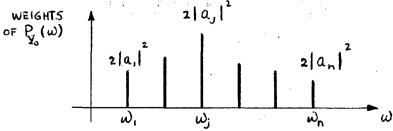
Hence σ_{γ}^2 depends upon a_k and ω_k and the absolute value of the frequency response squared of the vertical displacement:

$$A_{\gamma}(\omega) = \left| \frac{\omega_0^2 + i 2 \mathcal{J} \omega_0 \omega_k}{\omega_0^2 - \omega_k^2 + i 2 \mathcal{J} \omega_0 \omega_k} \right|^2$$

The frequency response squared, $A_{\gamma}(\!\omega)$, of the mass, m, as a function of w_1 would look like



If the track roughness is specified by the "a," for some fictitious type of roughness, the plot of the power spectral density weights as a function of ω may look like



Rewriting Equation 6.18 for 6_{γ}^{2} :

$$G_{Y}^{2} = \int_{0}^{\infty} \int_{1}^{n} \left| \frac{\omega_{o}^{2} + i + i + 2 \int_{0}^{\infty} \omega_{o}}{\omega_{o}^{2} - \omega^{2} + i + 2 \int_{0}^{\infty} \omega_{o}} \right|^{2} = 2 \left| a_{j}^{2} \int_{0}^{\infty} (\omega - \omega_{j}) d\omega \right|^{2}$$

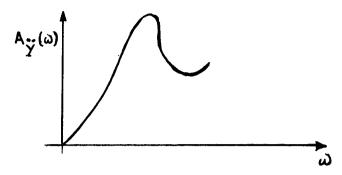
We can see that the magnitude of σ_{γ}^2 will depend upon how the peak of $A_{\gamma}(\omega)$ is placed with respect to peaks present in the weights of $P_{\gamma}(\omega)$. Therefore, for a rough track whose power spectral density contains one or more pronounced peaks, it is possible to change the variance of Y(t) by changing the system constants. m. c. -k.

The variance of the acceleration of Y(t), Y(t), is

The absolute value of the frequency response squared of the vertical acceleration of the mass is

$$A_{\tilde{Y}}(\omega) = \frac{\omega^{2} \left[\omega_{0}^{4} + (2 + \omega_{0}\omega)^{2}\right]}{(\omega_{0}^{2} - \omega^{2})^{2} + (2 + \omega_{0}\omega)^{2}} ... 6.22$$

A graph of this is



Again changes in the system constants will change the variance of $\ddot{Y}(t)$.

Examining Equation 6.21 from a different point of view and rewriting as $\frac{1}{2}$

$$\tilde{O}_{Y}^{2} = \int_{0}^{\infty} \int_{1}^{n} \omega^{4} \left| \frac{u_{o} + i 2 \int_{0}^{\infty} u_{o} \omega}{u_{o}^{2} - u^{2} + i 2 \int_{0}^{\infty} u_{o} \omega} \right|^{2} 2 \left| a_{j} \right|^{2}$$

$$\delta(\omega-\omega_i) d\omega$$
 6.23

The integrand may be written as

$$A_{ij}(\omega)$$
 $\sum_{j=1}^{n} 2 |a_{j}|^{2} \delta(\omega-\omega_{j})$

But with $\omega_j = v_0/\lambda_j$ in Equation 6.8:

$$P_{Y_0}(\omega) = \sum_{j=1}^{n} 2 |a_j|^2 \delta(\omega - \omega_j)$$

Hence

$$\sigma_{\mathbf{Y}}^{2} = \int_{\mathbf{0}}^{\infty} A_{\mathbf{Y}}(\omega) P_{\mathbf{Y}_{\mathbf{0}}}(\omega) d\omega$$

with the same reasoning

From Equations 6.14 and 6.15:

$$\sigma_{Y}^{2} = \mu_{Y}(o) = \int_{0}^{\infty} P_{Y}(\omega) d\omega$$

and from Equations 6.16 and 6.17:

 $\mathcal{L}_{\mathcal{F}}(\mathbb{R}^{n}) : \mathbb{R}^{n} \longrightarrow \mathbb{R}^{n} \longrightarrow \mathbb{R}^{n} \longrightarrow \mathbb{R}^{n} \longrightarrow \mathbb{R}^{n}$

$$6 \frac{2}{Y} = \mu_{Y}(0) = \int_{0}^{\infty} FY(\omega) d\omega$$

Therefore the power spectral densities of Y(t) and Y(t) are

$$P_{\Upsilon}(\omega) = A_{\Upsilon}(\omega) P_{\Upsilon_0}(\omega)$$

. 6.26

$$P_{Y}^{\bullet}(\omega) = A_{Y}^{\bullet}(\omega) \quad P_{Y_{0}}(\omega)$$

The results embodied in 6.26 are a special case of a general result. This result states that the power spectral density of the output of a linear time independent system, where the input is a weakly stationary random function, is equal to the product of the power spectral density of the input and the square of the absolute value of the frequency response of the output when driven simple harmonically at the input. By knowing an estimate of the input $P_{\gamma}(\omega)$ and varying $A_{\gamma}(\omega)$, the output $P_{\gamma}(\omega)$ can be varied.

Small values of 6°_{γ} are associated with sharp concentration of the distribution in the neighborhood of its mean. Hence, if we select m, c and k so as to make 6°_{γ} small, the probability that at any instant t, |Y(t)| will exceed some particular value sufficiently different from the mean is also small.

Rice, Reference 9, has shown that the expected number of times per second that $|\dot{Y}(t)|$ exceeds say y, is given by

where $6^{\circ}_{\dot{Y}}$ is the variance of $\dot{Y}(t)$.

Also, the expected number of times per second that $|\mathring{Y}(t)|$ exceeds $\mathring{y}(>0)$ is given by a similar formula

$$\overline{\mathbb{N}}_{\tilde{\mathbf{y}}} = \frac{1}{\pi} \frac{6\overline{\mathbf{y}}}{6\overline{\mathbf{y}}} = \frac{1}{\pi}$$

We now have equations to determine σ_{γ}^2 , $\sigma_{\tilde{\gamma}}^2$ and \tilde{N}_y , \tilde{N}_y . They indicate that, if we wish to design the model (which in this case could be a trailer) so as to smooth Y(t), then the selection of the system constants depends upon what aspects of Y(t) is to be smoothed. A few possibilities for the smoothing of the motion of the mass m will be mentioned:

For a fixed v_0 , select m, c, and k so that:

- a. σ_{γ}^{2} is a minimum (the probability of |Y(t)| exceeding a selected value is minimum).
- b. \overline{N}_{γ} is a minimum (the expected number of times per unit time that |Y(t)| exceeds some selected value, y, is minimum).
- c. $5\sqrt[2]{2}$ is a minimum (the probability of $|\tilde{Y}(t)|$ exceeding some limit is minimum)
- d. $\overline{N_{Y}}$ is a minimum (the expected number of times per unit time that |Y(t)| exceeds \tilde{y} is a minimum).
- e. The probability of one of the maxima occurring in a second, or $|\ddot{Y}(t)|$ exceeding a limiting value is a minimum (an analytical form for this probability exists, Reference 10).

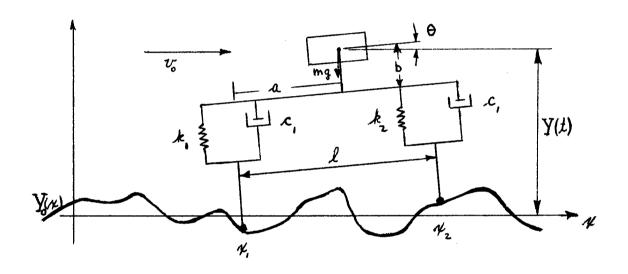
How do we select one of these possibilities to fit a specific application? Let us suppose that a man is to ride on the mass m. It is known that sharp acceleration peaks due to the follower coming against sudden rises in the track may cause damage to some of the organs in the lower region of the trunk of the body; sharp acceleration peaks when the follower executes a sudden drop causes the man and mass to separate unless strapped or fastened in some manner. Hence, it is appropriate to consider either paragraph b or e above. Whether reducing the expected number of times per unit time that |Y(t)| exceeds some limit y or reducing the number of peaks in |Y(t)| per unit time above \hat{y} produces a smoother ride remains for definitive clinical experiments on man to answer.

It is also known that oscillations of large amplitude and long period produce nausea in certain individuals. If δ_{γ}^2 is made a minimum by the proper choise of m, c, and k, all amplitudes will be reduced to a minimum, particularly for oscillations of long periods. Hence, it is appropriate in this case to consider the possibility mentioned in paragraph a above again. Experimental verification that a reduction in δ_{γ}^2 will reduce the tendency towards nausea is lacking.

These comments should indicate the many possibilities which exist for smoothing the motion of m and also indicate the need for gareful experimental work to validate the usefulness of any one of the possibilities selected. The close inter-relation between the three distinct

phases in the investigation of vehicle ride characteristics can now be clearly seen and that the progress of any one phase augments and directs the progress and development of the other phases.

Next in our approach to describing vehicular motion, the two dimensional vehicle model will be discussed, References 3 and 11. The model considered is a linear two degree of freedom vehicle moving with constant horizontal velocity on a track whose contour is a stationary random process. The system is



The vehicle is simplified to have linear springs and dampers for each follower with constants given as k_1 , c_1 and k_2 , c_2 . There is assumed to be a rigid horizontal connection between the followers such that the distance between contact centers is \boldsymbol{k} . The mass center is assumed to be at a point, a units, from the rear contact center and b units, above the rigid connection. With these assumptions, the differential equations of vertical motion of the mass center and of rotational motion about the mass center can be written down. Our study will be concerned with the symmetric 2-point follower vehicle with

$$k_1 = k_2 = k$$
 , $c_1 = c_2 = c$, $a = \frac{1}{2}$, $b = 0$, and the c.g. at $a = \frac{1}{2}$, $b = 0$

with the further assumption that $\cos \theta = 1$ (a 2% error for

 -10° < θ < 10°), the equations of motion are

$$\dot{Y} + \frac{2c}{m} \dot{Y} + \frac{2k}{M} \quad Y = \frac{k}{m} \left[Y_{o}(x_{1}) + Y_{o}(x_{2}) \right]
+ \frac{c}{m} \left[Y_{o}(x_{1}) + Y_{o}(x_{2}) \right] - g \qquad ... \qquad ...$$

where $x_2 = x_1 + \dots + x_m =$ the moment of inertia of the vehicle about its mass center and _____ denotes differentiation of the quantity under the bar with respect to time.

As in the previous study, we will assume the track is represented by the following Fourier series of the form

where $a_0 = 0$, $a_k = a_k^*$, $A_k = -A_k (a_k^*)$ is the complex conjugate of a_k),

 $\underline{f}_k = -\overline{f}_k$ and \hat{f}_k has dimensions of length. The $\underline{f}_{k's}$ are uniformly distributed random phases that generate this sample track from the given random process.

As a result of our assumption that the pitch is not large, \dot{x}_1 and \dot{x}_2 are equal to the velocity of the mass center:

$$x_1(t) = vt, x_2(t) = vt + \mathcal{L}$$

Therefore, in our case

$$Y_{o}(x_{1}) = \sum_{k = -n}^{n} a_{k} e^{i(\frac{vt}{\ell_{k}} + \frac{1}{\ell_{k}})}$$

$$\frac{1}{Y_{o}(x_{1})} = \sum_{k = -n}^{n} a_{k} e^{i(\frac{vt}{\ell_{k}} + \frac{1}{\ell_{k}})}$$

$$\frac{1}{Y_{o}(x_{1})} = \sum_{k = -n}^{n} a_{k} e^{i(\frac{vt}{\ell_{k}} + \frac{1}{\ell_{k}})}$$

$$\frac{1}{Y_{o}(x_{2})} = \sum_{k = -n}^{n} a_{k} e^{i(\frac{vt}{\ell_{k}} + \frac{1}{\ell_{k}})}$$

$$\frac{1}{Y_{o}(x_{2})} = \sum_{k = -n}^{n} a_{k} e^{i(\frac{vt}{\ell_{k}} + \frac{1}{\ell_{k}})}$$

$$\frac{1}{Y_{o}(x_{2})} = \sum_{k = -n}^{n} a_{k} e^{i(\frac{vt}{\ell_{k}} + \frac{1}{\ell_{k}})}$$

$$\frac{1}{Y_{o}(x_{2})} = \sum_{k = -n}^{n} a_{k} e^{i(\frac{vt}{\ell_{k}} + \frac{1}{\ell_{k}})}$$

$$\frac{1}{Y_{o}(x_{2})} = \sum_{k = -n}^{n} a_{k} e^{i(\frac{vt}{\ell_{k}} + \frac{1}{\ell_{k}})}$$

We can now solve Equation 7.1 explicitly. Assuming the system is at rest at the origin initially, we have

$$Y(t) = -\frac{g}{\omega_y^2} + \frac{e^{-\omega_y} \int_y^y t}{\omega_y (1 - \omega_y^2)^2} \frac{2 g \int_y^y sin(\omega_y \sqrt{1 - \zeta_y^2} t)}{1 - \zeta_y^2 t}$$

$$+ \frac{e^{-\omega_y} \int_y^y sin(\omega_y \sqrt{1 - \zeta_y^2} t)}{1 - \zeta_y^2 t}$$

$$+ \frac{1}{\omega_y} \frac{1 - \zeta_y^2}{1 - \zeta_y^2} \int_y^y sin(\omega_y \sqrt{1 - \zeta_y^2} t)$$

$$+ \frac{1}{\omega_y} \frac{1 - \zeta_y^2}{1 - \zeta_y^2} \int_y^y sin(\omega_y \sqrt{1 - \zeta_y^2} t)$$

$$\sin \left[\begin{array}{ccc} \omega_{y} \sqrt{1 - \frac{1}{5}} & \frac{1}{2} &$$

where
$$\xi_y \omega_y = \frac{c}{m}$$
, $\omega_y^2 = \frac{2k}{m}$ and $\omega_k = \frac{v}{k}$

Since we could have chosen initial conditions in such a way that the transient term outside of the integral vanishes, in the following calculation for Y, we neglect the transient term. Also, the following relation is used

$$\sin \left(\frac{\omega_y}{y}\sqrt{1-\frac{\zeta^2}{y}}\right)t \equiv \frac{1}{2i} \begin{bmatrix} \frac{\omega_y}{y}\sqrt{\frac{\zeta^2}{y}-1}t & -\frac{\omega_y}{y}\sqrt{\frac{\zeta^2}{y}-1} & t \\ e & -e \end{bmatrix}$$

Similarly for $\Theta(t)$, one obtains the solution, again neglecting the transient terms:

$$\Theta(t) = \frac{1}{\omega_{\Theta} \left(1 - \frac{5}{9}\right)^{2}} \int_{0}^{t} d\tau e^{-\frac{1}{2}\frac{\omega}{\theta}} (t - \tau)$$

$$\sin \left[\omega_{\theta} \sqrt{1 - \frac{5}{\theta}^{2}} (t - \tau) \right] \xrightarrow{\frac{\omega_{\theta}}{2}} \sum_{k=-n}^{\infty} a_{k} e^{i(\omega_{k} \tau + \phi_{k})} e^{i\frac{\pi}{2k}}$$

$$+ i \frac{\zeta_{\theta} \overset{\omega}{\theta}}{a} \qquad \sum_{k = -n} \omega_{k} a_{k} \qquad e \qquad (e^{i(\mathcal{L}_{k})} -1)$$

where
$$\omega_{\theta} = \frac{2 a^2 k}{I_m} \zeta_{\theta} \omega_{\theta} = \frac{a^2 c}{I_m}$$

Evaluation each of Equation 7.4 and 7.5 explicitly yields:

$$Y(t) = -\frac{g}{\omega_y^2} + \frac{1}{2i} \sum_{k=-n}^{n} a_k \left[\frac{\frac{\omega^2}{y} + i \zeta_y \omega_y \omega_k}{\frac{\omega_y}{y} \sqrt{1 - \zeta_y^2}} \right]$$

$$\begin{array}{c}
\frac{\ell}{\ell_k} \\
\text{(e} + 1)
\end{array}$$

$$x \left[\begin{array}{cccc} \frac{i(\omega_{k}t + \Phi_{k})}{k} & \frac{i\Phi_{k} - \omega_{k}(\zeta - \sqrt{\zeta^{2} - 1}) t}{\omega_{k}(\zeta_{y} - \sqrt{\zeta^{2} - 1}) + i\omega_{k}} \end{array}\right]$$

$$-\frac{i(^{\omega}_{k} + \Phi_{k})}{e} - \frac{i\Phi_{k}}{e} - \frac{^{\omega}_{y} (\zeta_{y} + \sqrt{\zeta_{y}^{2} - 1})t}{e}$$

$$-\frac{e}{\sqrt{(\zeta_{y} + \sqrt{\zeta_{y}^{2} - 1}) + i\omega_{k}}}$$

. . . . 7.6

$$\Theta(t) = \frac{1}{2 i} \sum_{k=-n}^{\infty} a_k \frac{\frac{\omega_{\theta}^2}{2} + i \zeta_{\theta} \omega_{\theta} \omega_k}{a \omega_{\theta} \sqrt{1 - \zeta_{\theta}^2}}$$

$$(e^{i} \mathcal{I}_{k} - 1)$$

$$-\frac{e^{i(\omega_{k}t+\int_{k})}-e^{i\phi_{k}}e^{-\omega_{\theta}}(\zeta_{\theta}+\sqrt{\zeta_{\theta}^{2}-1})t}{\omega_{\theta}(\zeta_{\theta}+\sqrt{\zeta_{\theta}^{2}-1}+i\omega_{k}}$$

. 7.7

The solutions 7.6 and 7.7 are random functions which represent the response of a linear system to random inputs. However, it is not these responses that are of direct concern but rather the significant characteristics of vehicle motion that can be inferred from their statistical properties. One can perform statistical analyses on Y(t) and Y(t) to determine their means, variances and covariances. The same can be accomplished for the velocities Y(t) and Y(t) and for the accelerations Y(t) and Y(t). Complete analyses of the statistical properties of the responses are presented in Section V, Reference 11. Expressions for

$$E\left[(Y(t) + \frac{g}{\omega_{y}}^{2})^{2}\right]$$
 and $E\left[(\Theta(t)^{2}\right]$

as well as expressions for the covariance and power spectral density of $\dot{Y}(t)$ are derived and presented.

Of direct interest is the time frequency form of the spectral density $P_{\overset{\bullet}{Y}}(\omega)$ of the vertical acceleration $\overset{\bullet}{Y}$ (t) of the c.g. of the frame. It is convenient to quote a form of this similar to the second of Equation 6.26 in the earlier section of this paper. It is obtained by a slight modification of Equation 45 of Reference 11.

$$P_{Y}(\omega) = \frac{\omega_{y}^{4}(\frac{\omega}{\omega_{y}})^{2} \left[1 + \cos(\omega + \frac{\omega}{\omega_{y}} + \frac{v_{0}}{v})\right] (1 + 4 \zeta_{y}^{2} + \frac{\omega^{2}}{\omega_{y}^{2}})}{2 \left[(1 - \frac{\omega^{2}}{\omega_{y}^{2}})^{2} + 4 \zeta_{y}^{2} + \frac{\omega^{2}}{\omega_{y}^{2}}\right]} P_{Y_{0}}(\omega)$$

. 7.8

where

$$\mathbf{v}_{\mathbf{o}}$$
 = Reference velocity

and $P_{Y_0}(\omega)$ is now the time frequency form of the power spectral density of $Y_0(x)$. The physical interpretation of the remaining parameters in 7.8 is

v = forward velocity of the vehicle.

 $\omega_{\mathbf{v}}$ = angular natural frequency in vertical translation.

 ζ_y = fraction of critical damping present in vertical translation.

 \mathcal{L} = distance between followers

Our interest in $P_{\frac{\omega}{Y}}$ (ω) is motivated by its possible significance to the comfort of a rider sitting at the c.g. of the vehicle frame. It was felt that one limit on the velocity of a vehicle set by driver (or rider) comfort. As soon as a driver reaches a velocity which bounces or shakes him with sufficient violence to cause discomfort, he reduces his velocity. Bouncing and shaking are related to the vertical displacement (and or acceleration) of the seat. Our attention for the moment will be directed to $\mathring{Y}(t)$, hence $P_{\mathring{Y}}(\omega)$. If some quantitative characteristic of $P_{\mathring{Y}}^{\omega}(\omega)$ could be related to driver comfort, it would

then form a possible criterion for determining a limiting velocity of a vehicle traveling on a rough surface, and such a criterion could then be used to study the effects of various vehicle parameters on limiting velocity.

A hypothetical example to illustrate the point is presented in Reference 3, supposing that driver comfort limits forward velocity whenever the maximum of $P_{\stackrel{\bullet}{\gamma}}(\omega)$ reaches some limiting value regardless of where this maximum occurs in the frequency (ω) range. The question posed is: what is the influence of the follower base length, λ , on the limiting velocity?

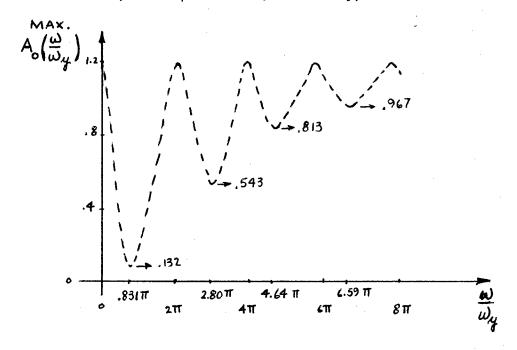
Taking a reasonable form for $P_{Y_o}(\lambda)$, namely

$$P_{Y_0}(\lambda) = \frac{\sigma_{Y_0}^2}{\lambda_0 \sqrt{2\pi'}} \quad e^{-\frac{\lambda^2}{2\lambda_0}} \qquad ... \qquad 7.9$$

where $\sigma_{\mathbf{X}_0}^2$ is the variance of $\mathbf{Y}_0(\mathbf{x})$ and λ_0 is a parameter that measures the spread of $\mathbf{P}_{\mathbf{Y}_0}(\lambda)$ about its maximum value which occurs at $\lambda=0$. We may write 7.8 as

We are interested in the maximum of $A_0(\frac{\omega}{\omega_y})$ as a function of d, since by the first of $7\cdot 1$, this is the only parameter containing ℓ . It is clear that for various choices of the parameters, $A_0(\frac{\omega}{\omega_y})$ will have different graphs. In particular, the maximum value of $A_0(\frac{\omega}{\omega_y})$ over the entire range of $\frac{\omega}{\omega_y}$ will change with changes in the parameters.

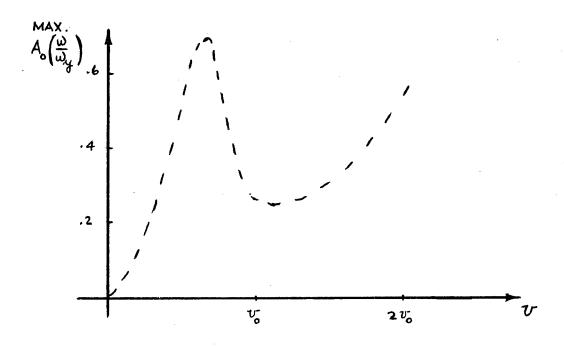
If we let the model vehicle have velocity $v=v_0$, with $\beta=1$ and $\zeta_y=\frac{1}{4}$, the maximum of $A_0(\frac{\omega}{w_y})$ as a function of $\frac{\omega}{w_y}$, for values of δ , would plot like (Reference 3):



 There are three features of the above figure which call for comment. The first is the large ratio between the largest and smallest values of the maximum of $A_0(\frac{\omega}{\omega_y})$, namely, $\frac{1.2}{.13} = 9$. Thus, follower base length, ℓ , is an important variable in determining limiting vehicle velocity if the limit on driver comfort is set by the maximum value of P. (ω). The second interesting feature is the sharpness of the minimum. That is, for a given $\zeta_y = \frac{1}{4}$, $\beta = 1$, the maximum of $A_0(\frac{\omega}{\omega_y})$ as a function of $(\frac{\omega}{\omega_y})$ is a minimum when $\alpha = \frac{1}{\sqrt{2}} = \frac{1}{$

It is interesting to note that since $\beta = \frac{\lambda_0 \omega_0}{\omega_y} = 1$, $l = .831\pi \frac{v_0}{\omega_y}$ also can be written as $l = .831\pi/\lambda_0$. Suppose we take $l = \pi \frac{v_0}{\omega_y}$ which almost minimizes the maximum value of

 $A_0(\frac{\omega}{y})$ and determine how changes in v in a certain range affect the peak value of $A_0(\frac{\omega}{w_y})$. Keeping $\zeta_y = \frac{1}{4}$, $\beta = 1$, the results would look like the following plot (Reference 3).



Observe that the minimum of the maximum values of $A_0(\frac{\omega}{wy})$ occurs slightly above $v = v_0$ and the peak of the maximum values of it occurs at v = .60 v_0 and has the value .670. Thus, for $l = \pi \frac{v_0}{wy}$, the maximum of $A_0(\frac{\omega}{wy})$ will remain near its minimum value for v in the range $(.95 \ v_0$ to $1.45 \ v_0)$. This suggests that for l near $.831 \ \pi \frac{v_0}{wy}$ it might be possible to come up to the velocity v_0 where the peak of $A_0(\frac{\omega}{wy})$ is almost a minimum without encountering as severe a peak as would occur with, say $l = .193 \ \pi \frac{v_0}{w_0}$.

Now let us suppose that the maximum value of P. (ω) consistent with driver comfort is known and that the length of \mathcal{L} , \mathcal{L}_y , \mathbf{w}_y , \mathcal{L}_y ,

calculation of limiting velocity of a given vehicle (of the type described, idealized and linear) traveling on a road or track of roughness specified by 7.9. Obviously, other forms for $P^{\bullet,\bullet}(\lambda)$ than given by 7.9 can be used without difficulty as can different limits on $P^{\bullet,\bullet}_{V}(\omega)$ instead of the constant values used.

While the hypothetical example produced some very interesting results concerning the possible significance of follower wheel base length as a significant parameter in establishing limiting velocity of a vehicle moving on rough ground, these results are necessarily tentative because of lack of experimental information. Still to be assessed are the effects of the other parameters. Also, a justification for use of many of the assumptions will have to be verified. It is apparent that much experimental work and careful analyses of the data will be needed before many of the indeterminancy can be removed. Questions such as the form of the power spectral density of ground roughness $P_y(\lambda)$, can only be solved by the analyses of actual ground survey data. As mentioned earlier, the survey data collected at the various army installations will aid us in establishing a more accurate form for $P_{y_i}(\lambda)$. The question of how well the idealized model represents the true vehicle can only be answered by comparing the results from actual field experiments with real vehicles. Here again, the data collected at one of the surveyed sites will aid us in determining the adequacy of the model and direct us in the modifications that will be necessary to give us a more accurate prediction. If now one assumes that ground roughness and vehicle response can be satisfactorily described, one obstacle remains to be hurdled, the involvement of man. In this study of vehicle ride characteristics, only he can determine whether a ride is smooth or rough and thus set the criteria which must be satisfied by the designer of the vehicle.

Reference 12.

Two phases in the vehicle ride characteristic study have been discussed up to now, the description of terrain roughness in quantitative terms and the use of the measurable roughness in describing simple vehicle motion. The third phase, the involvement of man in the study of vehicle motion, may be the most complex. The smoothness or roughness of a ride is a subjective evaluation by individuals experiencing the vibratory conditions and in dealing with humans, physiological as well as psychological factors must be considered. To be able to identify a ride condition as being rough, a criterion or criteria for ride roughness must first be established. The first step necessary in establishing criteria for ride from the driver or

or rider viewpoint is the establishment of a measurable relationship between the quantitative characteristics describing the motion of a vehicle and the subjective appraisal of this motion by man. If measurable characteristics of vehicle ride can be related to vehicle driver or rider comfort, this criteria could then be used to study the influence of various vehicle parameters on the ride and will direct the changes needed to make the ride more acceptable.

The ultimate aim of the studies, as stated earlier, is to develop a method of designing vehicle suspension systems whereby off-road vehicle speeds be increased. Maximum speed is largely a function of the driver's or rider's evaluation of his own ability to withstand the vibrations and violent motions associated with increased speeds over rough terrain.

It, therefore, became apparent that a "People Shaking" program be designed whereby the effects of random vibrations on man could be assessed. In our studies, by the nature of the quantitative description of roughness, the first question that needed to be answered was, "Is the human subject able to distinguish between member functions having the same spectral properties?", realizing that there could be an infinite number of member functions all having the same psd but each having point to point differences. The next question to be answered was, "Can member functions with different psd's be distinguished?"

The problem under investigation in general reduces to one of quantifying two different categories of events, one physical and the other psychological and of establishing quantitative relationships between the two. Once this information is quantified, an attempt can be made to establish an empirical relationship between these data and the various parameters of corresponding power spectra. Subjective evaluations, once quantified and related to psd, can then be used to determine necessary vehicle parameter changes for reducing objectionable vehicle vibrations. In addition, such information could be used to predict, within a measurable experimental error, maximum operating speeds over rough terrain.

Initially, some problems in experimental proceedures had to be resolved. First, the input vibration condition must be controllable and of known characteristics. To meet this need, the input member functions were machine generated. Although control of the input conditions could be attained, in answering the question whether member functions with the same psd be distinguishable, different segments of a vibration may have psd estimates that are different from one another; it is only when the record length becomes infinite that they are assumed to coincide. Therefore, the finite lengths of

the records may cause differences in the psd's to arise. Then, how long should the segments be? Two opposing requirements were recognized: First, the exposure had to be long enough to present a representative sampling of the random vibration condition. However, with the method selected for analyzing the results, if the exposure was too long, the subject may have trouble remembering the sensations perceived from previous conditions. Agreement was reached on a one minute exposure time, more or less on an arbitrary basis, with modifications later in the experiment if required.

Having established the objective of quantifying subjective appraisals of vibration intensity, the problem becomes one of selecting a scaling method that is most appropriate. The desired results of the scaling process in the early stages of the investigation were quantitative indices (based on qualitative judgement) of the various vibration conditions on a linear scale that approximates equal interval properties (i.e., numerically equal distances stand for empirically equal distances in perceived intensity of vibration). No anchor or psychological zero points were established, so it is not possible, without further extension of the method, to say that intensities above a given value is perceptible, annoying, alarming, etc.

Two distinct approaches to the quantification of psychological events, each with its advantages and disadvantages, seemed appropriate in our case. Of the two methods, that of paired comparison makes the least demanding assumptions concerning human observational powers. All stimuli to be scaled are presented to the subject in all possible The subject is required only to judge which one of the pair of stimuli is of greater quantity on some defined dimension. In the present case, the dimension is that of intensity. The chief limitation of this method is the number of observations required. With n different vibration conditions, there are (n)(n-1)/2 possible pairs. For n = 10 stimuli there are 45 pairs; for n = 20 stimuli conditions there are 190 possible pairings. A method of analyzing paired comparison experiments suggested by Sheff'e in the American Statistical Association Journal, September 1952, several advantages over the traditional paired comparison methods are offered. The negative time order error (i.e., other things being equal, the second member of a pair being perceived as more intense than the first) is not included in the scale values using the Sheffe method. Another advantage of this approach is that it affords the opportunity of testing the hypothesis of subtractivity, analogous to the hypothesis of additivity in the two-way layout. This hypothesis states roughly that the results for any pair, after order effects are eliminated, can be attributed entirely to differences of the main effects of the two vibration conditions in the pair.

As far as testing procedure is concerned, the Sheffe method requires one modification over the paired comparison method. Instead of reporting one member of the pair as being rougher than another, the subject also indicates how much rougher. The possible responses of the subject are:

1 was moderately greater than 2

1 was only slightly greater than 2

No differences could be detected

2 was only slightly greater than 1

2 was moderately greater than 1

The experimentor converts these preferences to a numerical score. When the subject responds that no differences could be detected, he is asked "If you had to make a choice, which would you say was the rougher?"

The other approach is that proposed by S. S. Stevens of Harvard, which he calls "Magnitude Estimation". Not only is the method very simple, but Stevens claims it leads to the highest level of measurement recognized (ratio scaling). The method consists of exposing the subject to a vibration of a given characteristic and telling the subject to call the intensity of the particular vibration some number, say, 100. Vibrations with other characteristics are presented and the subject is instructed: "If the intensity of the first vibration was 100, what would you call the intensity of this vibration? Use any number that seems appropriate, fraction, decimal, whole number - but try to make the number proportional to the intensity as you feel it."

The first question to be answered was whether individuals could differentiate between two vibration conditions, both having the same psd. In an attempt for an answer, six member functions with the same psd's were generated. The method of generation was to set fifteen (15) sine-wave generators to specified frequencies and one constant amplitude and randomize the phase relationship between them. Each of the six member functions consisted of the sum of sine waves at frequencies of 6.28, 7.28, 8.28, . . . , 20.28 radians/seconds (1.0 - 3.5 cps). The six member functions are shown in Figure 1. Six subjects were exposed to all possible pairs of the six-member functions, 30 pairs in all, and the data were analyzed using the modified paired comparison technique suggested by Sheffe. One member function, No. 2, was perceived as being significantly more intense than the others, with only small differences between the remaining five conditions.

	to I Stratefficated suffers - Str - age of			1 2 2 2 2 2 2 2 2 2 2 2 2 2 2 2 2 2 2 2	te destruction administration of the second second		1
	}				Morris		
WYWW.	Nr J. J.	Mond	Mylm	√√vvv~	Marall		
Wyw.	W/W/W	J.M.	Johnson	Moonly	VIMM		
	W. J. Vicam		J. J	MV M	Svw		
MM	MAJAM			Aleman .	W.M.		
January W	W. C.		MW(V)		Ww-w		
Z Z	My Jym	V. M. Morry		Arvolton, and a	MMM		
Now Mary	MATTA	M. M. Marine	Mymm	(Mary Jary)	W/w-m		
L/Crown	Modum	NVMM	سالهاكها	Walker	NVVIMM		, i
w/w/w/w	NVW V	Myran	Moham	MVVML	Mount		
JW/_J/J/	prody/rod	~ (V ^a 6)	No. No. No.	r.v.l	WWW.		1
Mony	MMIN	Moor	Morrand	Moody	MMm		
Mylym	Mondy	Mwy/hwW	WYVW	My In-In	Moder		. 4
Morry	Month	Morralla	Mr. Aronny	Mindle	www		
Wall.	Norm	Mrra	Jahan	J.M.M.	W. J. W.		
Moram	Mary James	Morrow	(Months of	. Mwy	Month		
- Andharas	Mww	Mondy	Johnston	NWW No-	man		
M-7/W2	my lawin	And profile or the transport of the condition of the cond	Lamor		JWW-JW		
July July	M. Marya	Www.W	WW.	www.dylphow	2)\5\max		
Individual production of the more of the m	ward war of the transford of the state of th	*	THE WAY WAY OF THE WAY		VINOWANDOWNANDO		
100 to 1 t	1 1	* * ! *		1	1 .	• 1	

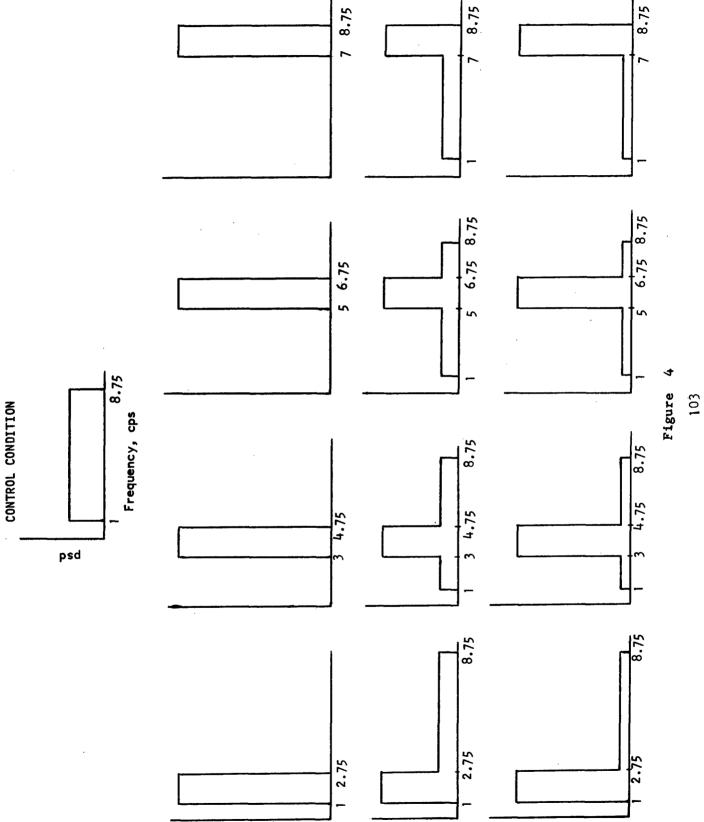
iillista liberkillis lihalisee iillisliski	War-way flow with	Samuel Am	
edellisti istematik filosopolisti edellisti istematik filosopolisti	v-vollo-vollo-vollo	SA PARAMANA AND AND AND AND AND AND AND AND AND	
	W. Word Word William	Tahaha Ananan ang ang ang ang ang ang ang ang an	
	moderal Magazillary	A Transaction of the state of t	
	WWW.WWW.		
	MANNIANATAVVVV		
	Confliction (All All All All All All All All All Al		
	And.		
		Mily Many Many Many Many Many Many Many Man	Constitution of the second constitution of the s

Figure 3

The consistency of judgement was remarkable, considering the nature of the task presented to the subjects. The 30 pairs of conditions were separated into an AM and PM session of 15 pairs each. After five pairs had been presented, the subject was allowed to relax and walk around for five minutes. There was a 35-40 second interval between presentations, the time needed to select the next condition, and the total time for one sitting of a subject averaged about one hour. No subject was tested with both AM and PM sessions in one day. Each volunteer subject received medical approval from the installation medical director to participate in the program. On the scheduled date of testing, each subject was briefed on the aims of the experiment, a detailed description of the procedure, and the requirements and duties as a subject.

A follow-up experiment was conducted to investigate the effects of changing the total power of the member functions. Using five of the member functions presented in the first experiment, member functions that were originally perceived as being the most intense, Nos. 1, 2, and 3, were presented at the same gain setting (total power), while two of the others that were perceived as being the least intense, Nos. 4 and 6, were increased in total power by 25% over the original setting, Figure 12. It was found that by changing the total power slightly, the ordering of the member functions as to intensity was significantly changed. Member functions increased by 25% were definitely perceived as being more intense.

Following the preliminary tests, the question presented itself: Is the difference in member functions small enough, when compared to the differences across conditions with different psd's to make the psd a useful description of the intensity of a vibrational condition? Fortunately, the answer to the preceding question appears to be "yes". Differences between two member functions having the same psd are relatively small when compared to differences in member functions with varying psd's. In a second experiment, the psd of the member function was varied. Two member functions from three different psd's were generated. All member functions contained the same number of frequency components. Spectrum I remained the same as for the previous experiments, with fifteen components in the 1.0 - 3.5 cps range. each component at the same amplitude. Spectrum II contained fifteen components in the 3.5 - 7.0 cps range with the amplitudes of the components equal to the Spectrum I amplitudes. Both of these have a flat spectrum in their respective frequency banks. Spectrum III contained the same frequency components as Spectrum I, but the amplitudes were varied so that the shape of the spectrum was ramp-like or triangular. The total power in each of the spectra was the same. These input waveforms are shown in Figure 3. A definite trend was noticed when the subjects were exposed to these vibratory conditions. As the range of frequencies moved up, the perceived intensity increased



Voltage and Frequency Settings for Sine Wave Generators

Used to Generate Random Voltages that Served as Forcing

Functions for the Ride Dynamics Simulator

RIDE NUMBER

Frequency Component (cps)	1	2	3	4	5	6	7	8	9	10	11	12	13
1.00	3#	12				6	9:	2	1	2	ì	. 2	1
1.25	3	12			•	6	9 :	2	1	2	1	2	1
1.50	3	12		•		6	9 .	2	1	2	1	2	1
1.75	3	12				6	9	2	1	2	1	2	1
2,00	3	12	1.			6	9	2	1	2	1	2	1
2.25	3	12	.*	,		6	9	2	1	2	1	2	1
2.50	3	12		9	,	6 :	9	2	1	2	1	; 2	1
2.75	3	12	;			6	9	2	1	2	1	2	1
3.00	3		12	*		2 + 2	1	6	9	2	1	2	1
3.25	3	٠	12			2 ·	1	6	9	2	1	:2	1
3.50	3		12		***	2]	1	6	9	2	1	. 2	1
3.75	3		12		4	2	1	6	9	, 2	1	2	1
4.00	3	-	12		ŝ	2 ₂₀₀	1	6	9	2	1	2	1
4.25	3		12			2 50	1	6	9	.2	1	2	1
4.50	3		12			2	1	6	9	2	1	2	1
4.75	3		12			2	1	6	9	2	1	# 2	1

*Entries in the table represent amplitudes (in volts) of the indicated frequency componets of the various vibration conditions (rides).

Figure 5.

RIDE NUMBER

Frequency Component (cps)	1	2	3	.4	5	6	7	8	9	10	11	12	13
5.00	3		•	12		2	1	2	1	6	9	2	1
5.25	3			12		2	1	2	1	7	9	2	1
5.50	3			12		2	1	2	1	6	9	2	1
5.75	3			12		2	1	2	1	6	9	2	1
6.00	3			12		2	1	2	1	6	9	2	1
6.25	3			12		2	1	2	1	6	9	2	1
6.50	3			12		2	1	2	1	6	9	2	1
6.75	3			12		2	1	2	1	6	9	2	1
7.00	3				12	2	1	2	1	2	1	6	9
7.25	3				12	2	1	2	1	2	1	6	9
7.50	3				12	2	1	2	1	2	1	6	9
7.75	3				12	2	1	2	1	2	1	6	9
8.00	3				12	2	1	2	1	2	1	6	9
8.25	3				12	2	1	2	1	2	1	6	9
8.50	3				12	2	1	2	1	2	1	6	9
8.75	3				12	2	1	2	1	2	1	6	9

Figure 5, Cont'd.

Also, in the same frequency band and with equal area under the spectral density curve, a flat spectrum was more bothersome than a ramped spectrum.

Based on information gained from the preliminary investigations, an experiment was designed to vary the parameters of the psd's that were felt to influence perceived vibrational intensities. Thirteen different conditions, all equated for total mean square amplitude values, were generated. The spectrum of these conditions are shown in Figures 4 and 5. The first condition was a flat spectrum with 32 sine wave components, all of the same amplitude and varving in frequency from 1 cps to 8.75 cps, in steps of 1/4 cps. This was our control condition. The second group of functions were generated using eight sine waves of the same amplitude and covered the frequency bands: 1.0 - 2.75; 3.0 - 4.75; 5.0 - 6.75; and 7.0 - 8.75 cps. The remaining eight member functions were generated using 32 sine wave components but the level of background power relative to the frequency bands described was systematically increased. The third group had one-half the power in the frequency band of interest and the other half distributed among the remaining frequencies. The last group had 75% of the power in the band of interest and 25% distributed over the remaining frequencies.

In the preliminary investigations a modified paired-comparison technique, the more conservative of the two methods discussed, was used. Later, results from both methods were compared. Since the scales developed using the two different methods were highly comparable, the decision was made to use the method of magnitude estimation proposed by Stevens, since it represents a considerable savings in the number of experimental observations required. In the analysis of the initial data, a definite ordering effect was found to be present. That is, everything else being equal, the second vibration condition was perceived as being more intense than the first. Such ordering effects are fairly common in psychological scaling using the paired comparison method and the method of analysis allowed for the removal of this effect by presenting all possible pairs in both orders, i.e., two conditions, 1 and 2, were presented in the order 1-2 and also in the order 2-1.

As mentioned above, the second phase of the experiment was conducted using the method of magnitude estimation suggested by Stevens. The thirteen conditions described were presented to thirteen subjects at three levels of gain, for a total of 39 vibration conditions per subject. The variations in perceived intensity of the vibration due to the location of the frequency band or bands containing the greatest power relative to the rest of the spectrum, the relative spread of power across the frequency range of interest

Physical Description of Subjects

Subject	Age	Height	Weight	Occupation
1	24	61111	180	Civilian
2	25	5'7"	115	Civilian
3	46	5'11"	170	Civilian
4	40	5!10!!	146	Civilian
5	30	5'10''	145	Military
6	24	61111	175	Civilian
7	35	51911	201	Civiliaņ
8	27	51911	195	Civilian
9	22	51911	153	Civili a n .
10	22	51911	150	Civilian
11	24	5'10"	175	Military
12	25	51811	185	Military

Figure 6.

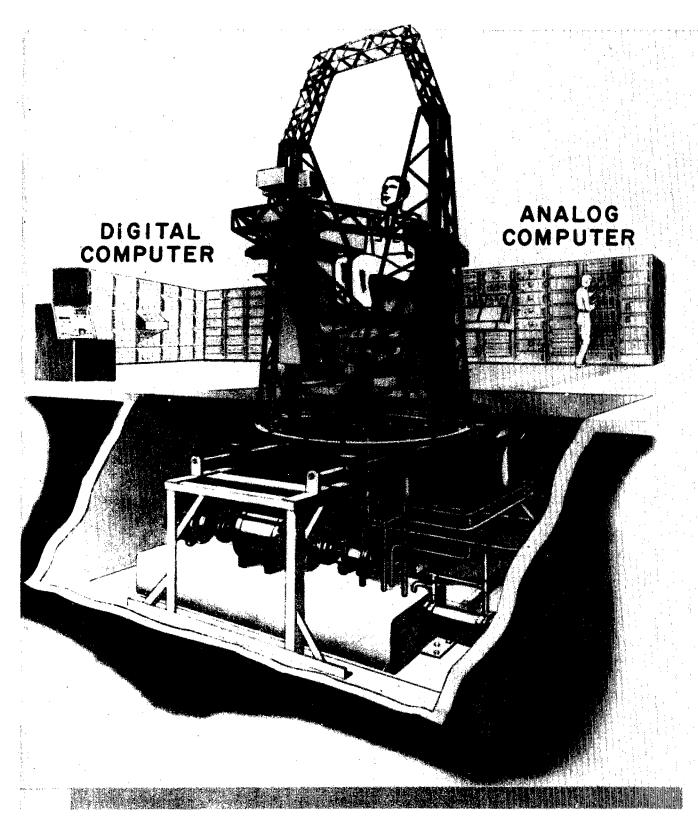


Figure 7.

SIMULATION

and the total power were investigated using a multi-factor analysis of variance scheme. Using the three parameters characterizing a single peaked spectrum, an attempt was made to develop a multiple regression equation whereby the perceived intensity of a vibration condition could be predicted, knowing the power spectral density characteristics of the vibration condition.

The thirteen subjects were divided into two groups of six subjects each. The thirteenth subject was one of the original twelve who completed a repeat of the experiment one week later to provide some information on the stability or repeatability of the scaling method employed. The data obtained from the first group of six subjects was used to develop the multiple regression equation and was cross-validated on the data provided by the second group of six subjects. The twelve subjects used in this phase of the experiment were male civilian and military employees of the U.S. Army Tank-Automotive Center. The subjects ranged in age from 22 to 46 years and in weight from 115 to 201 pounds. Figure 6.

The experimental equipment used in the study was the Ride Dynamics Simulator located at the U. S. Army Tank-Automotive Center, Warren, Michigan. The Simulator, Figure 7, is capable of motion in four degrees of freedom: bounce, pitch, roll and yaw, either simultaneously or singly in one direction. In the present study, only bounce (vertical motion) was employed. The Simulator is an electrically controlled, hydraulically powered feedback system. The input or command signal for the Simulator is a voltage and the seat will proportionally follow this voltage. The voltate may come from a standard signal generator or, as in our case, may be the output of an analog computer. The seat that actually vibrates is a modified U. S. Air Force F-101 Ejector Seat. Safety features were built into the Simulator that limits the maximum displacement. In addition. subjects were provided a "dead man" switch which they held in their hand while being exposed to the various vibrations. The subject was instructed that we could at any time stop the motion of the seat by simply releasing the switch or by a command to the seat operator through the intercom system. The seat automatically stopped when the seat displacement over-rode the maximum excursion limit switches.

On the day a subject was to serve, he was shown the simulation facilities, and the safety features of the apparatus were explained in some detail. The seat used was a hard plastic contour seat similar to those provided the drivers of tanks and armored personnel carriers. A standard type lap seat belt was adjusted to a loose position and the subject was then equipped with ear phone-microphone set for two-way communication between subject and experimenter. Instructions

Direct Magnitude Estimates of the Roughness
of 39 Vibration Conditions Obtained from 12 Subjects

SUBJECT

RIDE	1	2	3	4	5	6	7	8	9	10	11	12
1	Цж	5	4	8	2	3	2	3 -	2	5	5	3
2	3	8	2	3	3	2	2	5	2	6	3	2
3	7	13	. 5	6	10	12	8	9	12	6	5	6
4	8	10	12	15	13	18	12	12	3	8	12	6
5	11	16	16	22	20	15	11	15	18	14	13	12
6	5	7	2	4	4	6	3	2	3	· 3	5	4
7	4	6	3	5	5	4	2	3	5	4	2	4
8	4	5	4	5	7	7	3	3	4	5	12	4
9	4	5	4	6	8	6	6	5	6	3	6	4
10	5	8	5	7	3	7	6	5	4	4	4	4
11	8	15	7.	10	6	11	9	12	8	8	10	5
12	6	7	4	8	4	4	5	5	8	6	5	3
13	9	14	8	16	10	9	9	12	11	7	10	3
14	8	8	6	10	8	8	5	6	7.	6	4	5
15	5	6	2	3	5	3	7	5	7	7	3	5
16	9	12	7	9	9	12	12	15	15	7	18	7
17	12	14	15	20	19	21	13	20	15	11	20	13
18	15	25	16	25	22	22	15	20	20	18	22	13
19	5	12	4	9	9	9	9	5	10	7	4	5

Figure 8.

^{*}Entries represent the estimated magnitude of the roughness of a given vibration condition based on a control condition defined as having a roughness equal to 10 units.

SUBJECT

RIDE	1	2	3	4	5	6	7	8	9	10	11	12
20	6	9	3	5	8	5	8	5	5	5	7	4
21	7	10	6	10	8	10	10	7	8	10	9	3
22	6	9	5	6	8	8	7	5	4	12	4	6
23	10	10	7	10	9	12	5	8	7	11	10	5
24	10	14	12	9	14	15	12	14	11	9	12	12
25	9	10	13	12	10	9	10	15	8	9	8	4
26	13	17	13	25	15	15	12	20	13	14	16	9
27	8	13	7	12	10	15	9	13	12	9	12	7
28	3	10	4	4	2	4	6	8	8	6	5	4
29	12	20	17	12	12	16	13	15	14	12	15	12
30	17	30	18	35	20	25	14	27	25	25	25	15
31	16	50	20	35	25	30	18	30	30	30	27	14
32	8	14	6	11	11	11	10	17	9	15	5	5
33	7	10	3	4	5	9	12	8	8	8	9	4
34	8	15	9	18	9	9	10	15	11	12	10	8
35	11	30	8	8	12	12	10	9	13	11	9	7
36	12	14	14	10	12	15	12	18	20	12	18	9
37	16	45	16	30	20	18	13	22	20	16	18	12
38	12	16	14	25	15	18	12	17	16	12	18	12
39	17	30	20	30	18	20	16	20	18	20	22	14

Figure 8, Cont'd.

to the subject were read over the intercom and after it was determined that the subject understood his task, the first vibration condition was introduced. All conditions lasted for 60 seconds. The first vibration was the control condition. At the end of the first ride the subject was informed that he had just experienced a control condition defined to have a roughness equal to ten units on a roughness scale. The subject was further informed that his task was to rate the roughness of subsequent vibrations based on this control condition. He was allowed to use any number, fraction, decimal or whole, which he felt described the condition with reference to the control. Thirty seconds after the control condition ceased, the subject was exposed to a member of experimental vibration condition, each separated by a 30-second interval. During each interval the subject was asked to make a direct magnitude estimate of the roughness of the vibration he had just experienced, based on the control condition of ten units, Figure 8.

In one experimental session, the subject was exposed to all 39 vibration conditions with the order of presentation randomized. The control was presented at the beginning and subsequently after every fifth condition. After the tenth, twentieth, and thirtieth experimental condition the subject was allowed a seven minute rest out of the seat. An entire session lasted a bit over two hours. The twelve sessions (one for each subject) were conducted on six consecutive work days and one subject completed two sessions spaced one week apart. The noise level at the head of the subject varied between 90 and 95 decibels but this was undoubtedly attenuated by the earphones worn by the subject throughout the session. Room temperature and humidity were held constant at 76°F and 58% respectively. Civilian subjects wore ordinary street clothing and military personnel wore their U.S. Army Service Uniform with low quarter shoes. Care was taken to isolate the subjects from distracting conditions, however, he was still able to see the experimenter and some of the unrelated activity being conducted in the experimental area. Any information volunteered by the subject during a session was recorded. At the end of the session, the subject was asked if he had any comments about the experiment. The subject was asked not to discuss the experiment with anyone until the completion of the investigation.

There are several concepts of reliability that have been applied to psychological scaling data, Reference 12.

An estimate of the stability of a scale over time is provided by the correlation between two sets of ratings of the same objects rated by the same subject on two separate occasions. Another approach to the estimation of the reliability of a scale is to obtain some measure of internal consistency, i.e., a correlation of ratings obtained from different raters. Estimated Displacement Mean Squares of Bands of Frequency Components for Each of the 39

Experimental Random Vibration Conditions.

Frequency Band

Ride	1-3 cps	3-5 cps	5-7 cps	7-9 cps	Total Mean Square Displacement
1	47*	46	34	29	.02 in. ²
2	.16	50	38	31	.09
3	•39	.63	.44	31	.07
4	50	19	24	31	.04
5	50	52	35	.06	.04
6	36	48	33	30	.06
7	11	04	34	31	.07
8	44	30	35	30	.04
9	46	34	30	30	.04
10	48	47	02	30	.03
-11	48	42	36	29	.04
12	49	51	33	29	.05
13	49	51	26	22	•03
14	37	33	38	26	; = = =
15	2.25	52	35	31	
16	30	.91	.79	31	10
17	49	20	02	24	.04
18	50	52	30	1.23	.05
19	.04	32	33	29	÷ 406

^{*}Entries in the first four columns are the estimated mean square displacements (in standard score form) for the indicated frequency bands. The final column entries are the estimated total mean square displacements for the respective rides.

Figure 9.

Ride	1-3 cps	3-5 cps	5-7 cps	7-9 cps	Total Mean Square Displacement
20	.14	46	33	31	.09 in. ²
21	32	09	13	18	.05
22	34	.86	33	31	.06
23	41	38	06	25	.04
24	46	26	.71	29	.07
25	47	45	31	22	.04
26	48	49	21	08	.04
27	32	20	13	17	.07
28	3.54	52	38	31	.20
29	1.32	5.05	38	31	.25
30	33	27	5.72	.17	.18
31	43	52	38	5.71	.11
32	1.86	.23	09	07	.09

-.38

-.24

-.24

.03

1.05

-.08

-.06

-.31

-.24

-.22

-.22

-.26

•53

1.04

3.15

-.21

-.29

-.37

-.43

-.30

-.43

33

34

35

36

37

38

39

2.12

.62

.86

-.22

-.08

-.26

-.44

.14

.08

.08

.09

.13

.04

.06

Frequency Band

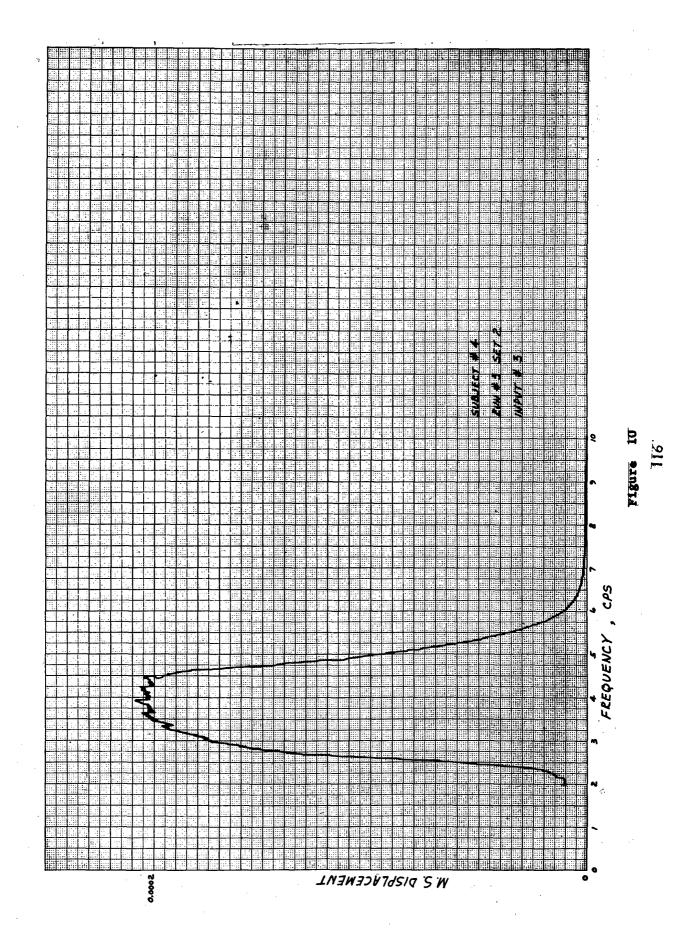
Figure 9, Cont'd.

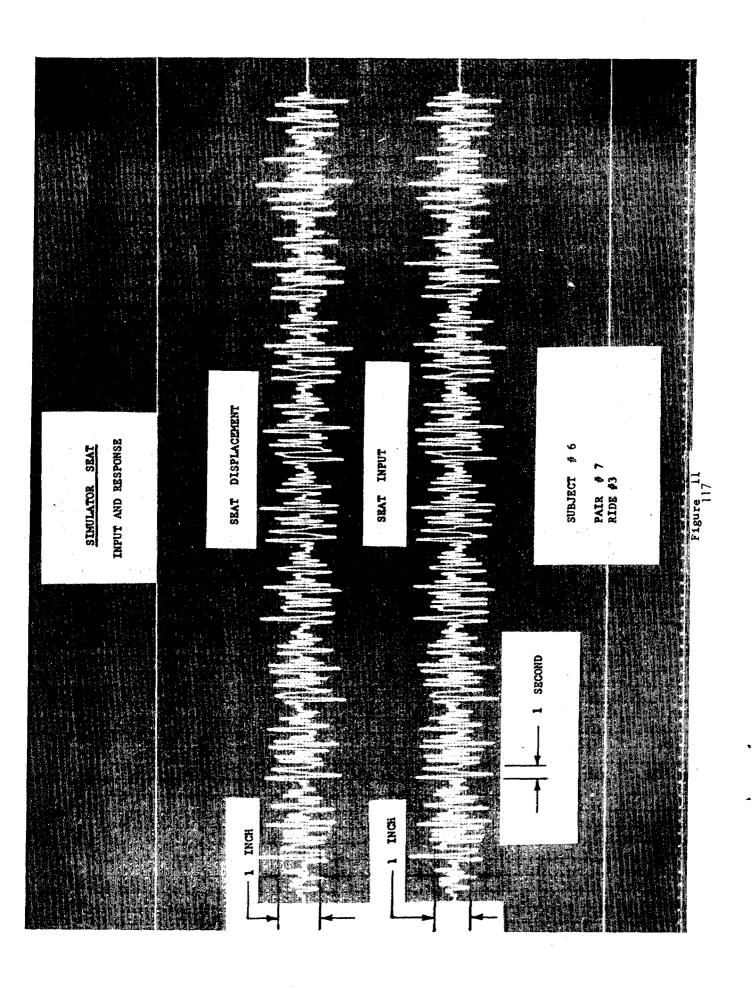
To provide an estimate of the stability of the roughness scale, the data from the subject was repeated. The experiment one week after his first exposure was used. An attempt was made to hold all conditions constant for the two administrations with the exception of the order of presentation of the vibration conditions. The product moment correlation between the scale values obtained for this subject on the two separate occasions was $\mathbf{r}=.919$, significantly different from zero at the .01 level.

Internal consistency estimates were based on a variance analysis proposed by Winer (1963). The average reliability of a single rating in the first group was $F_{11} = 707$. A similar estimate for the second group was $F_{11} = .727$. Estimates of the reliability of the average of six ratings were $F_{11} = .935$ and $F_{11} = .941$, respectively for the first and second groups (Reference 12).

To provide information on the actual displacement of the seat of the simulator, seat motion for the entire session of one subject (Subject 3) was recorded and analyzed to obtain estimates of the displacement power spectrum for each ride. This analysis made it possible to estimate the average mean square displacement of bands of frequency components. Four such averages, one for each of the four 2 cps bands between 1 and 8.75 cps were estimated for each ride, Figures 9 and 10. Similar displacement analyses were performed on the control ride to which the subject was exposed on seven different occasions during the session. The input signals for this control was identical so that the reliability of the simulator to faithfully reproduce a given input can be judged. An average inter-correlation of the four mean square estimates on each of the seven occasions was calculated. The obtained correlation was F_{11} = .98, significantly different from zero at the .01 level. A typical recording taken during one of the preliminary tests is shown in Figure 11.

In our attempt to develop an equation to predict the intensity of vibration conditions, a major hypothesis was that the roughness of random, whole body vibration is dependent both on the frequency and amplitude of major components of the vibration. To determine if mean square displacement alone would account for a significant portion of the variability of the roughness ratings, a product moment correlation was computed between the 234 ratings provided by Group I and the corresponding estimates of the total mean square displacements of vibration conditions measured with a true root-mean square meter. The obtained correlation was small (r = .15) but significantly different from zero at the .05 level.





Next an attempt was made to estimate perceived roughness of a linear combination of the estimated mean square displacements of the four frequency bands described previously. That is:

$$\hat{y} = \beta_1 x_1 + \beta_2 x_2 + \beta_3 x_3 + \beta_4 x_4 \dots 8.1$$

where \hat{y} = Predicted roughness rating in standard score form

 X_1 thru X_4 = The estimated mean square displacement of the 1-3, 3-5, 5-7, and 7-9 cps components.

 β_1 thru β_4 = Multipliers or weights which give the best linear combination of the several mean square estimates.

The best set of weights was defined as that set of weights which would minimize the sum of squares of the discrepancies between the predicted ($^{\circ}$) and obtained (y) ratings, i.e.,

$$(\hat{y} - y)^2 = a minimum.$$

The obtained multiple prediction equation:

$$y = -.136 X_1 + .321 X_2 + .383 X_3 + .554 X_4 ... 8.2$$

provided an uncorrected multiple correlation coefficient between predicted and actual ratings or $R_{y\ 1234}=.698$, significant at the .01 level. The developed prediction equation was cross-validated on the data provided by Group II. The cross-validated multiple regression coefficient of .718 was also significantly different from zero at beyond the .01 probability leve, (Reference 12).

From the results of the experimental program conducted to date, a few conclusions have been tentatively drawn:

- 1. Direct magnitude estimation provides a useful method for quantifying the subjective intensity of random vibrational conditions experienced by humans.
- The partitioning of total mean square displacement into components associated with bands of frequencies provides

a set of variables, which when properly weighted, predicts the roughness of a vibratory condition.

The results of the concluded experiments have proven encouraging, but still leaves many questions unanswered, both of a theoretical and of a practical nature. The experiments to date had been conducted with the motion in the vertical mode only. We feel that two other modes of motion, pitch and roll, will have to be investigated, both singly and in combination with vertical motion, before the quantity called roughness can be more totally defined. Another point needing investigation is the contribution of frequency components above 8.75 cps on the perceived intensity of random vibrations. Still another question is, how well does the simulated waveforms used in the tests resemble the profiles to be encountered in the field? Also, can roughness be defined in terms of the derivatives of displacement, specifically the acceleration?

Our aim is to define the undesirable characteristics of vehicle vibration which limits the maximum off-road speed of a vehicle. Another phase of the human studies which will have to be included, is the effect of these undesirable vibration characteristics on the performance of tasks by the occupants, such as driving and sighting. In other applications of the vehicle, the effects of the vibration on non-human occupants, such as cargo or instruments, may be the important consideration. These are some of the unanswered questions. In the end, if a relationship can be established between specific terrain profile characteristics and the undesirable effects on man and cargo, how can the vehicle characteristics be altered so that the objectionable quality of the ride be minimized? These questions reveal how closely the three elements of the terrain-vehicle-man complex depend upon one another. It is evident that the studies of this problem of increasing vehicular speeds over hard off-road terrains must be a paraleling and simultaneous attack on the individual elements of the complex before significant advances can be made. feel that inroads have been made in answering questions on vehicle ride characteristics but we also feel that much more needs to be done in the form of experiments and careful analyses of the results to augment and modify the theoretical considerations, before we can say with a fair degree of assurance that "good" ride in a vehicle can be built into a vehicle on the drawing boards.

REFERENCES

- Kozin, F., Cote, L. J. and Bogdanoff, J. L, "Statistical Studies of Stable Ground Roughness", Land Locomotion Laboratory Report No. 95, USATAC, Warren, Michigan, November 1963.
- 2. Bogdanoff, J. L., and Kozin, F., "Behavior of a Linear One Degree of Freedom Vehicle Moving with Constant Velocity on a Stationary Gaussian Random Track", Land Locomotion Laboratory Report No. 48, USATAC, Warren, Michigan, February, 1959.
- Bogdanoff, J. L., and Kozin, F., ''On the Statistical Analysis of the Motion of Some Simple Vehicles Moving on Random Track', Land Locomotion Laboratory, Report No. 65, USATAC, Warren, Michigan, 1959.
- 4. Moyal, J. E., "Stochastic Processes and Statistical Physics", Journal of Royal Statistics Society, Ser. B, Vol. II, p. 150, 1949.
- 5. Cramer, H., "Mathematical Methods of Statistics", Princeton University Press, Prince
- Rice, S. O., 'Mathematical Analysis of Random Noise', Bell System Technical Journal, Vol. 23, pg. 282 and Vol. 24, pg. 26, 1944 and 1945.
- 7. MacRoberts, T. M., and Gray, A., "A Treatise on Bessel Functions", MacMillian and Company, London, 1952.
- 8. Laning, J. H., and Battin, R. H., 'Random Processes in Automatic Control', McGraw-Hill Book Company, New York, 1956.
- 9. Rice, S. O., 'Mathematical Analysis of Random Noise, Selected Papers on Noise and Stochastic Processes', Edited by N. Wax, Dover Publications, New York, 1954.
- 10. Cartwright, D. E., and Longuet, Higgins, M. S., "The Statistical Distribution of the Maxima of a Random Function", Proc. Royal Society of London, Ser. A., Vol. 237, pg. 212, October, 1956.
- 11. Bogdanoff, J. L. and Kozin, F., ''On the Behavior of a Linear Two Degrees of Freedom Vehicle Moving with Constant Velocity on a Track Whose Contour is a Stationary Random Process', Land Locomotion Laboratory, Report No. 56, USATAC, Warren, Michigan, 1959.
- 12. Holland, C. L., Jr., "Human Response to Random Vibration", A Thesis submitted to the Faculty of Purdue University in partial full-fillment of the requirements for the Degree of Doctor of Philosophy, August, 1964.

STATE OF THE ART OF THE ANALYSIS

OF SOFT SOIL PERFORMANCE OF WHEELS

By: Z. J. Janosi

BACK GROUND:

Much has been done since the publication of Research Report No. 5 on the problem of wheels operating in soft soil. A number of papers were presented at the First International Conference on the Mechanics of Soil-Vehicle Systems in Turin (Italy) in 1961. These presentations represent the various avenues that have been explored to approach a solution which could be regarded as a new yardstick since Bekker's first book was published (1). Further work since the International Conference involved normal and shear stress measurements along the wheel-soil interface surface and the investigation of the "slip-sinkage" problem. In spite of all these efforts, no major breakthrough has been achieved since Bernstein, Goryatchkin, Garbari, and, more recently, Bekker worked out the mechanics of the rigid wheel-soft soil system on the basis of an expression in the form of

$$p = kz^n \qquad \dots \qquad 1.$$

where p is the normal pressure along the soil-wheel interface; z is the sinkage at the point where the pressure, p, acts; k and n are soil parameters.

The lack of really significant new results can be explained by the fact that the problem is the most difficult of the basic problems of land locomotion mechanics. For the sake of completeness, results reported in Research Report No. 5 and other Land Locomotion Laboratory publications will be briefly discussed.

When analyzing the equilibrium of a rigid wheel, Bekker arrived at the following equations. The sinkage of the wheel, z, is (1):

$$z = \left[\frac{3W}{(3-n) \text{ bk } \sqrt{D}}\right]^{\frac{2}{2 \text{ n}+1}} \dots 2.$$

where W is the load, b is the width of the wheel, D is the diameter.

The motion resistance due to soil compaction (R_c) may be written as:

The following assumptions are involved in Equations 2 and 3:

- a. Side-wall friction is negligible.
- b. The problem is two dimensional; p is constant across the wheel.
- c. The ground contact area extends from the undisturbed soil level to the bottom of the wheel.
 - d. Shear-stresses or tangential stresses are negligible.
 - e. $x \approx x^1$ (See Figure 1).
 - f. Only two terms are taken of the series expansion of

$$z - (z_0 - z)^2$$
.

- g. Sinkage does not depend on slip.

Substituting Equation 2 into Equation 3 one obtains:

$$R_{c} = \frac{1}{n+1} \left[\frac{3W}{(3-n)\sqrt{D}} \right]^{\frac{2}{2} \frac{n+2}{n+1}} \left(\frac{1}{bk} \right)^{\frac{1}{2} \frac{n+3}{n+1}}$$

Equation 4 implies that:

- a. Resistance is proportional to the load.
- b. It is inversely proportional with the diameter and the width, D having the stronger influence.
- c. The harder the soil is, the smaller the resistance becomes.

Research Report 5 also included some results on a low inflated towed tire, References (2), (3). It was shown that the sinkage is

where p_i is the inflation pressure and p_c is an empirical "pressure" which has to be included due to the stiffness of the carcass.

The resistance for this case may be expressed by Equation 3: the term z, however, will be represented by Equation 5 and not Equation 2.

It was shown that there exists a critical inflation pressure above which the tire acts as a rigid wheel in a given soil and below which the bottom of the tire deforms. This gives rise to a larger ground contact area, thus, less sinkage and, hence, less resistance than that which a rigid wheel would encounter. The lower the inflation pressure, the less the compaction resistance becomes. On the other hand, the resistance due to tire flexure increases. These opposite trends result in an optimum inflation pressure at which the resistance is minimum. The optimum inflation pressure is too low, however, in view of wear consideration for most tires.

The critical pressure is expressed as follows:

where z_0 is given by Equation 2.

The equation for the optimum inflation pressure includes the sum of the compaction resistance, Equation 5, and the resistance due to tire flexure (hysteresis). The inflation pressure at which this sum is minimum is then found. Since the hysteresis losses are expressed by an empirical formula which varies for each tire, this equation is not shown here.

THE "CYCLOID-METHOD":

The next step in tire-wheel research was the establishment of the equation for traction as a function of slip, Reference (4), (5).

The derivation of this important equation was first presented by the author of the present paper in Turin. A brief description of this work is given in the following.

The tractive force under a tire (or a track) is generated by shear stresses:

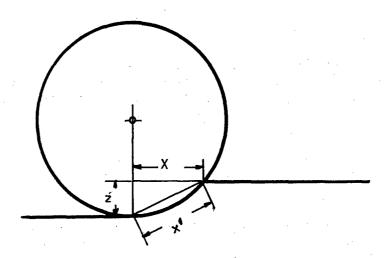


Figure 1.

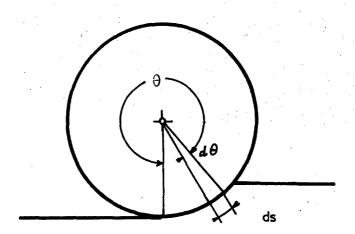


Figure 2.

$$H = \int_{S} \mathcal{T} \cos \theta \, ds \, \dots \, ... \, 7.$$

where H is the traction, τ is the local shear or tangential stress, s and ds represent the wheel-soil interface surface and surface element respectively. The angle θ is shown in Figure 2.

It is assumed that:

$$\mathcal{C} = (c + p \tan \beta)(1 - e) \dots 8.$$

The difficulties involved stem from the fact that the expression for j has to be derived from the equation of a looped cycloid, which is the path of a point of the wheel moving with positive slip.

The assumptions involved in the derivation are the following:

- a. Equation 7 holds.
- b. Soil values obtained from a vertical and a horizontal soil-loading test can be superimposed for the complex case of a wheel. In addition, the assumptions listed relative to Equation 3 are again made, with the exception of the neglection of the shear stresses.

The angle at which the point on the wheel perimeter moves vertically is called θ_V and the contact angle is Θ_0 . When $\Theta_V > \theta_0$ (see Figure 3), the sum of the tangential stresses are divided into two parts. The points on the wheel between θ_0 and Θ_V move forward (and downward), causing resistance. The points between θ_V and 2 m move backward (and downward) causing traction. Thus, the traction is the difference of the two "sub-sums".

$$H = H_1 - H_2$$
9.

In calculating H_1 , one has to use $j = j_1$, where

$$j_1 = \frac{D}{2} \left[(1 - i_0)(\theta_v - \theta) + \sin \theta - \sin \theta_v \right] \dots 10.$$

where ion is the slip. θ is the angle which varies between θ_{v} and 2π .

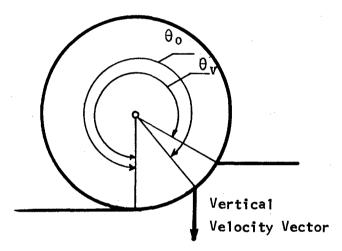


Figure 3.

 θ is the cos $^{-1}(1-i_0)$, the angle to which a point of vertical tangency belongs.

The limits of integration are $\,\theta_{_{\boldsymbol{V}}}\,$ and 2 π .

For Ho use

$$j_2 = \frac{D}{2}[(1 - i_0)(\theta - \theta_0) + \sin \theta_0 - \sin \theta]$$
. . . 11.

The limits of integration are θ_0 and θ_V .

In Equation 8, $p = kz^n$ where

$$z = \frac{D}{2}(\cos \theta - \cos \theta_0) \qquad ... \qquad .$$

When $\theta_{v} < \theta_{o}$ the "zone of resistance" does not develop because the soil is not in contact with the wheel along that zone which moves forward.

In this case,

$$j_3 = \frac{\nu}{2} \left[(1 - i_0)(\theta_0 - \theta) + \sin \theta - \sin \theta_0 \right] . . 13.$$

The limits of integration are $\theta_{\,o}$ and 2 $\pi.$

These equations can only be solved by means of a computer. The necessary steps are as follows:

a. Evaluate the sinkage from
$$z_{o} = \left[\frac{3W}{(3-n)bk\sqrt{D}}\right]^{\frac{2}{2}\frac{1}{n+1}}$$

b. Find On from

$$z_0 = \frac{D}{2} (1 - \cos^{\theta} 0)$$

Remember that $2\pi > \theta_0 > \frac{3\pi}{2}$

$$c. \ \ \, \text{Find} \ \, \theta_{V} \ \, \text{from:} \ \, \theta_{V} \ \, = \cos^{-1}\left(1-i_{0}\right)$$

$$\text{Note that } 2\pi > \theta_{V} > \frac{3\pi}{2}$$

$$d. \ \, \text{When} \ \, \theta_{0} > \theta_{V}$$

$$H = \frac{bD}{2} \frac{2}{\theta} \int_{0}^{2} \left\{c + k \left[\frac{D}{2}\left(\cos\theta - \cos\theta_{0}\right)^{n}\right] \tan\phi\right\},$$

$$\left(1 - e^{\frac{j_{3}}{K}}\right) \cos\theta \ \, d\theta \qquad ... \qquad ..$$

f. To obtain drawbar-pull, subtract

$$R_{c} = kb \frac{z_{o}}{n+1}$$
 from H.

The foregoing method applies for rigid wheels and tires whose inflation pressure is higher than critical.

When the inflation pressure is below the critical pressure, the ground contact area has to be established empirically and the track equation has to be used for the evaluation of the available traction.

Several other investigations will be described in the following. It should be emphasized, however, that none of them have been carried far enough to allow numerical evaluation of wheel performance for a wide range of conditions. Therefore, the method explained above is still the one which is used at the time of this writing, although it is recognized that it involves a number of gross neglections and crude assumptions.

UNIFORM STRESS DISTRIBUTION ON NON-FRICTIONAL SOILS

Uffelman (6) presented a paper at the Turin Conference describing a test series which was run by means of a steel-wheel equipped with normal-pressure sensitive cell and an instrumented spud to measure tangential forces.

The measurements are compared with theoretical results derived from a plastic theory of rut formation. It is interesting to note that Uffelman's equations for sinkage and motion resistance coincide with Equations 2 and 3 when n is set equal to zero. This value appears to be adequately accurate for "plastic" type soils.

To calculate the traction, Uffelman assumed uniform tangential force distribution, so that, for 100% slip

Equation 17 represents the sum of the horizontal components of the maximum shear-stress (or force) available in a soil for which $\phi = 0$.

Equating Equation 17 with the expression representing the resistance:

is obtained (where p = 5.7c is taken from Terzaghi's bearing capacity theory).

This result would mean that "a cylindrical wheel with no side walls would fail at the above sinkage on a purely cohesive soil irrespective of the actual value of soil cohesion or wheel width; it would stall before reaching this sinkage if the surface layers have a lower shear strength than the mean shear strength (slippery conditions".

When side-wall friction is also included, a similar method yields

$$\frac{z}{D} = 0.2 \dots \dots 19.$$

Finally, Uffelman proposes an equation for peak traction provided by a single spud per unit width:

$$p = \frac{W}{b \ell} h + 2 ch + \frac{1}{2} h^2 \dots 20.$$

where \pounds is the effective footing length, h is the effective spud height, and \digamma is the density of the soil.

Equation 20 is based on Rankine's retaining wall theory.

Figures 4, 5 and 6 are reproduced from Uffelman's paper. It can be seen that the assumption of uniform radial pressure is appropriate for the type of soil used. Figures 5 and 6 depict the difference between the tangential stress distributions, for a wheel operating under fairly high positive slip conditions, and a wheel which experiences negative slip (towed wheel).

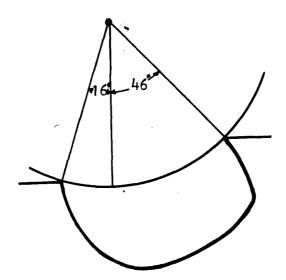
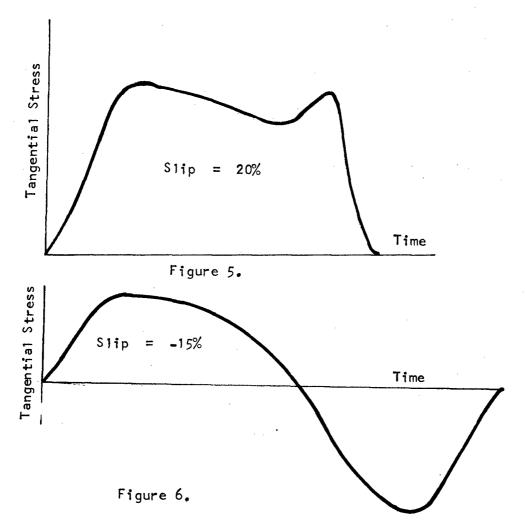


Figure 4. Radial Pressure Distribution



TANAKA'S METHOD:

In Tanaka's paper (7) presented in Turin, the equation of equilibrium for a wheel is shown to be:

T cos
$$\delta$$
 - N sin δ = DP (a)

T sin
$$\delta$$
 + N cos δ = W (b)

$$T \frac{D}{2} = M \qquad (c)$$

where

T is the resultant of the tangential stresses.

N is the resultant of the normal stresses.

M is the driving torque.

is the angle which characterizes the mutual point of attack of both T and N, Figure 7.

DP is the drawbar pull.

Thus, Tanaka assumed that δ is the common angle for both resultants. Even so, there are five unknowns (M, T, N, DP, and δ) in Equations 21. For a towed wheel M = 0, thus, T = 0. Therefore, the equations of equilibrium reduce to

$$N \sin \delta = DP$$

Equations 22 had also been used by Bekker (1). The change in sign has to be made because DP now represents the horizontal towing force acting on the axis. Thus, for towed wheels, the towing force is:

$$DP = W \tan \delta \qquad \dots \qquad 23,$$

When a driven wheel is not subjected to drawbar pull, Equation 21a becomes

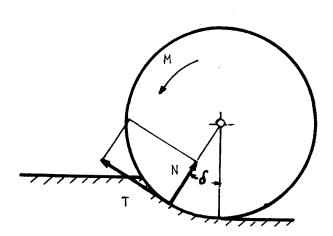


Figure 7.

The resistance, R, is represented by N $\sin \delta$. From Equation 22:

Substitute N into Equation 21b:

$$T \sin \delta + T \frac{\cos^2 \delta}{\sin \delta} = W$$

$$T \sin^2 \delta + T \cos^2 \delta = W \sin \delta$$

 $T = W \sin \delta$

Thus, $R = T \cos S = W \sin S \cos S \dots 26$.

When comparing Equations 23 and 26, it is seen that the motion resistance differs considerably between the cases of a towed and a driven wheel (W tan δ and W sin δ cos δ respectively).

Tanaka submits that angle δ is not the same for the two cases. Denoting the angle for the towed case by δ , one finds that

provided that the resistances are the same in both cases. Tanaka's test results support this hypothesis. However, this assumption should be regarded with reservations until a series of tests under a variety of soil conditions proves its validity.

One has to agree with Uffelman's discussion on Tanaka's paper. Uffelman pointed out that the assumptions of common angle $\mathcal S$, for T and N implies uniform stress distributions, and $\mathcal S$ is $\theta_0/2$. This is approximately valid for frictionless soil and high slip. If $\mathcal S'=\mathcal S$

where DP still denotes the rolling resistance of a towed wheel, and R is that of a self-propelling wheel.

COEFFICIENT OF ROLLING RESISTANCE AND ENERGY CONSIDERATIONS

The next pertinent paper was given by J. R. Phillips at the International Conference (8). The author analyzed the equilibrium of a powered wheel, utilizing the concept of the coefficient of the rolling resistance (8) as introduced by Chudakov.

Using the sign conventions shown in Figure 8, the author proposes to define g as follows:

It is important to note that Equation 28 is valid for the case when the driving torque M = 0.

According to Figure 8, the equations of equilibrium are,

$$R_z = W$$
 $R_x = DP$
 $M = R_z^a + R_x^k k_0 \dots 29$

from which

$$M = Wa + (DP)k_0$$
 30.

The "power input" through the axis of a driven wheel is M_{ω} , r being the angular velocity; the performance available at the drawbar (or where the chassis joins the axis) is DPv and the power absorbed by the soil $\bf S$ Wv. Thus,

Note that 9 differs from that shown in Equation 28 because M \neq 0.

If r is the rolling radius, v = r so that Equation 31 becomes

$$M = (DP)r + Wr$$
 32.

From Equations 30 and 32, one obtains

$$S = \frac{DP}{W} \left(\frac{k_0 - r}{r} \right) + \frac{a}{r} \dots 33.$$

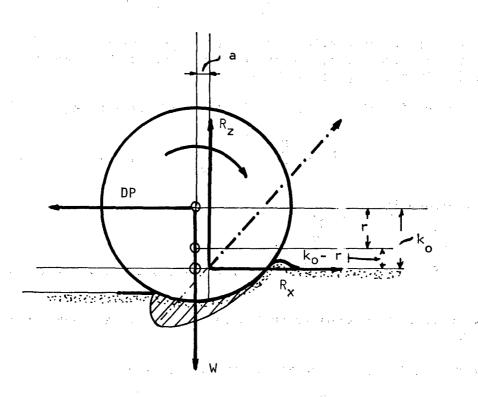


Figure 8.

or
$$g = \frac{a}{k_0} + \frac{M}{Wr} + \frac{k_0 - r}{k_0}$$
 34.

It is not difficult to show that the above equations yield the following:

$$DP = \frac{M}{r} - W \left[\frac{a}{k_0} + \frac{M}{Wr} \frac{k_0 - r}{k_0} \right] \cdot \cdot \cdot \cdot \cdot \cdot \cdot \cdot 35.$$

which shows that the available pull is always less than the "ideal" value of M/r. The resistance is now expressed as Wg, where g is the expression in the brackets in Equation 35.

In case of a rigid wheel rolling on hard surface, $k_0 = r$ from which

The resistance is,

It should be remembered that a and $\mathbf{k}_{\mathbf{0}}$ are not the same in the two cases.

When $i_0 = 1$ (one hundred percent slip) r = 0

$$DP = \infty - \infty$$
 38.

a finite but undefined value. For $r=0,g\to\infty$. The energy absorbed by the soil is § Wv. Since v=0 when $i\bar{\sigma}I$, § must approach ∞ in order to yield some finite value. When $r\to\infty$, the case of a blocked and towed wheel,

and

$$DP \longrightarrow -W \frac{a}{k_0} + \frac{M}{k_0} \qquad \qquad 40.$$

From the previous two expressions, it is seen that -9W = DP, when $r \rightarrow \infty$. The total input power is being lost in the soil $(DP_V = -9 W_V)$ since the moment M is doing zero work.

When $k_0 = 0$, the wheel sinks up to its axle. In this case

$$DP = \frac{M}{r} - [\infty - \infty] \qquad 41.$$

It is seen that one cannot devise a simple test which would yield definite information about ${\cal S}$.

Thus, Phillips' paper leaves "just one" problem unsolved: how to establish §. It is recalled that Tanaka's method depended upon the notion of d. Therefore, neither of the two authors were able to solve the equations of equilibrium, although both analyses allowed some new insight into the mechanics of the problem.

FLOW CONSIDERATIONS FOR SAND

Professor E. T. Vincent reported on his investigations which were concerned with the flow of sand past a rigid wheel (9). The author also ran a series of tests during which the normal pressure distribution under the wheel was recorded.

The author's conclusions are repeated here: ''As a result of this work, it can be concluded that, for a towed wheel in a dry sand:

- a. Compaction effects are small.
- b. Flow of sand occurs as a result of bulldozing forming a 'bow wave'.
- c. The normal pressure of the sand against the surface of a rigid wheel is of the form $p = kz^n$.
- d. The pressure of the sand on the surface of a rigid wheel can best be represented by two sets of soil values, one during the compaction phase, and the other as the stress is relieved (See Figure 9).
- e. The assumption of either compaction or flow has little effect upon the theoretical relationship for sinkage, drag, etc., provided the correct average values for the soil constants are employed.

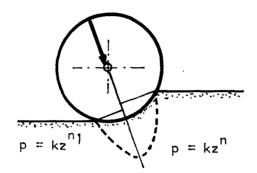


Figure 9.

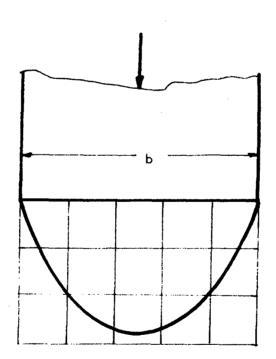


Figure 10.

- f. No assumptions are made in the Bevameter test concerning compaction or flow; thus, the use of the soil constant for either process appears legitimate.
- g. Acknowledging flow as the main process for the conditions considered offers a more realistic approach to the problem without throwing out all existing analysis."

NORMAL PRESSURE DISTRIBUTION AND "FRICTION CIRCLE" METHOD

Mr. E. Hegedus of the Land Locomotion Laboratory continued Vincent's efforts by measuring the normal pressure distribution under rigid wheels (10), (11), operating in various soils. Parallel to his experimental work, Hegedus analyzed the equilibrium of a rigid wheel as follows.

The elementary normal forces pass through the center of the wheel. The resultant of each element, dN and dT, will inclose the angle ϕ with the radius if the soil is purely frictional (c=0), and one disregards the initial portion of the contact surface where the shear-strength is not fully utilized. This assumption appears to be quite accurate when the wheel-slip is not too small. Thus, all reaction-element vectors form a tangent to a circle which is called friction circle in soil mechanics.

It is next assumed that the point of application of both T and N coincide and its characteristic central angle is θ_N (see the description of Tanaka's work). Using these assumptions

and the radius of the friction circle is

The equilibrium of moments states that

$$M - rV = 0$$
, or, $M - \frac{D}{2}V \sin \phi = 0$... 44.

where V is the resultant of T and N.

Also,
$$M - \frac{D}{2}T = 0$$
 45

The equations of equilibrium are:

These equations are similar to Equations 21, however, here the "existence of the friction circle" is assumed.

The unknowns are M, θ_N , V, and DP. Thus, Hegedus reduced the number of unknowns by one compared to Tanaka's case. Even so, there is one too many unknown. It is pointed out that the notion of θ_N is crucial for the solution of the wheel problem.

Hegedus' test program had the following goals:

- a. Establishment of the true shape of the normal pressure distribution and that of $\boldsymbol{\theta}_{\text{N}}$.
- b. Investigation of the effect of slip on normal pressure distribution.
 - c. Determination of the effect of wheel-slip on sinkage.

the second of the second second second second second second second second

- d. Investigation of the magnitude of the tangential or shear forces on the performance of powered wheels.
- e. Determination of the effect of soil properties or wheel slip-sinkage characteristics and frictional forces.

Tests were run in sand and sandy loam soils having various moisture contents.

The test results were summarized by Hegedus as follows:

a. The driving moment which depends on the tangential forces becomes constant in sand when the slip exceeds 30%. Thus, the assumption that ϕ = constant along the wheel-soil interface surface and the existence of the friction circle is valid, at least

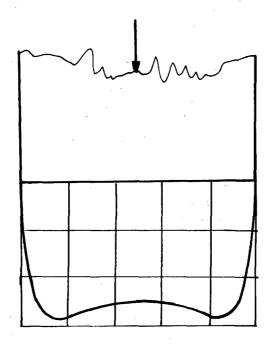


Figure 11.

above the aforementioned slip.

- b. The sinkage and the shape of the normal pressure distribution diagram depends on the slip. The angle θ_N decreases as slip increases in sand.
- c. The pressure is not zero at $\theta = 2\pi$. The pressure becomes zero at $\theta = 2\pi + 10^{\circ}$.
- d. The pressure distribution in the lateral direction is of the form shown in Figure 10 in sand.
- e. In the sandy loam tested, the sinkage and θ_N become independent from slip above 9% (or for c > 0.5) water content. Thus, θ_N is easier to express for soils having both frictional and cohesive properties than for purely frictional ones.
- f. The lateral pressure distribution is as shown in Figure 11 for cohesive soils.

Since the load, the resultant of the normal stresses, ϕ , D, and $\theta_{\rm N}$ were either known or obtainable from the test data, the equations of equilibrium could be checked for each test run.

For instance, the equation

was checked as follows. Plotting the vertical components of the elementary normal force, integrating them over the ground contact surface and adding the sum of the vertical components of the elementary tangential forces ($dT = dN \tan \phi$), one has to obtain a force equal to W. (Note that dT is calculated here and not measured).

If the above criteria is satisfied, T = N tan $\not p$ can be accepted along with the "friction circle" method. Hegedus found that V cos $(\not p - \Theta_N)$ was, at most, 5% less than W, indicating the correctness of the assumptions made.

Without going into details, it is pointed out that the friction circle concept can also be used for cohesive soils by separating the frictional and cohesive parts of the elementary reaction forces. The presence of cohesion results in an additional tangential force element $dT_{\text{\tiny C}}$ which is

$$dT_c = cdA$$
 48.

Lt. Colonel A. D. Sela (Israeli Army) spent a year at the Land Locomotion Laboratory. During this time, he conducted a series of rigid wheel tests using a special transducer embedded in the wheel which measured both the tangential and normal stress distribution along the contact surface. The transducer did not protrude from the wheel surface so that the stress pattern was not disturbed by the measuring device. Sela was mainly interested in dry sand - for obvious reasons.

The equation, valid for dry sand (c = 0), for shear stress versus deformation

$$-j/K$$

s = p tan ϕ (1 - e) 49.

was used.

It was shown earlier that it is moderately complex to express j in terms of the slip and the radius if one considers the cycloidal path of the wheel perimeter.

Colonel Sela introduced the simple assumption that

Obviously, $D/2(\theta-\theta)$ is the arc length between the leading point and an arbitrary point of the interface surface. Thus, it is assumed that the wheel behaves "like a track".

In order to follow the notations used by Sela, let us introduce

$$\Rightarrow = 2\pi - \theta$$
.

Then

According to Sela, "the flow of a soil particle under a wheel depends on the resultant force produced by the wheel on the particle".

This statement is not correct; however, it is the basis of the Russian school of thought (13) and may result in solutions of acceptable accuracy.

The horizontal component of the normal force element is

and that of the tangential force element is

When these two components are equal, the ratio s/p becomes

$$s/p = tan \propto_d$$

where $^{\alpha}$ d is that central angle at which the horizontal force-components cancel each other.

When
$$\alpha > \alpha d$$
, then $dN_h > dT_h$.

In this region, the particle is moved forward while for $\propto <$ < d, the particle moves backward.

When Equation 51 is plotted for various i values, Figure 12, the s/p vs. d curves are only valid below \propto d, that is, to the left from the intersection of s/p and tan \propto .

It is then necessary to construct an expression for the deformation (j) which takes place in the region characterized by $\infty > \infty d$.

Sela introduced the assumption that the displacement is a linear function of the distance from $\propto d$. So that

where m is the coefficient of proportionality. Thus, for a point in the region $\alpha_0 \ge \alpha \ge \alpha$ d, the total deformation becomes

$$j_f = \frac{D}{2} [(\propto_o - \propto) i + (\propto - \propto d) m \dots 53.$$

In case of a braked wheel (negative slip), the entire contact surface becomes a "bulldozing zone" which means that $\alpha_d = 0$.

Experimental results indicate that the shear stresses reverse their direction at a point, say, $\propto r$.

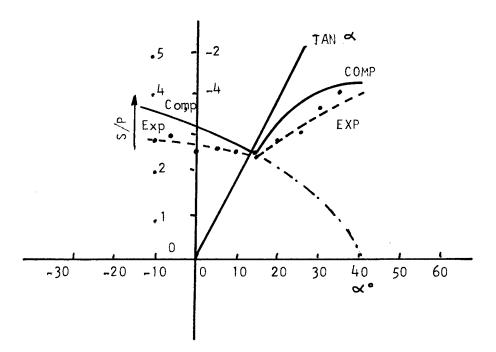


Figure 13.

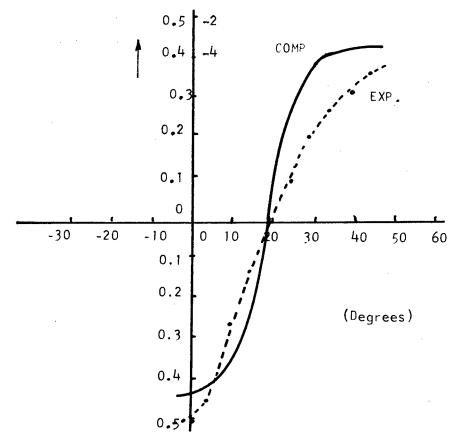


Figure 14.

For zero torque, one may assume symmetrical stress distribution expressed as.

Solving Equations 54 and 55:

In Figures 13 and 14, experimental and theoretical values are compared for the s/p vs. \propto relationship. For the soil used, tan $\phi = 0.44$ and K = 1.0 values were established. The numerical value of m was obtained from Equation 56 using \propto_o and β readings taken at "almost zero braking torque".

Sela acknowledges that further analysis of the data collected is needed to find a way "to define, theoretically, the rate of skid io, for zero torque. As is the case of a driven wheel, it is thought that qualitatively good agreement for the skid conditions exists between theoretical and experimental results. In spite of the fact that the behavior of 'm' has not been established, it seems that a fundamental understanding of the skidding wheel-soil relationship has been established."

SUMMARY:

It has been shown that since the publication of Research Report No. 5, workers in the field discovered that the tangential stresses play an important part in the mechanics of the wheel-soil interaction. Normal and shear stress distributions have been measured and the

equilibrium of the wheel has been investigated using various assumptions to establish the unknowns which are not defined by the three equations of equilibrium.

In spite of these efforts, the only method which allows one to calculate wheel performance is the one first presented by the present writer in Turin. The assumption of the $p=kz^n$ type normal pressure distribution and the lack of a slip-sinkage relationship make this approach of less than general validity. Other attempts to remedy these shortcomings yielded incomplete solutions since it was not possible to reduce the number of unknowns below four. Uffelman's solution is complete; however, it is only valid for very special soil conditions.

Future efforts should concentrate on the establishment of semiempirical methods for the description of the still undefined unknowns, such as Tanaka's " \mathcal{E} ", Hegedus' " \mathcal{E}_N ", or Sela's "m".

It should be pointed out that the dimensional analysis approach has been covered in another paper.

REFERENCES

- 1. Bekker, M. G. Theory of Land Locomotion, The University of Michigan Press, Ann Arbor, 1956.
- Bekker, M. G. and Janosi, Z. J. Analysis of Towed Pneumatic Tires Moving on Soft Ground, Land Locomotion Laboratory Report No. 62, OTAC, Centerline, Michigan, 1960.
- 3. Bekker, M. G. Off the Road Locomotion, The University of Michigan Press, Ann Arbor, 1960.
- 4. Janosi, Z. J. Performance Analysis of a Driven Non-Deflecting Tire in Soil, Land Locomotion Laboratory Report No. 84, ATAC, Centerline, Michigan, 1963.
- 5. Janosi, Z. J. An Analysis of Pneumatic Tire Performance on Deformable Soil, Paper No. 45, Proceedings of the First International Conference on the Mechanics of Soil-Vehicle Systems, Edizione Minerva Technica, Turin, Italy, 1961.
- 6. Uffelman, The Performance of Rigid Cylindrical Wheels on Clay Soil, Paper No. 7, Proceedings of the First International Conference on the Mechanics of Soil-Vehicle Systems, Edizione Minerva Technica, Turin, Italy, 1962.
- 7. Tanaka, The Statiscal Analysis and Experiments on the Force to the Tractor Wheel, Paper No. 18, Proceedings of the First International Conference on the Mechanics of Soil-Vehicle Systems, Edizione Minerva Technica, Turin, Italy, 1962.
- 8. Phillips, J. R. A Discussion on Slip and Rolling Resistance, Paper No. 54, Proceedings of the First International Conference on the Mechanics of Soil-Vehicle Systems, Edizione Minerva Technica, Turin, Italy, 1962.
- 9. Vincent, E. T. Pressure Distribution on and Flow of Sand Past a Rigid Wheel, Paper No. 50, Proceedings of the First International Conference on the Mechanics of Soil-Vehicle Systems, Edizione Minerva Technica, Turin, Italy, 1962.
- 10. Hegedus, E. A Preliminary Analysis of the Force System Acting on a Rigid Wheel, Land Locomotion Laboratory Report No. 74, OTAC, Centerline, Michigan, 1962.

- 11. Hegedus, E., Pressure Distribution and Slip-Sinkage Relationship Under Driven Rigid Wheels, Land Locomotion Laboratory Report No. 83, ATAC, Center Line, Michigan, 1963.
- 12. Sela, A. D., The Shear to Normal Stress Relationship Between a Rigid Wheel and Dry Sand, Land Locomotion Laboratory Report No. 99, ATAC, Warren, Michigan, 1964.
- 13. Goryachkin, V. P., Theoriya Kolesa, Sobranive Sochineniy, T2, Sel'khozgoz ("The Theory of the Wheel" Collected Works, Vol. II). Publishing House of Agr. Literature, 1937.

STATE OF THE ART OF VEHICLE

PERFORMANCE PREDICTION

By: T. F. Czako Z. J. Janosi

INTRODUCTION:

The ability to predict vehicle performance in off-the-road conditions is one of the primary goals of land locomotion research. Details of the basic system which describes the mechanics of soil-vehicle interaction have been refined and partially revised in recent years. The approach has remained the same in principle, however, as originally introduced by Bekker (1).

The Land Locomotion Laboratory is often requested by Government Agencies and industrial firms to participate in the evaluation of off-the-road performance of new vehicle concepts or to analyze the effect of certain changes in the design of current vehicles. Because of this continuing demand, it was felt that a brief but complete description of the analytical system would serve a useful purpose even though most of the basic information involved here is discussed in greater detail in other papers of this volume.

Since the problem is highly involved, simplifying assumptions must be made. This helps to keep the mathematics on a workable level. Certain factors which are known to affect vehicle performance must be neglected because the phenomenon in not fully understood.

The simplifying assumptions presented below and the wide scatter in soil strength under field conditions reduce the potential accuracy which could be expected from Bekker's basically sound approach. It is realized that off-the-road performance predictions are often inaccurate, especially for wheeled vehicles. However, the comparison of the predicted performance of various vehicles is not a futile exercise because the accurately predicted qualitative order in performance levels still yields a sound basis for the comparative evaluation of new vehicle concepts. The methods discussed in this paper are also useful when the advantages and disadvantages of certain proposed changes are to be weighed. The analysis may reveal, for example, that an increase in tire diameter would not sufficiently expand the range of strength of possible soils to warrant the added cost.

The soft soil performance of an off-the-road vehicle may be evaluated by means of several different measures. The Vehicle Cone Index, for example, is used by the Corps of Engineers for this purpose (2). The Land Locomotion Laboratory, however, has advocated the use of the drawbar-pull (DP) as the measure of performance. The drawbar-pull is the sum of all resistances subtracted from the gross traction available at the soil-vehicle interface. Gross traction is the horizontal component of the resultant of the stresses acting at the interface. The total resistance consists of the component due to soil compaction and one due to the so-called bulldozing. The latter is attributed to the weight of the soil mass being "pushed" out from the rut. The drawbar-pull can be related to the force-deformation relationship created in soil by a footing which moves in the horizontal and/or in the vertical direction. Problems associated with soil strength measurements are discussed in detail in Papers Nos. 1 and 2.

SIMPLIFYING ASSUMPTIONS:

The simplifying assumptions involved in the analysis of the mechanics of the wheel-soft soil system are listed in Paper No. 4. These assumptions are also inherent in the performance analysis of a vehicle.

The following assumptions are introduced in addition to those discussed in Papers Nos. 1, 2, and 3:

- a. The vehicle moves in a straight line on flat terrain at a slow uniform speed. Thus, forces due to steering action, inertia, slope climbing and speed effects in soil transportation under the wheel are eliminated. Conditions fulfilling these assumptions can be approximated by careful selection of the drawbar-pull test site and proper execution of the tests. Laboratory or outdoor soil bins approach these conditions closer than the best field test site.
- b. The slip of all wheels (or tracks) is the same. The interaction of unequal tractive forces created under the wheel is difficult, if not impossible, to analyze. Uniform slip conditions are not difficult to maintain with vehicles having locking differentials.
- c. Engine torque, and hence torque at the drive sprockets, or wheels, is always sufficiently large so that soft-soil performance is not limited by torque. Thus, the vehicle will stall only when the motion resistance is greater or equal to the maximum available traction (DP \leq 0). In case the vehicle pulls a trailer or a brake-vehicle

during drawbar-pull tests, stalling occurs when the sum of the drawbar-pull and the resistance is greater or equal to the traction. Note that drawbar-pull tests are conducted so that the required pull is gradually increased while the vehicle is in motion.

Military vehicles have engines powerful enough so that the vehicle "bogs down" in soft soil by spinning the wheels (100% slip) and not by stalling the engine.

d. The weight distribution on the ground contact elements does not change despite the presence of a moment created by the drawbar-pull. Thus, it is assumed that the moment arm of the drawbar-pull is small and its effect on the static load is negligible. This assumption is not really necessary; the actual load distribution could be found by trial and error solution of the equations listed below. A computer could easily handle the problem.

METHODS FOR CALCULATING THE DRAWBAR-PULL FOR TRACKED VEHICLES:

The following input data are required to perform the calculations:

```
W (1bs.) = Gross vehicle weight
b (in.) = Track width

$\mathcal{L}$ (in.) = Length of ground contact area
$k_c$ (1bs./in.^{n+1}) = Soil sinkage modulus
$k_c$ (1bs./in.^{n+2}) = Soil sinkage modulus
$n$ (dimensionless) = Sinkage exponent
$c$ (1bs./in.^2) = Cohesion
$\mathcal{L}$ (0) = Angle of internal friction
$K_{\theta}$ (dimensionless) = Coefficient of bulldozing resistance
$K_{\theta}$ (dimensionless) = Coefficient of bulldozing resistance
$K$ (in.) = Tangent modulus
$i_0$ (dimensionless) = Slip
$\mathcal{L}$ (1bs./in.^2) = Bulk density of soil
```

It should be pointed out that there is considerable controversy about the use of some of the factors listed above as well as about some of the equations listed below. The "arguments" are presented in other articles included in this volume.

According to practical observations, the vehicle may remain in a horizontal position while negotiating the terrain or it may proceed with its rear end sinking deeper than the front. Sometimes the front may even leave the ground. It is not fully understood how the trimmed attitude develops. A moment due to drawbar-pull; "excavation" of soil under high-slip conditions; and the static weight distribution of the vehicle are the influencing factors to be considered. It is known that Soviet track-layer tractors are built "nose heavy", so the drawbar-pull while pulling heavy implements "lifts" the front and the tractor assumes a horizontal attitude.

According to practical observations, most vehicles assume non-zero trim angle at high slip.

a. When a vehicle rides in a "horizontal" position, the following relationships are used:

(1) Ground contact area:
$$A = 2 b \ell (in.^2)$$
.

(2) Average ground pressure:
$$p = \frac{W}{A} (1bs./in.^2)$$
.

(3) Soil consistency:
$$K = \frac{k_c}{b} + k_p$$
 (1bs. in. n+2).

(4) Sinkage: $z_0 = (\frac{p}{k})^{\frac{n}{n}}$ (in.) This equation is obtained from Bekker's basic equation for sinkage $(p = kz^n)$.

(5) Compaction resistance:
$$R_c = \frac{2 b k z_0^{n+1}}{n+1}$$
 (1bs.),

This equation is obtained by calculating the work necessary to compact the soil to depth $\mathbf{z}_{_{\mathrm{O}}}$ under the tracks (Reference 1).

(5) Bulldozing resistance:

$$R_b = 2.b(2 K_\theta z_0 c + K_b T z^2)$$
 1bs.

This equation is derived in Reference 3 by assuming that the bull-dozing force is equal to the horizontal projection of the passive earth pressure. (See Figure 21, page 217, also).

(6) Gross traction:
$$H = (Ac + W \tan \phi) \left[1 - \frac{K}{i_0 \ell} (1 - e^{-\frac{i_0 \ell}{K}}) \right] (1bs.)$$

This equation has been derived in Reference 4. The expression is obtained by integrating the shear stresses along the track. The shear deformation - track slippage relationship is included in the formula.

(7) Drawbar-pull:

$$DP = H - (R_c + R_b)$$
 (1bs.).

This equation expresses that the drawbar-pull is equal to the gross traction less the sum of the resistances.

b. When a vehicle assumes a trim angle some of the equations take a different form. Since sinkage is assumed to be zero at the front, bulldozing is not present.

Equations (1), (2), and (3) are the same as above.

(4) Maximum sinkage:

$$z_{m} = \left[\frac{p}{k} (n+1)\right]^{\frac{1}{n}}$$
 (in.).

This equation is derived by assuming zero sinkage at the leading edge of the track, and linear increase of sinkage toward the rear, and by equating the weight of the vehicle to the sum of the vertical ground pressures.

(5) Compaction resistance:

$$R_c = \frac{W}{\ell} z_m$$
 (1bs.)

This equation is derived as before, taking the appropriate sinkage expression into account.

(6) Gross traction:
$$H = A \left\{ c \left[1 - \frac{K}{i_0 \ell} \left(1 - e^{\frac{i_0 \ell}{K}} \right) \right] + kz_{max}^n \cdot tan \phi \right\}$$

$$\left[\frac{1}{n+1} - \frac{1}{\ell} \frac{1}{n+1} \right] \left\{ x^n \cdot e^{\frac{i_0 x}{K}} dx \right\}$$

This is the integral (Reference 4) sum of the shear stresses acting along the track-soil interface. Due to the non-zero trim angle, the expression is more complex than the one for zero trim angle.

(7)
$$Drawbar-pull: DP = H - R_C$$

CALCULATIONS OF DRAWBAR-PULL FOR WHEELED VEHICLES:

In the following equations, W(lbs.) is the load on one wheel; D(in.) is the diameter of the undeflected tire; GW(lbs.) means gross vehicle weight; b(in.) is the width of the undeflected tire. Other symbols correspond to those listed before.

The following relationships are used in the calculations:

a. Sinkage:

$$z_0 = \left[\frac{3 \text{ W}}{(3-n) \text{ bk } \sqrt{D}}\right]^{\frac{2}{2 \text{ n+1}}}$$
 (1bs.)

This equation is derived (Reference 1) by equating the vertical load with the integral of the vertical stress components. The integration is carried out along the wheel-soil interface.

b. Compaction resistance:

$$R_{c} = \frac{b k z^{n+1}}{n+1}$$
 (1bs.)

This expression is obtained (Reference 1) by calculating the work needed to compress the soil to depth z_0 over an arbitrary length of wheel travel. This work is set equal to the work performed by

horizontal force (R_c) over the same length.

c. Gross traction:

$$H = \frac{bD}{2} \int_{2\pi - \beta_0}^{2\pi} (c + p \tan \phi)(1 - e) d0 (1bs.)$$

This expression represents the sum of the shear stresses along the wheel-soil interface. The relationship between the horizontal shear deformation j and the angle of wheel rotation & is involved. More details are given in Paper No. 4. The integration can be carried out numerically by a computer. The method has been first presented in Reference 5.

d. Drawbar-pull of one wheel:

$$DP_{W} = H - (R_{c} + R_{b}^{3})$$
 (1bs.)

e. Drawbar-Pull of the vehicle:

$$DP = \Sigma H - \Sigma R = \Sigma DP_W$$
 (1bs.)

Thus, the drawbar-pull of the vehicle is the sum of the drawbar-pull of each wheel.

Bulldozing resistance is used for front wheels only. It is assumed that for the uniformly loaded wheels of a multi-axle vehicle, the front wheels pull less than the following ones. Since the front tires compact the soil, the rear wheels encounter different soil consistency. This effect is not taken into account at the present time. Test results indicate that Bekker was right (Reference 1) when he indicated that the rear wheels "continue" on the pressure sinkage curve from the point where the front ones "left off". This means that when a vertical penetration test is interrupted by relieving the load and the load applied again, the record force-sinkage curve will follow the curve generated by an uninterrupted test. Thus, the trailing wheel's sinkage and compaction resistance should be calculated according to

$$p = k(z_1 + z_2)^n$$

where \mathbf{z}_2 is the sinkage of the second wheel relative to the rut formed by the first one and \mathbf{z}_1 is the sinkage of the first wheel.

Soil compaction is not the only cause of sinkage. It is known that slip causes additional sinkage. According to Hegedus (Reference 3), in soils having low cohesion the sinkage continuously increases with slip. The sinkage of a wheel operating in cohesive soil, however, is not significantly affected by slip.

Slip-sinkage is important because it influences bellying. It, however, does not affect the resistance due to compaction. There is not enough experimental evidence available at the present time about the mechanics involved in multiple pass and slip sinkage situations; thus, these phenomena are not accounted for in the method used for performance analysis.

GRAPHIC PRESENTATION AND INTERPRETATION OF RESULTS:

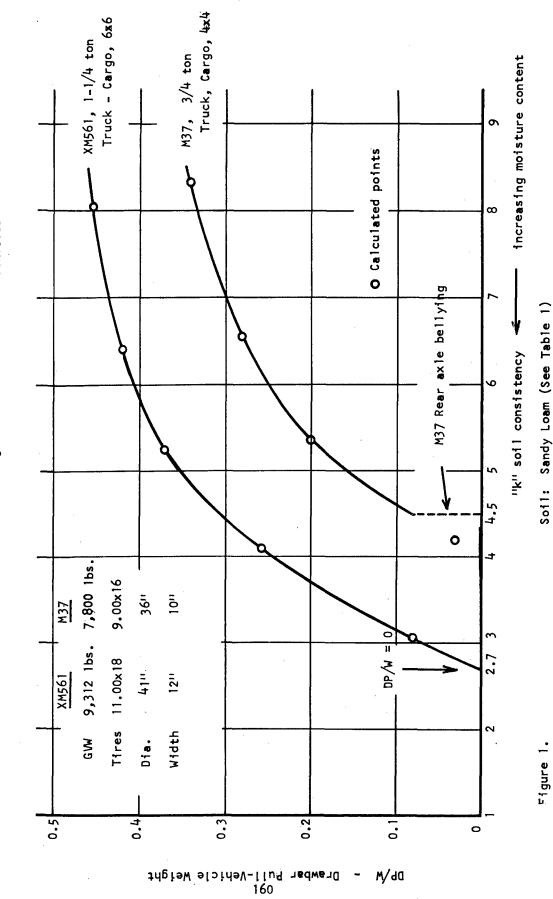
Drawbar-pull is seldom used as a variable. It is clear that a heavy vehicle is expected to develop more pull than a light one. Therefore, the drawbar-pull-weight ratio (DP/W) is considered the meaningful measure of performance.

For a given vehicle, the drawbar-pull-weight ratio depends on the strength of the soil and on the amount of slip between the running gear and the soil. Thus, it is not surprising that DP/W vs. soil consistency (k) and DP/W vs. slip (i_0) curves are frequently used to represent off-the-road vehicle performance.

Soil consistency is represented by 'k' which includes a critical length dimension (b) and curve fitting parameters (k_c, k_p) . Drawbar-pull, however, depends on the "horizontal strength characteristics" (c, p). Thus, DP/W vs. 'k' curves (Figure 1) would be uniquely defined only if there existed a one-to-one correspondence between c, p, and k. In reality, however, soils having different (c, p) sets may demonstrate the same 'k' value. Therefore, different DP/W ordinates may belong to the same abscissa of 'k' for the same vehicle.

Another difficulty stems from the fact that a vehicle exerts different drawbar forces at different slips. This does not present a serious drawback as long as it is understood that the ordinates represent the maximum pull available. If the maximum is reached at 100% slip, the pull available at $i_0 = 80\%$ is used. The lack of a one-to-one correspondence between c, ϕ , and k is taken into account by using i_0 values which are obtained from testing the same soil at various moisture contents. In other words, the abscissas of the points shown on the curve are not randomly selected values,

Calculated Drawbar-Pull-Weight Ratio of Two Wheeled Vehicles



but they are measured in a particular soil at various moisture contents. This way, when two or more vehicles (DP/W vs. k curves) are compared, (c, p) sets which belong to the same soil at the respective moisture levels are used. One has to keep in mind that the comparison is valid for one soil only.

A relatively "hard" dry soil can be converted into a soft "weak" material by increasing the moisture content. The DP/W vs. k curve depicts a corresponding deterioration in vehicle performance. The curves indicate the "type" of immobilization which can be expected after 'k' has been decreased sufficiently. A vehicle may "belly-out" before the traction diminishes to a level insufficient for supporting motion (z_0 = ground clearance). Conversely the vehicle may not be able to maintain minimum traction even though its sinkage is not too significant (H = R or DP = 0). Tropical soils often consist of a hard bottom layer covered with a thin "slippery layer". The sinkage can be plotted as a function of 'k' to interpolate that 'k' value at which bellying occurs (Figure 2). The points of Figures 1 and 2 were calculated by means of the values shown in Table I.

Since $k = \frac{k_c}{b} + k_p$ and b is a characteristic length dimension of the vehicle, k is not constant for two different vehicles even when the same soil is considered. The difference, however, is usually small.

The weaknesses inherent in the DP/W vs. k representation have been discussed. These plots are still often used mainly because this is the only method which demonstrates the variation of vehicle performance over a wide variety of soil strength conditions.

Drawbar-pull vs. slip curves (Figure 3) can only be plotted for a single soil condition. Thus, this representation is limited on the one hand, but, on the other hand it gives insight into the economy of operation and can be directly correlated with test data. A series of DP/W vs. slip curves, constructed for various soil conditions represent a better solution to the problem than one DP/W vs. k curve. One should keep in mind, however, that several detailed graphs may not be as useful for certain purposes as one approximate plot which covers a broad range of conditions.

The efficiency of operation is best emphasized on a (DP/W) $(1-i_0)$ vs. i_0 graph. This representation was first suggested by Dickson, Reference 6. It is seen that the ordinate of this graph becomes zero when DP = 0, (small positive slip) or when $i_0 = 1.0$

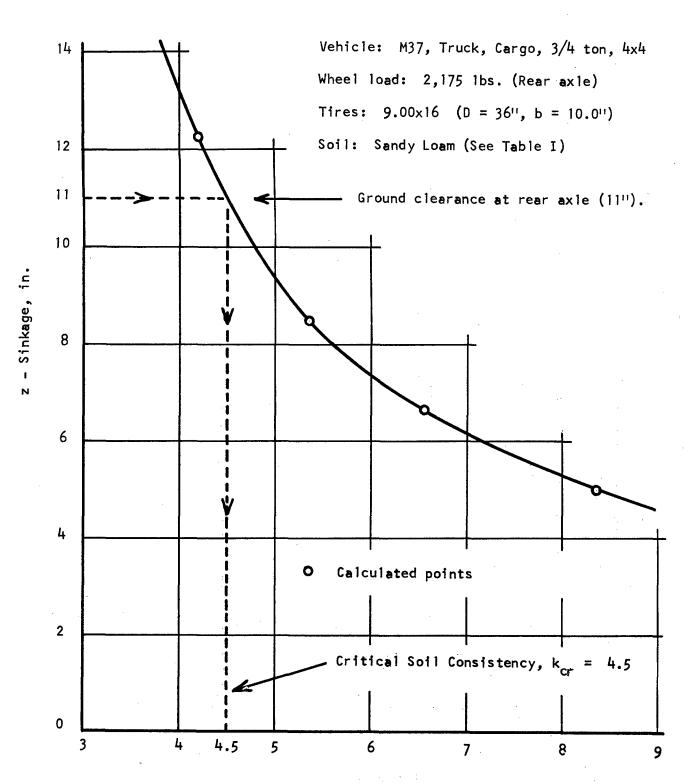
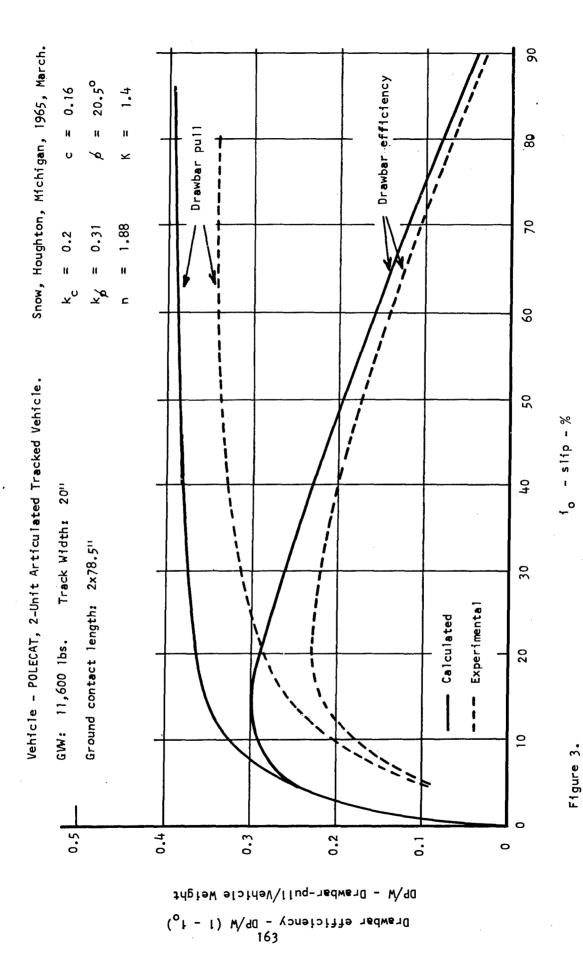


Figure 2. "k" Soil Consistency.



(running gear "spins out"). Between these two extremes, the graph shows the efficiency of the running gear as it is affected by slip. The curve reaches maximum at a certain slip which represents the point of highest efficiency.

TABLE I.

SOIL VALUES OF MICHIGAN FARM SOIL (SANDY LOAM)

AT DIFFERENT MOISTURE CONTENTS

Soi1	k _c	k _ø	n	С	þ	tan p	2 K	Kx	MC%
1	17.5	6.60	•53	1.6	29.2°	0.560	3.8	2.9	14
2	9.5	5.60	•5	1.9	27.5°	0.520	3.6	2.5	16
3	6.5	4.70	•47	2.00	25.5°	0.476	3.4	2.2	18
4	4.5	3.75	.42	1.6	23.5°	0.435	3.3	1.95	20
5	3.3	2.80	.39	1.0	21.5°	0.394	3.2	1.7	22
6	2.2	1.80	•35	0.8	19.7°	0.358	3.0	1.5	24

k = 1.0 in. = 0.06 lb./in.³ for soils 1 through 6.

REFERENCES

- 1. Bekker, M. G., "Theory of Land Locomotion", The University of Michigan Press, Ann Arbor, Michigan, 1956.
- Department of the Army, "Soils Trafficability", Technical Bulletin ENG 37, U. S. Government Printing Office, Washington, D. C., July 1959.
- 3. Hegedus, E., "A Simplified Method for the Determination of Bull-dozing Resistance", Report No. 61, Land Locomotion Laboratory, ATAC, Warren, Michigan, 1960.
- 4. Janosi, Z., Hanamoto, B., "An Analysis of the Drawbar-Pull vs. Slip Relationship for Track Laying Vehicles". Report No. 69, Land Locomotion Laboratory, ATAC, Warren, Michigan, 1961.
- 5. Janosi, Z., 'Performance Analysis of a Driven Non-Deflecting Tire in Soil". Report No. 84, Land Locomotion Laboratory, ATAC, Warren, Michigan, 1963.
- 6. Dickson, W. J., "Some Fundamental Soil/Vehicle Mechanics and a Method of Evaluation of the Soil/Vehicle System". Canadian Armament Research and Development Establishment, Val Cartier, Quebec, 1961.

DIMENSIONAL ANALYSIS IN LAND LOCOMOTION PROBLEMS

By: R. A. Liston

A popular pastime of many engineers, including the writer, working in or on the fringes of automotive design, is to indulge in a comparison of the "crude techniques" of the automotive engineer with the sophisticated systems analyses of the aeronautical, electronic, or aerospace engineer. In order to play the game, it is normal to draw a comparison between the design techniques of the automotive engineer and either the aeronautical engineer and the naval architect or, for the fully initiated, both. When dealing with the design of off-road vehicles, much of the design is purely empirical or it, in fact, may not follow any basis other than the dictates of the group which established the vehicle requirements. The vehicle requirements may establish weight, size, cargo area and configuration and other details in such a way that the designer is left with nothing to design. He may need no design technique beyond an ability to interpret the stated requirements.

The design of off-road vehicles is empirical for a rather straight-forward reason: it is reasonable from both safety and economic viewpoints to put ideas "into iron" and test the result. The aeronautical engineer and the naval architect have developed superb mathematical and model techniques for the design of their vehicles. Of course they have. They had no alternative. The aeronautical engineer could not in good conscience permit a pilot to test an untried aircraft. They were forced to develop mechanical and analytical models that would assure a high probability of success of a new concept. Thus, the aeronautical engineer was forced to develop his sophisticated techniques if for no other reason than to prevent the death of the crew.

The naval architect was forced to develop model techniques for economic reasons. It is not conceivable that a dozen full scale hull configurations could be tested for each new type of ship if the ship yard or ship purchaser were to stay in business. Therefore, in order to improve the performance of their vehicles, the naval architects had to either develop model techniques or face many years of slow evolution in vehicle form accompanied by random failures and successes.

The automotive designer had neither safety nor economic reasons to resort to model techniques. The failure of a major component is seldom tragic to the test vehicle driver. More often than not, the damage to the reputation of the engineer is greater than the physical

damage to the test driver. The cost of a prototype of a vehicle concept is quite modest particularly if the prototype consists of only the elements directly associated with off-road performance. In addition, suspension components can be varied or modified without an exceptional cost. Assuming that the empirical design approach produced satisfactory results, there was no obvious reason to resort to alternate methods.

The fact is that satisfactory results have apparently not been delivered since inadequate mobility has been and remains a constant source of criticism. For approximately twenty years, the Army has been supporting research programs having the objective of developing a basis for improved off-road vehicles. Other papers in this report have discussed the approach of the Land Locomotion Laboratory. This paper is concerned with the use of dimensional analysis and model techniques originally supported by the Transportation Corps to investigate the off-road vehicle problem. Before discussing the specific applications of dimensional analysis in land locomotion mechanics, a short defense of the approach is offered.

When dealing with a problem for which exact mathematical analysis poses extreme difficulties, it is often useful to utilize the techniques of dimensional analysis. Dimensional analysis does not permit the solution of difficult problems by a simple turning of a mysterious crank but instead requires an understanding of the problem equal to that required by "normal" mathematical analysis. In each case, one must understand the fundamental behavior of the phenomenon under study in order that basic assumptions can be proposed. If one attempts an exact mathematical analysis, the assumption is made in the form of one or more relationships and a set of boundary conditions. If the equations can be solved, the results can then be compared to experimental findings.

When applying dimensional analysis techniques, it is necessary that the controlling relationships be known even though the quantitative proportions need not be delineated. The relationships which are produced by the dimensional analysis do not indicate the value of coefficients and exponents. These are produced by experiments designed to satisfy the requirements of the analysis. If one begins with a set of assumptions and follows either exact mathematical or dimensional analysis, the same answers must evolve if both are to satisfy experimental results.

In the field of land locomotion mechanics, dimensional analysis has proven to be a very useful tool because the exact behavior of soil is quite fully misunderstood. It is generally agreed what soil

properties control the interaction between the soil and a loading device. However, other than for situations involving very small deformations not generally accepted, exact mathematical solutions have been developed in the field of soil mechanics. Because land locomotion mechanics deals with soil-vehicle interaction which involves large deformation, the use of dimensional analysis has been very inviting. It is inviting because we have an understanding of the controlling variables in the soil-vehicle system, but exact solutions have been denied us. The primary use of dimensional analysis has been in two areas: the development of a model theory and techniques (1,2,3) to evaluate vehicle concepts and the study of the behavior of soil subjected to large scale deformations (4,5).

Although Markwick (6) was the first researcher who attempted to apply dimensional analysis techniques to investigate the behavior of vehicles operating in soft soil, Nuttall should be credited with the first success. His initial studies (7) were based on the work of Markwick in which he attempted to verify Markwick's analysis by means of experiments using small wheels operating in a sandy loam and sand. The work was supported by the Ordnance Corps but was abandoned before useful results were obtained. The U. S. Army Transportation Corps picked up the task in 1956 and supported a study by Nuttall with the goal of producing a model theory for a wide range of soil types.

The dimensional analysis on which Nuttall's study was based produced the following functional relationships for purely frictional materials:

$$\frac{z}{d} = f_1(\frac{W}{C_s d^2}, p, i, \frac{h}{d}) \qquad \dots \qquad 1.$$

$$\frac{D}{W} = f_2(\frac{W}{C_c d^2}, \beta, i, \frac{h}{d}) \qquad ... \qquad 2$$

$$= f_3(\frac{W}{C_s d^2}), \, \phi, \, i, \, \frac{h}{d} \qquad \dots \qquad 3.$$

where:

z = Sinkage, inches

d = Characteristic length, inches

W = Weight, 1bs.

C_s = "Structural" cohesion, 1bs./in.²

ø = Angle of Internal Friction, non-dimensional

i = \$1ip, non-dimensional

h = Soil depth, inches

D = Drawbar-pull. 1bs.

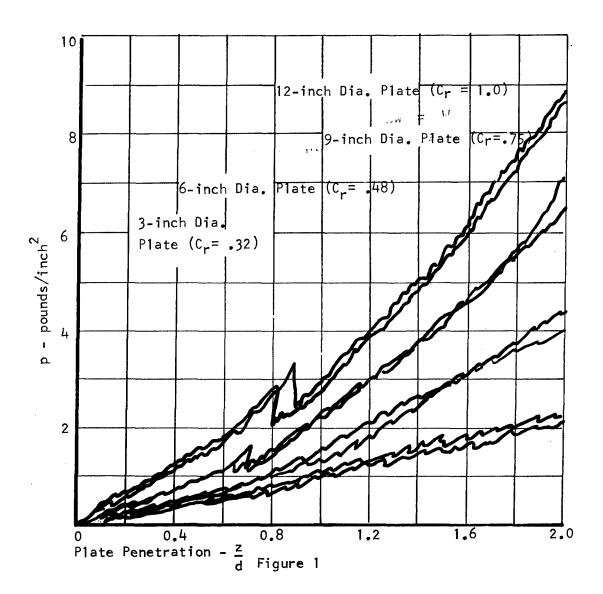
The retention of the factor

$$\frac{W}{C_s d^2}$$

for a purely frictional material is not very satisfying since C_S is the "structual" cohesion. In the opinion of the writer, the "structual" cohesion is equivalent to a bearing capacity factor similar to Bekker's k_C or k_C . The values are assigned to C_S dependent upon the scale factor involved in a particular test. Further, C_S is not established by means of a shear test of the soil but from a penetration in which it is assumed that the following relationship holds:

$$\frac{z}{d} = f_4(\frac{p}{C_s}) \qquad \dots \qquad 4$$

where p is the average pressure acting on a plate and the other variables are as previously identified. Bearing capacity theory provides a relationship between cohesion and unit loading, assuming negligible sinkage, for a cohesive material. By straining a point somewhat, Equation 4 could be considered to be appropriate for a cohesive material. However, Nuttall was dealing with purely frictional materials so that $C_{\rm S}$ can only be considered as a variable related to the bearing capacity characteristics of the soil. The value for $C_{\rm S}$ is taken as the relative structual cohesion, $C_{\rm r}$. In order to establish $C_{\rm r}$, a series of plate tests are conducted in which circular plates of varying diameters are forced into the soil and the relationship between sinkage and pressure recorded. The data are plotted in a semi-dimensionless form of pressure versus the ratio of sinkage and the plate



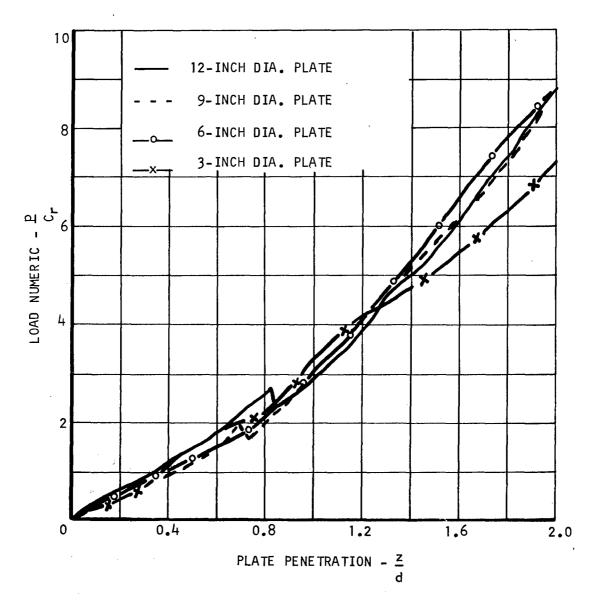


FIGURE 2

diameter. A non-dimensional plot of a load numeric, p/C_r , versus the sinkage diameter ratio is constructed so that all curves collapse upon an arbitrarily selected curve for which Cr is taken as unity. Figure 1 is a typical plot of p vs. z/d, and Figure 2 shows the 'collapsed" curves. These figures are taken from a paper by Nuttall and McGowan (8) in which Cr is unity for the twelve-inch diameter plate. It will be argued later that dimensional similitude or dimensional analysis techniques are appropriate to frictional, or non-cohesive. materials. It is proposed that the introduction of "structural" cohesion was an attempt to avoid the use of the conventional soil mechanics notion of bearing capacity valid for little or no deformation or the use of the Bekker sinkage parameters that are appropriate to large soil deformations. The disadvantage of the Bekker parameters from a dimensional analysis viewpoint is the fact that the sinkage variable dimensions that are dependent on the soil. In any event, it is not obvious that a connection exists between "structural" cohesion and the commonly accepted definition of cohesion.

All of Nuttall's reported work was conducted either in snow or He confined his studies to relatively large scale factors seldom attempting tests with models smaller than 1/4 scale. Experience has shown that his selection of a large scale factor was fortuitous from two viewpoints: the construction of a 1/4 scale model of the average vehicle of interest is relatively simple. If a very small scale vehicle is attempted, the cost becomes prohibitive because of the difficulty in maintaining exact scaling. In addition, dimensional analysis assumes that quantitative similarity is possible only if qualitative similarity exists. The behavior of soils is sensitive to the size of a loaapparatus. For example, a very small wheel will produce a soi. to tion quite different from that produced by a large wheel. A model wheel must, therefore, be of a size that will assure a similar soil reaction to that produced by the prototype wheel.

An example of the results achieved by Nuttall in correlating model and prototype performance in sand is shown in Figure 3. A considerable scatter of the data points is evident but the maximum error appears to be approximately 25% which is not particularly alarming to anyone dealing with vehicle tests in natural soil conditions. The correlation in soil can be considered as quite satisfactory especially when compared to Figure 4 in which Nuttall prescribes an experimental error of approximately 40% for tests conducted in snow. However, the results shown in Figure 5 tend to imply that some of the scatter attributed to experimental error may more reasonably be charged to poor correlation. The family of curves proposed in Figure 5 do not seem fully supportable after

CORRELATION OF 1/4 SCALE MODEL WITH MARSH BUGGY IN BEACH SAND

MODEL	FULL-SI	ZE	
•	0	8%	DEFLECTION
+		17%	DEFLECTION
X	Δ	30%	DEFLECTION

NOTE: Tests conducted in tilled and compact sand.

Deflections based on unloaded section height.

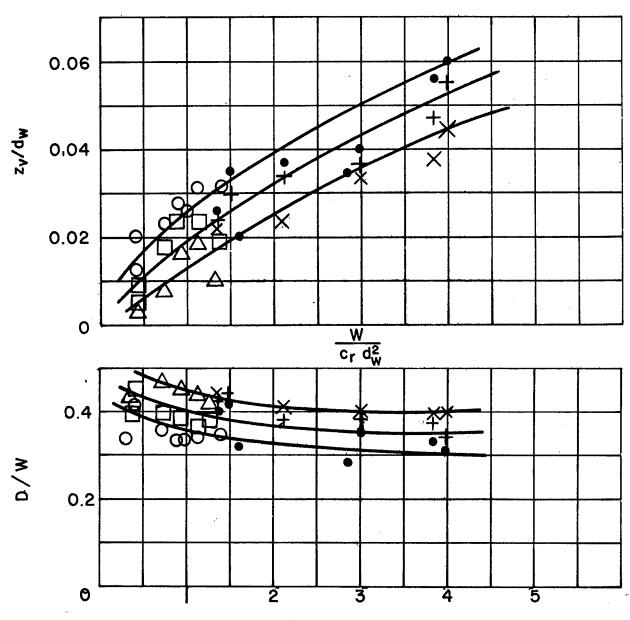


Figure 3

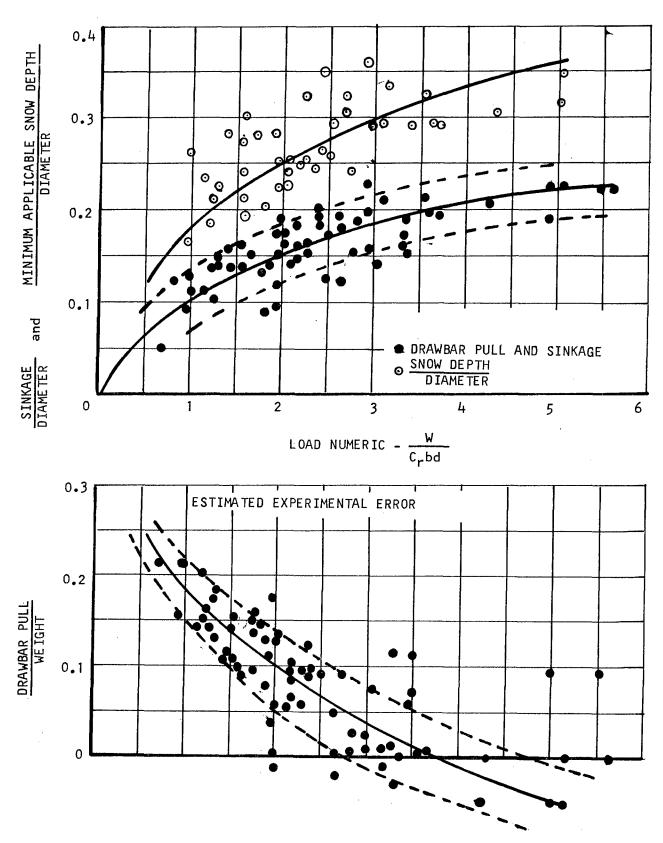


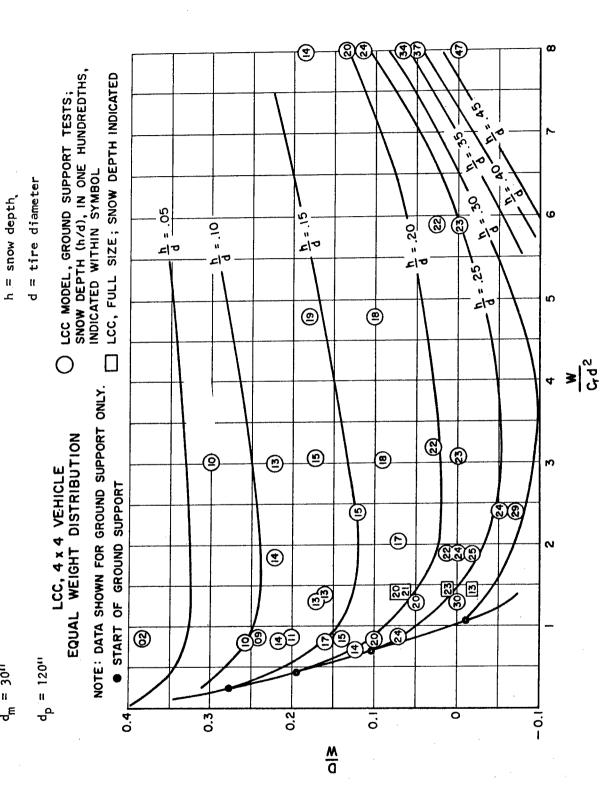
Figure 4

careful examination of the data points. Figure 6 is an alternate interpretation of a major portion of the data points of Figure 5 and one would reasonably conclude that the correlation is not very good. Figure 7 may give a clue as to one possible source of the lack of correlation - if the snow data presented in Figure 1 is actually representative of the snow on which the tests were conducted. If the curves in Figure 1 are replotted in the form of pressure versus sinkage, Figure 7 is produced. The curves for the various plates do not fall on the same line so that it is possible to condluce that the snow is not purely frictional. Because the snow apparently has cohesive properties, it is not surprising that the data do not correlate because of different scaling requirements imposed by the cohesion.

Upon completing his extension studies, Nuttall concluded that (9):

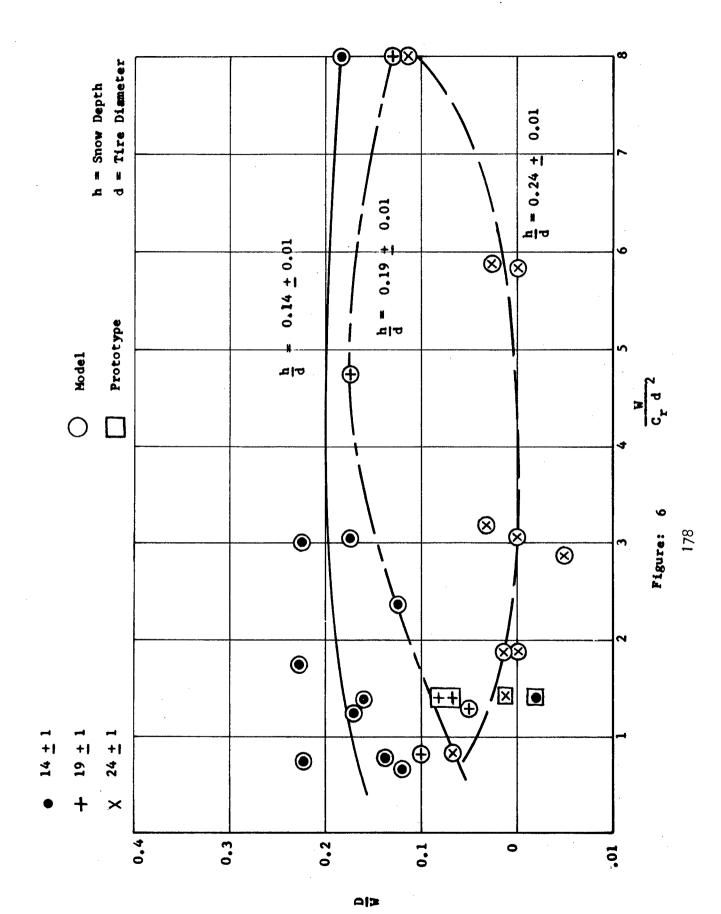
- a. The performance of any full-size, rubber-tired vehicle in sands can be predicted and studied with useful engineering accuracy by means of proper tests on a working scale-model.
- b. The performance in sands of any full-size, 4x4, vehicle on any type of pneumatic tire can be estimated with useful accuracy from data presented herein, i.e., Reference 9.

Although these conclusions are singular as engineering statements because of the absence of a hedge to hide behind, they are based on tire tests ranging from 6.00x16 to 36x41 so that considerable credance can be given the conclusions. However, before one becomes overly enchanted with the proposition of vehicle model tests, I would submit an unsolicited qualification for Mr. Nuttall: the "performance" in each conclusion should be preceded with the adjectives, "soft soil". Soft soil performance is only a part of offroad performance and may be less significant than obstacle performance. If a model is to be fully useful for the evaluation of a vehicle concept, all vehicle characteristics of importance must be included in the evaluation. This, of course, means that power, suspension, steering, ground clearance, angles of approach, and similar characteristics must be included in the model. The result is a very expensive model that may approach the cost of a full scale test rig. When conducting tests of aircraft or ship models. a model may cost two or three orders of magnitude less than a full scale mock-up prototype and there is no question concerning whether it is appropriate to conduct model tests or not.



 $d_{\rm m} = 30^{11}$

LCC TYPE TIRES IN SNOW, FLOTATION & GROUND SUPPORT FIGURE 5.



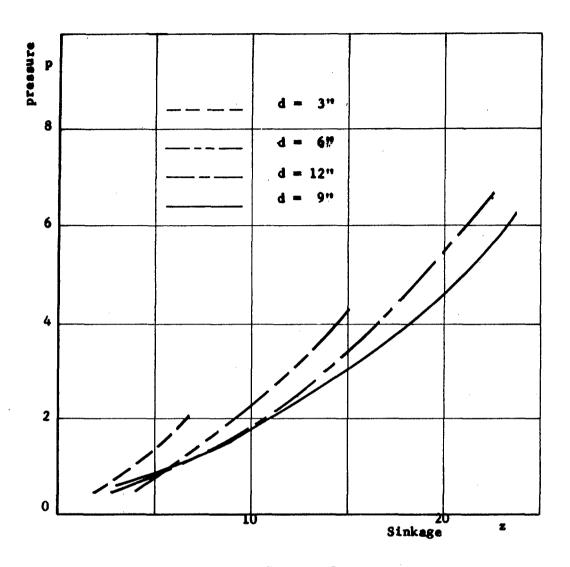


Figure: 7

Upon completion of the studies in sand and snow, the TRECOM study was extended to include cohesive materials. The continuation of the study was transferred to the Southwest Research Institute with Nuttall's results as a starting point. A dimensional analysis (10) using essentially the same set of parameters previously discussed produced the following functional relationships for a soil having both cohesive and frictional properties.

$$\frac{z}{d} = f_{4}(\frac{W}{C_{r} d^{2}}), \frac{\mathcal{T}_{b}}{C_{r}}, \frac{\mathcal{T}_{b}}{C_{t}}, i, \beta, f_{n}, m_{n}, \delta) \dots 5.$$

$$\frac{D}{W} = f_5(\frac{W}{C_r d^2}), \quad \frac{\mathcal{T}_b}{C_r}, \quad \frac{\mathcal{T}_b}{C_t}, \quad i, \not b, f_n, m_n, \not a) \quad . \quad . \quad 6.$$

The parameters not previously mentioned are: \mathcal{T} , soil density in lbs./ft.³; f, the coefficient of friction between soil and wheel surface; m, soil moisture in percent; \mathcal{S} , tire deflection, percent. The Nuttall study included f, \mathcal{T} and \mathcal{S} but assumed those values constant for both model and full scale tests. The use of moisture content as a parameter is perhaps questionable because the moisture content is established once the friction angle and cohesion are taken as constants.

The analysis for soils having cohesion departed somewhat from the earlier analysis in that it was assumed that the apparent structural cohesion for the model and prototype were related by:

$$(c_r)_p = \lambda (c_r)_m$$

where the subscripts refer to prototype and model and λ is the scale factor. However, careful analysis of the Nuttall studies indicates that the apparent cohesion does not follow the scale factor but some unrelated factor, g. This observation causes one to conclude that:

$$(c_r)_p = g (c_r)_m \dots 8$$

$$(c_t)_p = g(c_t)_m \dots 9.$$

where \$ is established experimentally. If the difference between \$ and \upalpha is not great, no particular problem exists. However, using the results of Figure 2, it is seen that for $\upalpha=4$, $\upalpha=3.12$. This would require that the density of the soil used for the model tests be greater than the prototype soil by a factor of 1.28. In order to accomplish this it is necessary that the soil density vary between the values of 90 lbs./ft. to 142 lbs./ft. which is not reasonable nor can it be accomplished without a significant change in other properties. It would appear that at the onset, the study of the cohesive soil scaling problem was hampered with a requirement that could not be met without resorting to "scaled" soils.

The initial results of the Southwest Research Institute study indicate that the scaling of performance in cohesive soil was not successful. Tests were conducted in three soil types: a silty clay, CH; a lean sandy clay, CL-ML; and a sandy clay, CL. In each case, the clay was a sub-surface material ranging from several inches below the ground surface to twenty feet below the surface. It was found that no correlation existed for any of the numerics except moisture content. However, moisture content cannot be considered as an independent numeric even though in a strict sense it meets the mathematical criterion which is that numerics are independent if one numeric cannot be obtained from another by an exponential relationship. However, as stated previously, moisture content is established by the frictional and cohesive properties so that it should be equally possible to obtain a similar correlation on the basis of cohesion or friction.

Figure 8 is taken from Reference 10 and indicates that the DP weight ratio and the coefficient of friction produce very similar curves when plotted against moisture content. One could infer from this result that the operation in the cohesive soils was such that performance was related primarily to tractive effort and secondarily to motion resistance. However, the relationship between the sinkage numeric and moisture content as shown in Figure 9 makes such a conclusion suspect since sinkage, hence motion resistance, becomes high as moisture content exceeds about 40%.

A possible explanation for this apparent anomaly is the very low bearing strength of the clay soils used in the tests when moisture content is high. At moisture contents in excess of 20%, the bearing strength began to decrease rapidly. However, the cohesion

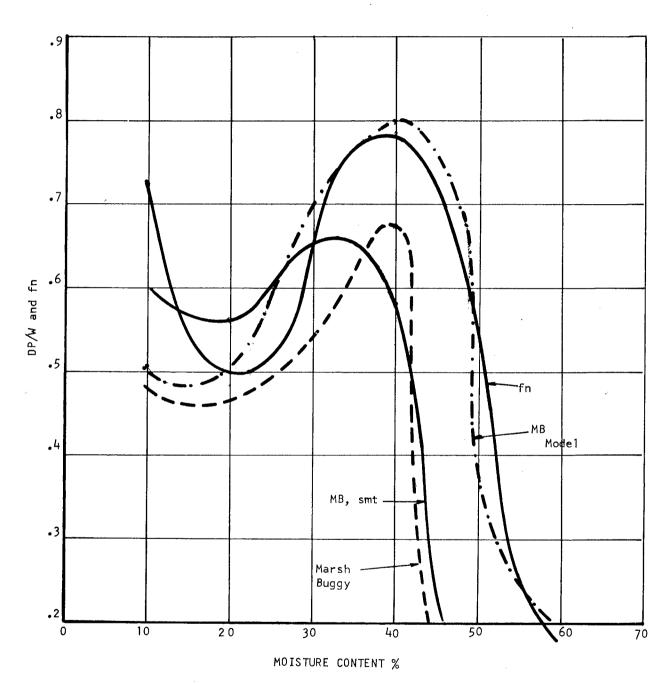


Figure 8

and therefore, traction, did not show a rapid decrease until a moisture content in excess of 40% was recorded.

An interesting aside is associated with measured values of $z/d_{\rm u}$ as high as .3 which still permits a positive drawbar-pull. It has been proposed (11) that in a purely cohesive material, immobilization will occur according to a geometric relationship established by the ratio of cohesion and bearing capacity. If, for example, the bearing capacity is 5.7 times the cohesion, it was proposed that a vehicle could be immobilized when the z/d ratio reached .03. However, a more germane observation concerning Figure 9 is that scaling of sinkage was not achieved and no correlation between the sinkage numeric and moisture content was evident. Since sinkage was not scaled, the idea of relative cohesion proposed by Nuttall would not be appropriate to the cohesive soil study and the numerics involving Cr would, therefore, not likely provide a basis for correlation. The avoidance of the requirement that soil density be scaled (without affecting cohesion) is an additional possible source of the lack of correlation. However, regardless of the source of the lack of correlation, it has not been shown that scaling of performance is or is not possible for vehicles operating in cohesive materials. There is, however, strong evidence that scaling of soil as well as the vehicle will be required if scale model testing is to be successful.

The dimensional analysis studies conducted by Vincent and Hicks at the University of Michigan (12) started from a different set of assumptions from those taken by Nuttall. The primary point of departure is the selection of dependent and independent variables. The dependent variables were taken as R, the horizontal component of motion resistance, z, the wheel sinkage, and T, the wheel torque. The independent variables are listed below:

It would appear that the selection of independent variables is appropriate to towed wheels but not for driven wheels. The basis of the Vincent-Hicks selection of independent variables was the well known Bekker sinkage equation:

which is used to determine sinkage and motion resistance of a rigid wheel. However, when computing traction, the cohesion and friction angle must be considered. It is possible to argue that k_{C} is related to cohesion; ky is related to the friction angle; and that n is related to the soil density making the Nuttall and Vincent-Hicks assumptions similar. Unfortunately, the argument does not hold since it has been repeatedly demonstrated that no such relationships exist. The Vincent-Hicks study produced the following numeric relationships:

$$\frac{R}{W} = f_1 \left[\left(\frac{W}{d^{n+2}k_{\not o}} \right), \left(\frac{k_c}{dk_{\not o}} \right), \frac{D}{d}, \alpha, \mu, n, i \right] \dots 12.$$

$$\frac{T}{Wd} = f_2 \left[\left(\frac{W}{d^{n+2}k_{\not o}} \right), \left(\frac{k_c}{dk_{\not o}} \right), \frac{D}{d}, \propto, \mu, n, i \right] \dots 13.$$

$$\frac{z}{d} = f_3 \left[\left(\frac{W}{d^{n+2}k_0} \right), \left(\frac{k_c}{dk_0} \right), \frac{D}{d}, \alpha, \mu, n, i \right] \dots 14.$$

The initial study was concerned with the performance of model and prototype wheels in sand. The properties of the sand were such that the requirements of similitude could be met. The value of $k_{\rm C}$ was zero so that the similitude requirements were:

where the subscripts refer to model and prototype. It is obvious that the model weight can be adjusted to maintain similitude and assuming that qualitative similarity is satisfied, scaling of performance is quite feasible. A typical plot of results is shown in Figure 10 in which the numeric T/Wd is plotted against slip. Although the scale factor is too large to cause one to become impressed with the accomplishment, the result is nonetheless encouraging.

One becomes quite discouraged, however, when the requirements for similitude are examined for soils having a non-zero k_c and k_c . In this case, the following numerics must be kept constant:

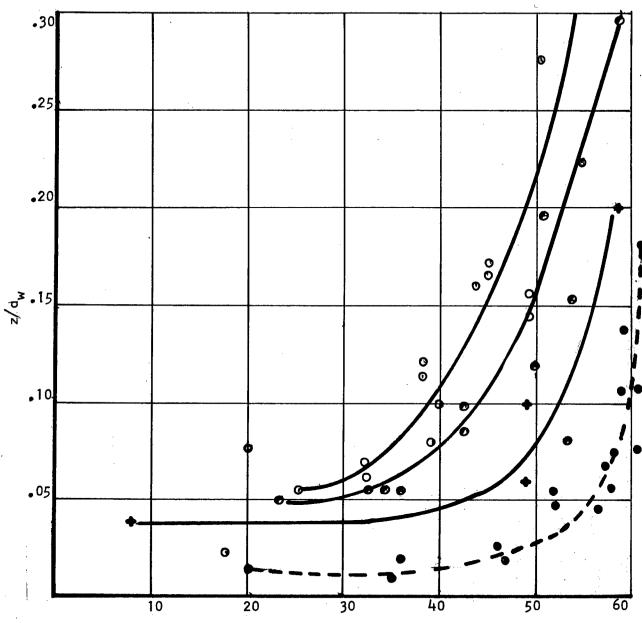
$$\left(\begin{array}{c} k_{c} \\ \hline d k_{p} \end{array}\right)_{p} = \left(\begin{array}{c} k_{c} \\ \hline d k_{p} \end{array}\right)_{m} \qquad . \ldots 20$$

$$(\mu)_{p} = (\mu)_{m}$$
 22.

$$(n)_{p} = (n)_{m} \dots 23.$$

$$(i)_p = (i)_m \dots 24$$

If χ is taken as the scale factor, the relationship between dp and dm is immediately dm = χ dp. Equation 20 states that unless χ = 1 the soil must be scaled. A scale factor of unity or the use of scaled or model soils appear to be equally unhappy prospects. However, test results (13) using a soil for which k_c and k_b were not zero



 M_h moisture content, %

OMB 12000 1bs

↑ MB 17400 1bs
 ↑ MB model 650 1bs
 ↑ MB smt 10640 1bs

 $WT_{\text{mod}} = (4.29)^2 = 12000 \text{ lbs}$

Figure 9 186

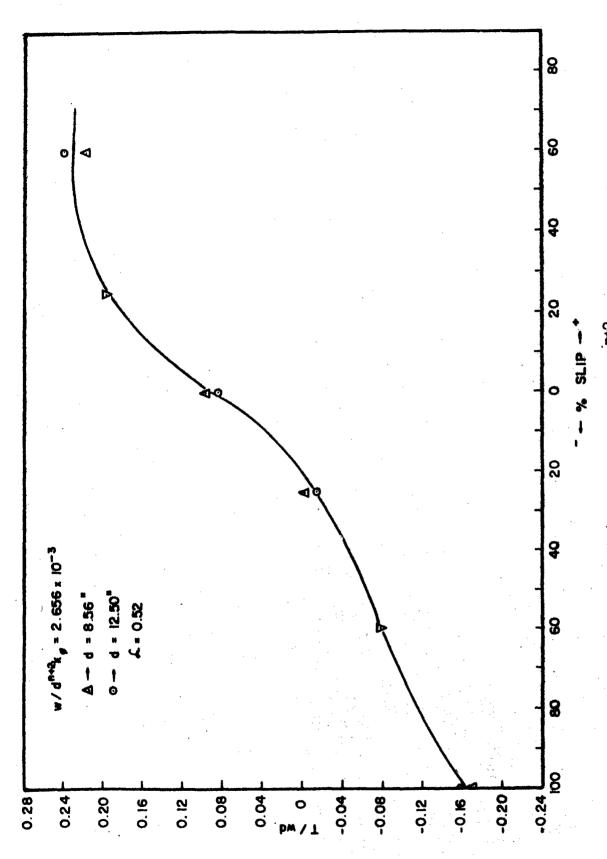


Fig. 10. Flot of (T/wd) vs. % slip for (w/d $^{\rm D+2}k_{\phi}=2.656 \times 10^{-3})$ under similitude conditions.

verified the conclusion that the similitude could not be maintained. An example of the lack of correlation between model and prototype is shown in Figure 10 in which the torque numeric is plotted against slip.

As a result of the requirement to provide model soils, Vincent and Hicks investigated methods of varying soil properties on a selective basis. If Equations 18, 19, 21 and 22 are examined, the magnitude of the problem is apparent. If Equations 18 and 19 are satisfied by taking $(k_c)_m = \lambda$ $(k_c)_p$, a rather clever adjustment will be necessary to satisfy Equations 21 and 22. The material on the surface of the model wheel could be varied to maintain a constant coefficient of friction but the requirement to maintain the sinkage exponent, n, constant may be difficult. It is not proposed that the development of a soil model is not possible. However, it is highly doubtful that the development of a sufficient number of model soils to permit a thorough evaluation of the soft soil performance of a vehicle concept is justifiable.

Several of the conclusions reached by the Vincent-Hicks study bear repetition. They conclude that: (a) dimensional analysis techniques are applicable to land locomotion studies in sand; (b) when the parameter k_c is not zero the soil values must be varied according to Equation 20; (c) the soil values may be changed selectively by addition of "foreign" materials to the soil.

The studies of Nuttall, Southwest Research Institute, and Vincent-Hicks were based essentially on quasi-static conditions in that strain rates were taken or assumed to be low enough to be outside of the range of dynamic effects. Several studies conducted in Canada will be reviewed subsequently which included a dimensional analysis of vehiclesoil interaction including dynamic effects. However, before addressing these studies, an alternate approach to the use of scale models will be discussed.

The Land Locomotion Laboratory does not advocate the use of models to evaluate the soft-soil performance of vehicles. The analytical techniques that are available are considered to be a more useful device for concept evaluation because of the considerable saving in time and money they permit. These techniques have been discussed elsewhere in the series making up this report and need no further discussion here. When the laboratory is required to conduct model studies, no real attempt is made to adhere to rules of similitude in a strict sense. Our model studies are based on an acceptance of the validity of the soil-vehicle relationships that have been developed supplemental by the selection of a scale factor sufficiently large to assure qualitative similarity between the soil reaction produced by the model and prototype.

The model technique used is essentially the following:

- a. A scale factor is selected and a model produced having geometric similarity to the prototype vehicle.
- b. Soil conditions are measured and identified by the values of k_c , k_p , n, c, and p.
- c. The drawbar-pull to weight ratio of the prototype is computed for the prototype vehicle.
- d. A trial and error solution is made to determine the proper scale weight of the model.

One can agree that the resulting model test is only as good as the equation used to solve for the drawbar-pull to weight ratio. This is quite true and we agree that a series of model tests conducted on this basis are no better than a series of analytical predictions. However, it has been demonstrated (14) that the technique can be used to produce model-prototype results that correlate satisfactorily for either frictional or cohesive soils without the requirement that model soils be used. However, there is no claim that the rules of similitude are statisfied because sinkage, along with pressure, for example, will only be scaled by happenstance. An additional drawback to the technique is that it is somewhat unwieldy. Before the weight can be selected for a given test, the soil characteristics must be measured and the data reduced so that the model weight can be computed. The computation of the weight is not difficult except in a physical sense. A simple example is given to indicate the method.

Assume that soil values have been measured and the results of the data reduction produce: $k_c=3$, $k_0'=5$, n=1, c=2, and $p=28^\circ$. A 1/4 scale model of the M113 Armored Personnel Carrier is to be tested. The pertinent characteristics of the M113 are: contact length of track, \mathcal{A} , equal to 105 inches; a 15 inch track width, b, and a 22,610 pound gross weight. In order to predict drawbar-pull, the standard measure of soft soil performance, one can write that

$$\frac{DP}{W} = \frac{H - R}{W} \qquad \qquad 25.$$

where DP/W is the drawbar-pull to weight ratio, W is the weight, H is the gross traction and R is the total motion resistance. H and R can be computed from:

$$R = \frac{bkz^{n+1}}{n+1} + b(2 zcK_b + y^2 z^2 K_{\theta}) \dots 27.$$

 \mathcal{T} is the soil density; K_b and K_θ are parameters related to the Terzaghi bearing capacity factors; $k = k_c/b + k_{\theta}$; b is track width; and z is the track sinkage. The value of z for a track can be computed from

$$z = \left[\frac{(n+1)W}{b \ell k}\right]^{1/n} \dots 28.$$

By combining Equations 25, 26, 27, and 28, the expression for DP/W is:

$$\frac{DP}{W} = \left(\frac{b \cancel{l} c}{W} + \tan \beta\right) - \frac{bk}{W(n+1)} \left(\frac{n+1}{b \cancel{l} k} + W\right)^{\frac{n+1}{n}}$$

$$- \frac{b}{W} \left[\left(\frac{n+1}{b \cancel{l} k} + W\right)^{\frac{1}{n}} + \left(\frac{n+1}{b \cancel{l} k} + W\right)^{\frac{2}{n}} \right] \dots 29.$$

Assuming that $\mathcal{T}=.06$ lb./in.³, and $K_b=K_\theta=1$, Equation 28 produces a DP/W = 0.78.

In order to establish the weight of the model to produce identical DP/W in the same soil, the expression for the drawbar-pull to weight ratio of the model and prototype are equated:

If λ is taken as the geometric scale factor, Equation 28 for the model can be expressed in terms of λ and the prototype characteristic lengths, b and $\mathscr{L}.$ The result is:

$$\left(\frac{DP}{W}\right)_{m} = \frac{c_{1}}{W} + \tan \phi - c_{2}(W)^{1/n}$$

$$- c_{3}(W)^{1-n/n} - c_{4}(W)^{2-n/n} \dots 31$$

$$c_2 = (k_c + \lambda \ bk_b)(n+1)^n \left[\frac{1}{\lambda \lambda (k_c + \lambda \ bk_b)} \right]^{\frac{n+1}{n}} ... 33.$$

$$C_3 = 2c \lambda bK_b \left[\frac{n+1}{\lambda \ell (k_c + \lambda bk_b)} \right]^{1/n} \dots 34.$$

$$c_{4} = \lambda \ b \ \delta \kappa_{\theta} \left[\frac{n+1}{\lambda \left(k_{c} + \lambda \ b k_{b} \right)} \right]^{2/n} \qquad35$$

Solution of Equation 31 by trial and error produces the result that the 1/4 scale model of the MII3 must weigh 520 pounds for the soil considered. A different soil or the same soil at a different moisture content will require that a new model weight be computed. If one used "conventional" model theory, the model weight would be taken as 350 pounds which would produce significant changes in performance.

It is necessary to re-emphasize that the model technique discussed is only as accurate as the equations used to predict performance of the model and prototype. It would seem that under such a circumstance, it would be more sensible to rely completely on an analytical analysis of performance. By and large, the above comment is subscribed to and models appear appropriate when the primary interest is in the mechanical feasibility of a wheel or track form or, in an unusual drive system. The model is used in such a circumstance to evaluate an aspect of performance in addition to the drawbar-pull.

Two complementary studies (3,15) have been conducted in Canada with the goal of developing model scaling laws. The approach pursued by the Mobility Research Laboratory of the Canadian Armament Research and Development Establishment (CARDE) was based on the use of a tilting plate penetrometer as a vehicle model. The penetrometer was forced into the soil by means of an oblique load so that the loading mechanism produced by a vehicle was duplicated. Although the CARDE study is of considerable interest, it is only briefly mentioned in this discussion because the basic philosophy is similar to that proposed by Bekker. The primary difference between the work at CARDE and that done by Bekker is that the latter used two soil tests and

the former a single soil test.

The work of primary interest to this discussion is that of Dickson and Yong (15) in which rules for dynamic similitude were proposed. The dynamic similarity numbers developed were not derived by use of dimensional analysis but on principles of soil mechanics. The approach considered the relationship between an external force and the behavior of a cube of soil located at an arbitrary point relative to the loading mechanism, be it a wheel or a track. The cube was assumed to be subjected to compressive and shear stresses and to gravity and inertia forces. The shear force, inertia force, gravity force, and air resistance were developed on the basis of a unit volume of soil. The development of the individual relationships would be of little help because it was necessary in each case to include a proportionality constant that would require experimental determination. However, when dealing with ratios of the various relationships, the proportionalities were excluded because it was assumed that the constant would be identical for various systems considered. This assumption does not appear strongly supportable because of the sensitivity of soil behavior to the size of the loading mechanism.

No attempt will be made here to present the derivation of all of the dynamic similarity numbers. However, the derivation of the shear force per unit volume of soil will be shown to demonstrate the approach. Consider a cube of soil having dimension L at a general location in the soil. The shear force acting on the soil is certainly

where:

 F_{s} = Shear force in pounds

s = Unit shear resistance in psi

L = Length and width of shear surface in inches.

The shear force per unit volume, V, is:

$$\frac{F_s}{V} = \frac{s}{L} \qquad 37.$$

Quoting from the authors (15) "If the size of vehicle were increased or decreased, the size of the significant soil mass (i.e., the volume of soil in any way affected by the vehicle), and hence

the size of the cube under consideration, would change proportionately. The size of cube is therefore proportional to the size of the vehicle, so that the dimension L is a measure of the size of the whole soil-vehicle system', and

$$\frac{F_s}{V} = K_1 \frac{S}{L_t} \qquad 38.$$

Where

 K_1 = the ratio of size of vehicle to size of cube

 L_{+} = track length or wheel foot print in inches

The development of the remainder of the relationships produced:

a. Inertial force per unit volume of soil:

where

F. = Inertia force in pounds

 $\mathcal{J} = \text{Soil density in 1bs./in.}^3$

 $g = Acceleration of gravity in in./sec.^2$

V₊ = Wheel or track speed in in./sec.

 ε = Soil unit strain in in./in.

 K_2 = Constant of proportionality

and V and L_{t} as previously defined.

b. Gravity force per unit volume of soil:

c. Air resistance per unit volume of soil:

where:

$$F_a = Air resistance$$

and the remaining variables are previously identified.

The dynamic similarity numbers were produced by considering the ratios of shear and gravity forces, inertia to gravity forces, air resistance to gravity forces, and inertia to shear forces and are:

$$DSN_1 = \frac{S}{\gamma L_+} \qquad \qquad .42.$$

$$DSN_2 = \frac{V_t^2 \varepsilon}{g L_+} \qquad 43.$$

It was assumed that geometric similarity in all respects was satisfied when dealing with soil-vehicle systems of different sizes. It would appear that the requirements of the similarity numbers could be met although a considerable amount of ingenuity would be required. If one assumed that — is constant for each system, the scale factor for shear resistance is the same as the geometric scale. However, the stress-strain relationship for soil is normally quite non-linear

so that in satisfying Equations 41 to 44, the sinkage will have to be distorted in order to produce the proper scaling of shear resistance. To overcome this problem is precisely the reason that Nuttall resorted to his relative cohesion.

As stated in another paper in this report, a fundamental proposition to land locomotion mechanics is that the behavior of either a wheel or a track can be predicted on the basis of the behavior of a series of plates. Two plates are forced vertically into soil and the relationship between pressure and sinkage established. A grousered plate is placed on the soil and the horizontal force-deformation curve is established by producing a shear failure in the soil. The penetration test assumes that a plate can be taken as a model of a wheel or track and can be used to predict sinkage, and hence, motion resistance. The shear test is used to predict the traction developed by a wheel or track. The details of the technique for predicting vehicle performance have been adequately reported elsehwere in this report and will not be repeated. The purpose of this discussion is to examine a study in which small and large plate sinkage tests were examined from the viewpoint of a dimensional analysis. This program was discussed in the paper written by Hegedus which appears in this report but is repeated in the interest of completeness. The objective of the study was to determine whether it is possible to predict the behavior of a large plate on the basis of the behavior of a small plate. This is obviously a simpler task then predicting the behavior of a wheel or track on the basis of a plate test. It is equally obvious that if one cannot treat simple plates as the basis of dimensional similitude, one cannot hope to predict the behavior of the more complex system on the basis of the simple system behavior.

A series of tests were designed on the basis of a dimensional analysis which assumed that the system variables consisted of:

```
s = Circumference of plate (inches, L)
```

A = Area of plate (L²)

b. = Characteristic width of plate

 \mathcal{L} = Characteristic length of plates (L)

z = Plate sinkage (L)

h = Depth of soil layer (L)

 $V = Velocity(LT^{-1})$

p = Average pressure beneath plate (M L T)

-1 -2

c = Cohesion (M L T)

b = Angle of internal friction (non-dimensional)

Coefficient of friction between soil and plate (non-dimensional)

-1 -2

Soil density (M L T)

In the conduct of the tests, the soil and the material were to be taken as identical for model and prototype and the depth of the soil was sufficiently great to permit the assumption of a semi-infinite soil mass. The variables—and h were eliminated at the outset. The rate of sinkage was taken as sufficiently low to assume an absence of inertia effects. Emori and Schuring (5) have shown that the critical velocity at which inertia effects become significant is approximately $\sqrt{5}$ gV. The critical velocity for the smallest plates tested was found to be 5 in./sec. All tests were conducted at a speed of 1 in./sec. so that velocity could be neglected in the analysis.

Taking sinkage, z, as the dependent variable, the following functional relationships were established:

$$\frac{z}{s} = f_1 \left[\frac{z l}{p}, \beta, \frac{l}{s} \right] \qquad ... \qquad .46.$$

$$\frac{z}{s} = f_2 \left[\frac{z}{p}, \frac{c}{p}, \beta, \frac{l}{s} \right] \qquad ... \qquad .47.$$

The relationship in Equation 46 is for a purely frictional soil and Equation 47 is for a soil having both cohesive and frictional properties. Equation 47 indicates that scaling of plate sinkage in soils having both friction and cohesion will be distorted because the numerics $\mathcal{T}_{\mathcal{A}}/p$ and c/p cannot both be satisfied if the same soil is used for both prototype and model systems. The numeric $\mathcal{T}_{\mathcal{A}}/p$ requires that model and prototype pressure be related by the geometric scale while the numeric c/p requires that the model and prototype pressure be equal. The numeric $\mathcal{T}_{\mathcal{A}}/p$ represents the ratio of external and gravity or body forces. If the body forces do not contribute significantly to soil strength, the $\mathcal{T}_{\mathcal{A}}/p$ numeric can be ignored and the

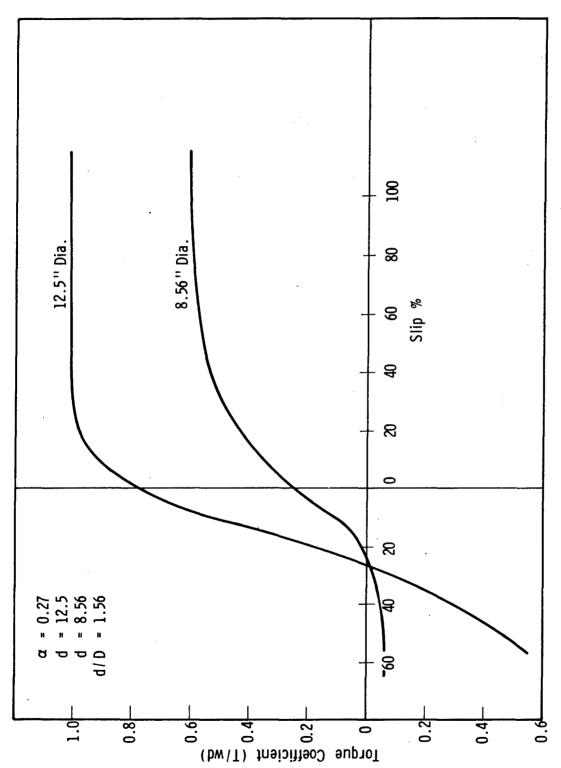
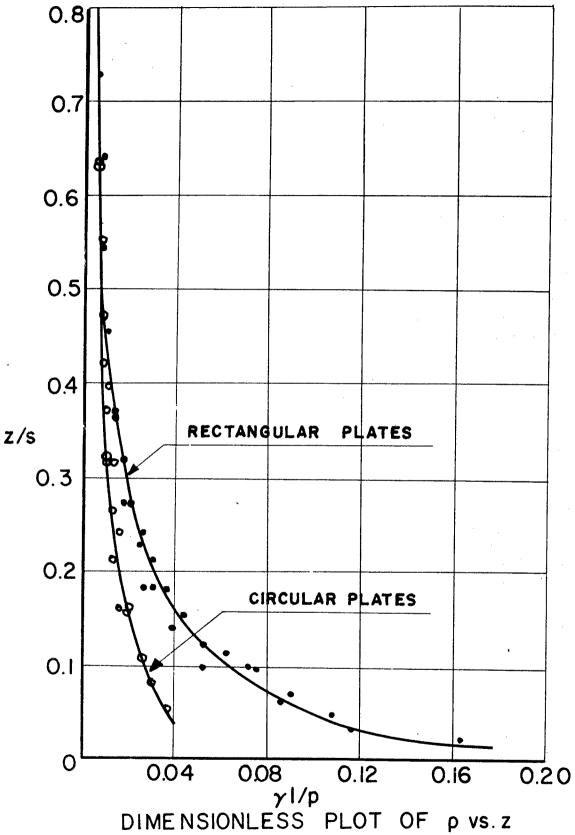


Fig. 11. Torque coefficient-slip for 12.5- and 8.56-in. dia wheels when α = 0.27, d/D = 1.56, and load coefficient = 15.0.



FOR WET OTTAWA SAND

Figure 12 198

relationship between dependent and independent numerics for a cohesive material taken as:

A series of tests were conducted using circular, rectangular, and square plates in sand, snow, and a clay. The object of the tests was to determine whether scaling was possible and to develop a pressure-sinkage relationship based on the experimental results if scaling was satisfactory. In order to evaluate the accuracy of the resulting equation, two criteria were to be used: the accuracy of predicting the sinkage of a large plate on the basis of the sinkage of a small plate and the accuracy of predicting the work involved in sinking a large plate to a given depth on the basis of soil parameters established from a small plate test.

The results of the tests indicated that scaling of the sinkage behavior of plates is possible in frictional soils and that a satisfactory pressure-sinkage relationship can be developed on the basis of tests satisfying the requirements of dimensional analysis. A similar conclusion was not supported for cohesive materials but the tests conducted in the clay were not adequate from either the viewpoint of quantity or of quality. A plot of the relationship between the numerics z/s and \mathcal{T}_{z}/s is shown in Figure 11. The same data are shown plotted on logorithmic paper in Figure 12. The data in Figure 12 show adequate collapse except for low values of z/s. Below a value of z/s = .06, the points are quite unsatisfactory. However, low values of sinkage are usually not dependable in any plate sinkage test because the soil is in a state of local failure or local compaction.

Writing the equation for the curves appearing in Figure 12, we have

$$\log(\frac{z}{s}) - \log A = m(\log \frac{z}{p} - \log B) \dots 49.$$

Where A and B are the coordinates of any point on the curve. Eliminating the logarithms:

Letting $-1/m = m_1$ we get:

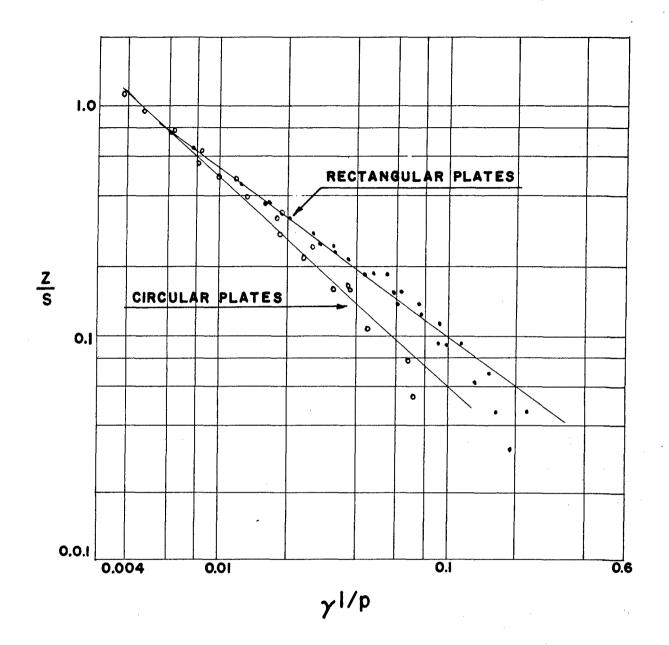
and taking $\mathcal{S}/\mathrm{S}(\mathrm{AS})^{\mathrm{m}}\mathrm{I}$ as a constant, the familiar Bekker Equation is produced:

Although the form of the constant is changed in that Bekker's equation for a frictional material would produce:

However, Bekker proposed that k was related to friction and the constant $\mathcal{TL}/B(AS)^m$ is also related to friction so that the form of the two equations appear quite similar. If plate sinkage tests can be scaled on the basis of the numeric c/p for purely cohesive materials, a similar procedure would produce:

and taking C/B(AS) as a constant, the equivalent of the Bekker parameter, k_{C}/b would be produced. It is thus evident that the dimensional analysis based equation will be quite similar in form to the Bekker equations for either purely frictional or purely cohesive materials. The parallel appears to collapse for materials having approximately equal contributions to strength by frictional and cohesive properties.

The plate studies discussed are only preliminary in nature and must be extended to include larger plate sizes and more careful set of experiments in clay. One series of tests have been completed in



LOG(z/s) vs. $LOG(\gamma I/p)$ FOR DRY OTTAWA SAND.

Figure: 13

sand in which plates ranging from 2 inches to 24 inches were used. The results appear in Figure 13 and the collapse of points into a single curve is quite satisfactory. The results of the initial tests have been reported in detail elsewhere (4) and will not be repeated here. Suffice it to say that the equation produced by dimensional analysis produced a somewhat better prediction of plate sinkage than the Bekker equation but there has been no demonstration that dimensional analysis will produce a sinkage equation that is as general as Bekker's equation.

The final application of dimensional analysis to land locomotion mechanics to be discussed is the study of Emori and Schuring (5). This study is included because it emphasized dynamic considerations even though the intended application was to earth working equipment rather than to vehicles.

Emori and Schuring assumed that the significant parameters affecting the behavior of a tool working soil are:

 \mathcal{L} = Characteristic length

F = Force

g = Acceleration of gravity

p = Mass density

V = Velocity

c = Cohesion of soil

A dimensional analysis produced the numerics: $K_1 = \phi$,

$$K_2 = \frac{c}{2 \pi \ell}$$
, $K_3 = \frac{V^2}{g \ell}$, $K_4 = \frac{F}{2 \ell 3}$ where $\mathcal{J} = gg$.

The numerics were taken as representing:

- 1. Inertia forces proportional to $\frac{d}{g} I^2 U^2$
- 2. Gravity forces proportional to $\mathcal{T}\mathcal{L}^3$.
- 3. Cohesive forces proportional to $c l^3$.

4. Frictional forces proportional to $\gamma l^3 \phi$

It was proposed that similarity was satisfied if the ratios of frictional, inertial, and cohesive forces to gravity forces were kept constant, that is,

The numerics $c/\sigma \mathcal{L}$ and $V^2/g\mathcal{L}$ are essentially the same as the Dynamic Similarity numbers 1 and 2 of Dickson and Yong, even though they were derived by quite dissimilar methods.

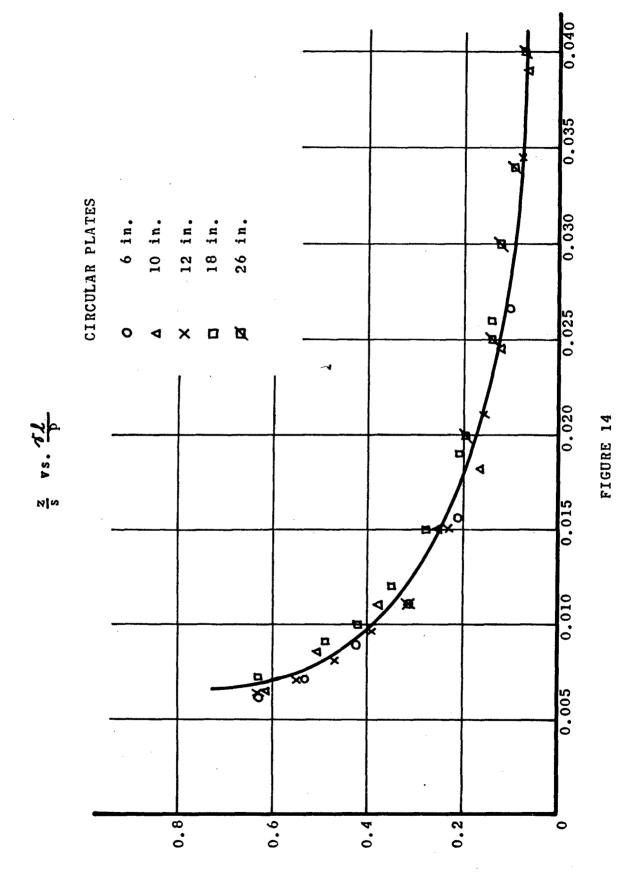
Emori and Schuring proposed two situations: the dimensional requirements for a small velocity and for a high velocity of soil deformation. For small velocities, three situations were argued: a sandy soil with c = 0, and clay soil with p = 0 and a loam type soil with c = 0. It was shown that for the case of sand, Equation 55 reduced to:

Equation 57 assumes that geometric and qualitative similarity is satisfied at the outset.

Equation 56 was reduced to

for a purely cohesive soil. Equation 58 is identical in form to Equation 42 in that S in Equation 42 would reduce to c for a purely cohesive material.

For a soil in which neither ϕ or c is zero, Emori and Schuring propose that



204

NIN

The equation is proposed as a speculation that needs many more experiments to be proven. The Terzaghi bearing capacity theory is quoted by Emori and Schuring as an example of Equation 59 in that:

can be written as:

This example may be a vain hope of support to the conclusion cited by Equation 59 because bearing capacity assumes negligible sinkage. Equation 59 permits, or more strongly, assumes, significant deformation even though the deformation rate is not high.

If the deformation rate is high, Equation 56 was reduced to:

in which only inertia forces are considered to be acting against the soil working tool. Experimental results were provided to support Equation 62 in which it was shown that for $V^2/g \mathcal{L}$ 100, the relationship between $F/g\mathcal{L}^3$ and $V^2/g\mathcal{L}$ was linear with a slope of 45°. The soil in which the tests were conducted had a cohesion of 0.27 psi and a zero angle of internal friction. Because of the very low strength of the soil, one is forced to question whether the controlling factor is inertia or viscosity. The significant point, however, is that a definite relationship between the external force and velocity was established. On the basis of their study, Emori and Schuring concluded that complicated soil working processes can be clarified by means of dimensional analysis and that model testing has been proven feasible.

The review of dimensional analysis applications presented in this discussion is by no means complete. The purpose of the review was not to consider all of the studies that have been conducted but to demonstrate the broad range of problems considered by various people. An earnest attempt has been made to place dimensional analysis in a proper perspective concerning its application to land locomotion mechanics. As a tool to develop insight into the soil-vehicle

system, dimensional analysis is of great significance. As a tool for vehicle evaluation, dimensional analysis is of limited value because we have no great need to resort to the use of models.

REFERENCES

- Nuttall, C. S., "Scaled Vehicle Mobility Factors", Wilson, Nuttall, Raimond Engineers, Inc., Chestertown, Maryland, July, 1956.
- 2. Vincent, E. T., Hicks, H. H., Jr., Oktar, E. F., Kapur, D. K., "Rigid Wheel Studies by Means of Dimensiona! Analysis."
- 3. Dickson, W. J., "Ground Vehicle Mobility on Soft Terrain", Journal of the Soil Mechanics and Foundations Division, Proceedings of the American Society of Civil Engineers, August, 1962.
- 4. Liston, R. A., and Hegedus, E., "Dimensional Analysis of Load-Sinkage Relationships in Soils and Snow", Report No. 100, Land Locomotion Laboratory, Warren, Michigan, 1964.
- 5. Emori, R. I. and Schuring, D. E., "Feasibility of Model Study in Earthworking Equipment", American Society of Agricultural Engineers, March, 1964.
- 6. Marwick, A. H. O., "Dimensional Analysis of the Bearing Capacity of Soils Under Tracked Vehicles and Its Application to Model Tests", Road Research Laboratory, October, 1944.
- 7. Nuttall, C. J., Jr., "Scale-Model Vehicle Testing in Non-Plastic Soil", Stevens Institute of Technology, ETT Report 394, December, 1949.
- 8. Nuttall, C. J., Jr., and McGowan, R. P., "Scale Models of Vehicles in Soils and Snows", Proceedings of the First International Conference on Mechanics of Soil-Vehicle Systems, Turin, Italy, June, 1961.
- 9. Wilson, Nuttall, Raimond Engineers Inc., "Scaled Vehicle Mobility Factors (Sand)", TREC Technical Report 61-67., U. S. Army Transportation Research Command, Fort Eustis, Virginia, April, 1961.
- 10. Roma, C. J., and Simon, Herman P., "Scale Model and Full-Scale Vehicle Testing in Cohesive Clay Soils", U. S. Army Transportation Research Command, Fort Eustis, Virginia, May, 1964, Report 64-6.

- 11. Uffelman, F. L., 'The Performance of Rigid Cylindrical Wheels on Clay Soils", The Proceedings of the First International Conference on the Mechanics of Soil-Vehicle Systems, Turin, Italy, 1961.
- 12. Vincent, E. T., Hicks, H. H., Jr., Oktar, E. F., and Kapur, D. K., "Rigid Wheel Studies by Means of Dimensional Analysis", Report No. 79, Land Locomotion Laboratory, Warren, Michigan, April, 1963.
- 13. Oktar, E., Mat, H., and Vincent, E. T., "Performance Coefficients for Powered Wheels in Michigan Farm Soil", Report 05600-16-F, The University of Michigan, Ann Arbor, Michigan, October, 1964.
- 14. Harrison, William L., Jr., "Analytical Prediction of Performance for Full Size and Small Scale Model Vehicles", The Proceedings of the First International Conference on the Mechanics of Soil-Vehicle Systems", Turin, Italy, 1961.
- 15. Dickson, W. J., and Yong, Raymond, "Principles of Similitude for Soil-Vehicle Models", Soil Mechanics Series No. 6, McGill University, April, 1963.

SOIL STRENGTH PREDICTION BY USE OF SOIL ANALOGS

By: William L. Harrison, Jr. Bong-Sing Chang

INTRODUCTION

The design of high performance military vehicles for off-theroad travel must be derived from specific parameters of the environment in which they will operate. To ignore such an approach in the establishment of design parameters could lead to gross inefficiency in performance.

The purpose of land locomotion research is to establish "vehicle environmental parameters" and a discipline relating these parameters to the performance of the locomotion element.

With the exception of highway vehicles, designers have looked to nature for guidelines to principles of locomotion. Seemingly. designers associated with the fluid mediums have followed nature's guidelines with greater success than designers of land vehicles. The guidelines presented by nature on land are at a minimum, as numerous as the variations in the physical environment. Animals which travel "overland" present the ultimate example of "special purpose" forms of locomotion. Mountain goats, moose, the cheetah, and snowshoe rabbits are all examples of these forms. The fact that special forms of land animals are so numerous, each suited to its environment, is indicative of the fact that the solution to land vehicle design is not singular nor one of simplicity. Although this study is concerned with soil strength characteristics, it is interesting to note that nature provides a wide variation in ground pressures, depending on the soil characteristics to which an animal is exposed and must negotiate. However, a characteristic common to all land animals is the principal of locomotion with levers, thereby having the inherent capability of negotiating geometric obstacles. Projection of this phenomenon tends to be evidence that geometric properties of terrain present the most severe design requirements for high performance off-the-road. The foregoing statement has been proven to be fact in several reported studies (1, 2). Nevertheless, soil strength remains an important factor of the environment; and a method for its prediction without access to the site is offered in the following pages.

TECHNICAL APPROACH

The current studies of soil strength prediction by the Land Locomotion Laboratory are in supplement to the overall study of terrain analogs. Many studies in terrain classification precede this paper, some of which are listed in the bibliography.

Several methods of predicting soil strength were investigated by short term study. The study which seemed at the time to offer the greatest probability of success proposed the establishment of soil analogs (3).

The soil analogs will be established by using the United States Department of Agriculture (USDA) Soil Classification System (4) by which a major portion of the United States has been sampled and mapped. In order to implement the proposed approach, soils in other areas of the world must be classified in terms of the USDA System. Work to this end has been in progress for a number of years by the World Soil Geography Unit in Hyattsville, Maryland. This system of soil classification gives the broadest description of soil properties available. It considers the properties of a soil mass, in situ, and describes each soil horizon to a considerable depth below the surface. Also considered is the natural vegetation, ground water, slopes, climate, and many additional facets that are lacking in other taxonomic systems (3). The USDA System comprises various levels of grouping starting with the Soil Associations. Following in descending order are the Great Soil Groups, Series, Soil Types, and Phases. An additional and valuable input to the classifications is the work of the Bureau of Public Roads in furnishing the Unified Soil Classification System (USCS) and the American Association of State Highway Offices (AASHO) designations for all major soil series.

What remains in the approach is to determine whether the USDA System lends itself to soil strength description by the Land Locomotion Laboratory soil strength parameters. This question is the basis for the study reported in this paper.

Field and laboratory experiments were designed to determine the following:

- a. The variation in Land Locomotion Laboratory Soil Values of USDA Soil Series from analogous sites. Sites were separated by distances of 100 to 300 miles.
- b. The possibility of grouping USDA Soil Series based on the Land Locomotion Laboratory Soil Value System. (5).



Figure 1.



Figure 2.

c. Determine the gross effect of the variation in soil strength parameters from analogous sites on vehicle performance predictions.

TEST PROCEDURE AND INSTRUMENTATION

Three sites of each series chosen for the study were sampled for the following information:

- a. Shear stress-deformation curves for determining cohesion and the angle of internal friction.
- b. Load-sinkage curves, for determining vertical load deformation parameters k_c , k_d , and n.
 - c. Moisture content.
 - d. Bulk density.
- e. Disturbed and undisturbed samples of the soil to a depth of 18 inches.
- f. Cone penetrometer readings at depths of three (3) and six (6) inches.

The majority of the sites were located in hay fields or grass-lands of a sort, requiring consideration of the vegetative cover. The procedure followed was to cut and roll back the turf. This allowed soil strength measurement without concern for variations in vegetative cover.

All sites were pinpointed by the local offices of the Soil Conservation Service who provided also a profile description of the site.

The instruments and supporting equipment were transported in a half-ton van. This included an AC-DC generator for power supply to recording instruments, wax melting pot, drying oven, etc.

The shear stress-deformation curves and the load-sinkage curves were measured with the Bevameters shown in Figures 1 and 2. Operation of this equipment and processing of the resulting data is described in Annex 8 of the report titled: "Mobility Environmental Research Study Mobility Testing Procedures", by the Land Locomotion Laboratory.





Figure 4.

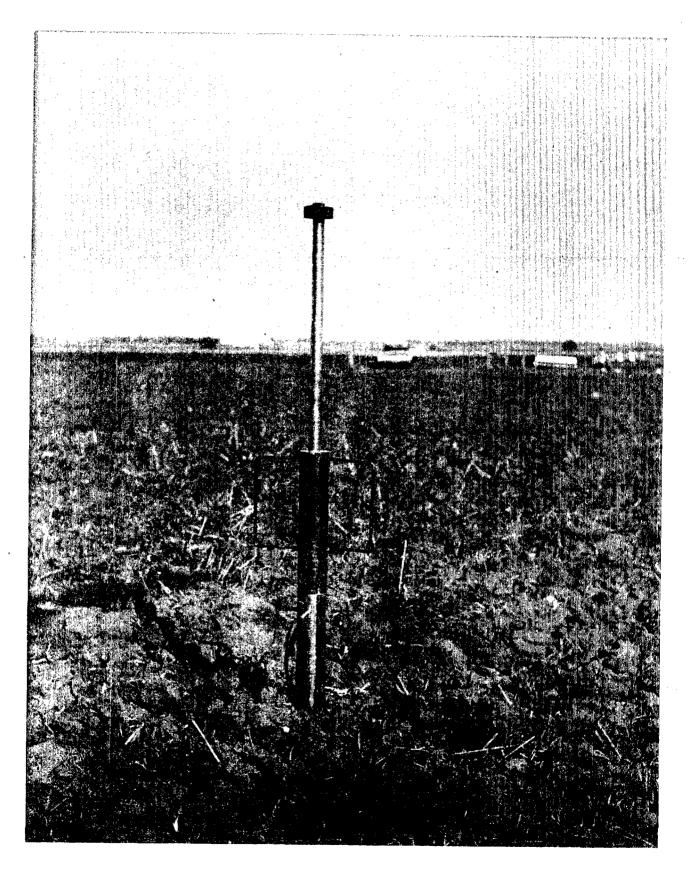


Figure 5.

Figures 3 and 4 show the nuclear devices used for measuring moisture content and density. Figure 3 shows the recorder and moisture meter in the process of calibration. Figure 4 shows the density device in place during measurement. Measurements were checked periodically by weighing and by the oven dry method.

Undisturbed samples were collected in thin walled tubes, 2-3/4 inch diameter and 2 feet in length. The tube and driving mechanism are shown in Figure 5.

The cone penetrometer is shown in Figure 6. A description of the use of this device is described in Annex 9 of the above report.

TEST RESULTS AND DISCUSSION

The test areas are referred to as the Northeastern and North Central sites. The northeastern sites were located in the States of Michigan, New York, Maine, and Connecticut. The soils on these sites were classified as sandy loams and loamy sands of the Gloucester, Charlton, Paxton, Adams, and Wallace series.

The North Central sites were located in the States of Indiana, Illinois, Iowa, Wisconsin, North Dakota, South Dakota, Wyoming, and Kansas. The North Central sites consisted of loams and silty clay loams of the Barnes, Bearden, Keith, Tama, and Fox series.

An Adams loamy sand located in Jefferson County, New York, and a Wallace loamy sand located in Emmet County, Michigan, were compared as possible analogs. The results of the field measurements are shown in Figure 7.

The grain size distribution of the Adams and Wallace Series is shown in Figure 8. The variation in density between the two sites of 14 lbs./cu.ft. is considerable. The cone index readings at 3 in. and 6 in. reflect this difference. The shear stress vs. normal load curves show a poor comparison. These soils cannot be considered as analogous although in the same Soil Association. The variation of the angle of internal friction (\not) with increasing water content is shown in Figure 15. Here again the two soils show dissimilar characteristics.



Figure 6.

Sites of the Paxton Series chosen for comparison were located in Jefferson County, New York; Androscroggin County, Maine; and in Tolland County, Connecticut. All sites of Paxton sandy loam measured were as close to the model as possible. Figure 10 shows the results of the field measurements. With exception of the variation in cone index readings the field test results are very uniform.

Figure 11 shows the comparison of two sites of Charlton sandy loam. One site was located in Androscroggin County, Maine and the other in Tolland County, Connecticut. In spite of a difference of 8% in moisture content, the field tests were for all practical purposes identical. Both test sites were grass covered pasture land.

The sites selected for measurement and comparison of the Gloucester sandy loam were located in Androscroggin County, Maine and in Tolland County, Connecticut. Both sites were under a cover of hay. The sites were considerably dissimilar in moisture content and density. These differences were not reflected to any considerable degree in the shear strength characteristics. Figure 12.

Figure 13 shows the variation in shear stress vs. normal load curves of the Paxton, Charlton, and Gloucester series under field conditions.

The disturbed samples collected for laboratory tests were used to determine the grain size distribution curves for each of the three series. The curves represent the analysis of the "A" and "B" horizons of all samples collected. Figure 14 shows the grouping of all series noting that soil types range from sand to sandy loam.

The three series had little apparent cohesion under field conditions (0 to 0.4 psi). Laboratory tests were conducted to examine the effect of changing moisture content. The maximum change occurred with the Paxton sandy loam. However, the differences between all samples were negligible. Figure 15 shows the variation of apparent cohesion (c) with increasing moisture content from samples of the Paxton loam. Also shown in Figure 15 is the variation of the angle of internal friction (b) with changing moisture content for all of the soils tested in the Northeastern area. With exception of the Wallace and Adams series, the results are uniform.

The test sites in the Northeastern Area were too firm for measurement of load-sinkage characteristics. The firmness of the soil is indicated in the distribution of cone index values shown in Figure 16.

NORTH CENTRAL SITES

Having gained experience from the tests conducted in the Northeastern area and on samples from these sites in the laboratory, the tests conducted in the Burosems and deep Chernozems of the North Central area were more detailed and informative.

The Tama, Fox, Barnes, Bearden, and Keith Series were selected for comparison within Series, and to determine the possibility of grouping different Series. The fifteen (15) sites (three of each Series) covered an area from Indiana to Eastern Wyoming and from North Dakota to Kansas. Measurements were made during the months of October and November.

Figure 17 shows the five Series measured in a comparison of profiles. Indicated are the comparative thickness of the A, B, and C horizons which were present in all cases with exception to the Bearden Series. This Series lacked a "B" horizon at Sites III and IV. VII, listed as Bearden in previous years, has been reclassified as the Forman Series. It differs in profile from the other sites by having a 15 inch "B" horizon. The Keith Series has a very shallow "A" horizon (5 to 7 inches) with exception to Site X (17 inches). The effects of these differences in profile within a series will be discussed later. In summary, the "A" horizon of the test sites ranged in thickness from 5 to 17 inches and the "B" horizon ranged from 0 to 35 inches. The most significant effects from the profile structure were the variation in depth of the "A" horizon within a series and the absence of the "B" horizon. These effects must be considered conjectural to some extent when considering that field moisture contents of the test sites had a variation of 21% and density varied from 62 to 113 pounds per cubic foot.

The table in Figure 18 shows a summary of all field data collected and the location of the test sites. Hardness of surface prevented measurement of k_c , k_f , and n at Sites II and VII. All vertical load parameters and cone index values measured indicated very firm soil conditions. A distribution of cone index values is shown in Figure 19.

Figure 20 shows the variation in c and \not values for all of the test sites. Cohesion ranges from 0 to 0.3 psi and the general body of curves range from \not = 20.1 to \not = 23.8 . Curves from Sites I, VIII, IX, and X which fell out of the general grouping can be explained as follows: Site IX was located on a mesa, which resulted in a low field moisture content. Surface shear was measured during a drizzle which had been in progress for about four hours, affecting only the first two inches of soil. This resulted in a low value of

 $\not b$ (18.5°) while the average moisture content of the first eighteen inches of soil indicated a rather dry condition (20%). Site X was located in a low area and had an "A" horizon which extended to approximately seventeen inches. The field moisture content (33%) was very near the liquid limit of the soil accounting for the low c and $\not b$ values (0.0 and 15.8° respectively).

Examples such as these can be used to explain the extremes in variation of the field test results, but of importance is the fact that the field tests had relatively small variation in spite of the variations in density and moisture content.

Tests in the laboratory were made to examine each soil series under like conditions and thereby establish a direct comparison of parameter ranges. Figures 21 thru 25 present summaries of the laboratory tests.

Figure 21 shows a band of grain size distribution curves for the fifteen test sites. The texture ranged from 22% clay; 48% silt; and 30% sand (loam) to 38% clay; 55% silt; and 7% sand (silty clay loam). The grain size distribution curves for the five series of the North Central area is included in the Appendix.

Figure 22 contains a table of the initial laboratory tests conducted on the disturbed samples with the Direct Shear Test Apparatus, and on the undisturbed samples with the Triaxial Test Apparatus.

Figure 23 shows the variation in apparent cohesion (c) and internal friction angle $(\not p)$ with changing moisture content. The average liquid limit for the fifteen samples was 25.4%. From 0 to 20% moisture content the samples show very close comparison. As each individual sample approaches its liquid limit, the magnitude of c and $\not p$ decreases rapidly.

Figure 24 illustrates the variation in shear strength (c + p tan $\not o$) of all fifteen samples as a function of moisture content. The variation is shown at normal loads (o) of 4, 8, and 10 psi. The large variation in shear strength beyond a moisture content of approximately 20% is to be expected with the large variation in liquid limits. This is also expected with the clay content of the samples varying from 22% to 38%.

Figure 25 shows the variation in shear stress as a function of normal load over a moisture content range of 0 to 22%. This illustrates the gross effect of the variations in soil strength parameters from the fifteen sites. Using the equation for gross

tractive effort: $H = Ac + W \tan \phi$ (5) where "A" is the contact area of the traction element and "W" is the load on the contact area, the total effect would equal the variation in apparent cohesion (c) from 0.15 to 0.5 psi.

CONCLUSIONS

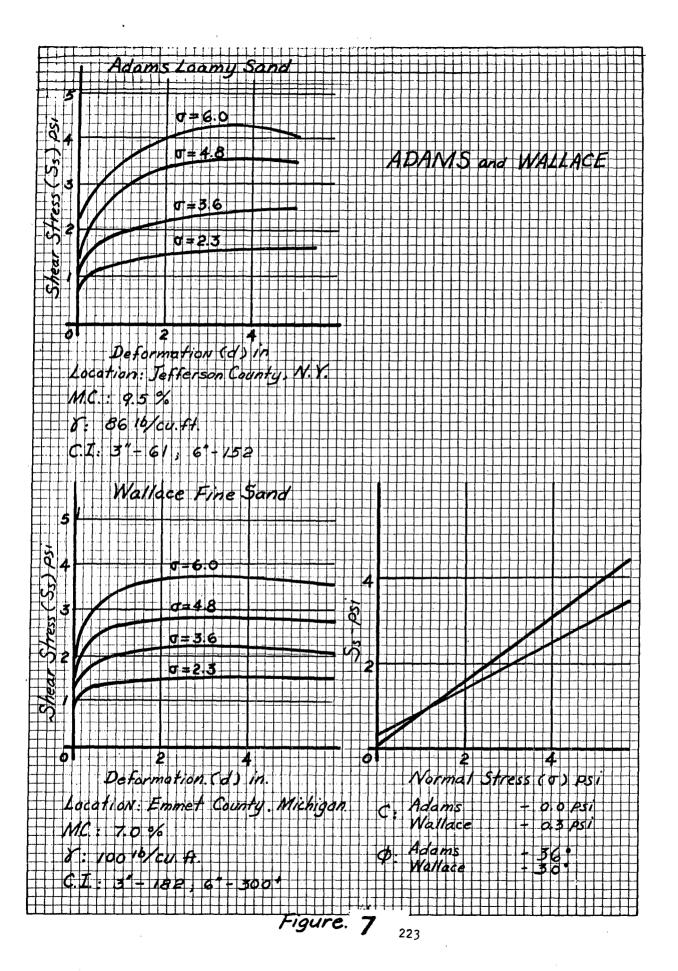
The United States Department of Agriculture Soil Classification System does lend itself to soil strength description by Land Locomotion Laboratory Soil Strength Parameters. For purposes of vehicle design and performance evaluations, prediction at the Series level should be sufficient. The attempted gain in accuracy by predicting at the level of Soil Type or Phase would be lost in the inherent variations within a Soil Series.

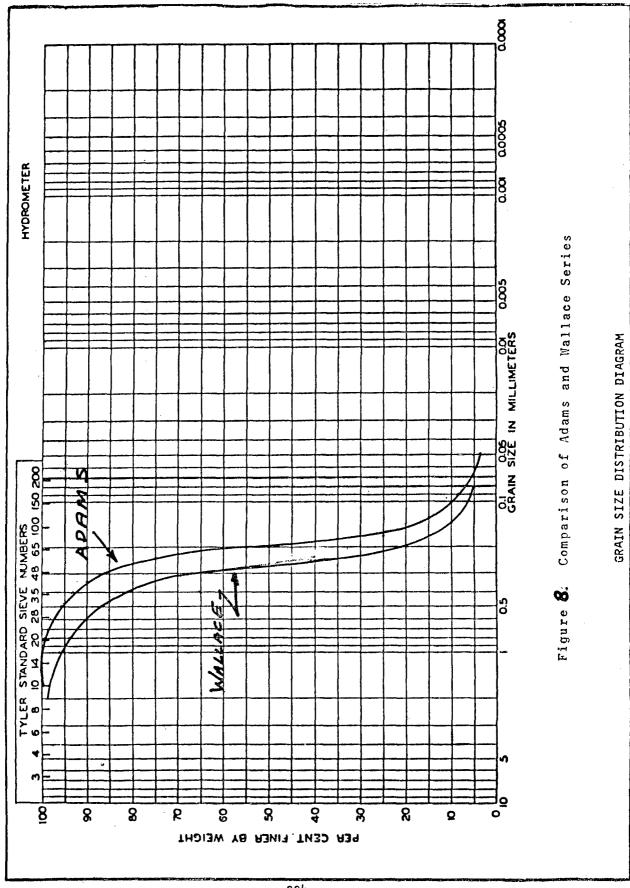
Based on the results from the laboratory tests, sites which are analogous in USDA Classification are equal in soil strength as described by the Land Locomotion Laboratory system of measurement.

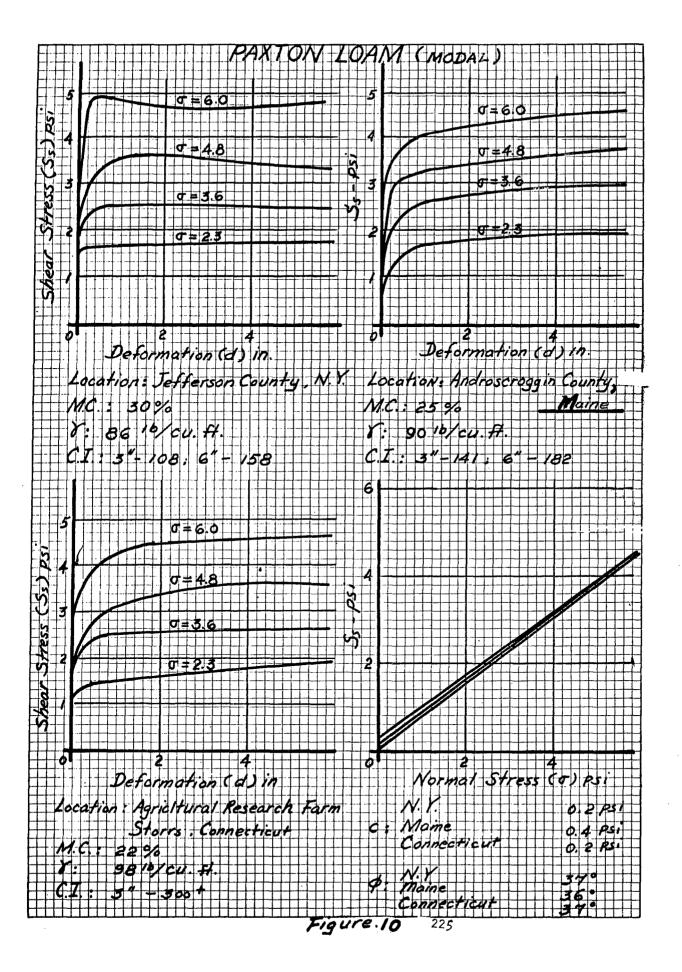
The results of measurements from both the Northeastern sites and the North Central sites lead to the conclusion that grouping of USDA Soil Series based on Land Locomotion Laboratory soil strength parameters is feasible.

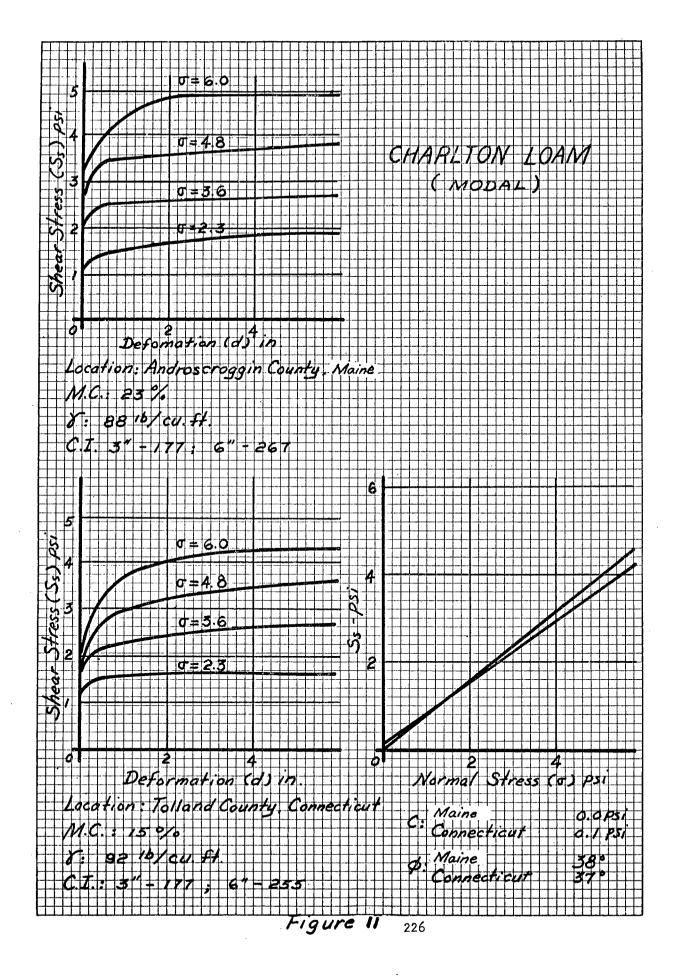
On the basis of the findings of this study, it is concluded that the establishment of soil analogs of remote and inaccessible areas of the world is a reasonable and practical approach to predicting soil strength parameters.

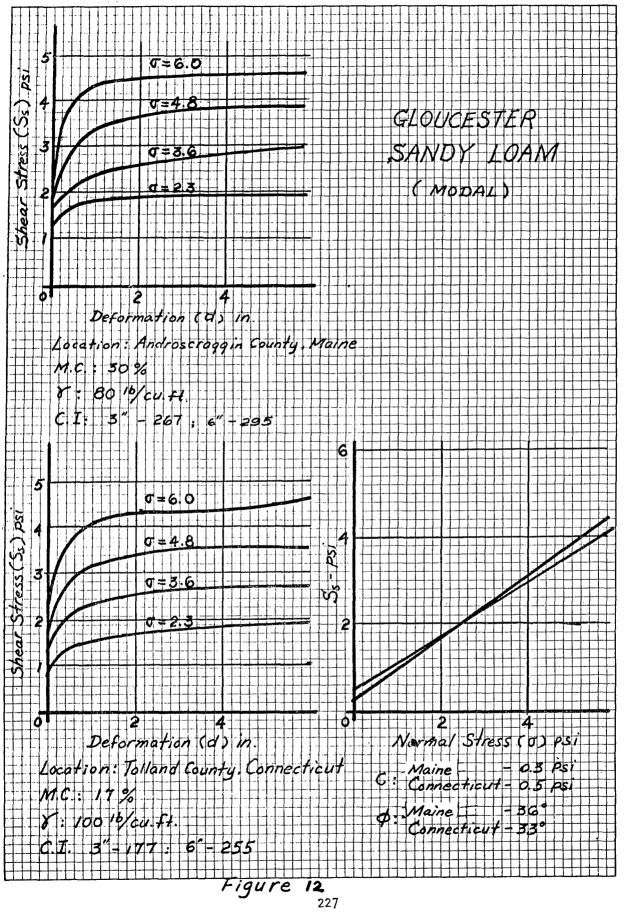
What remains is the final test of the proposed method by selecting sites located in the Eastern Hemisphere; determination and measurement of the accessible analog (Western Hemisphere); and finally on-site measurement of the remote area for determination of accuracy in description and strength prediction. In addition, a method is required to allow grouping of USDA Series into those having like Land Locomotion Laboratory Soil Strength Parameters. The initial investigation should consider the work of the Bureau of Public Roads. The Bureau is publishing the engineering properties of soils, i.e., texture classification, Atterberg Limits and the "Unified" and "AASHO" soil classifications of each established USDA Soil Series. This work could provide a significant shortcut in grouping USDA Series, and in the definition and location of accessible analogs.

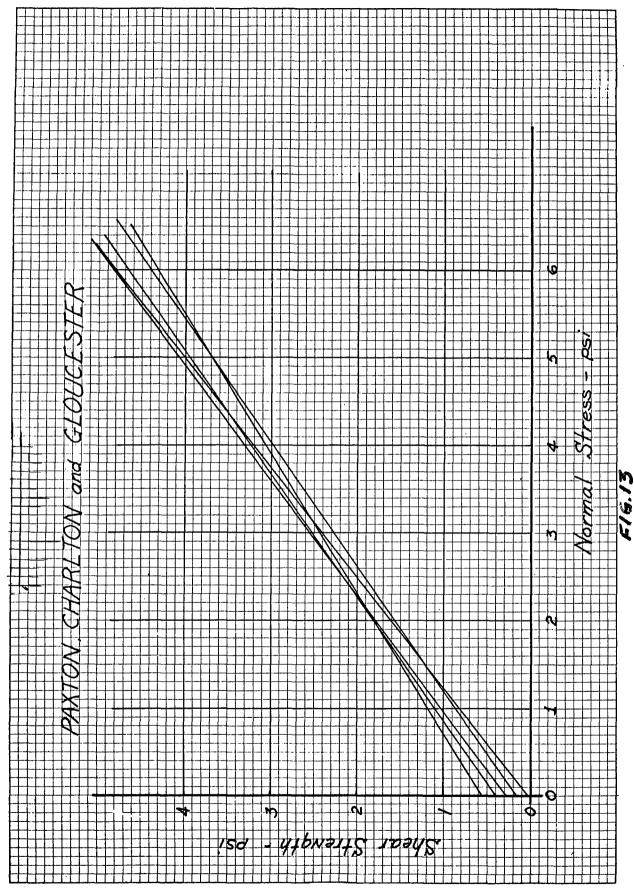


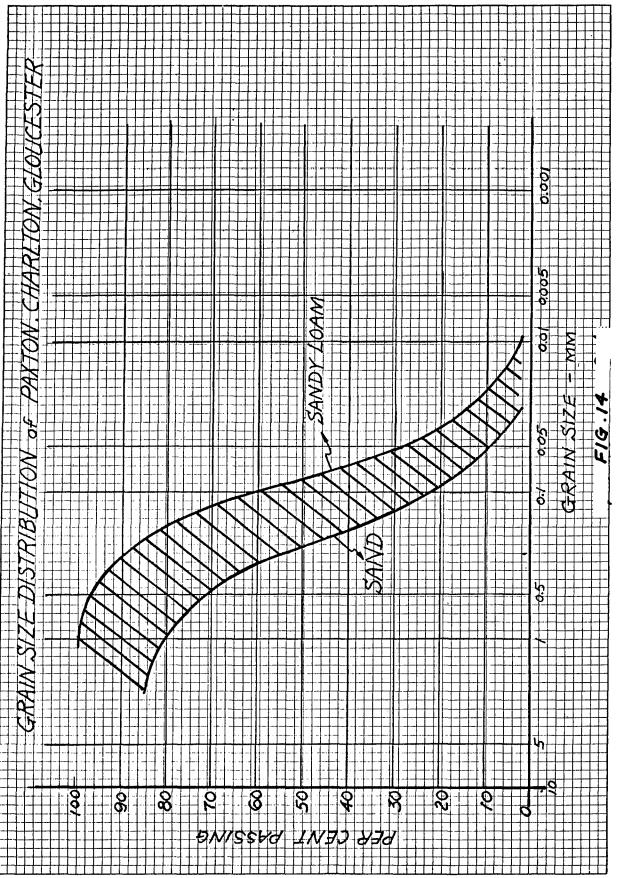


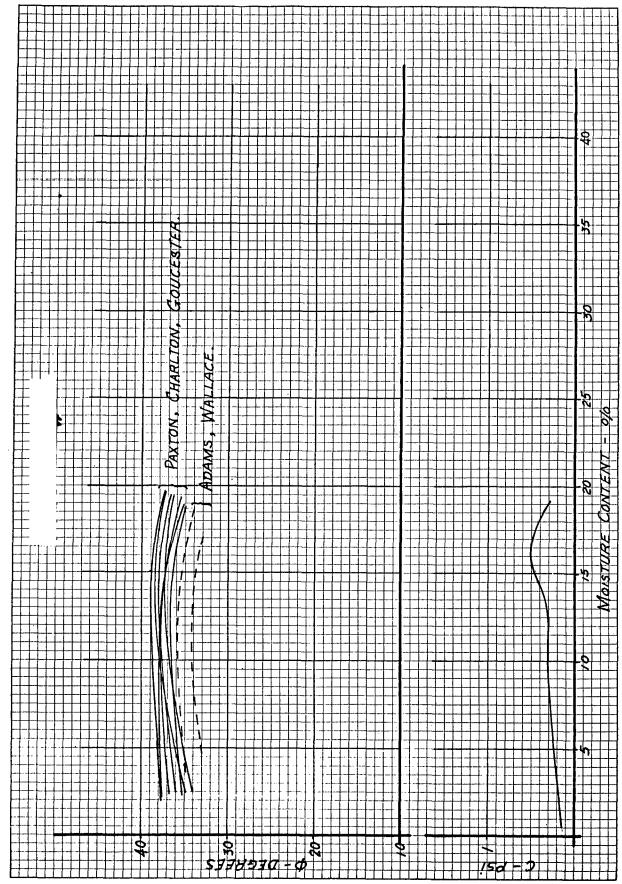


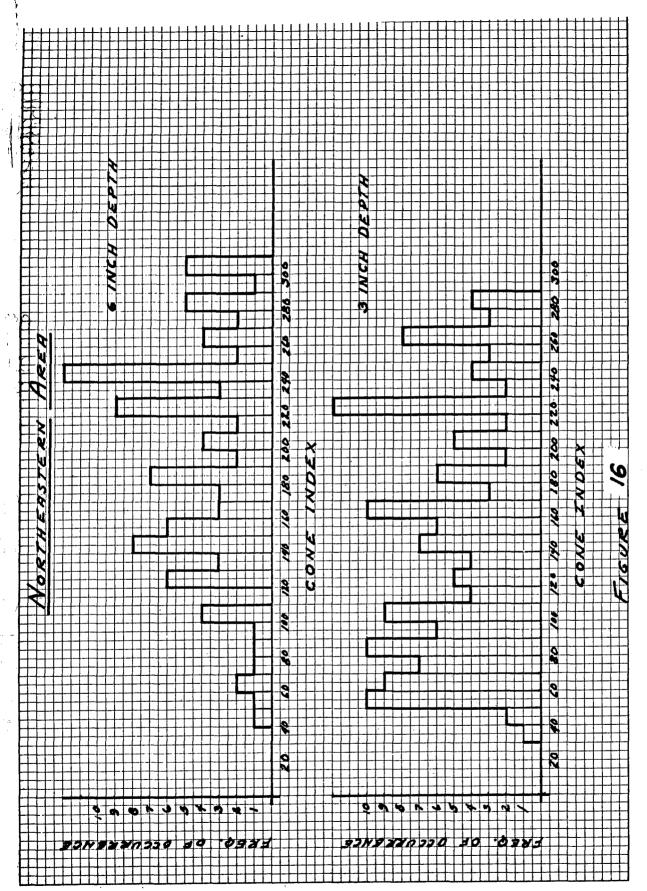






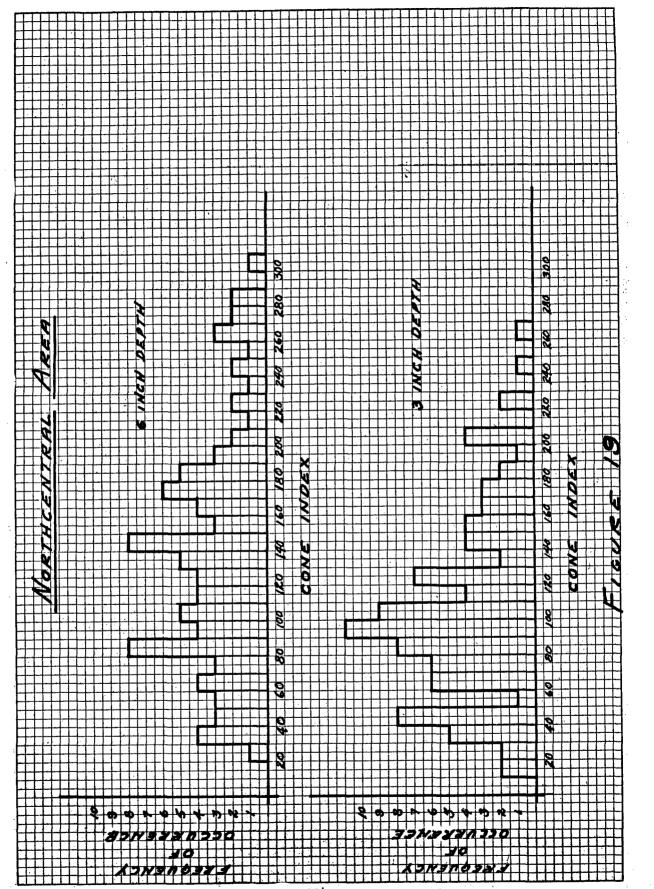


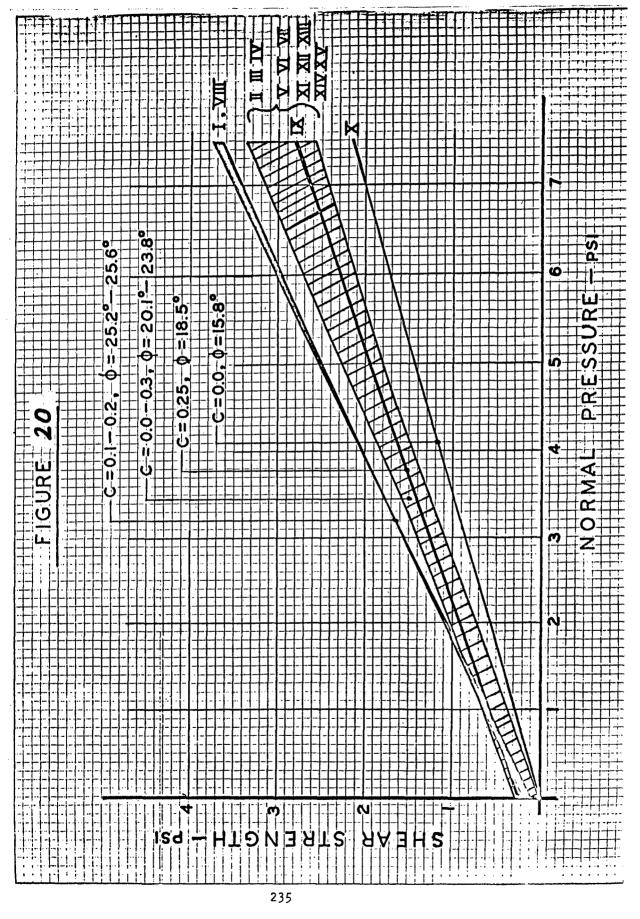


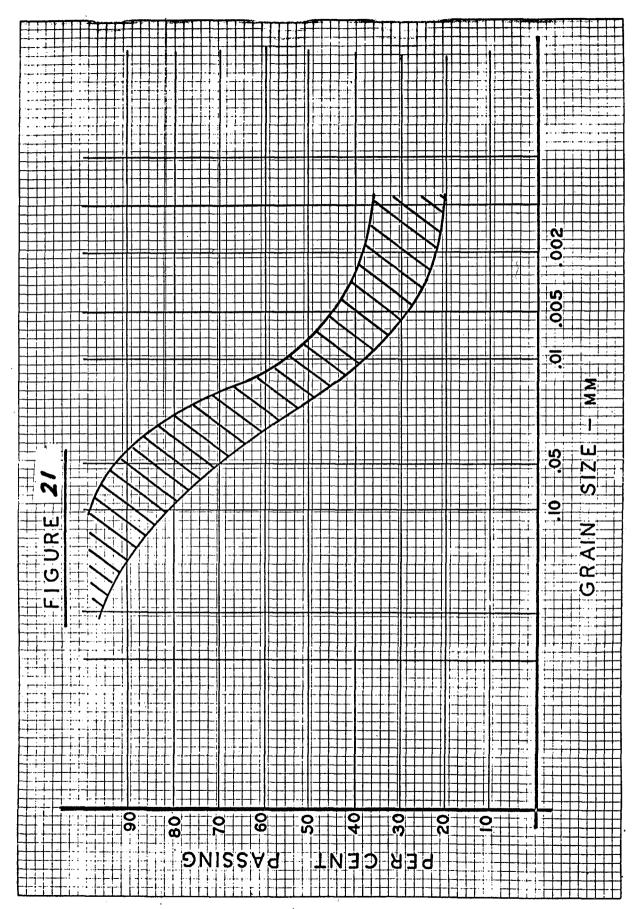


							-		1	
				Ü	1 1		S			
					"					<u>'</u>
	U			၂၂၂ပ	4					32
35					AT 41"-					right Hard
	-				3	C AT 48"			╢┼╢┼	
						-┨ ╌ ┪┤╏╏				
30										9
			O							
					$ \omega $		B			
										2
	B								Œ	
										┃┃ ┃ ┃ ┃ ┃ ┃ ┃ ┃ ┃ ┃ ┃ ┃ ┃ ┃ ┃ ┃ ┃ ┃ ┃
									ω	0 2
				8						HE 20
				11111111111				8		
				B						
m 2										
FIGURE		8						-		
<u>ပြု</u>			8							
[O		B								
	Α				A			-		
						 - 	A		Y	
9									A	8
			V	∀				A		
		1, 1, 1 1, 1						Ш		
SITE 国 国	則	KH	Ħ	H K	X	H		XIII	N N	
THO L	يا إلى					++1++		Pa		
ARDEN	38	'BNE'S	A 8	ELLH	K	AMA		X	P 0	
				232				111	<u> </u>	Literal III. III

				<u> </u>					
	H	 	1111111	111111			++++++++++++++++++++++++++++++++++++	++++++	+++++++
			<u> </u>			1111			
	┼┼┤	╁╁╅╂┼	╀┼┼┼┼┼┼	┋┋┋┋	╶┋┋┋	╌┼┼┼┼┼	┼┼┼┼┼	╎┧╎╏╏╏╏	┤┤╏╏ ┼┼┼┼
	口口	 	 	 			 	 	
╂┼┼┼┼┼	H	╂╂╂╂	╀╂╂╂╂╂╂	╂┨╏╏┩╏ ╄	╒╏┩╇	╶╂╂ ╁┼╂╂	╀┼┼┼┼	┞┋┋┋	┦╏╏╏
-									4111111
┠╏╋┩╏ ┪	Ш	▋ 	▋<u>┾</u>╁╏ ╆┼╏╬┼	╏┼┼┼┼┼	╘╻┼┼┼┼	<u>┪╅╅╏</u>		<u>▋</u>	▋<u>┼</u>╏┤ ╅┼┼┼┼
	Π		0 0		9 9		9 9	4 0 0	1
	丗		0 0		1911	2 1 1 2 1 1 2	119119		▋ ┆ ╅╅╅┪
H + H + H + H	H	┠┝┝ ╅╇	▋┤┤┨ ┽┼╂ ┥	╂┼┼┨┽╎ ┠┽╸	╌╏┼┼┼┼	╶╏┋ ┼┼╏┼┼	╂┼┼┼┼	╏┾┿╏ ┼┼╂┼┿	┫╁┼┼┼┼┼┼┼
	坩							▋ ▗ ▎ ▗ ▎▍	
┠┤┋╏╏╏	++	1 3	╏┼╬╏┼╬┞┼	╏┼┢┠┼ ╈╢┼ [┍]	7 +44 +4	┧┼┞┦┼╬	 + 	40 40 40	╻┼┼┼┼┼┼┼
	\Box			[-1]			$\Pi\Pi\Pi$		
				<u> </u>	. 				
		 	┇┽┼╏┽┼╂┼┼	┨┼┼╏┼┼╟┼	╌┇┼┼┼╂┼┼	╂┼┼╏┼┼	╂┼┼┼┼┼	┇┋┋	╻ ┾┼┼┼┼┼┼
	廿				11211	4 4 1	1112	121212	
	+	╏┼┼┼┼	╏┼╁╁┼╏┼┼	╿╌┼╼┼╌ ╏╾┼╌	╌┨┼┦╌╂┽┼	╌┼┼╌╏┽┼╴	╀┼┼┼┼	H + H + H + H + H	╏┼┼┼┼┼┼
	廿					T			
+++++++	++	+++	1-4-1-4-1-00	 - - - - - - - - - - - - - - - - - - -	1401+4	Ŋ- œ + 4 4	 	+40-40-00	▋┤┤╎┤┤ ┤ ┤┤
	#		2 5 5 3 6 5 6	22 22 0	7	7 8 4	2	22 23 63	
+++++	++	╿┤┼┼┼ ┆	 	1-4-1-4	<u> </u>	╏╏ ┼┼	19119	1-41-41-4	▋ ┼ ╏╏╏
	#		┇┆┆╏┆┆	┇┵┼┇┵┼┼┼		 			
++++++++++++++++++++++++++++++++++++	+	<u>╻╌┼╾┼╼┼</u> ╌┤		╽╅╽┼ध╌┧		1 2	1616	╏┼╆╏┼╆╏┼╈	▋┤ ┤┤┤┤ ┤
ППП	77	1	0 0 0		0 6		0 0	0 0 0	
t	#							<u> </u>	
H F	+F	Moisture Content D-18"	+++++	1-12-1-12	$1+\frac{1}{2}$,H,, I T I		+, ++++++++++++++++++++++++++++++++++	1 + 1 + 1 + 1 + 1 + 1 + 1 + 1 + 1 + 1 +
	#	# 0 = 0		0 0 7		2 - 2	8 7 9	\$ 6 4 \$ 6 4	
(C)	+	### H4	39.4	0 6 7	8 6	2	26. 50. 50. 50. 50. 50. 50. 50. 50. 50. 50	\$ 60 5 1 60 5	▋ ┊╸ ┼┼┼┼┼┼
	H.	##.h						┞┤╌┞╸╂╺┧┈╏╺╏╺╏╸	▋┼╀╀┼┼┼┼
t t	#					10 10		1+1+14	
H . F	++	7/18	80.3	0.00	36	2 2 88 88	8. 4.	98 6	┇┼┼┼┼┼┼┼
ا ليا إ	771				11911	774 179	## ##	96 88 66	
FIGURE	##	Dens:11y		┇╌┆╶┋ ═ ╏╌╽╌ ┩╌	┩╌┼╌┞╌┼╌┞╌┼╌┼╌				┇┆┆┆┆┆
<u>ዘ</u> ┗┹⊷ ∤	++1	- - - - - - - - - - - - -	81.3 66.2	103.6	12 8	6 9 6	8 8	9 6 6 8	┇ ┇ ┇ ┇ ┇ ┇ ┇ ┇ ┇ ┇
	#1	0 <u>-18</u>		 	1771128	12 12	1212	12112112	
	井	4-1-6						<u>+† + +</u>	<u>▋</u> ▐▐ ▐▐
H O F	++-1		+	+	4	[++]+-[+++++++	
	#					1++1++		<u> </u>	
H 1. F	$\pm \parallel$	<u> </u>	<u>╶╅╀┠</u> ╅┼┠╅┼╏	++++	 ¥ ++	╏┋┋	╶┤╌╏╸╏╸╏	┼┼╂┼╢┼┼┈	╏╎┼┼┼┼┼┼┼┼
H === E	H	1111						 	
ե է			VESOTA VKOTA	III MARSHALL, MINNESOTA V NEW ROCKFORD, NORTH DAK. VI LISBON, NORTH DAKOTA	FIT SHAWON CO, SOUTH DAKOTA	4 108	╌┼╌╂┼┼╌╏	NSTS NA	┇ ┼╎┼┼┼┼┼┼ ┼
H F	╁╀╏	++++		13 TEL 3	17517	11114		NA PER	
ti t	井	 	III: KENT, MINNESGT/ IV GROOKSTON, MINN WII: HURDN, SOUTH DA	III MARSHALL, MINNE V' NEW ROCKFORD, N		X GAKLEY, KANSAS I LEWISTON, MINNE	<u> </u>	HIT WAUKESHA, WISCO XIV KANKAKEE, ILLIN XV ANDERSON, INDIA	
┞╏╶╏╼╏╼╏╶╏╼┱	┼┼╏	+5	╫ ╃╟ ╫	 ⊈ - 6 #			-44	 \$ \$ 	
	口	AND LOCATION	III KENT, MINNESOT, IV GROOKSTON, MINN	T	VIII SHANNON CO.	CAKLEY, KANSAS LEWISTON, MINN	4 4 4 6 1 1 1 1 1	<u> </u>	<u> </u>
<u> </u>		<u> </u>	▗ ▋╟┋╟┇╟	+-14-14-14-1	119112	 	┤╬╏┤╬ ╏	 	╏╏┩┋ ┼┼┼┼┼┼┼┼
HHHH	H.	1211	14 14 11	1 ₹11811\$	1 3 1 2			ま 乗 ほ	
		<u> </u>			 		XII TOLEDO	 	┠ ┋╸╏╸╏╸╏╸╏╸╏
┝╊╂╂╂╂	┼┼╏	+&	13112115	14 18 19	1 1 1 8		12 13	3 3 9	
	II.		本 中 注	李 李	10 1 F		<u> </u>		
		- 40 - E		141-141-14	┋	┥┪	X H	╁╁╟┼╁┞┼┋┃	+
╺┨ ╏┩	┼┼┨	+	141-14-14	# T 		X + 1	X #		
	口			<u> </u>		▍ ▍		 	<u> </u>
	╁╏	<u> </u>		╡ ╃╃╃╃╃╇	┋				
	FI	 	BE ARDEN	BARNES	1 1 1 1 1 1 1	E KE	AMAT	FOX	
	土	1+++		++++			<u>+++</u> }-	 	╎ ╎╏╏╏╏╏ ╏
+++++		1111	+++++	++++++		11111	11111		
	Ш						<u> </u>	<u> </u>	<u>┼┼┼┼</u> ┼┼┼┤
-}-}-}-	++	1111	┞ ╊╂╇╋╃╃╃	┾╂┾╁╂╀Т	+++++		╁┼┼┼┼┼	++++++++++++++++++++++++++++++++++++	+
	\Box	 	 	 			<u> </u>	<u> </u>	<u> </u>
	出	1 	╂╂╂╂╂╂╂	┞╏╏╏ ╏	233	╅╅╂╂	╁╁╁┼┼	╂╂╂╂╂	++++++++++++++++++++++++++++++++++++
++++	\Box	HHH	 		1111				<u> </u>



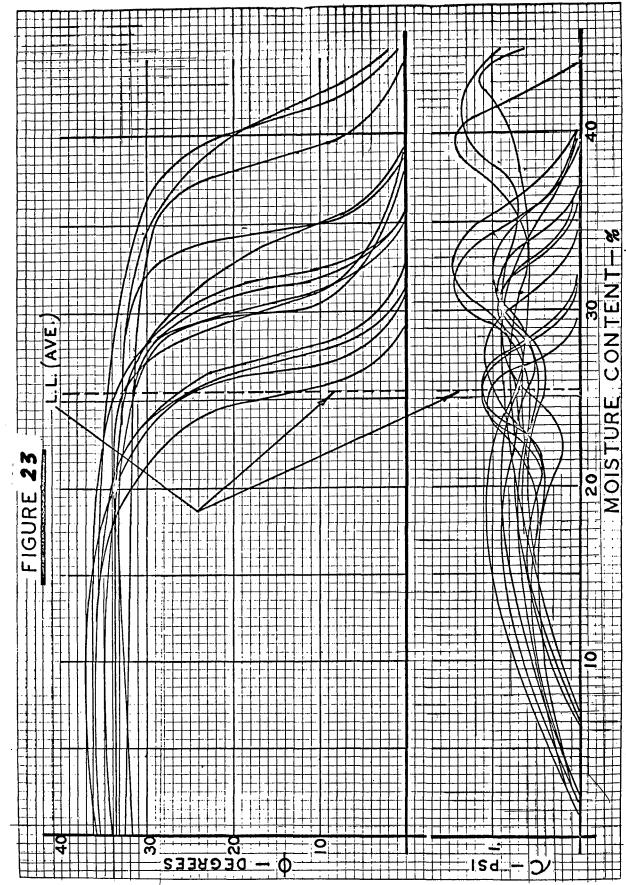


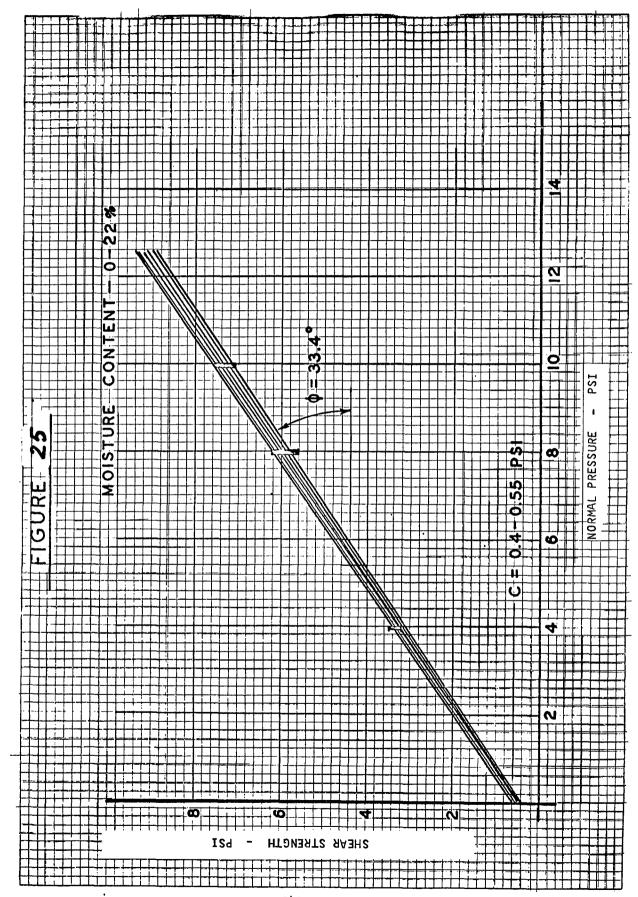


			١.		١.		١.				ŀ		ł
ĺ	Ì	į	ľ.	٠.	ľ		ľ	į		-			ĺ
	١.	4								. ,			
		1						1	l		ŀ		l
			L	-			ļ.,	-	_		ļ.,		ļ
		-			-		-	,		-	-	1	ŀ
			_	1							_		l
	-				-	_	-	-	Ļ.	_	_	-	ŀ
		1		-	٠	1		1	-	1	-	-	ŀ
1	_	1	_	,			_	-		1	_	-	ļ
		1	~	-		-	-	1	-	-	-	-	
		1			_				_			1	
1		-		-		-		-	-	4	-	-	ļ.
1		f	-	1	-	1	-	1	-	1	-	f	
-		1	_	1		-	-	1		-		1	
1	-	1	•	1	-	1		1		-	-	1	
1		1	_	1	_	1		-	_		_	1	
1	-	1		ł		ł	-	1	-	1		1	
١		1	_	1		1		İ	_	1	_	1	_
Į	_	+		1		1	_	1	_	+	_	+	
1	-	t		1	_	1	_	1		1	_	1	
1		f	_		•	1	•	•		•	ļ-	-	
l	**	t	_	•		_		١			۲	1	
I		Į					7	١	Į		-	1	
l		ł			1	1	h	٠	1		-	†	-
١		Į	_					•	•		_	1	-
ł		ł	-			1					H	1	
ı		1	_			ļ	Į	Ļ	J		_	1	
						ſ	٦	L				1	
ł		t	_	•		٠	J	ı			-	ł	
			_			•			•	-		ļ	
			_			•	111)		_		
						: ()				
						· · ·)				
					1)				
					1		7//-//)) ,				
					1	· · ·	7//-//)) ,				
				1	1		7//-//)) ,				
					1		7//-//)) ,				
					1	· · · ·	7//-//)				
					•		7//-//)				
					1	· · · · ·	7//-//)				
					1		7//-//						
					-								
					1								
					1								
					1								

	SILE	SITE NO AND LOCATION	Ulrect Shear Box	Irlaxiai	
			*	\$ \$ \$	11
	4				
	4	111. Kent, Minnesota	1.03 31.7 29.4	3.0 34.4 24.8 119.3	
	Aκι	IV. Crookston, Minnesota	0.72 29.7 39.4	3.7 0 39.5 116.0	
	Щ.			*	
	**	Vil. Huron, South Dakota	0.61 30.6 34.8	1.7 35.7 25.1 112.5	
	#	II. Marshall, Minnesota	0.83 33.5 20.0	1,7 31,8 -22,7 113,5	
	SAB	New Rock ford	1 57 31 (1 95 9	3,00	
				0.07 *	
	4	VI, Lisbon, North Dakota	0.50 29.2 34.3	2.0 34.0 22.6 110.1	
	VIII	VIII. Shannon County-South Dakota	0.72 32.5 13.2	2 3 32 2 1 3 3 102 5	
	1				
	;;1	LX. Torrington, Wyoming	0.33 33.2 20.0	SAKELE OTTED OUT	

	v	. Jakiey, Kansas	0.93 23.7 33.2	2.6 32.8 25.3 112.6	
		I. Lewiston, Minnesota	0.76 32 3 96.3	9-4-6	
	-				
	W.A.	. Hertan, Lowe	0.72 27.5 29.8	3.0 30.3 28.2 120.0	
	IX I	Toledo, Iowa	0.86 25.2 26.1	1.5 33.0 27.4 114.0	
	XIII.	. Waukesha, Wisconsin	0.76 27.0 17.6	1.7 34.0 20.6 104.2	
	XO	XIV. Kankakee, Illinofs	9 8 8 9 7 8 9 9 9	2000	
	+	1-1		313 8 45 7	
				7.04	
	*	* Samples lose of moisture.			
	*	** Sample Saturated - c 1s called	d apparent coheston.		
	3 3	Moisture content (%)			
	•	חבוופדרא דה/ דר			
X 42					





REFERENCES

- 1. Liston, R. A. and Hanamoto, B., "The Drawbar Pull-Weight Ratio as a Measure of Vehicle Performance", U. S. Army Tank-Automotive Center, Report No. 9349 (LL 107), August 1966.
- 2. "Mobility Exercise "A", Miscellaneous Paper No. 4-702, Page 61, U. S. Army Waterways Experimental Station, Corps of Engineers, February 1965.
- 3. Lassaline, D. M. and Harrison, W. L., "The Prediction of Soil Strength Parameters in Remote or Inaccessible Areas by Means of Soil Analogs", Report No. 8816 (LL 102), U. S. Army Tank-Automotive Center, April 1965.
- 4. U. S. Department of Agriculture, "Soil Classification, A Comprehensive System, 7th Approximation", August 1960.
- 5. Bekker, M. G., "A Practical Outline of the Mechanics of Automotive Land Locomotion", Land Locomotion Laboratory, Detroit Arsenal, January 1955.

PORTABLE SOIL TEST DEVICES

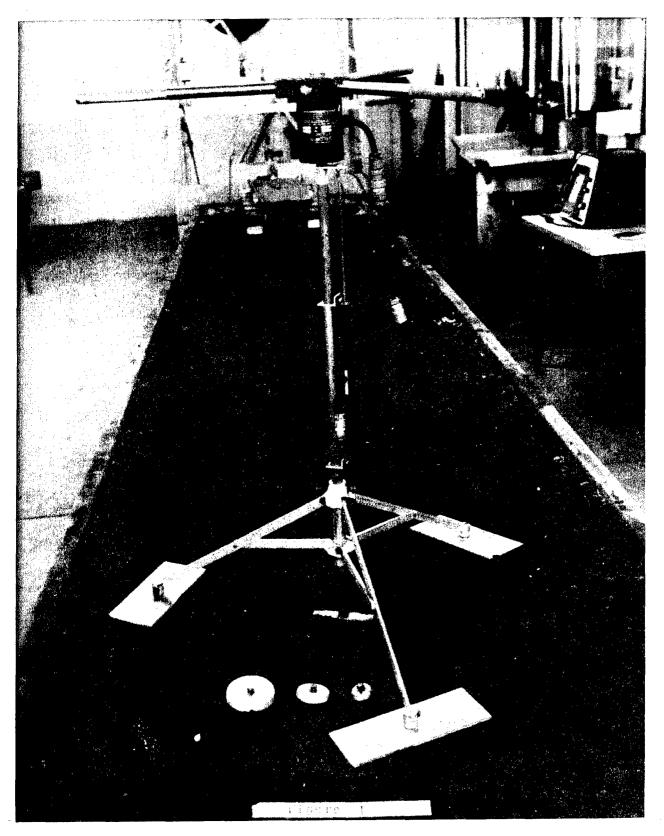
By: Paul Spanski

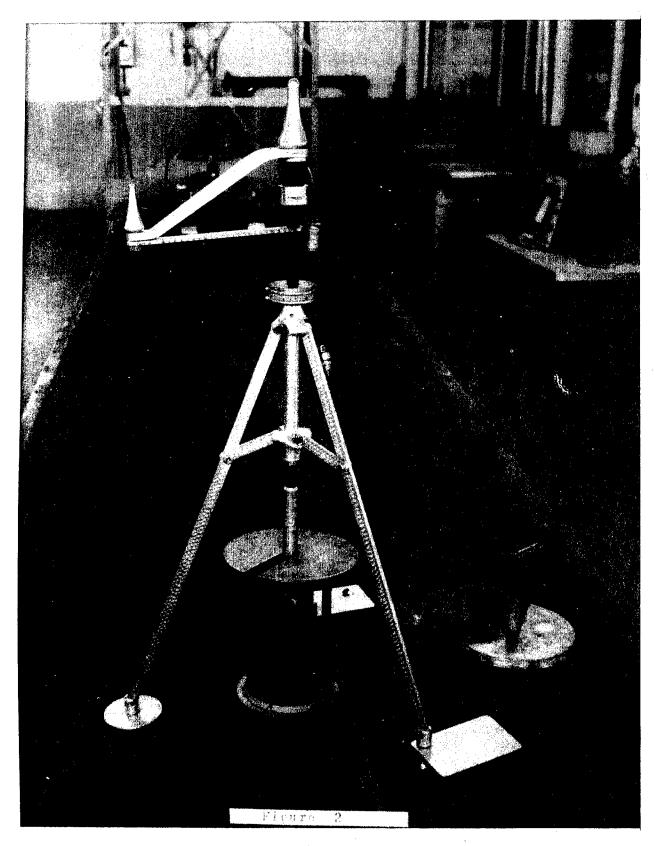
A valid objection to the use of the Bekker Soil Value System for routine soil strength measurements is the cumbersome equipment available to obtain a valid set of data. Until recently, field equipment was merely an adaptation of laboratory equipment to fit the chassis of various vehicles. The result has been a series of heavy, rather clumsy, and expensive Bevameters or soil strength measuring devices.

Several years ago, it was recognized that if the Bekker Soil Value System were to become accepted for field testing, some definite attempt would be necessary to design a simple, easy to operate, light, portable Bevameter. The first set of such instruments is shown in Figures 1 and 2. Some of the requirements were met, but the data produced by these devices were extremely sensitive to operator techniques. The shear unit relied on dead weight to produce the required normal pressures and the over-all rigidity of the two units was judged to be inadequate.

In the fall of 1961, it was decided to begin a fresh approach to the design of portable Bevameters. The following criteria were established for the design of a manually operated, portable penetrometer (load-sinkage device):

- a. The sinkage rate must be controllable.
- b. The geometry of the device must allow a minimum of 6 inch sinkage.
- c. The load-sinkage device must be capable of exerting a minimum of 500 lb. force on the soil.
 - d. Easily damaged components must have ample protection.
- e. The frame of the load-sinkage device must be sufficiently rigid to prevent errors in sinkage measurement.
- f. The load-sinkage device must be capable of being carried by one man.





DESIGN CONCEPT

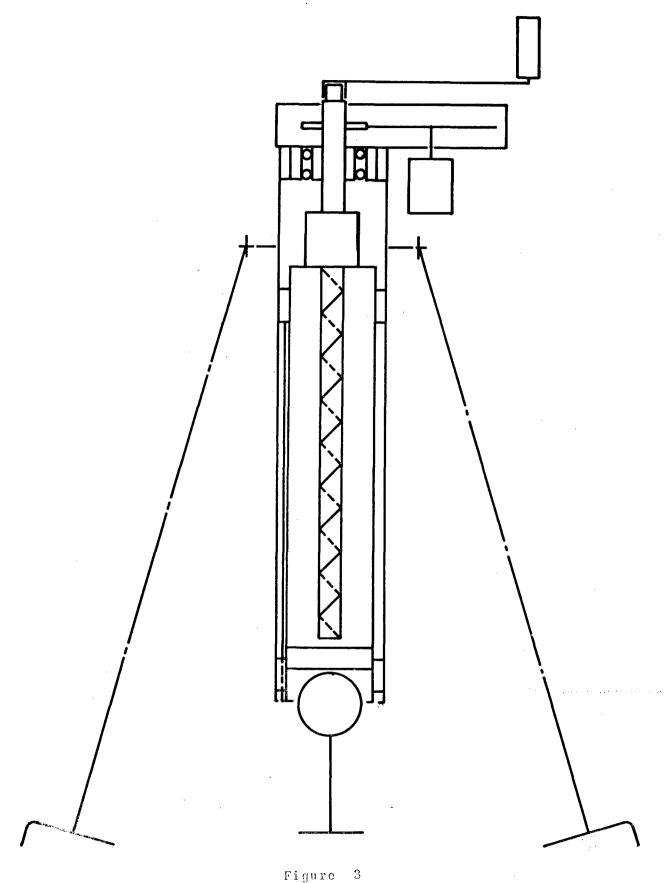
To obtain sufficient rigidity in this device during axial motion of the sinkage plate, it was decided to use concentric sliding tubes as the basic structural elements. Tubing offered the twofold advantage of rigidity and minimum weight (See Figure 3). The outside tube is held stationary, the inside tube carries the sinkage plate. Precise control of the relative motion between the two tubes is provided by a screw and nut arrangement. The choice of tube size and material was a compromise among the requirements of light weight, rigidity, commercial availability of tubing and space necessary for the screw and nut. The final selection was a 3-inch 0.D. x 14 gauge wall outer tube and 2.50 O.D. x 14 gauge wall inner tube. The material used was 6061 T6 aluminum alloy which has approximately the strength of hot finished mild steel. Two oil impregnated bronze bushings separate and maintain the concentric alignment between the two tubes. A thin steel quide rail is fastened to the inner tube and passes through a groove in the lower bronze bushing. The rail prevents any rotary motion between the inner and outer tubes.

Controlled motion between the two tubes is accomplished by a recirculating ball nut and screw. The mechanical efficiency of the system is very high. The screw thread lead is one inch per turn. This means that by cranking at one turn/second, a sinkage speed of 60 inches/minute can be maintained. This figure is about the lower limit for power operated laboratory equipment.

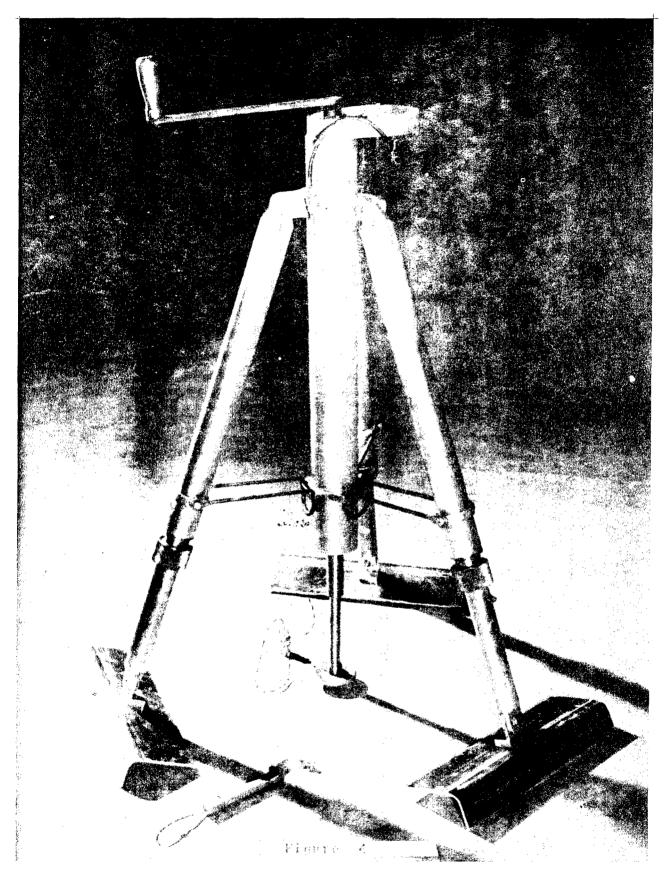
The screw thread shaft is anchored in a double row ball bearing fixed in a housing at the upper end of the 3 inch diameter tube. A 1/2 inch square drive tang projects above the top cover, providing a convenient location for manually cranking the penetrometer. The re-circulating ball nut is fixed in a plug in the upper end of the inner tube. The arrangement of these components allows a total axial movement of over 15 inches.

A ring type load cell is interposed between the lower end of the inner tube and the shaft which supports the sinkage plate. The load cell is recessed into the lower end of the inner tube, thus, providing a maximum amount of protection from physical damage. In this location the load cell has the advantage of measuring only the force required to sink the penetrometer plate and not the frictional forces, which may develop in the sinkage mechanism.

Sinkage is measured by means of a 10-turn potentiometer which is geared to the screw thread shaft at a ratio of 2:1. The gear box and potentiometer are located at the upper end of the device. The gear box is sufficiently heavy to withstand blows that would easily damage the potentiometer.



igure 3 **24**6



The electric signals from both sensing units are fed to an X-Y Plotter, thus giving a permanent visual record of a load-sinkage test.

The mechanism described above is supported by a tripod when set up for operation as shown in Figure 4. Each leg of the tripod is made from two telescoping aluminum tubes and can be adjusted by means of an eight blade collet and locking collar. Clamping force is applied by means of a tapered thread on the collet. The total adjustment available is about 22 inches. The top of each leg is anchored to a heavy aluminum spider at the top of the penetrometer and braced near the bottom by a U-shaped wire brace of 1/4 inch diameter steel. At the foot of each leg is a grouser type support plate with an area of 53 sq. in. This area is sufficient to support the device on any surface except dry, fluffy snow.

The tripod, in addition to supporting the device, also acts as an anchor to counter lifting forces generated during a sinkage test on each of the tripod feet during operation. Thus, the maximum available force to sink a footing is equal to three times the weight of the lightest operator plus the weight of the device itself. A given sinkage test is ended if a tripod leg leaves the ground, since after that point the sinkage measurement becomes inaccurate.

In order to minimize weight, every effort was made to use aluminum alloy in the construction of the device. Alloy 6061-T6 was chosen because of its high strength, (37,000 psi yield strength), good machineability, and availability in a variety of forms. The result was a final weight of only 34 lbs., a weight readily carried by one man.

Portability of the device, however, is limited by the recording instruments. The weight, sensitivity and power requirements of the X-Y Plotter dictate the use of an instrument vehicle to accompany the penetrometer in the field.

In numerous, but not exhaustive, field tests the penetrometer device has performed as expected. Within the limitation of the force available (a maximum of 480 - 500 lbs.) the device produces smooth load-sinkage plots characteristic of laboratory, power-operated equipment. The device is only mildly sensitive to operator's technique and thus, a given operator can quickly develop the skill necessary to produce smooth curves.

The portable penetrometer has been used in the field in conjunction with several test programs. Two of these projects have so far been reported on in a published form (1)(2). It was found that the penetrometer performed satisfactorily within its load limitations.

Considering these favorable results with the penetrometer, it was decided to construct a manually operated portable shear unit. The design was initiated in the Fall of 1963. The first step was the establishment of the following design criteria:

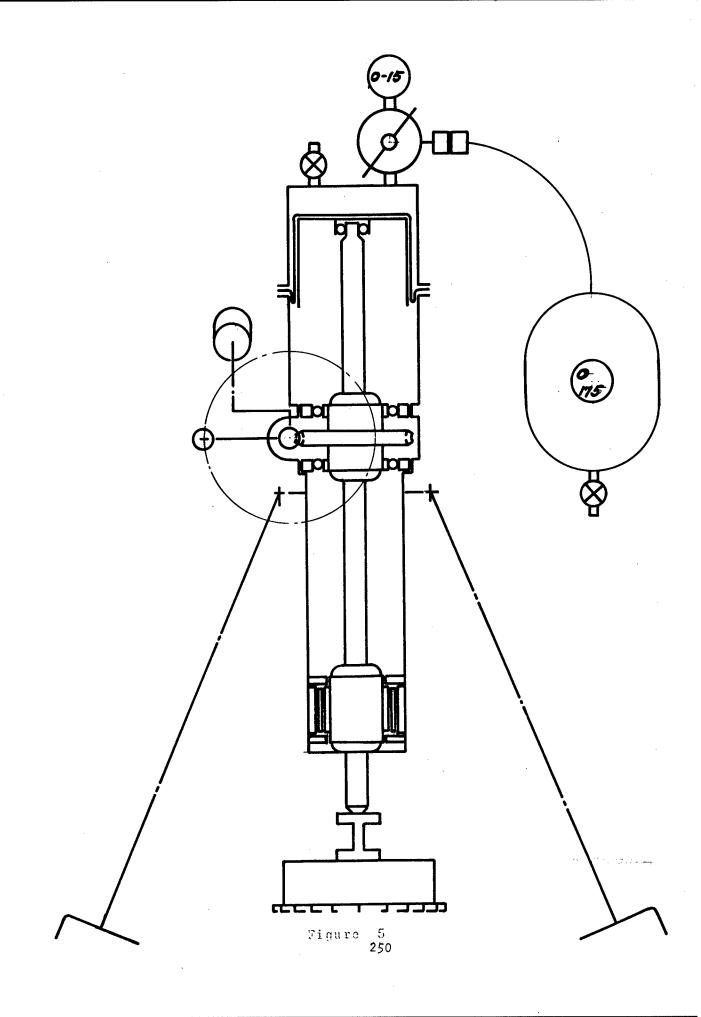
- a. Eliminate the use of dead weight to obtain normal loads.
- b. Provide a sufficiently rigid structure to prevent the shear annulus from "walking" during operation.
- c. The shear-deformation device must be portable by one man.

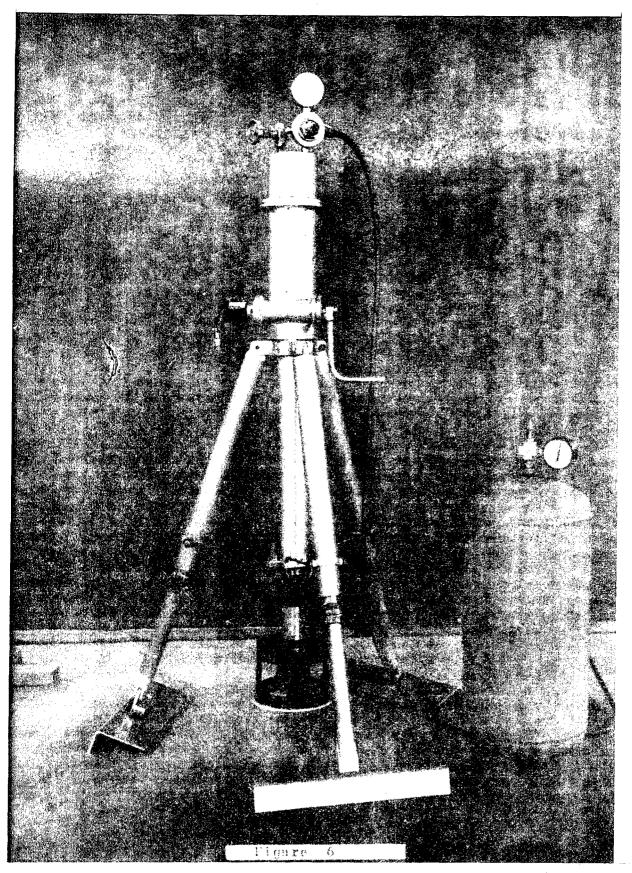
Previous shear deformation devices relied on application of dead weight to obtain the required normal pressure. In the conception of the new unit, air pressure was used to obtain normal loading (See Figure 5).

At the top of the shear-deformation unit is a piston in a cylinder. A fabric reinforced, rubber-coated, rolling diaphragm provides an almost frictionless seal. Air pressure applied to the volume above the piston loads the shear annulus through the ball spline shaft and torque cell. The maximum travel of the piston-shear annulus is 6 inches. By varying the air pressure in the cylinder any desired normal load may be imposed on the shear annulus.

In operation, the shear annulus generally experiences some sinkage. To compensate the increase in volume and the consequent loss of pressure above the piston, air is added by means of a sensitive pressure regulator. Thus, the normal load on the annulus remains constant regardless of sinkage. After each reading, the pressure regulator is shut off and the pressure released through a drain cock.

The shear annulus is rotated manually. A worm and gear rotate the upper ball spline, which transmits torque to the spline shaft. Due to frictional properties of the ball spline, the applied torque has negligible effect on the axial travel of the spline shaft. The lower ball spline nut is carried in a needle bearing and supported by thrust rings. A rigid exterior housing holds all components in alignment. The torque sensing unit is located immediately after the shear annulus and, thus, senses only the torque required to shear the soil.





The cranking effort to rotate the shear annulus is very low. The cranking ratio is 12.5:1, which results in a cranking torque of 20 in.lbs. or less, even in strong soils. A ten turn helipot coupled to the worm shaft senses this motion. The gear ratio allows about 5/6 of a turn of the annulus to be recorded. The helipot is protected from over-travel by a small torque limiting coupling.

Normal loads may be varied from about 13 lbs. to 193 lbs. This corresponds to ground pressures of less than 1 psi to more than 9.5 psi. The sensitivity of the gas pressure regulator is sufficient to obtain readings at 1 psi ground pressure intervals.

Air pressure for operation in the field is supplied from a .9 cu.ft. volume ASME pressure vessel. Based on a charging pressure of 175 psi, the tank will provide air for 50 to 60 individual readings. The exact number depends on the normal loads required and the sinkage. (See Figure 6).

Support for the instrument is nearly identical to that used on the penetrometer. The weight of the operator's counter-balance is employed to vertical soil reactions as in the case of the penetrometer.

Aluminum alloy 6061-T6 was used wherever possible in the construction of the shear-deformation unit. The weight of the pilot model was 58.5 lbs. This was considered excessive and a revised design has produced a lighter more compact device which weighs 44 lbs. The previous weights cited do not include the 20 lb. weight of the air supply system or recording instruments.

The pilot model shear-deformation device has successfully been used in the field at various locations in the United States and in Puerto Rico (2).

REFERENCES

- Harrison, William L., Jr. and Bong-Sing Chang, "Analogs: For Soil Strength Prediction", Technical Report No. 9367 (LL 108), U. S. Army Tank Automotive Center, Warren, Michigan, 1966.
- 2. Sloss, David A., Jr., and D. M. Lassaline, "A Study of Tropical Soil Strengths". Presented at the Second International Conference of the International Society for Terrain-Vehicle Systems, Quebec City, Quebec, Canada, 1966. (Paper available through the University of Detroit, Detroit, Michigan).

WHEELED BEVAMETER FIELD TESTS

By: David Sloss

INTRODUCTION

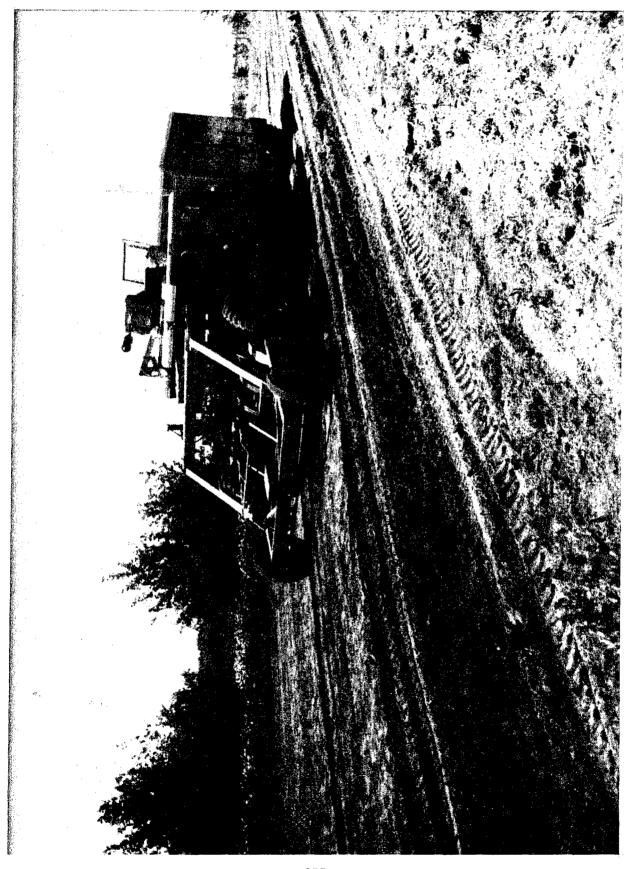
The acquisition of a "soil value profile" of a test site is a time consuming procedure if a conventional penetrometer and a shear annulus (Bevameter) are used. Dr. M. G. Bekker developed the concept of a wheeled Bevameter which would record the strength of the soil continuously and much more rapidly than conventional methods. laboratory model was built and is described in detail in Reference 1. The same reference describes the theoretical considerations used for the evaluation of the recorded inputs. The theory is based on the assumption that if it is possible to predict what a wheel will do from taking soil values, it should then be possible to predict the soil value from the wheel performance. In the final design, two wheels are used to obtain k_c , $k_{\acute{c}}$, and, n. Three wheels are run simultaneously to establish c, p, and k. Two reference wheels are also needed to establish the "ground reference zero" for the loadsinkage and the shear-deformation data.

Laboratory tests conducted in 1958 showed that a Wheeled Bevameter was feasible, and that better prediction of wheeled vehicle performance might be expected using the Wheeled Bevameter data. These tests were conducted in a well-graded sharp sand, and a sandy loam. A sufficient number of trials (i.e., 20 to 25) were run to establish the statistical accuracy of the data.

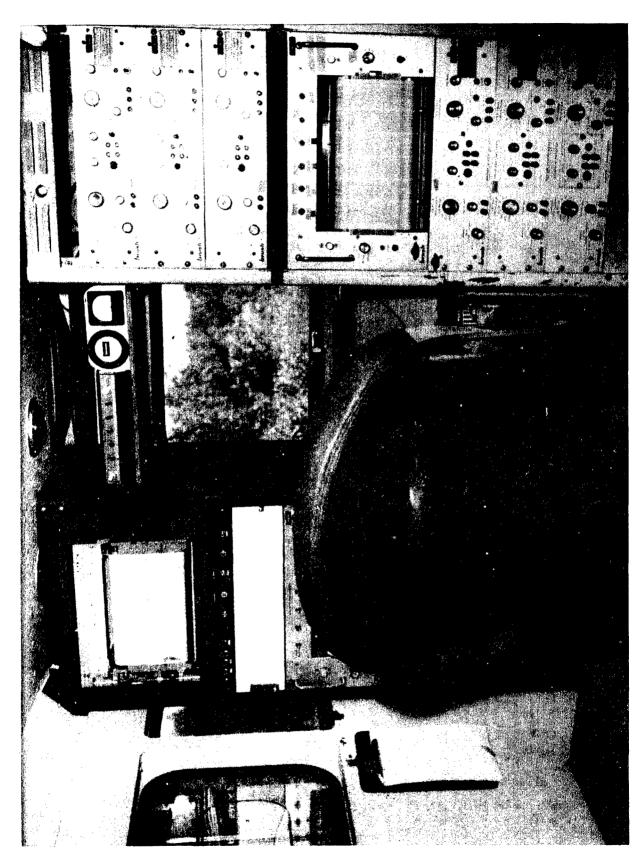
A contract was awarded to Wettlaufer Engineering Company, Detroit, Michigan in 1962 for the design and construction of a Wheeled Bevameter suitable for field use. The completed unit, shown in Figure 1, differed in two major respects from the laboratory version.

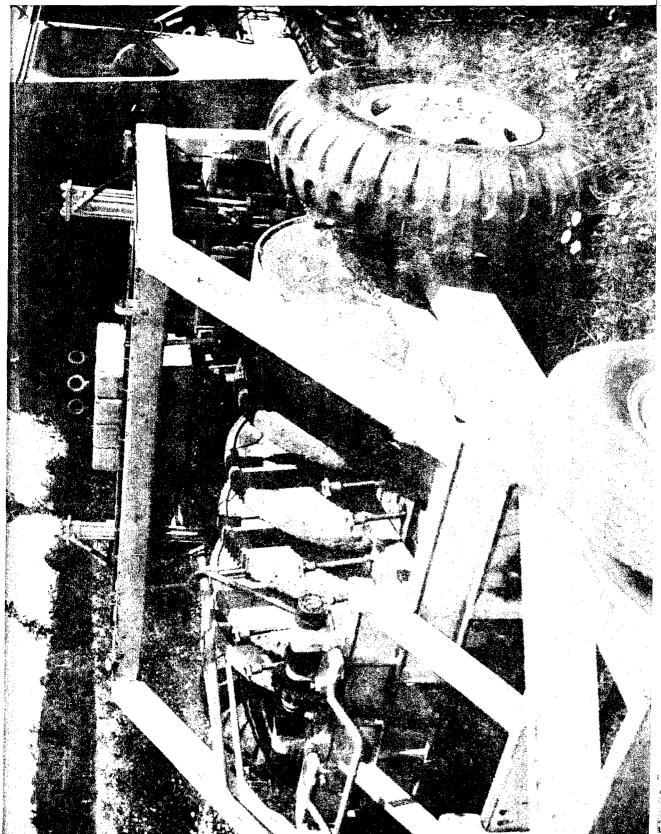
- a. The shear, sinkage, and reference wheels are mounted side by side in a row for a total of seven (7) wheels. This requires a much wider sampling path than the laboratory unit which used only two wheels at a time.
- b. Shear wheels are powered rather than braked, as in the laboratory unit.

As shown in Figure 1, the field unit is pushed over the soil to be measured by a POLE CAT vehicle which also carries the hydraulic power unit and the instrumentation required (See Figure 2). A close-up of the Bevameter unit is shown in Figure 3.



Figure





OLUC ON

FIELD TESTS

The Wheeled Bevameter was tested in snow and soft soil at the Keweenaw Field Station, Houghton, Michigan during 1964. The objective of these tests was to discover and eliminate the "bugs", always present in a new design. The purpose of this paper is to discuss the experience gained during these tests.

For snow tests, the Bevameter frame was supported by skis, and the balast weights were reduced to a minimum. A number of test runs were made in snow and the following conclusions were made:

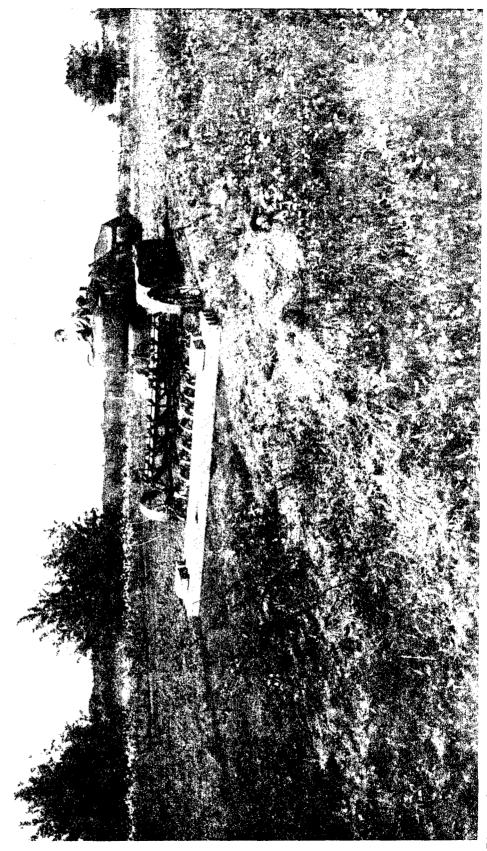
- a. The area required for a test run was extremely large (i.e., approximately 8×100 ft.), when compared to conventional equipment.
 - b. The instrumentation required further refinement.

In general, the first field test of the equipment was disappointing, both with respect to the operation of the equipment, and to the quality of the data.

In the Spring of 1964, further tests were conducted in farm soil and in uniform coarse grained stamp sand to further evaluate the Wheeled Bevameter. During this test, a portion of the data was reduced after each run to determine its acceptability. The initial runs on a plowed field resulted in very erratic data. This was attributed to the plow furrows which caused the two reference wheels to ride above, below, or at an angle to the true ground reference required for the proper operation of the load-sinkage and shear wheel instrumentation.

In order to obtain data that could be reduced, it was necessary to prepare the test site. Preparation, shown in Figure 4, consisted of tilling the soil with a spring plow, followed by a mold-board which filled in the furrows left by the plow. This procedure produced what appeared to be a relatively uniform and fairly soft soil condition.

The data from the prepared test site was examined qualitatively and it was determined that the sinkage data could be reduced. The shear data was still not acceptable because 100% slip could not be obtained on the shear wheels, due to a lack of power in the hydraulic system. Additional tests were made at the prepared test site for load-sinkage values, using both the Wheeled Bevameter and a hand-carried Bevameter unit shown in Figure 5.



igure 4



A sample of the raw load-sinkage data in shown in Figure 6. Readings were taken at points 1 through 6 where the curve indicated that the sinkage had stabilized. The sinkage was stabilized by loading the sinkage wheels in increments. Data reduced from these, and similar curves, are shown in Figures 7 through 9.

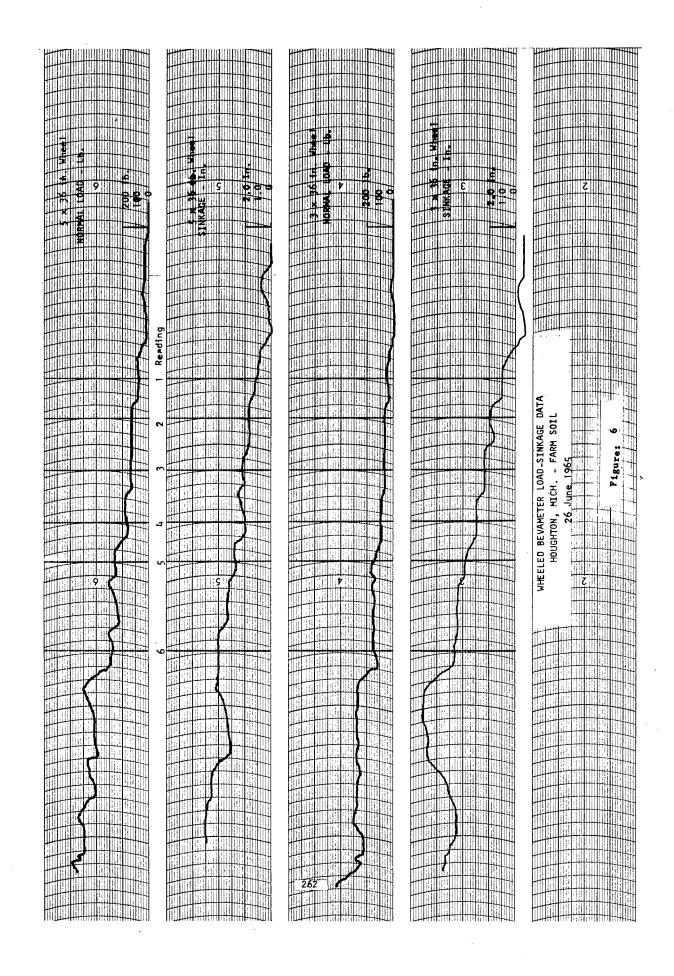
The soil values obtained from the data were not consistent between runs, nor did they correlate with the Hand Bevameter data shown in Figures 10 through 12. Analysis of the Hand Bevameter data indicated that there was considerable variation in soil strengths within each test site. The wide variation in soil strengths is considered to be a major cause for the inconsistent Wheeled Bevameter soil values.

Data interpretation can have a large influence on the soil values. Figure 13 shows a smooth curve drawn through the original data, Figure 6. Figure 14 shows the soil values obtained from the smooth curves. When these values are compared with the original values, Figure 7, it is quite evident that a small shift of the data will produce a large change in soil values.

The long test run required to obtain soil data can be considered an advantage, because it automatically averages the soil strength data over a large area. It also has an advantage because it will not produce accurate data if the test area has irregularities, or extremely varied composition. In this series of tests the site was prepared carefully and the length of the run was not a factor.

Additional work was done in checking out and calibrating the instrumentation associated with the shear wheels. After a number of tests on two prepared test sites, it was concluded that the hydraulic system powering the shear wheels could not be controlled accurately enough to produce uniform reducible data. It was also found that the system did not have sufficient power to produce the required 100% shear wheel slip. It was further determined that there was an interaction between the hydraulic loading system, for the load-sinkage wheels and the hydraulic drive for the shear wheels. This prevented the load-sinkage and the shear data from being taken simultaneously.

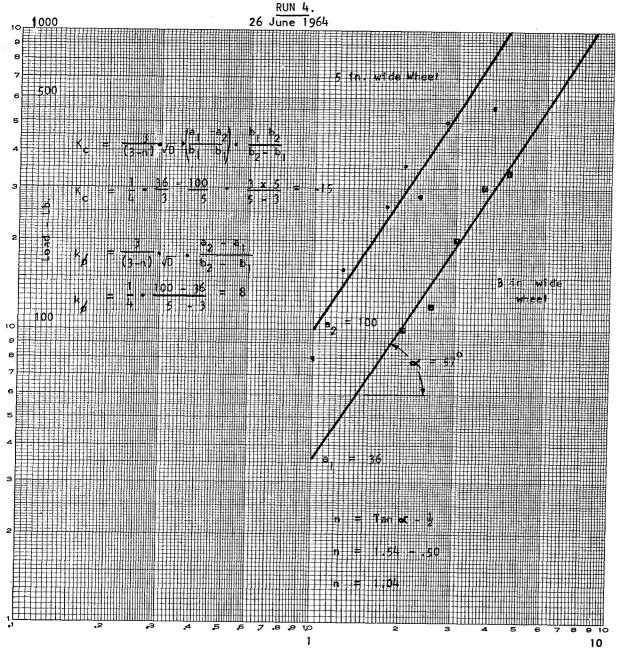
The winter and summer tests demonstrated that the Wheeled Bevameter was capable of producing soil strength data; however, a number of mechanical problems require correction before a complete evaluation can be performed. These refinements include:



LOGARITHMIC PLOT OF

WHEELED BEVAMETER LOAD-SINKAGE DATA

HOUGHTON, MICH., FARM SOIL

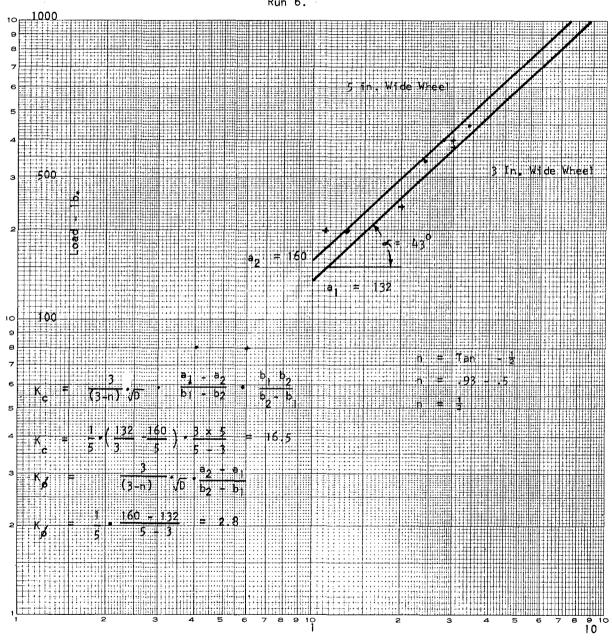


Sinkage - In.

Figure: 7

LOGARITHMIC PLOT OF WHEELED BEVAMETER LOAD-SINKAGE DATA HOUGHTON, MICH., FARM SOIL 26 June 1964

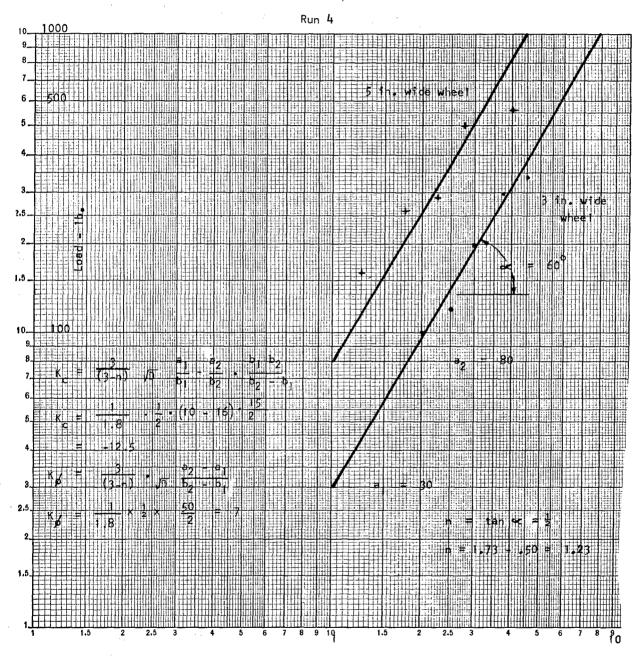
Run 6.



Sinkage - In.

Figure: 8

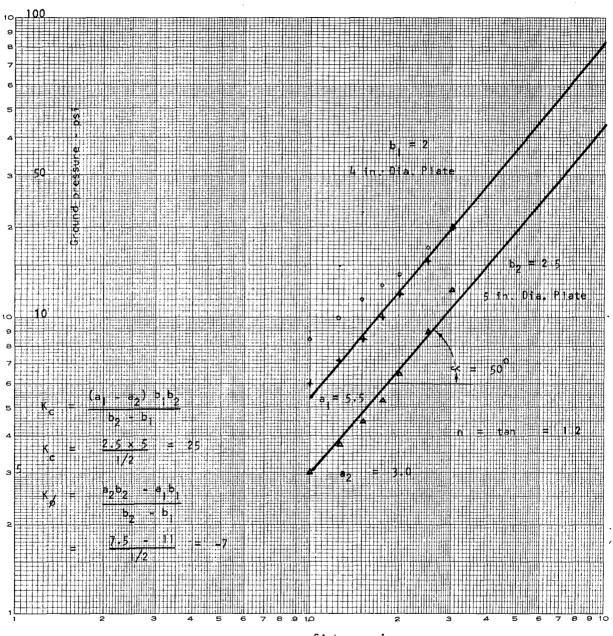
LOGARITHMIC PLOT OF WHEELED BEVAMETER LOAD-SINKAGE DATA HOUGHTON, MICH., STAMP SAND 26 June 1964



Sinkage - In

LOGARITHMIC PLOT OF HAND BEVAMETER LOAD_SINKAGE DATA HOUGHTON, MICH., FARM SOIL

25 June 1964



Sinkage - in.

Figure: 10

LOGARITHMIC PLOT OF

HAND BEVAMETER LOAD-SINKAGE DATA HOUGHTON, MICH., STAMP SAND 26 June 1964

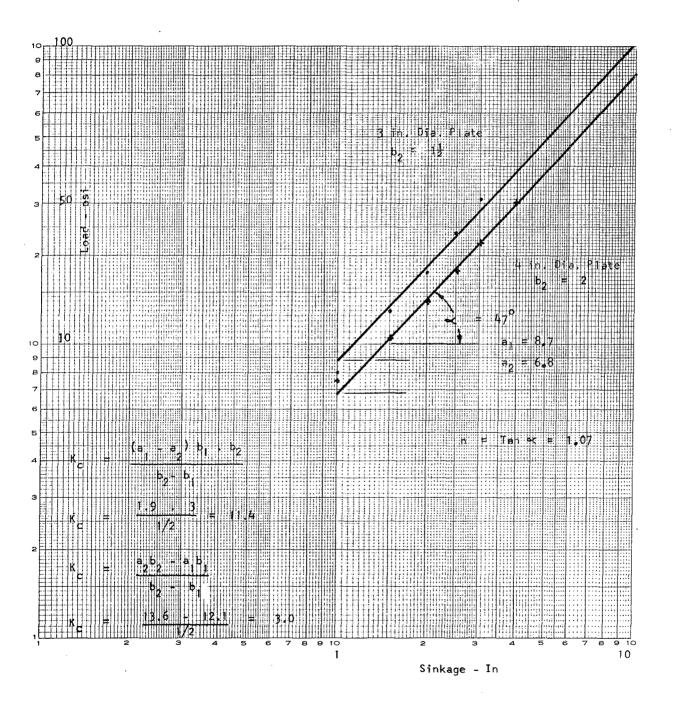
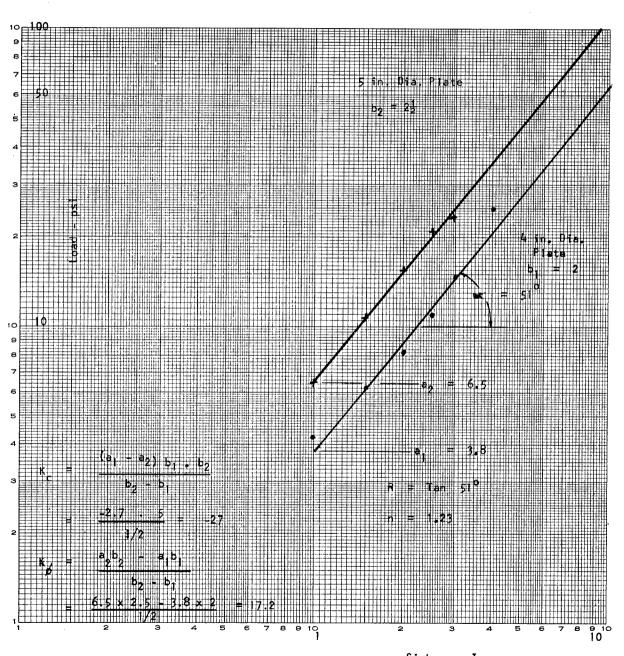


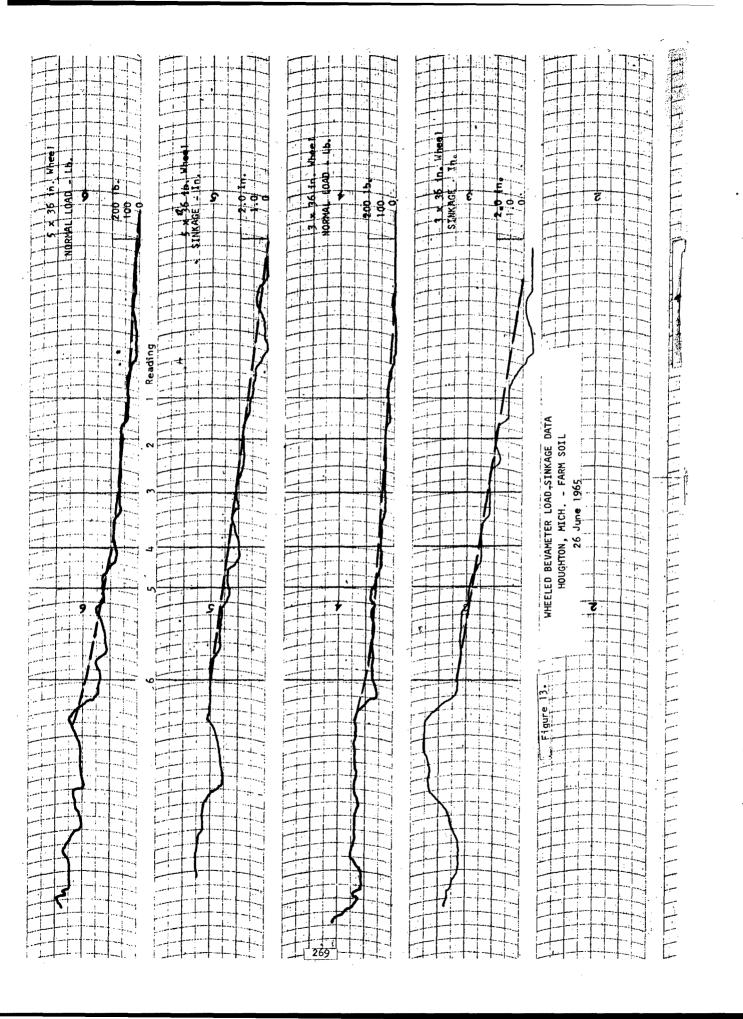
Figure: 11

LOGARITHMIC PLOT OF HAND BEVAMETER LOAD-SINKAGE DATA HOUGHTON, MICH., STAMP SAND 26 June 1964



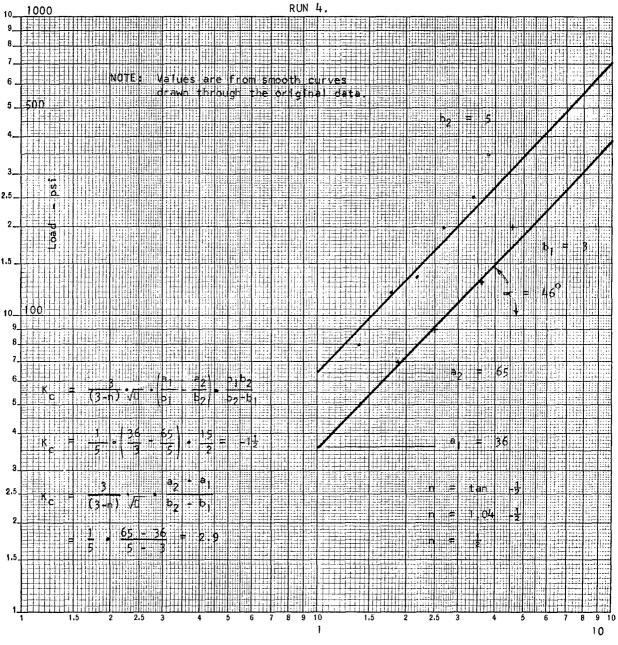
Sinkage - In.

Figure: 12



LOGARITHMIC PLOT OF

WHEELED BEVAMETER LOAD-SINKAGE DATA HOUGHTON, MICH., FARM SOIL 26 June 1964



Sinkage - In

Figure: 14

- a. Installation of idlers on the chain drives for the shear wheels. Considerable "hash" was apparent on the shear wheel torque R.P.M. traces. The idlers should reduce the "hash" to a tolerable level.
- b. Redesign of the load-sinkage controls. The present control system does not allow the load to be applied uniformly.
- c. Redesign of the shear wheel speed control. The present control system does not allow the speed, and hence the slip, of the wheel to be increased uniformly.

The Laboratory's original intention was to have the necessary refinements made to the equipment and then to re-test the wheeled Bevameter in snow during March 1965. Due to numerous delays these modifications were never completed.

During this period an improved version of the Hand Bevameter was developed and tested with good results. This prompted reevaluation of the need for the Wheeled Bevameter. It was concluded that even if the wheeled unit worked perfectly, the cost and time required for transportation of the equipment and set-up, versus that for the hand units, made the wheeled unit economically impractical. Therefore, all work on the development of the Wheeled Bevameter was stopped.

REFERENCE

Pavlics, F., "Bevameter 100. A new type of Field Apparatus for Measuring Locomotive Stress-Strain Relationships in Soils". Proceedings of the First International Conference on the Mechanics of Soil-Vehicle Systems, Turin, Italy, 1961.

TERRAIN GEOMETRY MEASURING EQUIPMENT

By: L. A. Martin

INTRODUCTION:

Vehicle tests are conducted in varying environments which must be described in quantitative terms. Without proper description of the test conditions, the results are nearly useless.

Soil strength measurements and, sometimes, the quantitative description of the test course profile must accompany off-the-road vehicle tests. Fear of damaging one or more elements of the vehicle-driver-cargo system, often limits the speed of a vehicle. Therefore, the systematic investigation of vehicle ride over rough terrain is just as important as the establishment of the true relationship between the traction of the vehicle and soft soil. The first step in the former problem is the development of a quantitative system for the description of random terrain profiles. This system must be based on the knowledge of the exact shape of actual terrain profiles, if the work is to attain any practical significance.

The profile measuring system, shown in Figure 1, to be discussed here is the result of the need for a quick, reliable system for measuring off-the-road profiles. The system uses the slope integration method of terrain geometry measurement.

THEORY OF OPERATION:

The slope integration method of ground profile measurement uses the two equations:

where s = total distance traveled along the surface of the ground,

x = horizontal component of distance along the ground for total travel s.

y = elevation of the ground at horizontal distance x,



U.S. ARMY TANK.AUTOMOTIVE COMMAND NEG. NO. 71669 DATE 1 Apr 63
Terrain-Geometry Equipment mounted on a M-113, Armored Personne!
Carrier. Armor Board, Fuel Test Loop, Fort Knox, Ky. Jul 62.

 y_0 = elevation of the ground at the beginning of the run,

9 = slope angle of the ground at the distance s from the origin.

The two quantities which must be measured to implement these equations are the slope angle of the ground (θ) and the distance traveled along the ground (s).

The data reduction reconstructs the terrain profile by calculating horizontal and vertical distances for a known increment of distance traveled (DS). These equations are:

The reconstructed profile is the summation of these discrete distances over the total profile length traveled. s.

$$x = \begin{array}{ccc} \mathbf{i} \\ \mathbf{\Sigma} & Dx_{\mathbf{i}} \\ \mathbf{o} \\ \mathbf{i} \\ \mathbf{y} & = \begin{array}{cccc} \mathbf{\Sigma} & Dy_{\mathbf{i}} \\ \mathbf{o} \\ \end{array}$$

The accuracy of the reproduced profile is dependent on the increment of traveled distance (DS) chosen. The distance DS is approximately six inches and results are good.

EQUIPMENT DESIGN:

The two quantities required for data reduction are the slope angle θ and the distance traveled, s, where s = Σ DS.

A fifth wheel is used to indicate the distance traveled along the profile path. The fifth wheel has a breaker point and cam system which gives an electrical pip for each DS of travel.

The slope angle θ is the angle of the ground measured from the horizontal. This measurement is taken with the equipment shown in

SIGNAL GENERATED by PROFILE WHEEL

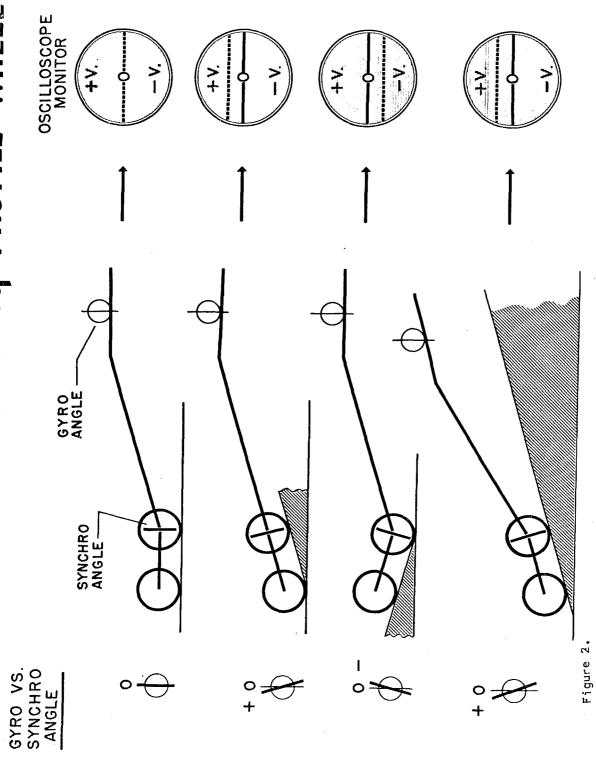


Figure 2. The angle θ is the angle of the wheel frame, with the horizontal as datum. The wheel frame supports two eleven inch diameter wheels in tandem, a wheelbase of 14 inches, which follow the ground profile. A trailing arm, which is towed, carries the equipment. The wheel frame is free to rotate about its support point on the trailing arm, which is the axis of the front wheel. This rotation about the pivot point in the trailing arm is measured electrically and compared to the horizontal datum, with the resulting signal being proportional to the wheelbase angle. A gyroscope also mounted on the trailing arm establishes the horizontal datum. An example of the wheelbase signal generated is shown in Figure 2.

The data is recorded on three channels of an Ampex AR200 tape recorder, two FM channels and one AM channel. The slope angle signal (0) and the constant increment of distance (DS) pip are recorded on the FM channels. The AM, or voice channel, records pertinent data and comments. Examples are identification of run, calibration data, general topography, the beginning of the run, and the end of the run. Figure 3 illistrates the complete data as recorded on all three channels, and the reproduced profile compared to the original profile. It should be emphasized that this is a theoretical profile and should not be misinterpreted as actual data.

CALIBRATION:

The two data signals, θ and ds, must be calibrated before and after each run. The angle θ is calibrated as a voltage proportional to the wheelbase angle -- plus voltages for positive angles (rear wheel higher than front), zero voltage for zero angle (horizontal), and minus voltage for minus angles (rear wheel lower than front). These voltages are kept within a range of +2 volts to -2 volts as recommended for the tape recorder, but the complete range of 0 ± 2 volts should be used for the greatest accuracy. Therefore, the maximum slope angle expected should be set equal to 2 volts. For example, $10^{\circ} = 2$ volts.

The demodulator is used to adjust the output voltage to the desired value. An oscilloscope is used to observe the output voltage and the screen grid is used for the voltage calibration. The oscilloscope is also used to monitor the magnetic tape to insure that a signal is being recorded.

The constant distance increment, ds, should be calibrated on the media over which the profile will be measured. Two fifth wheels are used, a rubber tire bicycle wheel and a grousered bicycle rim. The rubber tire wheel is used in hard surface tests, whereas, the

<u>┅╌┄╌╌╌╌╌╌╌╌╌╌╌╌╌╌╌╌╌╌╌╌╌╌╌╌╌╌╌╌╌</u> DATA RECORDED BY PROFILE WHEEL Figure: TOTAL SUBSTANCE ALONG CURVE -VOICE CHANNEL WHEEL ANGLE M-ONE PULSE EVERY 5-1/4 IN. DISTANCE • DATA RECORDED mmmm. · REDUCED DATA •PROFILE HCRIZONTAL **NOITAV3 J** 3 277

grousered wheel is used in mud or soft soil.

By calibrating the wheel on the media to be measured, the negative slip or skid of the wheel can be taken into account. The calibration procedure is: (1) run the wheel two complete revolutions, (2) measure the distance traveled on the surface, and (3) divide the distance traveled by the number of pips in two revolutions. Each pip indicates that a known distance has been traveled. When a smooth surface cannot be found for calibration, then the distance per pip can be estimated as

DS = circumference of the wheel number of pips per revolution

For varying conditions and depending on the required accuracy, DS can be adjusted by replacing the cam with one having the desired number of lobes to meet required accuracy and varying conditions. The number of cam lobes partially determines the speed at which the profile can be measured. The fifth wheel pulses are used to trigger the digital computer in the data reduction stage, and these pulses must be very 'clean' (no noise). When DS equals six inches, the maximum hard surface speed is approximately two mph. Off-the-road speed is limited to one mph due to wheel bounce.

DATA REDUCTION:

The slope angle θ , and the distance, DS, traces should be checked in the field to be sure that these traces are continuous and 'clean'.

The field data on magnetic tape must be transformed into digital computer language. A data logging system accepts the field data, multiplexes these inputs and converts their values into a digital number. These data are recorded on magnetic tape in a manner compatible with the digital computer to be used.

Dx and Dy are computed from Equations 3 and 4 at each pip (a known distance has been traveled). This output can be taken either in printed tabular form or on paper tape to be used in an automatic X-Y plotter to get the reproduced profile.

UNUSUAL VEHICLE AND COMPONENT CONCEPTS

By: R. A. Liston

There will be no attempt in the following discussion to include all unusual concepts with which the laboratory has come into contact. The selection of concepts will be confined to those that were formulated in the Land Locomotion Laboratory or supported by the laboratory on a contract basis. It is necessary to be quite selective when writing about unusual vehicles simply because there have been so many ideas proposed to solve the off-road problem that a complete coverage would be of unacceptable proportions.

As a general guide, an unusual vehicle concept is one which attempts to satisfy the requirements of off-road terrain by means of a significant departure from conventional solutions. Conventional solutions depend on the use of slightly modified suspensions for either a tracked or wheeled vehicle. A conventional solution would, for example, attempt to increase soft soil performance by increasing the dimensions of the track and thereby decrease the ground pressure. An unconventional or unusual solution to the same problem could use an air cushion to reduce ground pressure. Interest in the unusual is often high simply because we are aware that a radical change in performance is only likely to be achieved by a radical change in basic vehicle morphology. When attempting to evaluate an unusual vehicle concept, it is necessary to relate vehicle characteristics to a set of general requirements imposed by off-road terrain. If a concept stands up to the general requirements, a more complete investigation is appropriate.

The general requirements for an off-road vehicle fall into five categories: (1) Soft soil; (2) Geometric obstacles; (3) Hard, rough ground; (4) Vegetation; and (5) Water obstacles. In order to provide adequate performance in soft soil, both the size and the shape of a tire or track must be considered. It appears obvious that size of a wheel is important but the role of form is somewhat more subtle. To examine the effect of wheel shape, it is helpful to examine what theory tells us.

It is possible to describe the behavior of a wheel in soft soil by means of the following equations:

$$R_{c} = \frac{bk}{n+1} z^{n+1}$$
 2

 $R_{b} = b(2 z c K_{b} + 7 z^{2} K_{\theta})$ 3

 $H = c b(Dz - z^{2})^{\frac{1}{2}} + W t an \phi$ 4

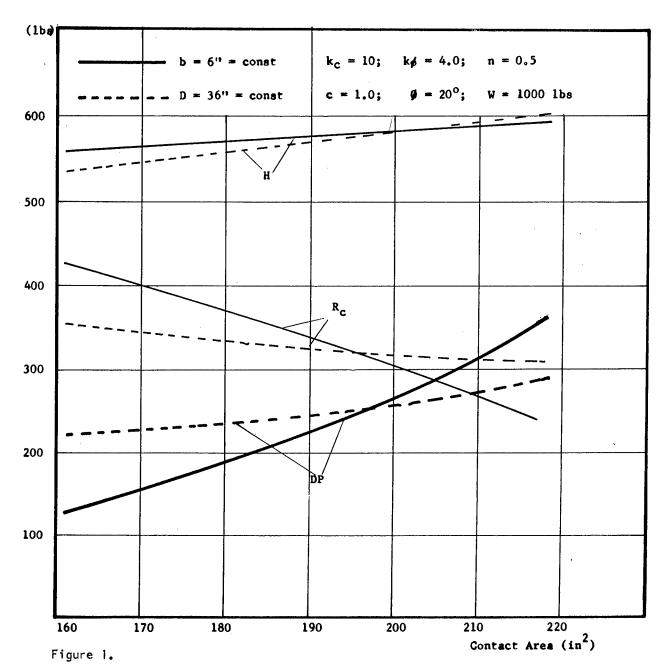
 $R_{T} = R_{c} + R_{b}$ 5

 $DP = H - R_{T}$ 6

where: z is sinkage; W is wheel load; D is wheel diameter; b is wheel width; k, n, \not o, K_b , K_0 , \not o, and c are soil properties; R_c is compaction resistance; R_b is bulldozing resistance; R_T is total resistance; H is gross traction; and DP is drawbar-pull. (See Figure 21).

If Equation 1 is introduced into Equations 2, 3, and 4, it is possible to examine the effect on performance of a change in diameter or width.

$$R_{b} = 2 cK_{b}(\frac{1}{b}) \frac{\frac{2}{2} + 1}{(\frac{1}{D})} \frac{\frac{1}{2} + 1}{(\frac{1}{D})} \left[\frac{3}{k(3-n)}\right]^{\frac{2}{2} + 1}$$



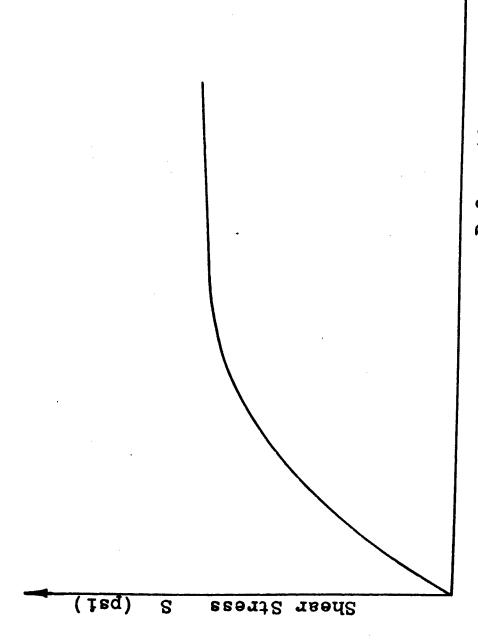
$$H = c \begin{cases} \frac{2 \text{ n}}{2 \text{ n+1}} & \frac{4}{2 \text{ n+1}} \\ (D) & (b) \end{cases} = \left[\frac{3 \text{ W}}{k(3-n)} \right]^{\frac{2}{2 \text{ n+1}}} \\ - \left(\frac{1}{D} \right) & (b) & \left[\frac{3 \text{ W}}{k(3-n)} \right]^{\frac{4}{2 \text{ n+1}}} \end{cases}$$

$$+ \text{ W tan } 6$$

Figure 1 is a graphic presentation of Equations 7 and 9. The figure was developed to depict the effect on performance of changes in contact area produced by increasing either wheel width or diameter. Examination of the figure reveals that a given area change obtained either by increasing width or diameter produces an equivalent increase in performance as measured by the gross traction. However, under most circumstances, the area change should be obtained by increasing the wheel diameter instead of the width. Gross traction is proportional to area and load but independent of area shape. However, motion resistance is proportional to contact area and width. A given area increase will produce a fixed increase in traction independent of whether the increase is produced by greater width or diameter. But, because resistance is proportional to width, drawbar pull is less for the wide than for the narrow area. Therefore, it is better to increase area by increasing diameter than width.

In addition to the consideration of motion resistance, we should examine the mechanism through which traction is developed. In order to obtain traction, soil must be deformed. The relationship between shear strength and deformation is shown in Figure 2. The maximum shear strength occurs after significant deformation has occurred this may be one or several inches. If the contact area of the wheel is oriented so that the longer dimension is in the direction in which the soil is sheared, the wheel is more efficient than if the shorter dimension were oriented in the direction of shear. That is, shear of the soil can only be achieved by means of wheel slip. If the wheel must slip one inch and the length of the contact area is two inches, the wheel must develop 50% slip to achieve maximum traction. If instead, the contact length is four inches, the same traction can be developed at 25% slip.

There seems, therefore, several reasons why a wheel designed for optimum performance in soft soil should be relatively narrow and have a large diameter. Theory is, of course, totally meaningless unless it is confirmed either by experiment or experience. Experience



Deformation j (in)

Typical soil shear stress-strain curve.

unquestionably verifies the conclusions obtained from the figure. When carriages were developed for operation in soft soil, it was obvious from experience to the builders that it was easier to pull a narrow, large diameter wheel through the mud than a wide, small diameter wheel.

A similar argument holds for a tracked vehicle because the equations describing the behavior of a track are similar in form to those for a wheel. The more efficient soft soil performance available from a long, thin track has been one of the reasons that articulated vehicles have been attractive.

Efficient utilization of soil strength dictates a long track; however, there is a definite limitation to track length if a vehicle is to be steered by means of skid-steering. The obvious way to accommodate the conflict between steering and efficiency is to use a long track and steer by articulation of the vehicle.

Until recently, there has been a general tendency to overlook the performance requirements imposed by geometric obstacles. This is understandable because it is seldom that a vehicle becomes immobilized by an obstacle even though it is unable to negotiate the obstacle. When one considers adverse terrain, the usual image is a quagmire with vehicles sinking to their axles and recovery crews knee-deep in mud. However, the frequency of occurrence of such obstacles is relatively low and the time and place at which they will be found is quite predictable. However, when we consider the frequency of occurrence of geometric obstacles, it is evident that off-road terrain contains an almost continuous variation in profile. A major component of the profile consists of variations sufficiently severe to be considered as obstacles. An obstacle is defined in this context as a variation in terrain profile sufficiently severe relative to the vehicle to require a specific response on the part of the operator. Examples of geometric obstacles are ditches, steep slopes, river banks and rice paddy dikes.

In order to provide adequate obstacle performance, it is necessary that a vehicle: (1) have large ground clearance; (2) have angles of approach and departure of 90° ; (3) have a break angle such that the vehicle will not be immobilized on a "crown"; (4) provide uniform loading of wheels or tracks even though the ground surface is not uniform; and (5) sufficient flexibility either in the frame or through articulation, to permit large relative motion between parts of the vehicle. It may be offensive to read a list of qualitative statements concerning vehicle requirements which appear to be simple to quantify. For example, what is meant by "large ground

clearance" when the usual method of stating ground clearance is to specify 18 inches as a minimum? The qualitative statement was made because ground clearance, along with the other characteristics listed, except for approach and departure angles, tends to be a vehicle term. A large vehicle may require much more than the 18 inch ground clearance and a small vehicle considerably less. Despite the vagueness of the criteria offered, they provide a good rule of thumb for the evaluation of the obstacle performance of a concept offered as an off-road vehicle.

It was previously stated that most off-road terrain has a continuously varying profile. In the absence of soft soil or of geometric obstacles, it is still not possible to travel at high speed. Anyone who has had the experience of driving across a pasture in a jeep will recognize the fact that even a modest amount of roughness will severely restrict speed. The speed restriction is the vibration of the vehicle which becomes sufficiently severe that the operator chooses to go no faster because of real or feared damage to himself or the vehicle. A reasonable understanding of vehicle characteristics required to reduce vehicle vibration response has been at hand for many years. To reduce vibration, a small unsprung mass and a large wheel travel are the starting points. A "live" suspension which permits the wheels to be driven up and down in conformance with the ground profile appears necessary if a significant increase in speed is to be achieved. This appears to be a most unhappy situation because a live suspension is of necessity a complex system involving the sensing of profile and instantaneous change of suspension characteristics in response to the profile senser. However, if a conventional suspension having conventional mass and wheel travel is proposed on a vehicle concept, it requires no analysis to establish that the concept will not provide high off-road speed.

The problem of the negotiation of areas covered with vegetation has only recently been recognized as significant because of the emphasis on operation in jungle environments. The problem has, of course, always existed but has been largely ignored because forests have been accepted as impenetrable with no great thought as to whether vehicles might in fact be able to overcome the obstacle. There are two obvious ways to operate through a heavy forest: avoid the trees by passing between them or knock the trees down. The ability to avoid the trees is considerably more attractive than knocking them down since the latter approach involves a huge expenditure of energy that is largely wasted and the noise of crashing through a forest would alert any enemy troops in a wide radius. It is obvious, however, if a vehicle is to negotiate between trees, it must be quite narrow and highly maneuverable. On the other hand, if the vehicle is to knock down trees, it must be powerful, massive, and be driven by a fearless operator. Operation in areas of heavy

vegetative cover is a sufficiently new idea to prevent an appreciation of the required vehicle characteristics. It can be concluded that a vehicle must either be small and maneuverable or large. Small can be taken as no wider than the jeep and large as the size of an M113 Personnel Carrier. The vehicle must provide adequate protection for personnel and should place the operator as high as possible to improve vision. This latter requirement has been shown to be highly significant in dense vegetation. If vegetation is dense, it will usually consist of small trees and bushes which do not stop the vehicle but obscure vision to the point that the operator becomes lost.

It has become required that vehicles be capable of either swimming or floating. In the opinion of the writer, this is largely a futile requirement because a swimming capability leads the tactician to believe that he has an ability to move across waterways which he, in fact, does not have except in very unusual circumstances. The unusual circumstances consist of smooth, slow moving water accompanied by a gently sloping exit from the water. In order to make a vehicle float or swim, the vehicle can be designed to provide adequate buoyancy or flotation kits can be installed. Designers have been very successful in providing flotation. However, the problem of getting out of a river has hardly been admitted much less addressed. In order to negotiate a modest river bank, the bank must be prepared or else outside aids, such as a winch, must be used. The primary advantage of a swimming or floating capability is in the reduction, not elimination, of the engineer effort required to negotiate a river.

If negotiation of water obstacles is accepted as a requirement, the negotiation of river banks is an immediate auxiliary requirement. Good water performance is associated with freeboard, water speed, and control. The capability to negotiate river banks is related to geometric obstacle performance except that a river bank normally represents a more severe obstacle. A winch having a load rating equal to the vehicle weight appears as a starting point. It is not apparent that river banks can be negotiated without the development of a radical change in vehicle form.

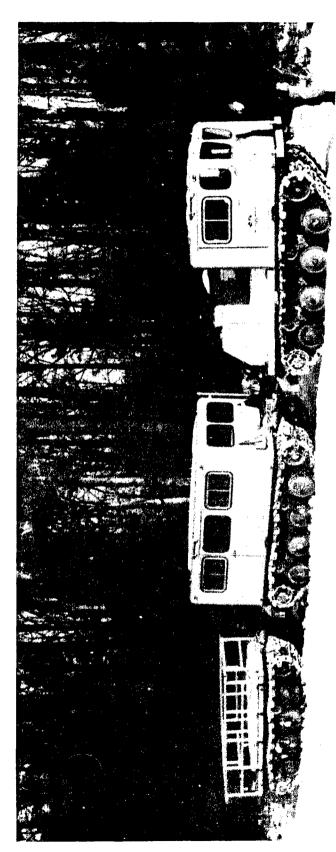
The general requirements for vehicles have been enumerated. We will now turn to an examination of concepts that satisfy some of the requirements. None of the concepts satisfy all of the requirements nor does it seem likely that any vehicle can meet them all. The first vehicle concept that will be examined is the COBRA ——a three-unit, articulated vehicle having a spaced-link track. The track will not be discussed at this point since it is better to treat the track along with other novel suspension concepts. The COBRA was based on the combining of two different but similar ideas: the articulated

vehicle and the land train. The articulated form of vehicle has normally been considered a two-unit machine which makes the most efficient utilization of a given track area. Articulation was conceived as a method to steer a tracked vehicle. The land train was proposed as a method for moving large loads without paying the penalty of increased vehicle size. For example, a series of identical self-propelled units each having a payload of 10 tons could move 100 tons simply by coupling ten of the units together into a train. The railroad train could be mimicked and a vehicle constructed with an "engine" and a series of cars. The cars would be self-propelled but receive power from the engine. The thought was that there would be virtually no limitation on the load that could be carried by a land train and the performance of the train would be independent of load, since each additional unit would provide its own motive force. It would thus be possible to have a 1,000 ton vehicle with the same ground pressure as a 20-ton vehicle. Unfortunately, the idea does not work as well as anticipated because of the occurrence of obstacles. In most off-road conditions, it is not possible to go very far before a steep slope, ditch, hill crest, or similar obstacle must be negotiated. In order to negotiate the obstacle, it is usually necessary to reduce vehicle speed. If a vehicle train is very long, it soon occurs that some part of the train is in contact with an obstacle all of the time. An additional factor that must be considered is that the maximum speed of a vehicle must be increased in a direct proportion to the length of the vehicle. Consider the average speed of a three-unit vehicle compared to that of a conventional vehicle having dimensions equal to one unit of the three-unit vehicle. The three-unit vehicle must be able to transverse an obstacle at a higher rate or move over the smooth ground between obstacles at a higher rate in order to have an average speed equal to that of the conventional vehicle. If one writes the equation for the average velocity of an n unit articulated vehicle negotiating two obstacles, it is found that

$$V = \frac{\cancel{l} + \frac{6}{5} nx - \frac{x}{5}}{(\frac{12}{5} nx - \frac{2x}{5}) + (\cancel{l} - \frac{6}{5} nx + \frac{x}{5})}$$

$$v_0$$

Where: V is the average velocity, n is the number of visits; ℓ is the distance between obstacles; x is the length of the units and $\frac{x}{2}$ is the spacing between units; v_0 is the speed at which an obstacle can be negotiated and v_ℓ is the speed between obstacles. If Equation



10 is differentiated with respect to n, the following proportion is found:

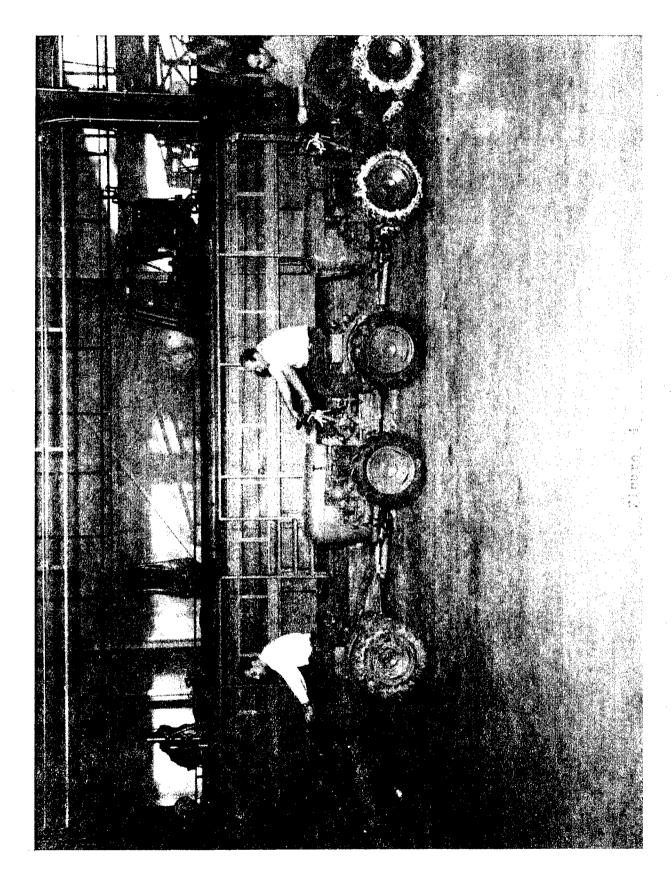
Since Equation 11 is negative for a given v_0 and v_ℓ with $v_0 < v_\ell$, a single unit vehicle will have the highest average speed.

Experience has shown that an articulated vehicle can operate at a higher speed over rough terrain than can a conventional vehicle. However, as the number of units is increased, the gain is rapidly lost and a rule of thumb is that a vehicle having more than four units represents the limit to the usefulness of the articulation principle.

The preceding discussion was not intended to discourage the use of articulated vehicles. Rather, it was written to establish the limitations in the application of the vehicle form. The COBRA, shown in Figure 3, was designed to investigate the limitations discussed above in addition to evaluating the spaced-link track. The vehicle was of limited success because of a considerable over load on the suspension system which reduced its durability severely. However, valuable experience was gained and it become obvious that articulated vehicles having more than two units must incorporate a flexible steering system. When moving forward, the third and following units should not have positive steering at the articulation point but should merely trail. When operating in reverse, the two rearmost units should provide steering with the remaining units trailing. It was also apparent that multi-unit articulated vehicles require the use of a joint which can be connected and disconnected rapidly if the potential flexibility of the concept is to be utilized.

The use of articulated vehicles inspired the so-called inching principle. The inching principle utilizes the articulation joint to provide a mechanism to eliminate soft soil immobilizations of articulated vehicles. If the articulation joint incorporates a set of hydraulic cylinders for steering, the cylinders can also be used to provide a driving force. If a two-unit articulated vehicle is immobilized in soft soil, the motion resistance is obviously greater than the available traction. Assuming tracked vehicles having equal traction and motion resistance for each track, we can state that:

where H is traction and R is resistance. If the rear unit is braked, the force required to push the unit to the rear is:

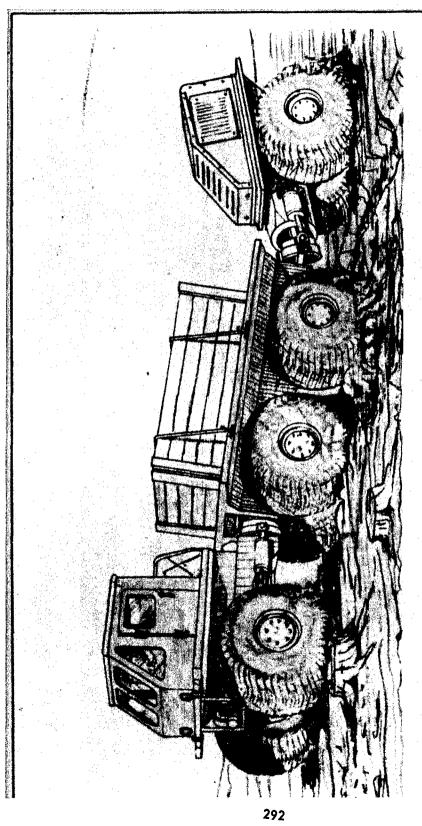


$$F = 2H + 2R_1 \dots 13$$

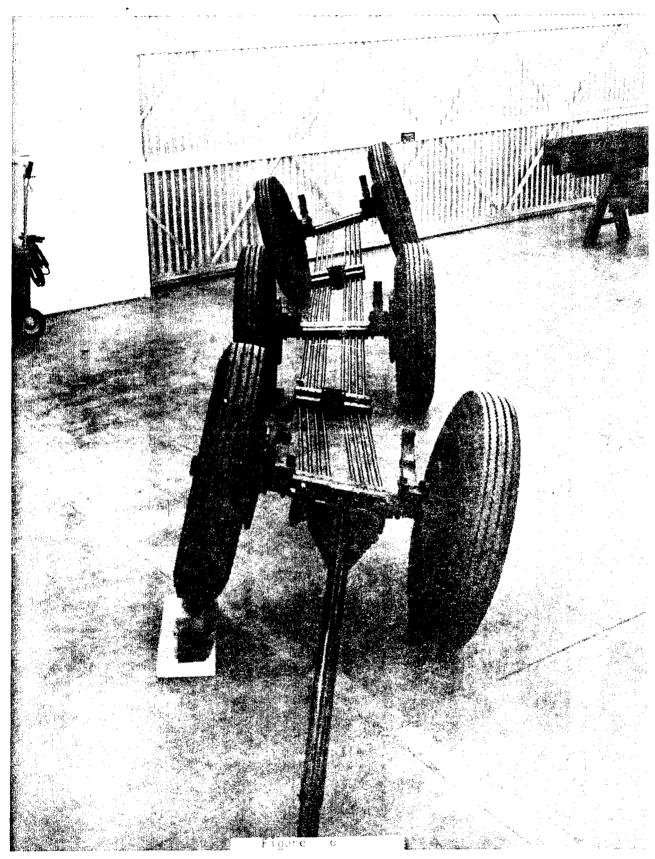
where R₁ is the compaction and bulldozing resistance acting to oppose the rearward movement of the track. This means that the force, F, is available as a reaction for the steering cylinders. If the front unit attempts to move forward and the steering cylinders are extended, the front unit will move forward if Equation #4 holds, the rear unit will move backward if Equation #4 holds, and merely oscillate in place if Equation #4 holds. Except in this latter, and unlikely, case, the vehicle will be able to move in one direction or the other so that the immobilization is eliminated.

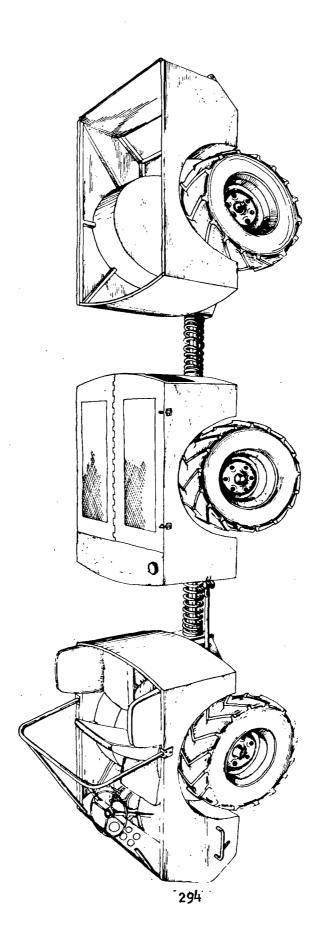
For a three-unit vehicle, the two rear units act as a "deadman" to push the front unit. The front and rear units then pull and push the middle unit. Finally, the two front units pull the rear unit so that the vehicle inches forward until the cause of the immobilization has been passed. It is, of course, possible that the motion resistance is sufficiently high that the hydraulic cylinders are overloaded. In addition, the inching principle may not assist in overcoming the very common cause of immobilization - a slope covered with a thin layer of weak soil. In order to negotiate the slope-soil obstacle, it is necessary that the "coefficient of friction" between the soil and track or wheel be greater than the percent slope to be climbed. The quotation marks are used since the parameter under consideration is the ratio of the tractive force and the vehicle weight component normal to the soil. In any event, if a vehicle is unable to negotiate a slope as described and the complete vehicle is on the slope, the inching principle will be of no assistance. The saving grace is that the combined slope and "slippery" soil obstacle is usually not so long that a multi-unit vehicle cannot span the obstacle and inching may be of some use.

A test rig using the inching principle is shown in Figure 4. The rig consists of three 4x4 farm tractors with inching cylinders installed. The rig is obviously rather unwieldly but the purpose of assembling it was to investigate the inching principle to determine whether the idea had any practicability. The rig was tested in four foot deep snow in Houghton, Michigan and the results were quite gratifying even though the rig was severely damaged. The inching cylinders permitted the three tractors to be moved, albeit slowly.



ARTIST CONCEPTION OF 8X8 WHEELED CONCEPT





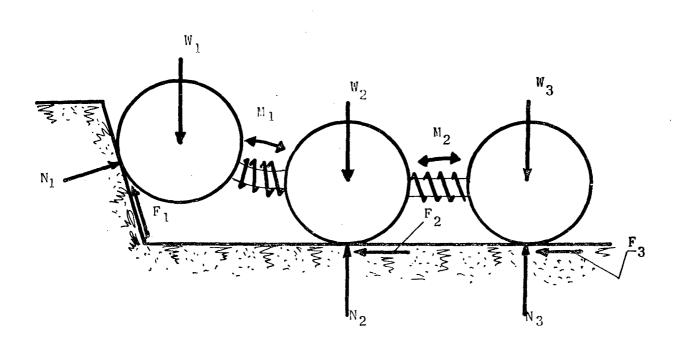


Figure 8

through the deep snow. Unfortunately, the design of the connecting linkages to the tractors was somewhat weak and both sets of inching cylinders were broken from the tractors. It is interesting to note that the vehicles were moving in sufficiently difficult conditions that once the cylinders failed, it was necessary to disconnect the tractors and drag them out simply with a vehicle operating on a near by road. The inching principle has been incorporated in a series of high mobility test rigs which are currently being procured for test purposes. An artist's sketch of one of the concepts appears as Figure 5.

An attempt to gain the benefits of being articulated without paying the full penalty of the articulation joint was proposed by Bekker (1) for lunar application. The concept was later examined for application to earth vehicles and a test rig is currently under construction in the Land Locomotion Laboratory. The concept has been designated as the flexible frame and derives its name from the fact that the primary frame element consists of a flexible member. The frame shown in Figure 6 makes the concept obvious.

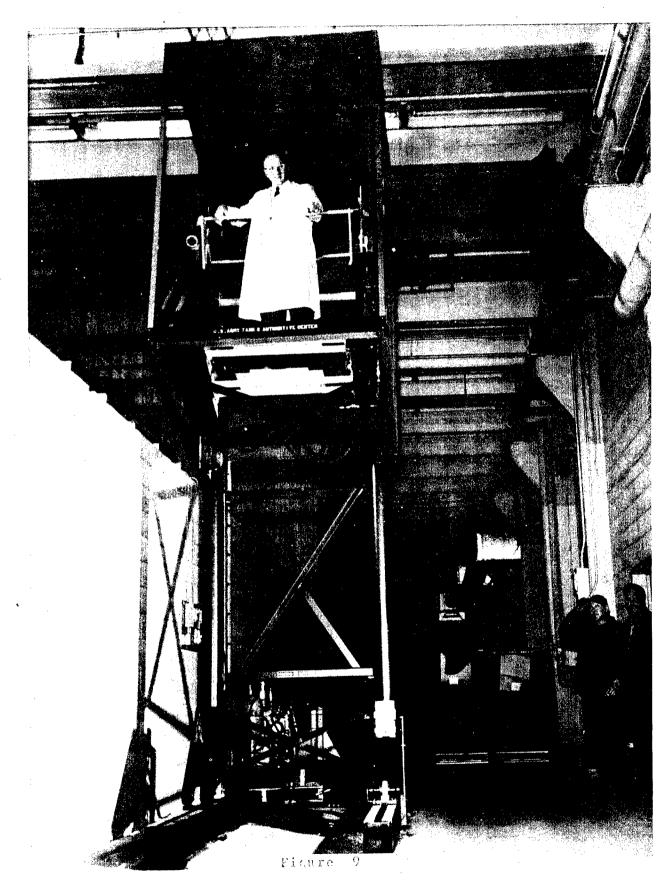
The flexible frame test rig currently under construction is shown in Figure 7. The test rig departs from Bekker's original concept in that coil springs are used as the joints between units. The springs are mounted so that no restriction is provided in roll while the motion in pitch or yaw is restricted by the bending strength of the spring. The primary advantage of the flexible frame concept is its simplicity and in the reduction of the space required by the joint. However, the obstacle performance of the vehicle is superior to a conventionally articulated vehicle of similar proportions. If the front unit of a flexible framed vehicle moves upward as shown in Figure 8, the front and second unit soil loading is increased in proportion to the deflection of the flexible element. In many cases, traction is a function of both contact area and normal pressure. increasing normal pressure, the wheel in contact with the obstacle develops an increase in traction at the precise time at which the increase can make its greatest contribution. The outstanding obstacle performance of Bekker's lunar vehicle model has verified the potential of the concept.

The following unusual vehicle concept may more rightfully be called bizarre than unusual. The concept resulted from a consideration of the solutions evolved by nature for locomotion over unmodified terrain. Almost without exception, animals that have survived the long process of evolution are walking devices. Despite its apparent simplicity, nature has nowhere produced a wheel but has relied

on a much more complex set of levers for locomotion. This has been true for a cogent set of reasons: it has been shown (2) that the walking device is more efficient in soft soil operation than vehicles based on the wheel and that the walking mode of locomotion produces a significant smoothing of rough terrain by selection of the parts of the terrain which will be used. In addition, if extremely rough terrain is to be negotiated, it is necessary that the propelling mechanism be sufficiently flexible to permit major changes in the orientation of the driving elements without an equally major change in orientation of the cargo being propelled. The "Daddy Long Legs" can be taken as an extreme example: the legs on this vehicle can go through violent excursion without the least effect on the cargo. I will not go into the background studies that led us to the point of proposing a quadruped walking machine instead of a leaping vehicle, for example, since this has been amply reported elsewhere (2).

Early studies by and for our laboratory had indicated that regardless of the type of levered vehicle one proposed, the primary problem was one of control. How could an operator sense where to place a leg of the machine and how could he place it once the decision was reached? The design and construction of a levered vehicle was straightforward - how to control the resulting machine appeared an insurmountable problem since it would require an unacceptably complex computer system. Mr. Henry Aurand, at the time with the TEMPO organization of the General Electric Company, came to our rescue in 1961. He proposed that a biped walking machine be constructed using the force feedback control system developed by General Electric to control the Handy-Man Manipulator. The potential solution to our problem was recognized and a series of feasibility studies were begun forthwith.

Force feedback is one of the three primary means by which we control our body motor functions. We make our judgments on the basis of one or a combination of visual, tactile, or kinesthetic signals. To demonstrate: if we are to pick up a glass filled with a liquid, our visual sense tells us where to place our hand; our kinesthetic, or force, sense tells us when we have reached the glass and how much force to apply to pick it up; our tactile sense tells us whether the glass is rough or smooth and to drop it if it is too hot. Under most circumstances, the force cue is the most reliable signal. Our visual cues may be totally misleading under many ordinary circumstances. For example, a cube of tungsten carbide looks like a cube of steel. Because most people are far more familiar with steel than with tungsten carbide, our system is prepared by visual cue to pick up a cube of steel. When our force cue tells that the cube weighs several times as much as we expected, we are momentarily dismayed.



The dismay is only momentary because our control system immediately responds to the force cue and rejects the visual misguidance. Our tactile sense may often be equally misguiding as shown by the incapability to distinguish between very hot and cold objects. In this situation the fact that our tactile sense cannot tell us whether we are being burned or frozen is of little significance because the response to either signal is the same - eliminate contact forthwith.

It is quite simple to think of many examples of visual vs. tactile miscues but it is difficult to imagine a kinesthetic miscue because there is no interpretation involved in a force signal. It is scarcely likely that difficulty could occur in distinguishing a very light weight from a very heavy weight. The object of the, perhaps over-long, discussion of our sensory system was to establish that much of our activity is controlled by a force feedback type of response. Although the force feedback is supplemented with other feedbacks, it is the primary means of control. If one is concerned with the development of a device that mimics human motions, the most obvious means of controlling the device is by the same signal and response system used by the human. Because it is not reasonable to reproduce the human response system electronically, it is again obvious that the human should be included in the control network.

The feasibility of a walking type device using the force feedback control was studied and it was concluded that the idea was sound from mechanical and control viewpoints. The human factors aspects of such a device required a further study which produced the conclusion that static balance was the most difficult phase of biped walking. Technically speaking, static balance has nothing to do with walking so that the conclusion can be rephrased to the following: if a control system can be devised to permit static balance of a biped having adequate degrees of freedom for walking, the control system is adequate for the walking mode. This conclusion can be demonstrated by observation of a child learning to walk. When progressing from the creeping mode to the walking made of locomotion, the child is capable of the leg motions involved in walking but is unable to walk except for short distances between balance aids. The child will balance with the aid of a chair and then progress by means of a semi-controlled fall to another chair. Once an ability to maintain static balance is achieved, the child is competent at walking and is almost immediately able to run.

In order to investigate the static balance problem, the device shown in Figure 9 was constructed. The rig consists of two twelvefoot long legs and a cab. The motions of the balance demonstrator are confined to a single plane and consist of an ankle joint and hip



joint. The operator is placed in a crude harness designed so that he receives a force feedback response at his ankle and hip joints. Both the joints are operated by hydraulic cylinders which are actuated by a servo-valve. A large number of people have been tested in the balance demonstrator and it has been established that the force feedback control system is completely satisfactory and static balance is simple. The operator does not have to balance the rig; he must merely balance himself and the machine mimics him exactly so that it is in balance. Although a part of our balance capability is controlled by vestibular responses, this does not appear very significant in the static balance problem because the level of the signals is quite modest.

It has been demonstrated that a control system is available that will permit static balance and, therefore, a walking machine. The control of a quadruped walking machine appears much simpler than the biped because the balance requirement is greatly reduced. A proposed quadruped is shown in Figure 10 in which the device is depicted as operating in terrain similar to that found in jungles. The dimensions of the proposed machine are: ten feet long; ten feet high; and three and one-half feet wide. The leg length has been selected as six feet. A potential payload of 500 pounds is proposed for a machine of these proportions. Adaptation of an operator to the quadruped appears to be no more difficult than for a biped. The front legs could be controlled by the operators arms and the rear legs controlled by his legs. The operator would be suspended in a harness and be tilted approximately 200 from the vertical so that both arms and legs receive a proper force signal. It is expected that the high speed control of a quadruped walking machine will be more difficult than a biped simply because the human is not adept at moving on all fours. This, however, is not considered a difficult long term problem because of the remarkable ability of the human to adapt himself to change.

Despite the fact that the walking machine remains in the exploratory stage of rather fundamental problems, the device appears to have great promise for off-road applications. The soft soil performance can be adjusted to suit the area in which the vehicle is to operate by the simple expedient of changing the size of the foot pad. If very large pads are to be used, it may require a learning process on the part of the operator similar to learning to walk with snow shoes. However, with even a little experience, one can walk while wearing snow shoes -- admittedly not very well, but this is considerably better than not at all. When compared to the effort involved in modifying a tracked or wheeled vehicle for operation in variable soil conditions, the slight training time involved in "changing feet" is insignificant.

The obstacle performance of a quadruped should be competitive with its natural counterpart, the mule. An animal smooths terrain by selection of the parts of the terrain which it chooses to use and, in addition, smooths its response to terrain roughness by changing the length of its stride. The quadruped has the potential of similar performance. The selection of the point at which the operator will place his foot can be by visual means just as he would place his foot when walking or, in this case, creeping. When negotiating extreme slopes, the leg lengths can be modified to maintain the "body" in a relatively level attitude. The quadruped device is considerably more efficient than a biped when attempting to negotiate extremely difficult terrain. It is common for a human to resort to creeping when climbing severe slopes or particularly rough ground.

The performance of a quadruped through dense vegetation should be good because of the narrow, long, animal-like dimensions. The legs can be made long enough so that surface vegetation can be stepped over. The trees can be avoided by a combination of the narrow shape of the vehicle and its high degree of maneuverability. An additional advantage of the quadruped for operation in vegetation is that the location of the operator's head will be approximately eight feet above ground level which will provide an increased vision capability.

One of the most exciting aspects of the quadruped is its potential ability to negotiate river and canal banks without assistance. The machine can be made to swim by using either a sculling or kicking motion of the feet. It does not appear at all difficult to provide adequate buoyancy to float the vehicle with ample freeboard. The vehicle can be made to float and to swim. However, for the first time, the quadruped offers the possibility of a vehicle exiting from the water without assistance even though the bank may be quite severe. Without question there will be many banks which cannot be negotiated without assistance. On the basis of our understanding of the requirements for an off-road vehicle, the quadruped appears to offer great potential.

Earlier in this paper, a discussion was presented in which it was argued that a large diameter, narrow wheel represents the optimum use of a given wheel volume. In view of that reasoning, our laboratory has been interested in the development of wheels which produce the equivalent effect of a large diameter without paying the penalty of a large diameter. Two approaches, both proposed by Bekker, have been followed: a tire design permitting greater than normal deflection and the use of a flexible rim to permit large wheel deflections.

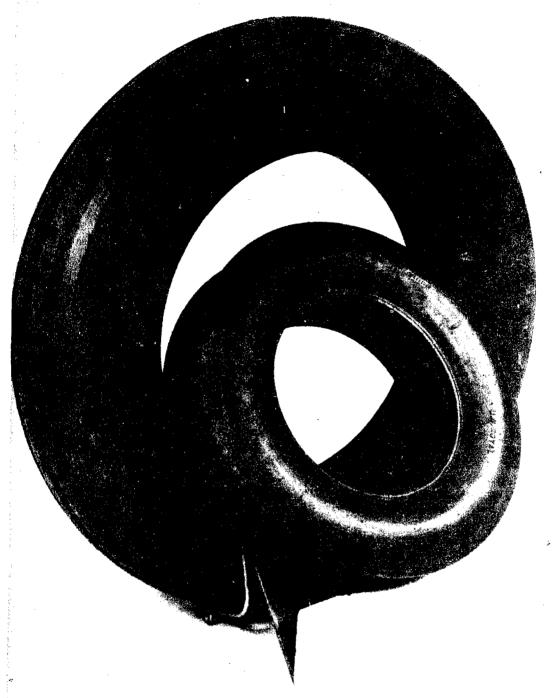


Figure 11

U. S. ARMY TANK AUTOMOTIVE CENTER NEG. NO. PR 2805-65-3 DATE 24 May 65 Inner and Outer Tire Components of Condual Tire Concept.



Figure 12

CONDUAL TIRE,

Before examining these two approaches, one thing should be emphasized. A large diameter, wide wheel is more effective than a equally large, narrow wheel. However, to optimize performance for a given volume and weight, a narrow, large diameter wheel should be used.

The first device to be examined is the condual tire. The name condual refers to a concentric-dual tire and is made obvious by Figure 11. The condual tire was conceived to obtain a long, thin contact area by means of large tire deflection. Under normal circumstances, it is possible to deflate a pneumatic tire so that the tire deflection is equal to 15% of the wall height. Thus, to increase contact area without damage to the tire, it is necessary to increase the section height. However, the section height is limited by mechanical considerations. It would not appear to be feasible to construct a tire which doubled the permissable deflection by doubling the section height. However, if the tire were constructed so that it consisted of two tires, each of which had "normal" section heights, the mechanical problems could be avoided. The condual tire was assumed to have potential stability problems during highway operation because the tire would deflect laterally during turning maneuvers. It would be possible to avoid the stability problem by inflating the inner tire to a high pressure so that it behaved as a solid rim. During off-road operation, both inner and outer tires could be deflated to produce maximum deflection. It was assumed at the outset that the tire would deflect laterally at low inflation pressures, but this was not considered significant because of the low operating speed. However, in the event that the lateral deflection did pose a problem, several devices were proposed to provide support for the tire and prevent excessive deflections. Subsequent tests with a prototype tire revealed that the lateral deflection problem was nonexistent.

Figure 12 shows the assembled condual tire. The present configuration requires that a pressure differential of 10 psi exist between the inner and outer tires – the inner tire having the higher pressure. A tire of similar construction was tested by the manufacturer on a standard tire dynamometer. The tire operated at 50 mph for a period of 40 minutes before failure occurred. This does not seem much of an achievement until compared with the performance of the original prototype: $2\frac{1}{2}$ minutes at 50 mph. Furthermore, the manufacturer of the tire does not see any reason why the tire cannot be made to operate with a durability approximately equal to a conventional tire.

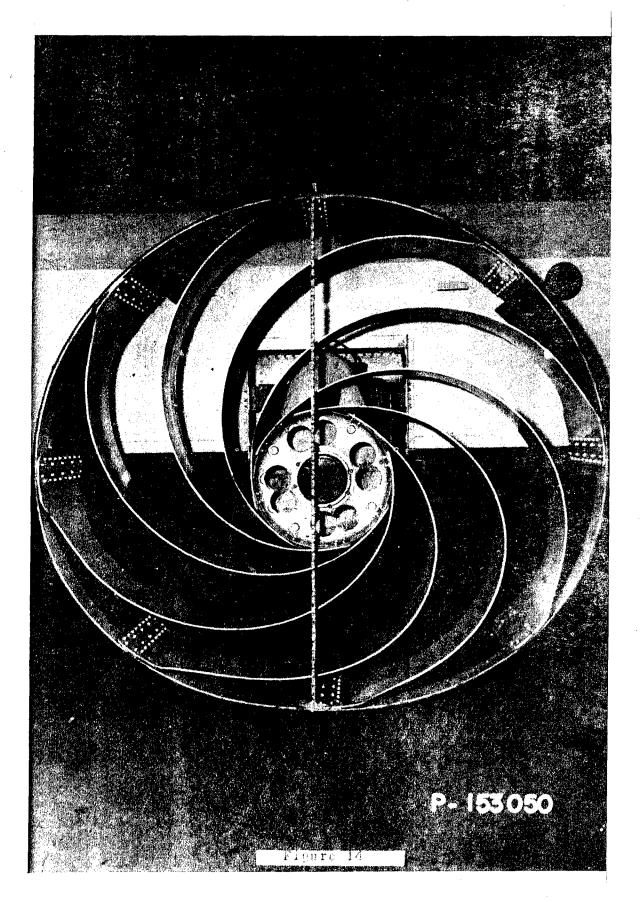
The remainder of the discussion of wheels will be concerned with concepts based on the use of a flexible rim. The original flexible

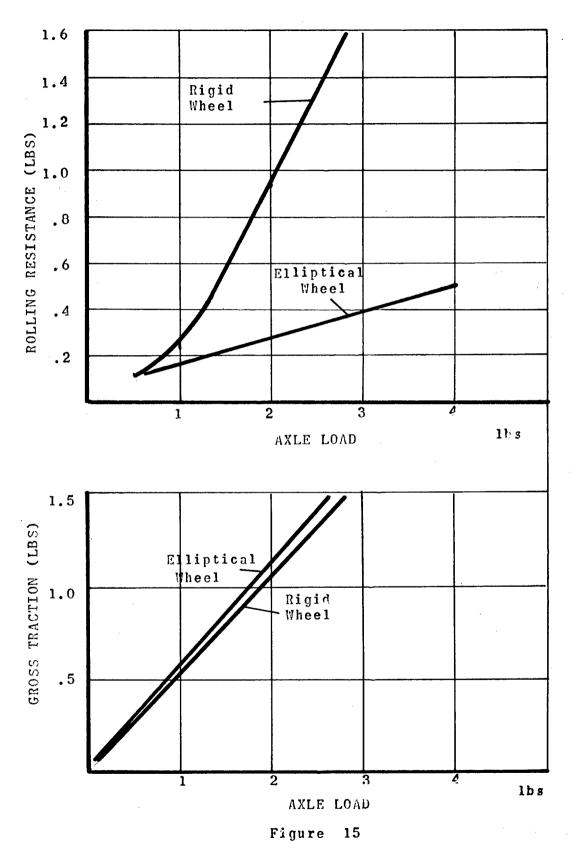


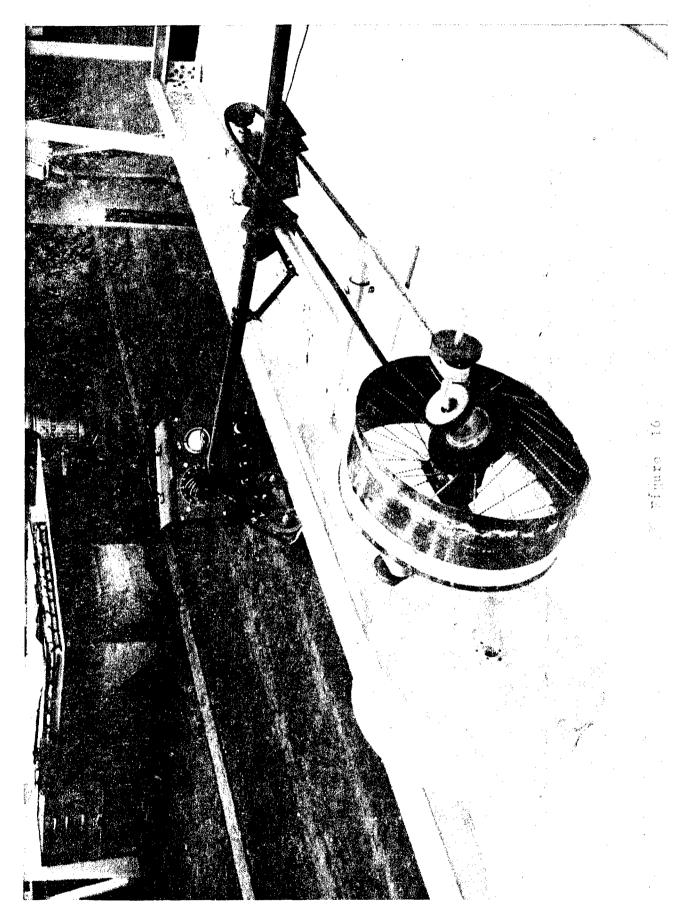
Figure 13

-DETROIT ARSENAL-

NEG. NO. 63835 DATE 29 Jul 60 Elastic, Hubless Wheel Vehicle, 3/4 View.







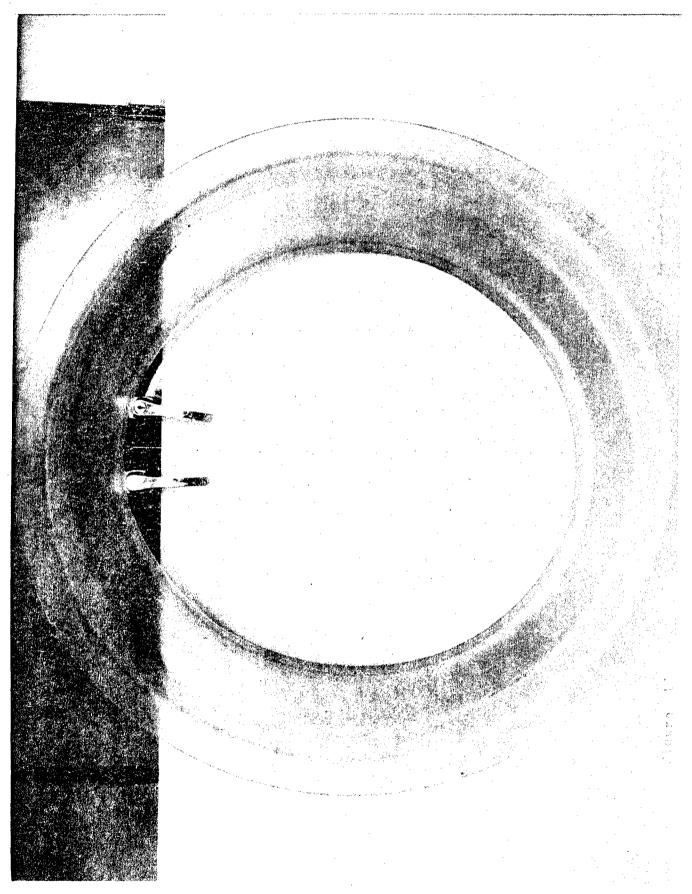
rimmed wheel, and inspiration for the remaining wheels to be discussed, was the hubless wheel proposed by Bekker. The hubless wheel was nothing more than a rim. The rim consisted of two hoops joined by solid cross-links. The cross-links served the dual purpose of joining the two hoops and providing a means for driving the wheel. The hubless wheel is shown in Figure 13 mounted on a modified "Mule".

The hubless wheel was not carried beyond the first prototype stage because of a series of problems that appeared to be soluble only by complicating the device so much that its greatest asset of simplicity was lost. The idea of the flexible rim was picked up by Mr. Ed Markow of Grumman Aircraft who, developed the 'Metalastic' wheel.

This wheel, proposed for application to a lunar vehicle, is shown in Figure 14. The wheel consists of a flexible rim joined to a hub by means of a series of springs. The springs are wide at the rim and narrow at the hub so that considerable lateral stability is achieved without an undue weight penalty. Compared to conventional wheels of equal diameter. the metalastic wheel develops a higher drawbar-pull because of the large contact area produced by deflection of the rim. A series of tests were run by Mr. Markow using a 12 inch diameter, 3 inch wide metalastic wheel and a conventional rigid wheel of equal dimensions operating in a purely frictional soil. The parameters evaluated were traction, rolling resistance, and the drawbar pull versus slip relationship. Typical results of the test series are shown in Figure 15. Because the tests were conducted in a purely frictional material, the gross traction produced by the wheels was identical. The difference in performance shown in Figure 15 is due solely to the reduced rolling resistance of the flexible wheel. This point is sufficiently important to be repeated at frequent intervals: the potential payoff associated with a reduction of rolling resistance is usually greater than the payoff available from an increase in traction.

Because of the simplicity of the metalastic wheel and the suspension properties achieved with no moving parts, the wheel developed considerable interest for its lunar vehicle potential. An outgrowth of the development of the metalastic wheel was the elliptical wheel.

This wheel, shown in model form in Figure 16, is also based on the flexible rim. The rim is connected to the hub by means of flexible straps. As seen in the figure, the hubs are tilted so that they appear as ellipses when viewed along the wheel axle. Since the straps are inextensible and the rim flexible, the rim also assumes an elliptical shape. The result is a wheel having a large contact area



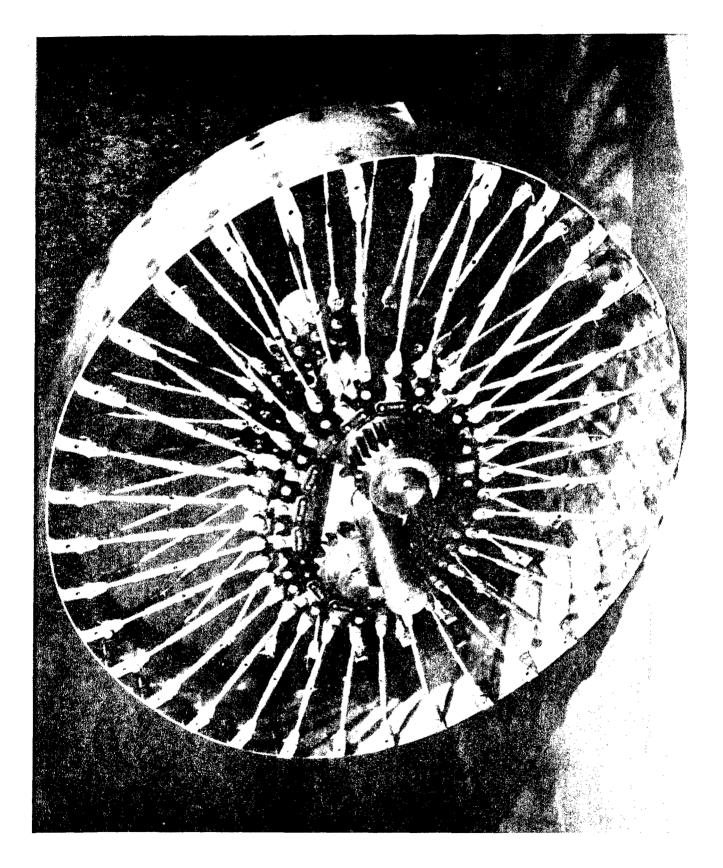
for a given wheel diameter. In cohesive materials, the elliptical wheel increases drawbar-pull by reducing motion resistance and increasing traction. In frictional materials, the performance improvement is achieved by a reduction in motion resistance.

There was no attempt to establish the relative performance of the elliptical wheel compared to a conventional wheel by experiment. The potential improvement was obvious permitting us to concentrate our effort on the examination of the mechanical feasibility of the wheel. The first, and most obvious, problem with the elliptical wheel was the provision of a drive mechanism. The radial straps connecting the rim and hub were capable of carrying a tensile load but were deliberately pivoted at the hub and rim connection points eliminating the feasibility of transmitting torque through the "spokes". A proposed solution is shown in Figure 17. Subsequent work has produced a simpler, cheaper, and more rugged means of transmitting torque but the idea is the same. Torque is transmitted by means of a membrane-like device which offers slight resistance to compressive loads but has high torsional strength. Thus, the wheel can be driven, or towed, without affecting the elliptical shape of the wheel.

A second problem, so far unsolved, with the wheel is the provision of a running surface that is sufficiently flexible to have no appreciable affect on the rim deflection characteristics but, at the same time, sufficiently strong to provide a good wearing surface. A small section height, pneumatic tire has been proposed by a tire company that appears to be a reasonable solution.

The third problem appears at this time to be the most difficult to solve without introducing unreasonable complications to the wheel form. This problem is the dynamic behavior of the wheel during high speed turns. Although the drive membrane has high torsional stiffness in the plane of the membrane, it offers little or no resistance to rotation of the rim relative to the vertical axis of the wheel. In other words, relative motion between the hub and rim is possible because of the flexibility of the rim and spokes. When attempting to turn at high speed, the rim will behave as a gyroscope and resist the attempt to change its direction of motion. The wheel has not been analyzed from this viewpoint but previous attempts to use flexible spokes have failed because the wheel was destroyed by high amplitude oscillations which occurred during steering at high speeds.

An alternate form incorporating similar principles as the elliptical wheel, has been proposed to provide dynamic stability without undue complication. The wheel, shown in Figure 18, has the

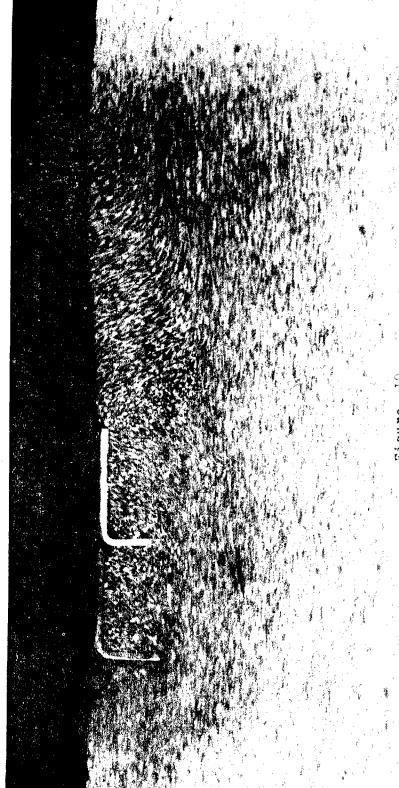


disadvantage of a fixed shape. The elliptical wheel is capable of a wide variation of the relationship between the major and minor axes. This can be accomplished by making the titlt of the hub controllable. For highway operation, the hubs could be vertical: as required, the hubs could be tilted in increments up to the maximum tilt depending on the soft soil conditions. It would be most logical, of course, to have the wheel operate in either of two configurations: at no hub tilt for highway operation and at maximum hub tilt for off-road operation.

The driving torque for the modified elliptical wheel would not have to be transmitted by means of a membrane. Because the spokes of the modified wheel are not radial, torque can be transmitted by the spokes by means of a tensile load much in the same way as a bicycle wheel transmits torque. An additional useful characteristic of the modified elliptical wheel is the oscillation permitted around the axle. The long axis of the wheel can move around the axle which means that the wheel can behave in a manner similar to a bogey suspension and thereby reduce the severity of the motion of the axle as the wheel negotiates a vertical obstacle. The result is a capability to move at higher speeds off-road.

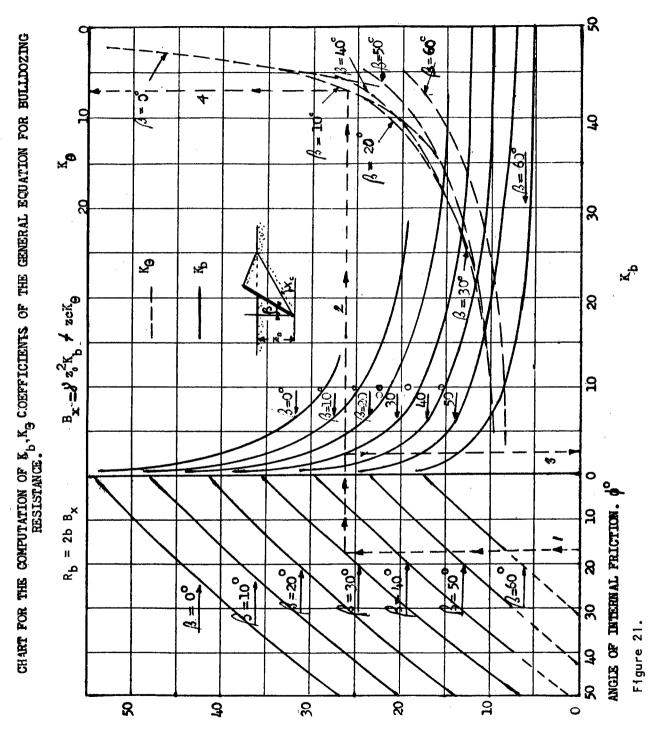
All of the wheel or track forms discussed attempt to accomplish the same result: increase contact area and develop the contact area so that the longer dimension of the area is oriented in the direction of wheel motion. The objective is, of course, to provide a wheel form that will produce an increase in soft soil performance by increasing traction and decreasing motion resistance. The emphasis in the wheel forms discussed has been on the reduction of motion resistance. When attempting to improve performance by increasing traction, it is necessary to cause either more soil failure or to cause the soil to fail in such a way as to increase the resistance to failure. The former is achieved by an increase in contact area and the latter by means of proper grouser design. When attempting to provide adequate grousers to produce a significant performance improvement, one is usually stymied because the grouser is quite unacceptable for operation on hard ground.

The final unusual concept to be discussed is the spaced-link track. The track is a device which attempts to utilize the maximum strength available from a given soil mass. In Figure 19, two types of soil failure are demonstrated. The soil failure that occurs between the two grousers has been identified in Bekker's book (3) as "grip" failure. The failure produced by the front grouser is called general failure and it is apparent that a considerably larger mass of soil is involved in this latter failure mode. The spaced-link track attempts to utilize the additional traction available from the general failure mode by spacing the grousers sufficiently widely apart to permit the general failure to occur. The spaced-link track



NGNO 47217 DAIL 19 March 1948
Comparison of Kamm vs. Standard Track. Models were tested in a medium texture sand at 15 inches per min. travel Standard track showing difference in soil failure between a closed-link and spaced-link track.

HIGNO 42387 DAMS SEPT DAR SENAL-HIGNO 42387 DAMS SEPT 1954
CARTIER CARGO Amphibious T60, Spaced-Link Track Test-High Rear view



A : SUALT SHUTTION OF RUPTURE PLANE: x,

shown in Figure 20, was designed for operation in soft soil. The track was installed on a test rig and demonstrated excellent soft soil performance but had obvious drawbacks for hard soil operation. A modified track is currently being designed for installation on the COBRA. The new track will provide a running surface for highway and hard soil operation that will reduce the vibration caused by the spaced-link track and reduce the excessive wear rate caused by operation on non-deforming materials. It is anticipated that the running surface will not significantly reduce the soft soil performance characteristics of the track so that a practical spaced-link track will evolve.

A fairly wide range of concepts has been included in this discussion. There has been no attempt to include all of the unusual concepts that have been proposed as that would be a task for a dedicated automotive historian. The concepts that have been included all have two characteristics: they attempt to adapt to the terrain to produce optimum performance; they demonstrate an application of land locomotion mechanics. Some may object that the concepts may be too radical to have practical application. It is argued that a radical improvement in off-road vehicle performance can only be achieved by radical solutions. All permutations and combinations of conventional solutions have been tried without producing a major change in performance. It is predictable that this should be true. When off-road terrain is examined, it is found that a given amount of traction is available and a given force resists motion. If a device either does not use all of the traction available or contribute to the motion resistance, the performance will be kept at a modest level. The conventional vehicle concept falls into the above category and no amount of rearranging of pieces can overcome the basic incompatibility of the vehicle to the off-road terrain.

REFERENCES

- "Evaluation of Elastic-Frame Vehicle Concept", by G. M. Defense Research Laboratories, Santa Barbara, California, November 1963.
- 2. Liston, R. A., "Unusual Wheel and Tire Concepts", Proceedings of the 5th Meeting of the Quadripartite Standing Working Group on Ground Mobility, Kingston, Ontario, Canada, 1965.
- 3. Bekker, M. G., "Theory of Land Locomotion", The University of Michigan Press, Ann Arbor, Michigan 1956.

DISTRIBUTION LIST

Commanding General		No. of
U. S. Army Tank-Automotive Command		Copies
Warren, Michigan 48090		
Attention:		
Chief Scientist/Technical Director of Laboratories, AV	ISTA-CL	1
Chief Engineer, AMSTA-CR		1
Director, Development & Engineering Directorate, AMSTA	∖-R	1
Vehicular Components & Materials Laboratory,		
ATTN: General Support Branch, AMSTA-BSG		2
Vehicle Systems Division, AMSTA-RE		2
International Technical Programs Division, AMSTA-RI	e de la Caracia	1
Engineering Control Systems Division, AMSTA-RS		2
Systems Concept Division, AMSTA-RR		2
Maintenance Directorate, AMSTA-M		2
Quality Assurance Directorate, AMSTA-Q		2
Commodity Management Office, AMSTA-W	•	2
Vehicular Components & Materials Laboratory,		
ATTN: Research Library Branch, AMSTA-BSL		3
Safety & Reliability Division, AMSTA-RB		1
Land Locomotion Division, AMSTA-UL	the second	10
Propulsion Systems Laboratory, AMSTA-G		5
Fire Power & Sub-System Integration Division, AMSTA-HF		1
Frame, Suspension & Track Division, AMSTA-UT		6
Scientific Computer Division, AMSTA-US		1
Technical Data Division, AMSTA-TD		2
Operations Support Division, AMSTA-RP		2
Combat Dev Comd Liaison Office, CDCLN-A		2
Marine Corp Liaison Office, USMC-LNO		2
AF MIPR Limison Office, SGRPD-USAF		2
Canadian Army Liaison Office, CDLS(D)		. 2
USA EL Liaison Office, AMSEL-RD-MN		2
USA Weapons Comd Liaison Office, AMSWE-LCV		2
Reliability Engineering Branch, AMSTA-RTT		I
Sheridan Project Managers Office, AMCPM-SH-D		1
General Purpose Vehicles Project Managers Office, AMCPI	M-GP	1
M60, M60A1, M46A3 Project Managers Office, AMCPM-M60		. !
Combat Veh Liaison Office, AMCPM-CV-D		I
US Frg MBT Detroit Office, AMCPM-MBT-D	•]
XM561 Project Managers Office, AMCPM-GG		1

	No. of Copies
Commanding General U. S. Army Materiel Command Washington, D. C. ATTN: AMCRD-DM-G	
Commander Defense Documentation Center Cameron Station Alexandria, Virginia 22314	20
Marry Diamond Laboratories Attn: Technical Reports Group Washington, D. C.	1
U. S. Naval Civil Engineer Res & Engr Lab Construction Batallion Center Port Hueneme, California	. 1
Commanding General U. S. Army Test and Evaluation Command Aberdeen Proving Ground, Maryland ATTN: AMSTE-BB AMSTE-TA	. 1 . 1
Commanding General U. S. Army Supply & Maintenance Command Washington, D. C. 20310 ATTN: AMSSM-MR	1
Commanding General 18th Airborne Corps Fort Bragg, North Carolina 28307	1
Commanding General U. S. Army Alaska APO 409 Seattle, Washington	1
Office, Chief of Research & Development Department of the Army Washington, D. C.	2
U. S. Army Deputy Chief of Staff for Logistics Washington, D. C.	2

ė,

	No. of <u>Copfes</u>
President U. S. Army Airborne Electronic & Fort Bragg, North Carolina 2630	
President U.S. Army Arctic Test Center APO Seattle, Washington 98733	un en el esta el el esta el
Director, Marine Corps Landing Forces Development Center Quantico, Virginia 22134	
Commanding Officer Aberdeen Proving Ground, Maryland Attention: STEAP-TL	
Commanding General Headquarters USARAL APO 949 Seattle, Washington ATTN: ARAOD	The second of th
Commanding General U. S. Army Aviation School Office of the Librarian Fort Rucker, Alabama ATTN: AASPI-L	
Plans Officer (Psychologist) PP&A Div, G3, Hqs, USACDCBD Fort ORD, California 93941	
Commanding General Hq, U. S. Army Materiel Command Research Division	erikansa (h. 1865) 18 - Arian Barris, eta erikansa (h. 1865) 18 - Arian Barris, eta erikansa (h. 1865)
Research and Development Director Washington, D. C. 20025	ate specification of the second specification of the secon
Canadian Army Staff 2450 Massachusetts Avenue Washington, D. C.	
British Joint Service Mission Ministry of Supply Staff 1800 K Street, N. W.	

	No. of Coples
Commander U. S. Marine Corps Washington, D. C. Attention: A0-rH	1
Commanding Officer U. S. Army Aviation Material Labs Fort Eustis, Virginia Attention: TCREC-SDL	1
Commanding General U. S. Army General Equipment Test Activity Fort Lee, Virginia 23801 Attn: Transportation Logistics Test Directorate	1
Commanding General U. S. Army Medical Services Combat Developments Agency Fort Sam Houston, Texas 78234	2
Commanding Officer Signal Corps Fort Mommouth, New Jersey 07703 ATTN: CSRDL	2
Commanding Officer Yuma Proving Ground Yuma, Arizona 85364 ATTN: STEYP-TE	1
Corps of Engineers U. S. Army Engineer Research & Development Labs Fort Belvoir, Virginia 22060	1
President U. S. Army Maintenance Board Fort Knox, Kentucky 40121	. 1
President U. S. Army Armor Board Fort Knox, Kentucky 40121	1
President U. S. Army Artillery Board Fort Sill, Oklahoma 73503	1
President U. S. Army Infantry Board Fort Benning, Georgia 31905	1

	No. of Coples
Director U. S. Army Engineer Waterways Experiment Station Corps of Engineers P. O. Box 631 Vicksburg, Mississippi 39181	
Unit X Documents Expediting Project Library of Congress Washington, D. C. Stop 303	•
Exchange and Gift Division Library of Congress Washington, D. C. 20025	; 1
United States Navy Industrial College of the Armed Forces Washington, D. C. ATTN: Vice Deputy Commandant	. 10
Continental Army Command Fort Monroe, Virginia	1
Department of National Defense Dr. N. W. Morton Scientific Advisor Chief of General Staff Army Headquarters Ottawa, Ontario, Canada	1
Chief Office of Naval Research Washington, D. C.	ı
Superintendent U. S. Military Academy West Point, New York ATTN: Prof. of Ordnance	
Superintendent U. S. Naval Academy Anapolis, Maryland	1
Chief, Research Office Mechanical Engineering Division Quartermaster Research & Engineering Command Natick, Massachusetts	1

Security Classification			
DOCUMENT CO (Security classification of title, body of abstract and indexis	NTROL DATA - R&		the overall report is classified)
1. ORIGINATING ACTIVITY (Corporate author)			RT SECURITY C LASSIFICATION
Land Locomotion Laboratory		Und	classified
		2 b. GROUF	N/A
3. REPORT TITLE			
Research Report No. 6			
4. DESCRIPTIVE NOTES (Type of report and inclusive dates)			
State-of-the-Art Report on Off-the-Ro	ad Mobility Re	search	
5. AUTHOR(S) (Leet name, tiret name, initial) Liston, Rona Czako, Tibor F.; Harrison, William L. Martin, Lynn A.; Wills, Brian M.D.;	ild A.; Janosi , Jr.; Spansk	, Zoltar 1, Paul	ı J.; Hegedus, Ervin;
6. REPORT DATE	74. TOTAL NO. OF P	AGES	75. NO. OF REFS
November 1966	329		70
Sa. CONTRACT OR GRANT NO.	Sa. ORIGINATOR'S R	EPORT NUM	BER(S)
b. PROJECT NO.	9560		
c.	S. OTHER REPORT	NO(S) (Any	other numbers that may be assigned
	this report)		
d.	<u> </u>		
Distribution of this do	ocument is unli	nited.	
11. SUPPLEMENTARY NOTES	12. SPONSORING MIL	TARY ACTI	VITY
	U.S. Army T	ank Auto	omotive Command
13. ABSTRACT	<u> </u>		
This report is a comprehensive co Staff of the Land Locomotion Laborator volume, a picture of the state-of-the- The following topics are covered: in Vertical and Horizontal Directions diction; The Analysis of Wheel Perfor istics Studies; Application of Dimens Remote Area Soil Strength Prediction b Portable Soil-Strength Measuring Appar Strength Measuring Device; Discussion High Mobility Vehicle and Component Co	y. Its purpos art of soil-vel Description and Its Use in mance in Soft Sional Analysis by Means of Soi atus; Field T	e is to nicle me of Soil Vehicle Soil; \ in Land 1 Analogests wit	offer, in a single echanics. Stress-Strain Behavior e Performance Pre- /ehicle Ride Character- d Locomotion Mechanics; gs; Description of a th a Wheeled Soil

DD 150RM 1473

Security Classification

OFF-THE-ROAD MOBILITY SOIL STRENGTH VEHICLE RIDE WHEELS PERFORMANCE PREDICTION DIMENSIONAL ANALYSIS SOIL ANALOGS SOIL TEST DEVICES UNUSUAL VEHICLES	14.	KEY WORDS	LINK A		LINK B		LINK C	
SOIL STRENGTH VEHICLE RIDE WHEELS PERFORMANCE PREDICTION DIMENSIONAL ANALYSIS SOIL ANALOGS SOIL TEST DEVICES	L	KET WORDS	ROLE	WT	ROLE	WT	ROLE	WT
	•	SOIL STRENGTH VEHICLE RIDE WHEELS PERFORMANCE PREDICTION DIMENSIONAL ANALYSIS SOIL ANALOGS SOIL TEST DEVICES						

INSTRUCTIONS

- 1. ORIGINATING ACTIVITY: Enter the name and address of the contractor, subcontractor, grantee, Department of Defense activity or other organization (corporate author) issuing the report.
- 2a. REPORT SECURITY CLASSIFICATION: Enter the overall security classification of the report. Indicate whether "Restricted Data" is included. Marking is to be in accordance with appropriate security regulations.
- 2b. GROUP: Automatic downgrading is specified in DoD Directive 5200.10 and Armed Forces Industrial Manual. Enter the group number. Also, when applicable, show that optional markings have been used for Group 3 and Group 4 as authorized.
- 3. REPORT TITLE: Enter the complete report title in all capital letters. Titles in all cases should be unclassified. If a meaningful title cannot be selected without classification, show title classification in all capitals in parenthesis immediately following the title.
- 4. DESCRIPTIVE NOTES: If appropriate, enter the type of report, e.g., interim, progress, summary, annual, or final. Give the inclusive dates when a specific reporting period is covered.
- 5. AUTHOR(S): Enter the name(s) of author(s) as shown on or in the report. Enter last name, first name, middle initial. If military, show rank and branch of service. The name of the principal author is an absolute minimum requirement.
- REPORT DATE: Enter the date of the report as day, month, year; or month, year. If more than one date appears on the report, use date of publication.
- 7a. TOTAL NUMBER OF PAGES: The total page count should follow normal pagination procedures, i.e., enter the number of pages containing information.
- 7b. NUMBER OF REFERENCES: Enter the total number of references cited in the report.
- 8a. CONTRACT OR GRANT NUMBER: If appropriate, enter the applicable number of the contract or grant under which the report was written.
- 8b, 8c, & 8d. PROJECT NUMBER: Enter the appropriate military department identification, such as project number, subproject number, system numbers, task number, etc.
- 9a. ORIGINATOR'S REPORT NUMBER(S): Enter the official report number by which the document will be identified and controlled by the originating activity. This number must be unique to this report.
- 9b. OTHER REPORT NUMBER(S): If the report has been assigned any other report numbers (either by the originator or by the sponsor), also enter this number(s).

- 10. AVAILABILITY/LIMITATION NOTICES: Enter any limitations on further dissemination of the report, other than those imposed by security classification, using standard statements such as:
 - "Qualified requesters may obtain copies of this report from DDC."
 - (2) "Foreign announcement and dissemination of this report by DDC is not authorized."
 - "U. S. Government agencies may obtain copies of this report directly from DDC. Other qualified DDC users shall request through
 - (4) "U. S. military agencies may obtain copies of this report directly from DDC. Other qualified users shall request through
 - (5) "All distribution of this report is controlled. Qualified DDC users shall request through

If the report has been furnished to the Office of Technical Services, Department of Commerce, for sale to the public, indicate this fact and enter the price, if known

- 11. SUPPLEMENTARY NOTES: Use for additional explanatory notes.
- 12. SPONSORING MILITARY ACTIVITY: Enter the name of the departmental project office or laboratory sponsoring (paying for) the research and development. Include address.
- 13. ABSTRACT: Enter an abstract giving a brief and factual summary of the document indicative of the report, even though it may also appear elsewhere in the body of the technical report. If additional space is required, a continuation sheet shall be attached.

It is highly desirable that the abstract of classified reports be unclassified. Each paragraph of the abstract shall end with an indication of the military security classification of the information in the paragraph, represented as (TS), (S), (C), or (U).

There is no limitation on the length of the abstract. However, the suggested length is from 150 to 225 words.

14. KEY WORDS: Key words are technically meaningful terms or short phrases that characterize a report and may be used as index entries for cataloging the report. Key words must be selected so that no security classification is required. Idenfiers, such as equipment model designation, trade name, military project code name, geographic location, may be used as key words but will be followed by an indication of technical context. The assignment of links, rules, and weights is optional.